POLYTECHNIQUE MONTRÉAL

affiliée à l'Université de Montréal

Synthesis and Characterization of Novel Energetic Materials Based on NTO & Energetic Binder Through Cast-Cured Technique

MOHAMED ABDALLA A. I. ELNEGOUMY

Département de génie chimique

Thèse présentée en vue de l'obtention du diplôme de *Philosophiae Doctor*

Génie chimique

Novembre 2025

POLYTECHNIQUE MONTRÉAL

affiliée à l'Université de Montréal

Cette thèse intitulée :

Synthesis and Characterization of Novel Energetic Materials Based on NTO & Energetic Binder Through Cast-Cured Technique

présentée par **Mohamed Abdalla A. I. ELNEGOUMY**
en vue de l'obtention du diplôme de *Philosophiae Doctor*
a été dûment acceptée par le jury d'examen constitué de :

Abdellah AJJI, président
Charles DUBOIS, membre et directeur de recherche
Etienne COMTOIS, membre et codirecteur de recherche
Julian SELF, membre
Jonathan LAVOIE, membre externe

DEDICATION

To God, my supervisor, my family, my beloved parents, my wife, my sons, lab members, and to everyone *who has ever supported me……*

Thank you for your support and care

ACKNOWLEDGEMENTS

During my PhD journey, I was fortunate to meet truly several wonderful people from whom I learned a great deal. Without their efforts and support, this work would not have come to light or reached its final form.

I would like to begin by expressing my appreciation to my supervisor, Professor Charles Dubois, thank you for your guidance, thank you for your help, thank you for your encouragement, thank you for everything. I am especially grateful for his trust and patience, which gave me from the very first moment and throughout my entire Ph.D. journey. I would also like to extend my sincere thanks to my co-supervisor, Dr. Étienne Comtois for supporting this project, and for his valuable suggestions that greatly contributed to my personal and professional development. Additionally, I would like to appreciate the members of the jury to review and evaluate my thesis. I am deeply grateful to my lab members, Dr. Ricardo Pontes, and Dr. Silvia for their invaluable support, and willingness to help me overcome both scientific and technical challenges. I feel fortunate to have met and worked with them. I also want to extend my gratitude to all wonderful peoples that encouraged me and helped me during the past three years including Ms. Martine Lamarche, Ms. Claire Cerclé, Mr. Gino Robin, Mr. Matthieu Gauthier, and Ms. Lucie Jean. My thanks to all.

I am truly thankful to the Egyptian Ministry of Defense (MOD) for supporting my studies during my PhD journey. Their financial support help gave me the resources and opportunities; I needed to complete my research. I would also like to thank important peoples and friends that were beside me during the development of this work: Dr. Ahmed Elbeih, Dr. Ramy Sadek, Dr. Mahmoud Youssry, Dr. Ahmed Emam.

Without the support of my parents, I would never have been able to complete my journey during my life. Finally, I would like to thank my lovely wife, Mai, my sons, Basem and Ahmed, my daughter, Nada for their support, help, and encouragement. I would not have been able to finish this work, especially during the times I felt like giving up, without Mai and her constant love and support. She was always there for me, and still is. I'm truly lucky to have her in my life.

Mohamed…

RÉSUMÉ

Le domaine des matériaux énergétiques évolue constamment en réponse au potentiel destructeur considérable résultant de stimuli involontaires et d'initiations accidentelles, des événements qui entraînent des pertes importantes en vies humaines et en biens. Par conséquent, ce domaine de recherche suscite une grande attention et un intérêt croissant visant à développer de nouveaux matériaux énergétiques.

Les explosifs plastiques (PBXs) constituent une classe de matériaux énergétiques reconnus pour leur manutention sécuritaire et leur insensibilité à divers stimuli. D'importants efforts ont été consacrés au développement de la prochaine génération de PBXs afin d'améliorer leurs performances et leurs caractéristiques de sécurité. L'intégration de polymères énergétiques et d'explosifs intrinsèquement insensibles tels que le 3-nitro-1,2,4-triazole-5-one (NTO) et le 1,3,5-triamino-2,4,6-trinitrobenzène (TATB), comme substituts potentiels aux explosifs traditionnels tels que le 1,3,5,7-tétranitro-1,3,5,7-tétrazocane (HMX) et le 1,3,5-trinitro-1,3,5-triazinane (RDX), attire aujourd'hui beaucoup d'intérêt. L'objectif est la synthèse et la caractérisation de matériaux explosifs avancés, en particulier par la technique du moulage-coulée, afin de développer de nouveaux PBXs combinant une performance de détonation améliorée avec une meilleure sensibilité mécanique et une stabilité thermique accrue. De plus, cette recherche propose une nouvelle méthode de synthèse de NTO basée sur un microréacteur, visant à surmonter les limitations et les risques des procédés traditionnels en batch.

Les activités de la thèse sont divisées en cinq axes principaux. La première partie vise à étudier la nature et les paramètres critiques associés à la synthèse conventionnelle du NTO par la technique en batch et par la procédure (one-pot). Ce travail a pour objectif de proposer une voie de synthèse plus sûre et plus efficace. Les données obtenues à ce stade, en particulier la température de nitration, ont été essentielles pour orienter le développement d'une nouvelle méthode de synthèse du NTO dans un microréacteur.

La deuxième partie consiste à développer une approche de synthèse innovante du NTO en utilisant un microréacteur et la chimie en flux pour répondre aux défis et risques associés aux méthodes conventionnelles. L'un des principaux avantages de cette technologie appliquée aux explosifs est sa capacité à gérer en toute sécurité les dégagements de chaleur intenses au cours des réactions

ainsi qu'à limiter la formation de points chauds. La troisième partie concerne le développement du matériau explosif lui-même à base de NTO, afin d'obtenir une énergie améliorée, une sensibilité mécanique réduite et une stabilité thermique contrôlée. L'objectif est d'atteindre un équilibre optimal entre énergie et sensibilité en enrobant les particules de NTO d'oxyde de graphène (GO) et d'oxyde de cuivre (CuO) sous forme nanométrique.

La quatrième partie porte sur la synthèse et la caractérisation de nouveaux matériaux PBXs basés sur le NTO et le polymère énergétique GAP, en utilisant une technique de moulage-coulée. Une série de matériaux a été développée afin d'évaluer systématiquement les paramètres de performance et les caractéristiques de sensibilité. Pour garantir une dispersion optimale et une bonne homogénéité, les échantillons ont été préparés à l'aide d'un mélangeur centrifuge sous vide (Thinky mixer). En plus de la composition explosive de base (NTO/GAP), des PBXs modifiés incorporant du NTO enrobé de GO ainsi que du NTO enrobé de GO et de nano-CuO ont été préparés.

Enfin, les caractéristiques de performance des PBXs ont été calculées théoriquement à l'aide du code thermochimique EXPLO5. De plus, une simulation temporelle du test de Cook-off à confinement variable (VCCT) a été réalisée avec COMSOL multiphasiques pour évaluer le comportement thermique et la sécurité d'un PBX à base de NTO-GAP soumis à un chauffage lent. La structure chimique, la morphologie, la sensibilité et la stabilité thermique ont été examinées de manière systématique. Les principales caractéristiques de performance, notamment les propriétés de détonation et la chaleur de combustion, ont été évaluées pour déterminer l'aptitude des matériaux aux applications énergétiques.

Les résultats montrent que commencer la nitration à 25 °C permet une préparation plus sûre du NTO par la méthode en batch, et qu'augmenter la température à 65 °C pendant environ 2 heures donne un rendement de 67.2 %. En comparaison, la méthode one-pot fournit un rendement plus élevé de 72.3 %, offrant une voie de synthèse plus évolutive mais légèrement plus risquée.

Le NTO a été préparé avec succès par chimie en flux dans un microréacteur, offrant une alternative plus sûre et plus efficace. Le meilleur rendement a été obtenu avec le mélange de solvants DMF: DMSO (80 :20) atteignant 59.6 % en seulement 5 minutes à 65 °C, contre 2 heures nécessaires en batch.

Le GO a été préparé avec succès par la méthode de Hummers modifiée, et les matériaux enrobés NTO/GO et NTO/GO/CuO ont été élaborés par ultrasons. Les résultats ont montré que le NTO/GO conservait sa structure polymorphique. Les enrobages de GO ont amélioré la sensibilité mécanique (frottement et choc) et la stabilité thermique du NTO. Un enrobage de 3 wt. % GO a augmenté l'énergie d'activation de 45 kJ/mol par rapport au NTO pur, tandis que des teneurs plus élevées ≥ 4 wt. % ont réduit la stabilité thermique. Une innovation notable a été l'intégration réussie de moins de 1 wt. % de CuO dans le NTO sans accélérer de manière significative sa décomposition catalytique tout en augmentant l'énergie libérée grâce à la combinaison avec le GO.

Les PBXs ont été préparés avec succès en utilisant le GAP et le NTO, avec un mélange bimodal de deux tailles de cristaux pour améliorer le compactage, permettant une charge solide maximale de 76.5 wt. % de NTO. D'autres compositions incorporant du NTO enrobé de GO et du NTO enrobé de GO et CuO ont également été élaborées. Les PBXs développés ont présenté des améliorations significatives de la sécurité mécanique par rapport au NTO pur et à plusieurs compositions modernes d'explosifs insensibles. Le PBX à 76.5 % NTO/GAP a montré une sensibilité au frottement de 360 N, surpassant l'IMX-101, l'IMX-104, ainsi que des PBXs à base de GAP contenant du BCHMX ou du CL-20. L'ajout de GO et de GO/CuO a encore amélioré la sensibilité mécanique. L'analyse thermique a montré que tous les PBXs conservaient un unique pic exothermique caractéristique du NTO. L'intégration du GAP et des additifs nanométriques a diminué les températures de décomposition et les énergies d'activation par rapport au NTO pur. La présence du GO et d'autres additifs a modifié le comportement de décomposition, réduisant généralement la stabilité thermique par rapport au système NTO/GAP non modifié. Globalement, les PBXs ont montré une nette amélioration de la sécurité mécanique, avec des variations modérées de la stabilité thermique. La chaleur de combustion et la chaleur d'explosion ont augmenté pour toutes les compositions, et l'ajout de GO et CuO a encore renforcé ces valeurs. En termes de performance de détonation, toutes les compositions ont montré une amélioration notable par rapport aux matériaux insensibles tels que l'IMX-101, démontrant l'efficacité des PBXs développés. Enfin, selon les résultats de la simulation VCCT réalisée sous COMSOL, la température maximale dans le cœur du PBX a atteint environ 213 °C, ce qui se situe entre les températures d'initiation mesurées par DSC, indiquant que dans ces conditions simulées, la composition PBX peut atteindre ou légèrement dépasser le seuil de décomposition thermique.

ABSTRACT

The field of energetic materials continually evolves in response to the substantial destructive potential resulting from unintended stimuli and accidental initiation. These events result in significant loss of human lives and assets. Consequently, this research area has attracted much attention and substantial interest aimed at developing novel energetic materials.

Plastic bonded explosives (PBXs) represent a class of energetic materials recognized for their safe handling characteristics and unsensitivity to diverse stimuli. Great efforts had been devoted to developing the next generation of PBXs, aiming to improve their performance and safety attributes. The incorporation of energetic polymers and intrinsically insensitive explosives such as 3-nitro, 1, 2,4-triazole, 5-one (NTO) and 1,3,5-triamino-2,4,6-trinitrobenzene (TATB), as potential replacements for traditional explosive materials like 1,3,5,7-tetranitro-1,3,5,7-tetrazocane (HMX) and 1,3,5-trinitro-1,3,5-triazinane (RDX) has attracted much attention nowadays. The objective is the synthesis and characterization of advanced explosive materials, particularly through the cast cured technique to develop novel PBXs that combined between enhanced detonation performance with enhanced mechanical sensitivity and thermal stability. In addition, this research proposes a novel microreactor based synthesis method for NTO explosive, aiming to overcome the limitations and risks of traditional batch processes.

The thesis activities are divided into five main trusts; the first part is to investigate the nature and critical parameters associated with the conventional synthesis of NTO explosives using the batch technique and the one-pot procedure. This work aims to propose a safer and more efficient synthesis route. The data obtained from this stage particularly the nitration temperature was critical for guiding the development of a new method for NTO synthesis inside the microreactor.

The second part is to develop a novel synthesis approach for NTO utilizing microreactor employing flow chemistry to address the challenges and risks associated with the conventional methods. One of the key advantages of this technology to use in explosives synthesis, is its ability to safely handle, intense heat releases during the reactions. Also, its ability to limit hot spot formation.

The third part concerns the development of the explosive material itself based on NTO to exhibit enhanced energetic output, reduced mechanical sensitivity and controlled thermal stability. The

goal is to achieve an optimal balance between energy and sensitivity by coating NTO particles with graphene oxide (GO) and copper oxide (CuO) nanomaterials.

The fourth part focuses on the synthesis and characterization of new PBXs materials based on NTO and glycidyl azide polymer (GAP) as the energetic binder using a cast-cured technique. A series of materials were developed to systematically evaluate both performance parameters and sensitivity characteristics. To ensure optimal dispersion and consistency, samples were prepared using a high-speed planetary centrifugal vacuum mixer (Thinky mixer. In addition to the base explosive composition (NTO/GAP), modified PBXs materials incorporating NTO coated with GO and NTO coated with GO and nano-CuO were also prepared.

Finally, the performance characteristics of the PBXs materials were calculated theoretically using EXPLO5 thermochemical equilibrium code. Additionally, a time-dependent simulation of the variable confinement cook-off test (VCCT) was carried out using COMSOL Multiphysics to assess the thermal behavior and safety of an NTO-GAP-based PBX under slow heating conditions.

The chemical structure, morphology, sensitivity, and thermal stability were systematically examined. Key performance characteristics, including detonation properties and heat of combustion, were evaluated to assess the suitability of the materials for energetic applications.

The results show that starting nitration at 25 °C allows safer preparation of NTO using the batch method, where increasing the temperature to 65 °C for about 2 hours yields 67.2% NTO. In comparison, the one-pot method provides a higher yield of 72.3%, offering a more scalable but slightly riskier synthesis route.

NTO was successfully prepared through the flow chemistry using a microreactor that offers a safer and more efficient new alternative technique for NTO preparation. The best yield was obtained using DMF: DMSO solvent mixtures (80:20) that achieving high yield as 59.6% in just 5 minutes at 65 °C compared to 2 hours required in the batch methods.

GO was successfully prepared using the modified Hummers method, and the coated materials NTO/GO and NTO/GO/CuO composite were prepared through an ultrasonic technique. The results indicated that the coated NTO/GO material retained their original polymorphic structure during the preparation process. GO coatings successfully improved the mechanical sensitivity (friction &impact) and thermal stability of NTO, specifically, when the coating content of GO was 3 wt.%,

this led to increasing the activation energy by 45 kJ/mol compared to pure NTO, whereas higher GO contents ≥ 4 led to a reduction in thermal stability. One of the new innovations was the successful incorporation of approximately less than 1wt.% CuO as a nano-metal oxide in the NTO without significantly accelerate the catalytic decomposition of NTO and in the same time increase the energy release of NTO by combination the coating layer with GO.

PBX materials were successfully prepared using GAP and NTO, employing a bimodal mixture of two NTO crystal sizes to improve packing efficiency, enabling a maximum solid loading of 76.5 wt.% NTO in the PBX compositions. Additional compositions of PBXs incorporated NTO coated with GO and CuO were prepared. The developed PBX compositions showed significant improvements in mechanical safety compared with pure NTO and several modern insensitive munition compositions. The 76.5% NTO/GAP PBX demonstrated a friction sensitivity of 360 N, outperforming IMX-101 and IMX-104 (by 50% and 125%) as well as GAP-based BCHMX and CL-20 PBXs (by 22% and 46%). The addition of GO and GO with CuO further enhanced the mechanical sensitivity. Thermal analysis showed that all PBXs retained a single exothermic peak characteristic of NTO. Incorporating GAP and nanomaterial additives into the PBX compositions lowered the decomposition temperatures and activation energies compared with pure NTO. The presence of GO and other additives altered the decomposition behaviour, generally reducing thermal stability compared with the unmodified NTO/GAP composition. Overall, the PBX composition showed significant improvements in mechanical safety, with moderate variations in thermal stability. Both the heat of combustion and the heat of explosion increased for the PBX compositions. Adding GO and CuO further enhanced these values. In terms of detonation performance, all PBX compositions showed a clear improvement with detonation velocities compared with other insensitive materials such as IMX101. This improvement in performance highlights the effectiveness of our PBXs materials. Additionally, according to the results of COMSOL-based simulation of the VCCT, the maximum temperature within the PBX core reached approximately 213 °C that falls between the DSC onset values, indicating that under these modelled conditions the PBX composition may reach or slightly surpass the threshold for thermal decomposition.

TABLE OF CONTENTS

LIST OF TABLES

LIST OF FIGURES

LIST OF SYMBOLS AND ABBREVIATIONS

Symbols

ρ	Density
D	Detonation velocity
V_o	Specific volume of detonation gases
Q_v	Heat of detonation
Tg	Glass transition temperature
Mn	Molecular weight
P	Explosion pressure
T	Explosion temperature

Abbreviations

PBXs	plastic bonded explosives
HEMs	High energy materials
RIM	Reaction injection molding
DOZ	Dioctyl azelate
DOA	Dioctyl adipate
MAPO	Tris-1-(2-methylaziridinyl) phosphine oxide
HMDI	Hexamethylene-diisocyanate
TDI	Toluene diisocyanate
IM	Insensitive munitions

GAP	Glycidyl azide polymer
BAMO	3,3- Bis azido methyl oxetane
HE	High Explosive
JWL	Jones-Wilkins-Lee
TO	Triazole one
DSC	Differential scanning calorimeter
KAS	Kissinger-Akahira-Sunose
FTIR	Fourier transfer infrared
SEM	Scanning Electron Microscopy
TGA	Thermo gravimetric Analysis
PETN	Pentaerythritol Tetranitrate
HMX	Cyclotetramethylene-nitramine
RDX	Cyclotrimethylene-trinitramine
TATB	Triamino-trinitrobenzene
NTO	3-nitro, 1, 2,4-triazole, 5-one
TNAZ	1,3,3-Trinitroazetidine
CL20	Hexanitrohexaazaisowurtzitane
FOX-7	1,1-Diamino-2,2-dinitroethene
NOL	Naval Ordnance Laboratory
DMSO	Dimethyl sulfoxide
GO	Graphene oxide
DMF	Dimethyl formamide

SC	Semicabazide hydrochloride
DNAN	2,4-Dinitroanisole
SST	Stainless steel
PTFE	Polytetrafluoroethylene
PFA	Perfluoro alkoxy alkanes
FEP	Fluorinated ethylene propylene
SAR	Split and recombine
HNS	Hexanitrostilbene
WHMIS	Workplace Hazardous Materials Information System
DRDC	Defence Research and Development Canada

CHAPTER 1 INTRODUCTION

1.1 Context

The need for increased safety concerning explosives materials during their handling, storage, and transportation arises from the significant damage caused by the accidental initiation of these materials [1]. This requires the development of new energetic materials to mitigate these risks effectively. However, it is important to note that enhancing the safety of energetic materials by making them less sensitive often comes at the expense of their explosive performance. For the successful development of new energetic materials, two essential factors must be combined, both of which are imperative: superior performance and safety requirements. [2]. Often, the energetic materials that have relatively low velocity of detonation and low detonation pressure as 3-nitro, 1, 2,4-triazole, 5-one (NTO) are less sensitive to accidental initiation (lower impact and friction sensitivity). These energetic materials that have reduced sensitivity led to the development of important application called insensitive munitions (IM). Insensitive Munitions (IM) could be defined as those that consistently fulfill performance, readiness, and operational requirements only on demand, and minimize accidental initiation by external stimuli [3]. Advancements in this field include the development of new explosives and the use of less sensitive energetic compounds in energetic compositions. For example, specific energetic materials as IMX101 and IMX104 have been developed for being used in insensitive munitions applications. While these materials meet safety requirements, they exhibit lower performance characteristics than their no counterparts [4].

In broad terms, energetic materials (EMs) are a category of materials capable of releasing stored chemical energy within their molecular structure, when subjected to external stimuli like heat, shock, or electrical current, these materials rapidly emit its energy [5]. Traditionally, energetic materials are categorized based on their applications into low-energy explosives like propellants and pyrotechnics, and high-energy explosives like primary and secondary explosives. The latter are further classified into primary explosives such as mercury fulminate, silver fulminate, and lead azide, secondary explosives such as 1,3,5-trinitro-1,3,5-triazinane (RDX), 1,3,5,7-tetranitro-1,3,5,7-tetrazocane (HMX), and trinitrotoluene (TNT), or tertiary explosives encompassing, ammonium nitrate fuel oil (ANFO) and dynamite compositions [5].

Explosives can be categorized in various ways, one of which is based on their chemical composition, distinguishing between pure individual explosives and explosive mixtures [5].

Explosive mixtures can consist of multiple single explosives, such as Composition B, a blend of 60% TNT and 40% RDX [6], or single explosives combined with fuels, oxidizers, binders, or plasticizers, as seen in PBXs and slurry explosives [7]. The key distinction between different types of explosives, propellants, and pyrotechnics lies in the rate of energy release. Propellants and pyrotechnics involve relatively slow deflagration processes (taking several seconds), whereas explosives release their energy through rapid detonation processes (occurring within microseconds) [5].

All researchers aim to develop new explosive materials that optimize both performance and safety aspects. Several strategies have been employed to desensitize explosive materials. These methods include coating explosive materials with insensitive polymers [8], refining explosive crystals through recrystallization techniques [9], creating new insensitive explosives such as 1,3,5-triamino-2,4,6-trinitrobenzene (TATB) and NTO [10], and incorporating nano-explosive materials into the energetic material compositions [11]. Additionally, co-crystallization techniques have been explored, leading to the formation of larger crystals with enhanced properties compared to the original individual explosives [12]. On the other hand, typically, there are two approaches employed to increase the energy of the system, utilizing melt-castable explosives or incorporating energetic binders and plasticizers when formulating new energetic materials [13].

A common strategy to attain a balance between safety and performance criteria involves developing compositions of PBXs materials. PBXs are compositions consisting mainly of secondary explosives like RDX, HMX, or pentaerythritol tetranitrate (PETN), dispersed within a rubbery matrix with binders and plasticizers [8]. This encapsulation enhances thermal stability, burn rate, and resistance to external forces (mechanical sensitivity). Several PBXs materials have been developed, but these traditional PBXs have proven inadequate in addressing the challenges related to the storage, transportation, and handling of ammunition under extreme conditions, as well as the risk of accidental initiation [1]. On the other hand, melt casting insensitive compositions provides safety advantages and succeeded in overcoming the problems related to the storage, transportation, and handling of ammunition, as well as reduced the risks of accidental initiation, but it often results in reduced performance and detonation parameters, as in IMX-101 and IMX-104 compositions [4]. Consequently, an alternative approach is needed to resolve this dilemma. This alternative approach involves employing intrinsically insensitive explosives like TATB or

1,3,3-Trinitroazetidine (TNAZ), or NTO through a cast cured technique instead of the traditional ones HMX and RDX. Additionally, in contrast to traditional PBXs. This innovative method utilizes energetic binder to effectively balance between safety and performance, providing a solution to this challenge.

NTO is considered a favorable solution for use in Low Vulnerability Ammunition (LOVA). It exhibits lower sensitivity to friction and impact compared to RDX, HMX and PETN while its sensitivity is similar to TNT and TATB. However, it is slightly more sensitive to shock than TATB and less sensitive than PETN, RDX and HMX [14].

Recently, carbon nanomaterials, such as carbon nanotubes (CNTs), carbon nanofibers (CNFs), graphene and its derivatives (graphene oxide (GO) and reduced graphene oxide (RGO)) have been active fields of research that shown great potential in improving safety while maintaining the explosive's efficiency or having minimal impact on energetic properties [15]. CNTs have demonstrated a significant positive impact on reducing sensitivity, especially mechanical sensitivity as they act as desensitizers for several explosives due to their large specific areas and unique thermal, electrical and mechanical properties [16]. Among these carbon nanomaterials, GO stands out as an important derivative of graphite due to the presence of oxygen containing functional groups on its basal planes and edges. It has several characteristics that make it highly suitable for energetic materials applications. Its high theoretical specific surface area and abundant oxygen functional groups enhance its interaction with energetic components. GO offers also thermal reactivity, which is beneficial in energy releasing reactions. Additionally, GO is more hydrophilic and dispersible compared to other carbon nanomaterials, reducing agglomeration during coating processes and allowing for better encapsulation and desensitization of energetic materials. [17-18]. Also, GO itself is considered to be a potential energetic materials (EM) because it liberates oxygen stored on its basal plane and long edges functional groups through violent exothermic reaction [19].

Energetic polymeric materials are characterized by a hydrocarbon-based fuel component and one or more oxidizing “explosophoric” groups integrated into their polymer backbone are considered favourable solution to enhance the performance of the EM compositions by elevating the overall energy output of the energetic materials [20]. This led to the development of high-performance explosives and advanced rocket propellants. These polymers contain different energetic functional

groups include azide group ($-N_3$), nitro ($-NO_2$), nitrate ester ($-O-NO_2$), nitramino ($-N-NO_2$), or other similar explosive-functional groups [21]. Glycidyl azide polymer (GAP) is an important energetic polymer characterized by the presence of ($-N_3$) groups in its molecular structure. GAP is commercially available in multiple grades that differ significantly in molecular weight, and these differences determine whether the material functions as a binder or as a plasticizer. For example, GAP-5527 is a prepolymer with a typical number average molecular weight in the range of several thousand g/mol, allowing it to form a cross-linked polymer network suitable for use as an energetic binder. In contrast, GAP based plasticizers have much lower molecular weights typically a few hundred g/mol which gives them high mobility and makes them effective at reducing viscosity and improving flexibility in propellant or PBX compositions. Also, GAP remains non-sensitive to mechanical stimuli and yields a higher proportion of low molecular weight combustion products like CO, H_2, and N_2, rather than CO_2 and H_2O [22].

1.2 Problem statement and motivation

The development of high explosive manufacturing has become a major focus for many scientists and researchers nowadays due to the serious problems and hazardous incidents associated with their production. These dangers and risks are not solely due to the use of hazardous reagents. But also, from the various hazardous synthesis processes including nitration reactions, azide reactions and amination reactions, etc. that contribute to the overall risk [23,24]. Furthermore, researchers have systematically formulated various energetic composition materials in an attempt to harmonize the essential demands for both safety and performance, in accordance with the prerequisites of insensitive munition applications. These efforts have employed several compositions of energetic materials.

As a result of these efforts, several approaches have been published on NTO synthesis from its discovery in 1905 to the present, employing methods such as the two-step process and the one-pot synthesis procedure using different nitrating agent including the use of fuming nitric acid [25-26], concentrated nitric acid (70%), as well as mixed acids [27]. These conventional methods involve significant risks during the nitration step due to the relatively high nitration temperature of 65 °C for approximately 1.5-2 hours [27]. Moreover, the exothermic nature of the reaction throughout the nitration poses additional challenges and risks. During the nitration reaction, the temperature

rapidly increases and can exceeds 100 °C within a few minutes. To overcome some of these challenges, alternative approaches have been explored such as the use of metal nitrates such as potassium nitrate (KNO_3) and silver nitrate ($AgNO_3$) in the nitration process [28]. Also, some researchers have also utilized unconventional heating methods, such as microwave irradiation, as an energy source to carry out the nitration step [29]. All of this effort is aimed to synthesizing NTO explosive in a safe manner while maintaining a reasonable production yield. However, these alternatives still face challenges related to the nature of the nitration process.

Additionally, the driving force behind every research in the area of energetic materials is often to maximize the performance of the military warheads. But, the design of future weapon systems requires the utilization of explosive and propellant materials that strike a balance between high performance and enhanced safety measures. The handling, storage, and transportation of explosives also have substantial risks, given the potential for accidental initiation leading to significant damage and human loss [1]. Consequently, there is a need for the development of new energetic composition materials that prioritize safety and at the same time have high detonation characteristics. Balancing this equation proves challenging since enhancing safety tends to come at the expense of performance. In this direction as well, researchers have made a lot of efforts on designing explosives that address both requirements, seeking solutions that minimize sensitivity while maintaining the necessary operational effectiveness. One of these explosive compositions has been developed utilizing nitramines such as RDX and HMX in combination with various polymers including inert and energetic ones employing the cast-cured method. However, the authors of these energetic composition materials discovered that while these compositions exhibited high performance and detonation characteristics, but in the same time, these energetic materials exhibited high impact and friction sensitivity [30-32]. On the other hand, through melt cast method, researchers introduced new energetic composition materials of explosives, such as IMX-101 and IMX-104, in an effort to address the challenge that stated above (high impact and friction sensitivity). These materials are based on a low sensitivity high explosive, NTO in combination with 2,4 dinitroanisole (DNAN) explosives. IMX-101 and IMX-104 successfully addressed sensitivity problems, but in the same time, these energetic composition materials exhibit a lower detonation velocity when compared to nitramine-based compositions, with detonation velocities of 6885 m/s and 7420 m/s respectively [4,33-35].

So, it is essential to create an alternative composition to resolve this dilemma to refine the above two categories of the energetic composition materials. This alternative approach should combine the high detonation characteristics of nitramine-based compositions and the low sensitivity to the external stimuli of IMX-101 and IMX-104.

1.3 Originality and impact

Researchers are now exploring alternative technologies to synthesis the NTO explosive materials instead of the traditional techniques due to the dangers and risks related to these traditional techniques [36]. In that manner, we wish to develop a novel approach for the synthesis of NTO. A novel approach will be employed for synthesizing NTO through the synthesis in microreactors, aimed at addressing the challenges associated with the conventional methods. These microreactors offer distinct advantages, enabling precise regulation of reaction temperatures and enhancing process safety. In this methodology, we will systematically vary parameters such as, solvent selection for1,2,4-triazol-5-one (TO) dissolution, solvent concentration and reaction time. Each of these parameters will be investigated within the microreactor to pinpoint the optimal conditions that yield the highest NTO output using microreactor flow technology. Also, we aim to develop a range of PBXs materials using the cast-cured method. These novel materials will be primarily based on NTO and GAP binder. The objective is to determine the maximum achievable explosive content in the polymer matrix that achieve a balance between high performance and reduced sensitivity. Furthermore, novel ternary composites consisting of NTO, GO, and nano- CuO embedded in the GAP matrix will be prepared and studied to evaluate the thermal, mechanical sensitivity and detonation performance of the resulting PBXs.

1.4 Dissertation objectives

The objective of this thesis is to design, synthesize, and characterize novel advanced PBXs with enhanced detonation performance, while maintaining mechanical sensitivity (impact and friction) within acceptable limits for use in IM. The study emphasizes the use of cast-cured compositions incorporating NTO as the primary intrinsically insensitive pure explosives and GAP as the energetic binder as well as the modified PBXs materials. Additionally, this research introduces a novel microreactor-based synthesis method for NTO, designed to overcome the limitations associated with traditional batch processes. This novel approach seeks to improve the safety and

thermal control of NTO synthesis. Ultimately, the research aims to produce novel PBX material with superior performance and safety profiles compared to current IMX explosives and conventional PBXs materials. The detailed objectives of this thesis are outlined in chapter 3. This chapter presents the specific objectives and research goals that guide the entire work, from the synthesis NTO explosive material via a novel microreactor based synthesis to the synthesis and characterization of advanced explosive materials, particularly through the cast cured technique to develop novel PBXs compositions for use in insensitive munitions applications.

To achieve the overall research objective, the work is organized around five goals. First, optimization of the conventional synthesis of NTO via batch and one-pot procedures. Second, a novel microreactor approach for a safer and controlled synthesis of NTO explosive material, aiming at addressing the challenges associated with the conventional methods. Third, development of novel NTO-based nanocomposites using graphene oxide and copper oxide coatings for enhanced thermal stability and reduced mechanical sensitivity. Fourth, creating an alternative technique instead of melt cast technique (IMX101-IMX104) for developing new PBXs materials based on NTO and energetic binder GAP, with systematic variation of composition and processing conditions to assess their structural, energetic performance and sensitivity characteristics.

Finally, the theoretical detonation parameters of the newly developed PBX compositions were calculated using the EXPLO5 program. In addition, a time-dependent simulation of the variable confinement cook-off test (VCCT) was carried out using COMSOL Multiphysics to assess the thermal behavior and safety of an NTO-GAP-based PBX under slow heating conditions. The detailed description of the research objectives is presented in Chapter 3.

1.5 Dissertation overview

Chapter 2 presents a literature review covering six key areas related to this work. It begins with an overview of energetic materials and PBXs from their components to production methods. It then focuses on NTO synthesis approaches, its properties, and reaction parameters. The chapter also covers the GAP binder, recent IM compositions using cast-cure and melt-cast techniques, and the role of GO in energetic materials. Finally, it discusses the use of microreactors in flow chemistry to improve safety during energetic material synthesis.

Chapter 3 presents the specific objectives of the research and the main research goals that guide the whole work, from the synthesis NTO explosive material via a novel microreactor based synthesis to the synthesis and characterization of advanced PBXs materials.

Chapter 4 presents the experimental procedures, optimization strategy, and discussion of the conventional synthesis of NTO through batch methods. This chapter focuses on identifying and evaluating key reaction parameters affecting the yield and purity of the intermediates and final product. It begins with a general overview followed by a detailed description of the materials and methods used, including the chemicals involved and the synthesis routes for TO and NTO. The results and discussion section highlights the influence of variables such as reaction time, temperature, and reagent ratios on the efficiency of TO and NTO synthesis. The data obtained from this stage particularly the optimized nitration temperature was critical for guiding the development of a new and safer method for NTO production inside the microreactor.

Chapter 5 presents a novel microreactor-based approach for the safer, more controlled, and continuous synthesis of the NTO explosive material. Building on the findings of conventional synthesis methods discussed in the previous chapter. The chapter begins with an introduction to the motivation behind using flow chemistry, followed by a detailed description of the materials and methods used in the microreactor synthesis route. The results and discussion section explores the solubility behavior of TO in various solvents, the nitration of TO under continuous flow conditions, and the successful preparation of NTO using the microreactor setup. This chapter demonstrates the potential of microreactor systems in the synthesis of high-energy materials with improved safety.

Chapter 6 presents the development of the explosive material itself based on NTO to exhibit enhanced energetic output, reduced mechanical sensitivity and controlled thermal stability through surface coating techniques. This chapter focuses on the synthesis of graphene oxide (GO) and the synthesis of NTO/GO and NTO/GO/CuO materials. The results and discussion provide comprehensive characterization of the synthesized materials. In addition, the thermal behavior, kinetic stability, heat of combustion, and mechanical sensitivity of prepared samples are evaluated.

Chapter 7 presents the development of a new composition based on NTO and GAP binder, proposing an alternative to the conventional melt-cast techniques used in IMX-101 and IMX-104 explosives. This chapter focuses on combining NTO with the energetic binder GAP to produce safer and thermally stable PBX compositions. The materials and methods section detail the

recrystallization process of NTO particles and the preparation of the composite PBXs using GAP as a binder. The results and discussion encompass morphological analysis, elemental composition, mechanical sensitivity measurements, and thermal characterization of the prepared compositions. Additionally, the chapter concludes with the calculation of detonation parameters using the EXPLO5 program to assess the performance potential of the developed PBXs compositions.

Chapter 8 presents the numerical modeling results and analysis of the slow cook-off behavior of the developed NTO-based PBX composition. A time-dependent simulation of the VCCT was performed using COMSOL Multiphysics to assess the thermal response and decomposition behavior of the explosive under slow heating conditions. The model incorporated temperature-dependent material properties and decomposition kinetics derived from differential scanning calorimetry analysis. This chapter includes temperature distribution profiles, identification of critical regions, and evaluation of the risk of thermal runaway. The simulation results provide valuable insights into the thermal stability, ignition threshold, and compliance of the PBX materials with insensitive munitions requirements.

Chapter 9 presents an integrated analysis of the experimental and simulation results obtained throughout the study. This chapter introduces key findings from the optimization of NTO synthesis by both conventional and microreactor-based methods, the development of coated NTO nanocomposites using graphene oxide and copper oxide, and the formulation of new PBX materials based on NTO and GAP binder. The impact of these modifications on thermal stability, sensitivity, and detonation performance is critically examined. Furthermore, insights from the COMSOL-based simulation of the VCCT are discussed in relation to the thermal behavior of the developed PBXs under slow heating conditions.

Finally, chapter 10 discussed the main and significant conclusions from this research and the future recommendations.

CHAPTER 2 LITERATURE REVIEW

2.1 Overview of energetic materials

Energetic materials, in the simplest terms are substances that can store chemical energy within their molecular structure and can release it rapidly when triggered by different external stimuli such as heat, shock, or electrical discharge. These materials are generally classified into several types, each of them serving specific functions and applications as illustrated in the following classification diagram. But their design goes far beyond just delivering power and make a huge detonation. From my experience in studying with energetic materials, it is clear that their design must strike a careful balance: on one hand, they must demonstrate high performance and explosive power to accomplish their intended purpose in munitions and missile system applications. On the other hand, they need to remain stable and safe over long periods of storage, handling and transportation under severe or unpredictable conditions. Additionally, they should exhibit insensitivity to external stimuli such as impact, friction, and fire, in order to minimize the risk of accidental initiation. This dual requirement means that when exploring or developing these energetic materials, we must account for both their performance characteristics during detonation and their safety characteristics [5].

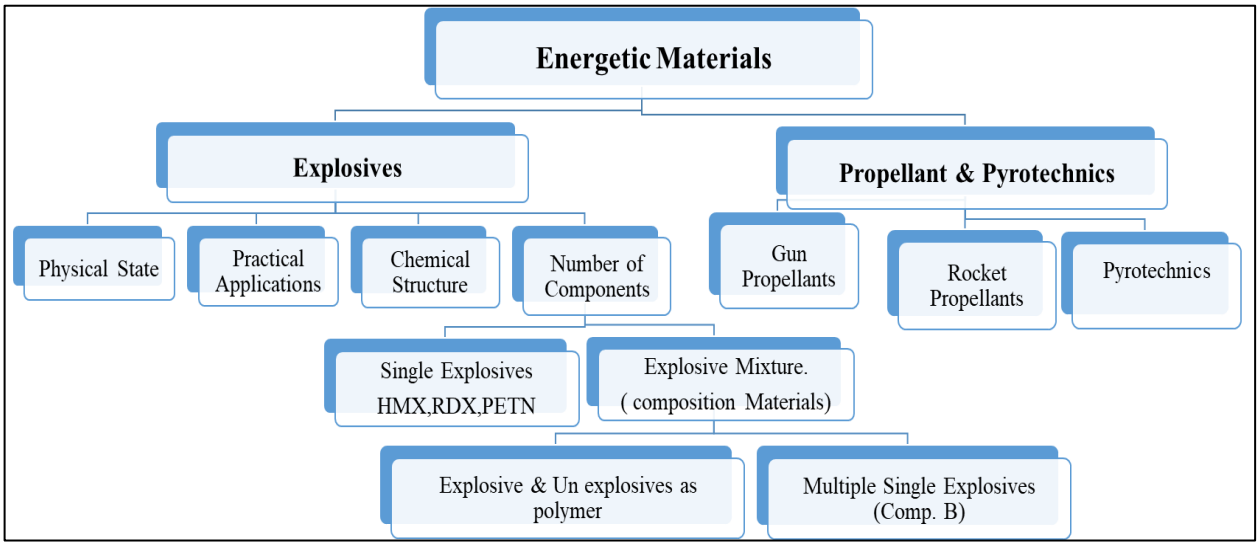

Figure 2-1 Typical classification of energetic materials.

Energetic materials can be exposed to a range of external threats such as heat, impact, and shock from different sources such as bullets, fragments, or shaped charges as illustrated in the diagram.[37]. From these threats, thermal hazards are particularly critical, especially in the design of insensitive munitions because, when these energetic materials are confined within sealed casings as they typically are in missiles or shells, they can become highly vulnerable [38]. If the released heat from slow thermal decomposition of these energetic materials accumulates faster than it can dissipate, the result can be catastrophic: rapid pressure rise, deflagration, or even full-scale detonation [39]. Thermal risks are carefully categorized into two types. Fast heating risks that mimic emergency fire scenarios like those that might erupt on a ship's deck, or in an ammunition depot [40]. Slow heating risks represent the more dangerous risk. These risks arise from the gradual heat transfer during storage of these energetic materials [41]. But heat is not the only concern. Other hazards like unexpected fragment impacts from nearby detonations, bullet strikes, or shaped charge attacks from anti-armor weapons also pose serious threats [42]. And we cannot ignore sympathetic detonations, that happen when the explosion of one munition set off others nearby [43]. Moreover, mechanical initiation from impact and friction during the storage or transfer of the ammunitions is also possible [44].

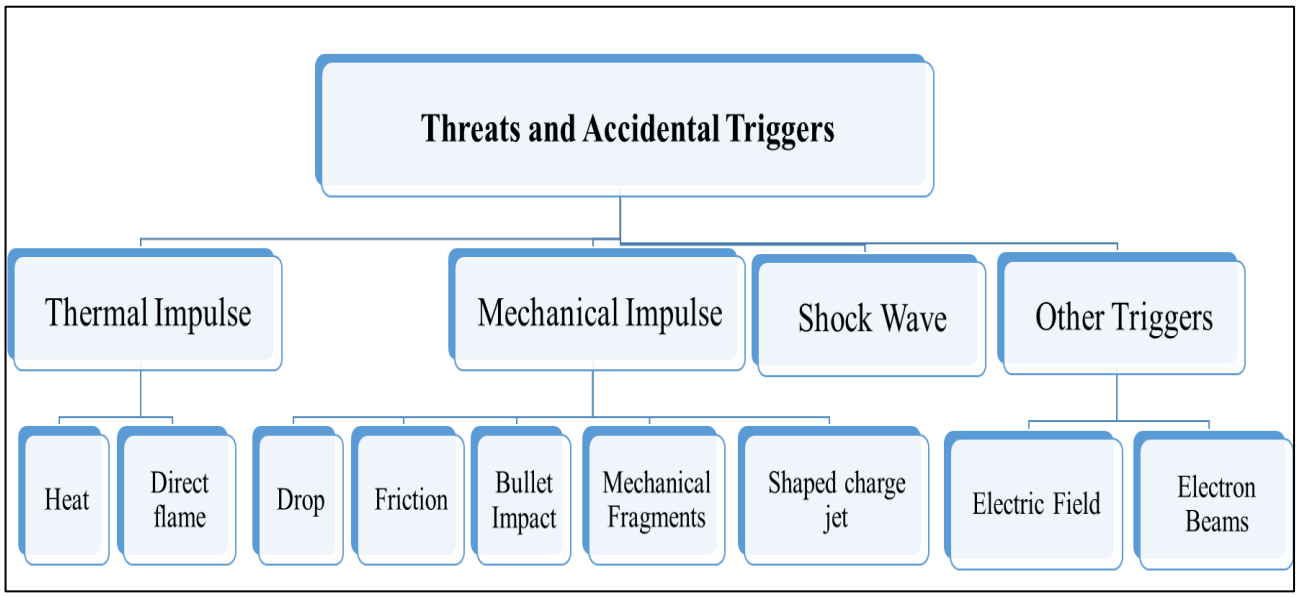

Figure 2-2 External stimuli and threats of energetic materials

The primary goal of any research in energetic materials has often been to enhance the performance characteristics of military warheads. These powerful compounds come with serious risks and dangers. This led to the attention of the concept of insensitive munitions (IM). The shift toward IM was not just a technical evolution. But it was a necessary response to the very real dangers posed by these conventional munitions that reacting violently to external stimuli like fire, impact, or shock as shown in Figure 2.3. History is full of such catastrophic incidents, and they still occur today: explosions aboard ships, in storage depots, or during transport, that often triggered by relatively minor events but have resulted in the loss of valuable assets such as aircraft, submarines, bases, and countless human lives.

Figure 2-3 Accident due to the large explosion in Lebanon in 2020 of ammonium nitrate due to unsafe and inadequate storage (Death of over 200 people and more than 6500 injuries) [45], [46].

Insensitive munitions as illustrated before are munitions that consistently fulfill performance, readiness, and operational requirements only on demand, and minimize the accidental initiation by external stimuli [3]. When designing insensitive munitions, it is essential to consider three main components: the energetic material, the casing or architecture and the packaging. But the response of the munition to various threats like bullet impact, rapid or slow heating, impact and friction stimuli primarily depends on the energetic material [47,48]. It is widely accepted that explosive components characteristics play a vital role in determining the response of an energetic material formulation. As the importance of insensitive munitions has been growing, numerous test methods and standardized protocols have been established to assess their safety and performance [49-51]. Understanding how a munition reacts to various external threats helps in safeguarding personnel

and mission platforms, and it ensures safer logistics and storage practices. One of the key evaluations for these IM are fast heating and slow heating tests. The fast-heating test involves exposing the munition to a liquid fuel fire that produces flame temperatures above 800 °C [52]. In contrast, the slow heating test is conducted in a controlled chamber, where the ammunition is heated gradually under forced convection at predefined heating rates [53].

2.2 Overview of plastic bonded explosives (PBXs).

Plastic bonded explosives (PBXs) or polymer bonded explosives are energetic material compositions consisting mainly of secondary explosives like RDX, HMX, or PETN dispersed within a rubbery matrix made of binders and plasticizers [8]. PBXs involve the binding of explosive crystals within a matrix to encapsulate the explosive particles with a protective layer to enhance its properties [54].

Compared to traditional casted TNT based explosives, PBXs overcome most of the problems that encountered casted explosives such as insufficient thermal stability, increased sensitivity with increased performance, high shrinkage after casting with the risk of large internal voids and bubbles of air that increased the sensitivity of these explosives, violent explosive reaction in a fuel fire and cracking, liquid exudation during extended storage [55].

Figure 2-4 Prima sheet 1000: a PETN-based flexible sheet explosive [56].

On the other hand, PBXs have several advantages such as excellent chemical stability and resistance to humidity, so they have increased shelf life and lower vulnerability. Also, they demonstrated lower sensitivity to various mechanical and thermal stimuli, so they are safer during handling and storage [57].

One of the key advantages of PBXs lies in their excellent mechanical properties, including high flexibility, improved toughness and resistance to cracking under mechanical stress. These characteristics make PBXs particularly suitable for different application where casted TNT-based explosives fall short of meetings the requirements. PBXs can exist in different forms as sheet explosives as shown in Figure 2-4. Also, plastic explosives that used in controlled demolitions of specific objects. These properties significantly broaden their use in both military and industrial applications [58-59].

2.3 Production methods of PBXs:

PBXs can be manufactured through different techniques including cast cured techniques, slurry, non-aqueous process, and reaction injection molding methods [60-62]. The selection of the production technique is depended upon several factors; the most important one is the application of the PBXs materials.

2.3.1 Cast cured technique

PBXs materials incorporating polyurethane binders derived from hydroxy terminated prepolymers like hydroxyl-terminated polybutadiene (HTPB), glycidyl azide polymer (GAP), bis azidomethyl oxetane (BAMO), and similar compounds are manufactured using the cast cured method. Figure 2-5 illustrates the casting cured technique for PBXs production [63]. The production process of these PBXs materials can be divided into four keys steps:

(a) Prepolymer preparation and powder treatment.

(b) Mixing of the ingredients under vacuum.

(c) Addition of crosslinking agent.

(d) Casting and subsequent curing at constant temperature.

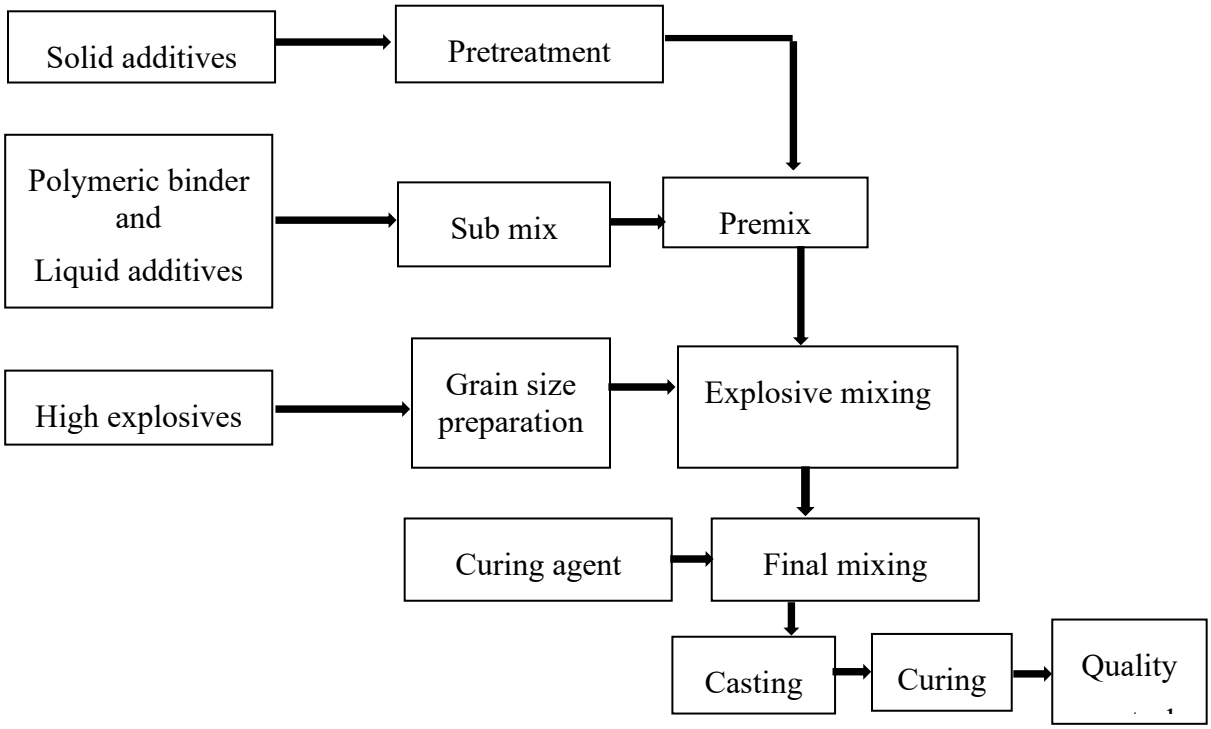

Figure 2-5 Block diagram of casting technique for PBX production [63].

2.3.2 Reaction injection molding (RIM)

RIM involves the rapid mixing of reactive liquid components as a polyol component including HTPB or GAP polymer and isocyanate components as hexamethylene diisocyanate (HMDI) or toluene diisocyanate (TDI) which are immediately injected into a mold containing the explosive materials. The polymerization and curing occur inside the mold, forming composite PBXs [64]. Although RIM is a feasible method for producing PBX materials, it has not been widely adopted in the energetic materials industry. This is primarily due to safety concerns, process complexity. A schematic representation of an RIM process is shown in Figure 2-6.

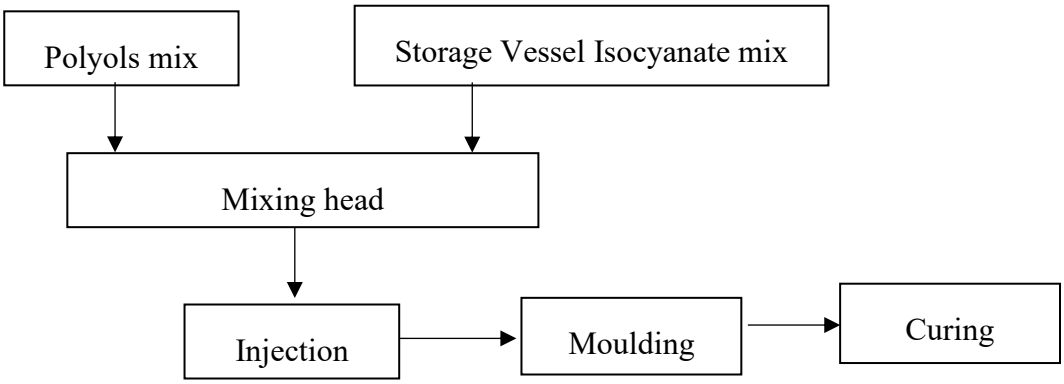

Figure 2-6 A schematic representation of an RIM process [64].

2.3.3 Slurry technique

Slurry technique involves dispersing the explosive materials into inert, non solvent liquid medium commonly water or any other solvent to reduce their sensitivity during mixing. Then, the binder typically dissolved in organic solvent with curing agent, then all added slowly to the slurry under controlled agitation. By using heat, air sweep, and slight vacuum to remove the solvent. The coated explosive agglomerates, which are then filtered and dried to create molding powder [65]. Figure 2-7 illustrates the slurry technique for PBXs production.

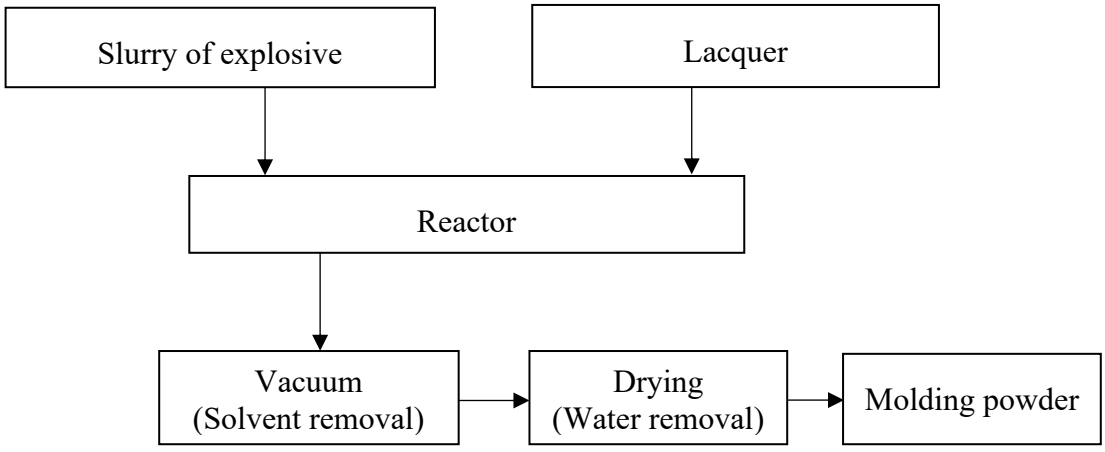

Figure 2-7 Water slurry technique for production of PBXs [65].

2.3.4 Non-aqueous process

When working with moisture-sensitive explosive as HMX, hexa-nitro-hexa-azaisowurtzitane (CL-20), a non aqueous method is often used in which the dry explosive materials are mixed with polymer binder that dissolved in an organic solvent and with isocyanates under controlled condition. The mixture is gentle stirred and shaped into molds [66]. Figure 2-8 illustrates the steps of non-aqueous process for PBXs production.

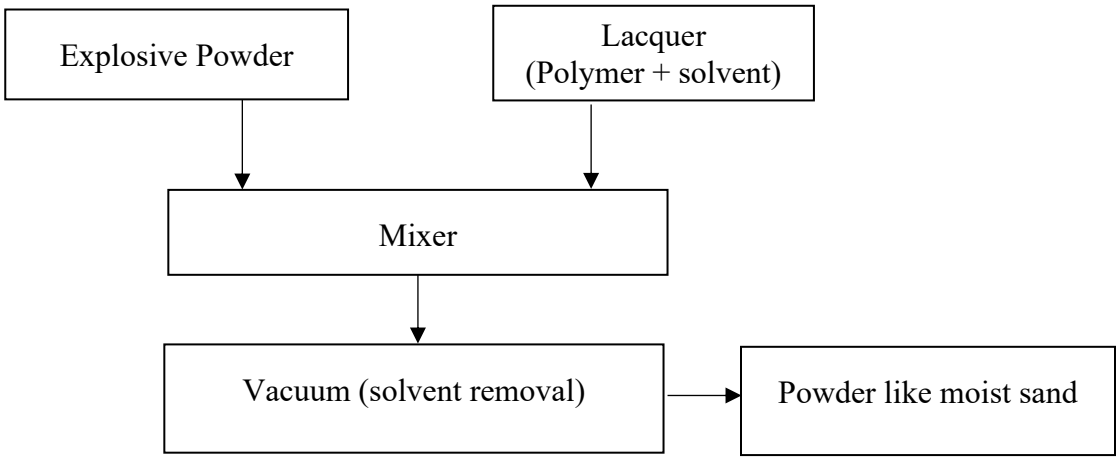

Figure 2-8 non-aqueous process for production of PBXs [66].

2.4 Main ingredients of PBXs

PBXs is a composite material comprising solid explosive particles dispersed within a polymeric matrix. Additional minor additives, including plasticizers, catalysts, curing agents, emulsifiers, dispersing agents, anti-freezers and wetting agents, are incorporated [67]. The typical components of PBXs and their respective functions are detailed in Table 2-1.

2.4.1 Plasticizers

A plasticizer is incorporated into the energetic materials to decrease the viscosity of the mixture, make the mixing and casting easier and to increase its workability, flexibility and lower the glass transition temperature (Tg) of the polymer binder [68]. Plasticizers can be energetic or non-energetic (inert) just as their polymeric counterparts. Some of the important plasticizers are Dioctyl azelate (DOZ), Dioctyl sebasate (DOS) and Dioctyl adipate (DOA) [69].

2.4.2 Curing agents

Curing agent plays a crucial role in transforming the plastic binder into a solid, coherent, and mechanically stable matrix as it effectively holds together the explosive particles within the plastic matrix. This process of curing, also known as cross-linking or polymerization. This enhances the mechanical properties and stability of the explosive material, also it improved thermal stability making it suitable for various applications. Some of the important curing agents are toluene diisocyanate (TDI) and hexamethylene diisocyanate (HMDI) [70].

Table 2-1 Main components of PBXs [67].

No.	Component	Examples	Function
1	High Explosives	RDX, HMX, PETN, TATB, NTO, etc.	To produce high detonation velocity, high brisance, and high heat of explosion.
2	Polymeric Binder	-Thermoplastic: (Poly-isobutylene, etc.) -Thermoset: (Polyurethane, etc.)	To reduce sensitivity and provide a wide range of mechanical properties.
3	Plasticizers	- Dioctyl azelate. (DOZ) - Dioctyl adiapate (DOA)	To increase flexibility, reduce melt viscosity, improve mechanical properties and lower the glass transition temperature (Tg) of the polymer binder.
4	Bonding agent	- Tris-1-(2-methylaziridinyl) phosphine oxide (MAPO)	To prevent settling of solid ingredients.
5	Curing agent	-Hexamethylene-diisocyanate (HMDI) -Toluene diisocyanate (TDI)	To induce polymerization.
6	Accelerators	- Cobalt naphthenate	To increase the polymerization rate.
7	Additives	- Dispersing agent, and wetting agent.	To facilitate better wetting of the filler particles by the polymeric binder.

2.4.3 Polymeric binders

Binders are cross-linked polymers that create a matrix that binding the solid materials of explosives together, with the addition of plasticizers to facilitate the processing of uncured mixture and modify the mechanical properties of the final energetic materials [71]. In the context of explosives, the polymer function as a protective coating around explosive crystals that preventing direct contact between crystals and thereby reducing sensitivity to various mechanical stimuli. This preventive measure minimizes the risk of hot spot ignition caused by frictional heating [72]. Then, they play a crucial role in decreasing the sensitivity of explosive materials to impact and friction. As they have the ability to absorb and dissipate energy from potentially hazardous stimuli, making them ideal for applications in insensitive ammunitions [73]. Also, thermoplastic polymers are incorporated into plastic explosives due to their melt processability and flexibility such as polystyrene, polyethylene that provide good mechanical toughness, straightforward processing and reliable compatibility to energetic crystals. Their ability to melt and flow allows uniform coating of crystals at relatively low temperatures and offers greater ductility than thermosetting binders. Various polymeric materials, both energetic and non energetic, have been incorporated into PBX compositions to improve their mechanical strength, thermal stability and processing behavior.

Yu et al. reported the preparation of CL-20-based PBXs materials using non-energetic binders such as fluorine resin (FPM) polyurethane, and cis-butadiene rubber. His results confirmed that FPM demonstrated superior performance, achieving a characteristic drop height of 28 cm compared to 15 cm for pure CL-20, and reducing the friction explosion probability from 100% to 70%. These results confirmed an improvement in mechanical sensitivity and thermal stability without significantly affecting the decomposition temperature [74]. Liao et al. [75] reported the coating of CL-20 using polyurethane resulting in reduction in its mechanical sensitivity. Similarly, Lan et al. [76] studied several CL-20-based PBXs materials and found the addition of RGO increased the thermal stability of the CL-20- based PBXs with 551 glue binder. Another recent attempt at the beginning of 2025 was reported by Gao et al. [77] who investigated CL- 20/NTO -based PBXs materials aiming to achieve a balance between high energetic performance and improved safety. In his work, two non-energetic binders, cellulose acetate butyrate (CAB) and fluor elastomer (F2603) were used. They reported that the CAB-based PBXs demonstrated enhanced thermal

stability, lower sensitivity and higher detonation velocity that suggesting it to be a more promising candidate for safer high-performance explosive application.

However, further development is still required to adapt such new energetic materials for use in LOVA-type applications, where both performance and insensitivity must be simultaneously optimized.

As presented in Table 2-2, a wide range of PBXs materials have been developed globally, relying on different types of inert polymers such as HTPB, Estane, and Viton in combination with different high explosives including RDX, PETN, HMX, and TATB. These PBXs materials represent traditional PBXs systems. Despite their high detonation performance with detonation velocities approximately approaching 8000 m/s, they still require further development. In particular, their mechanical sensitivity (impact and friction) remains a limiting factor for their use in insensitive ammunitions applications [78-82]. Therefore, there is a clear need to enhance the insensitivity characteristics of these systems while maintaining or improving their energetic performance.

However, increasing the polymer content in PBXs materials to enhance safety and reduce sensitivity (impact and friction) typically leads to a reduction in overall energetic performance, because inert binders do not contribute to the energy output. Therefore, achieving a PBX material that combines high detonation performance with low sensitivity during storage and handling remains a critical challenge in the field of energetic materials. A promising trend to address this limitation involves the substitution of inert binders with energetic polymeric binders such as GAP and poly BAMO. These binders not only provide the required mechanical properties and processability but also contribute significantly to the total energy that released from the whole material of PBX, thereby enabling the design of PBXs with both enhanced performance and improved safety characteristics.

Table 2-2 Typical PBXs materials based on different high explosives [78-82]

Name	Compositions	Velocity of detonation m/s	Application
C- 4	91% RDX / plasticizer/Binder /Mineral Oil	8100 / ρ = 1.65 g/cm^3	Demolition and old weapons
Semtex H	41.2% RDX / 40.9% PETN / plasticizer Antioxidant / Binder	7568 / ρ = 1.6 g/cm^3	Old weapons
Comp. A	91% RDX / wax	8470 /ρ = 1.61 g/cm^3	Main charges in land mines & rockets
HEXOWAX	RDX / Wax or Binder	8350 / ρ =1.71 g/cm^3	Pressed composition for main charges and boosters
PBX 9007	RDX / Polystyrene / DOP	8009 / ρ = 1.66 g/cm^3	Weapons
PBX 9010	RDX, Kel-F 3700	8370 / ρ = 1.79 g/cm^3	Nuclear weapons
PBXN-3	RDX / nylon	-	Missiles
PBXW-17	RDX / Polyacrylate	8100 / ρ =1. 66 g/cm^3	Pressed composition for shaped charges and boosters
EDC-29	95% HMX / 5% HTPB	-	UK composition
EDC-37	91% HMX / NC	-	-
LX-04-1	85% HMX / 15% Viton-A	8046 / ρ = 1.86 g/cm^3	Nuclear weapon
PBX 9011	90% HMX, 10% Estane	8500 /ρ = 1.77 g/cm^3	Nuclear weapons
PBXN-5	95% HMX and 5% Viton	8800 /ρ = 1.86 g/cm^3	Pressed composition for boosters
OCTOWAX	HMX / Wax or Viton	8850 /ρ= 1.78 g/cm^3	Pressed composition for high performance warheads and
PBX-9502	95% TATB+ KelF 800 5%	-	Main-charge explosive with very low explosiveness and shock
RX-26-AF	TATB+ HMX +Estane	-	Main charge explosive but increased shock sensitivity

2.4.3.1 Glycidyl azide polymer (GAP)

Glycidyl azide polymer (GAP) is an energetic azide polymer characterized by the presence of N_3 groups in its molecular structure (high nitrogen content). It is a hydroxyl-terminated polyether featuring pendant alkyl azide groups. It consists of a polyethylene oxide backbone with azidomethyl groups replacing nitromethyl groups [23, 83-86] as shown in Figure 2-9. GAP stands out as a promising polymer due to its low molecular weight and acts also as an energetic plasticizer in advanced solid gun propellants [87]. GAP remains non-sensitive to mechanical stimuli and yields a higher proportion of low molecular weight combustion products like CO, H_2, and N_2, rather than CO_2 and H_2O [23]. The energetic properties of GAP arise from the chain scission of the azide group, leading to the production of nitrogen gas with a high heat of reaction, rather than the oxidation products. The exothermic decomposition of GAP occurring at temperatures ranging from 202 to 277 °C that accompanied by a 40% weight loss [86]. GAP exhibits a low glass transition temperature of - 45 °C and a minimal percentage of polymer weight-bearing chains that making it an energetically favorable binder system [23,87]. GAP of Mwt 500-1000 is used as an energetic plasticizer while GAP of Mwt 1500:6000 is used as a prepolymer to produce PBXs materials and composite soild rocket propellant (CSRP) using casting technique [88].

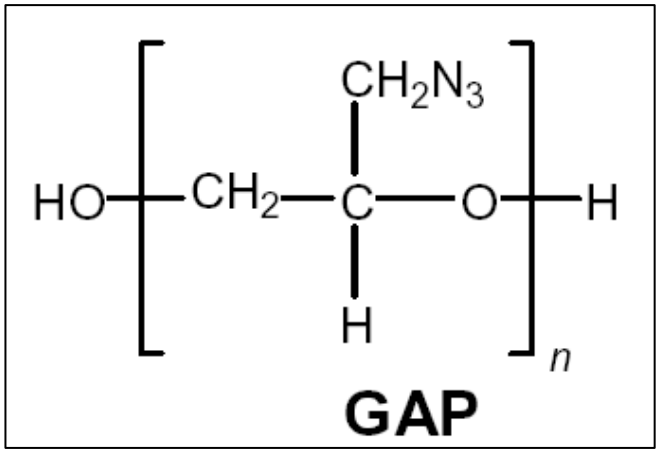

Figure 2-9 Structure of Glycidyl azide polymer [85].

Elbeih et al. reported the preparation of different PBXs materials based on GAP with several nitramine explosives including cis 1,3,4,6-tetranitrooctahydroimidazo-4,5-dimidazole (BCHMX), CL-20, and HMX. The study demonstrated that incorporating GAP led to increase in energetic performance, as the heat of explosion was observed to be 1.13-1.16 times higher compared to traditional PBXs materials using HTPB. Also, the CL-20/GAP achieved the highest experimental detonation velocity that reaching 8676 m/s. On the other hand, its desensitizing effect was found to be slightly lower than that of HTPB because the impact sensitivity remained relatively high indicating that the PBXs materials were still sensitive despite improved energy output [89].

Wei Yanju et al. prepared GAP/CL-20 based PBXs material for use in initiation systems to prepare a booster explosive containing 82 wt.% CL-20. The material was successfully cast into initiation grooves. This study determined that when the charge density reached 1.68 g/cm^3, the detonation velocity reached 7290 m/s. In addition to its high performance, the GAP/CL-20 material showed low mechanical and shock sensitivity that with a drop height of 38.2 cm and a card gap of 7.74 mm, making the martial GAP/CL-20 a promising candidate for miniaturized booster charges in small-sized initiation networks [90].

Zeng et al. developed core-shell structured aluminized explosives by coating nano-aluminum particles with GAP with HMX. His study revealed that the use of GAP-coated aluminum in a core-shell structure significantly improved dispersion, mechanical strength and creep resistance. Also, the thermal decomposition of HMX was slightly advanced, and the combustion process showed more vigorous and sustained burning and the detonation velocity of the core- shell structured HMX composite with 15 wt.% of GAP-encapsulated aluminum reached 8567 m/s. The study demonstrates that the GAP shell not only stabilizes nano-aluminum but also contributes to enhanced detonation and combustion characteristics that offering a promising approach for improving aluminized explosive materials [91].

Despite the important advancements that achieved by researchers in recent years, the use of polymeric materials such as GAP and similar binders proved that the use of these polymers improved the performance characteristics and energy output of PBXs materials. This enhancement is not solely due to the decreasing the binder content in the explosive materials, but more importantly, based from the energetic nature of these polymers, which actively contribute to the overall energy release during detonation. Also, theses explosive materials maintaining acceptable

levels of mechanical sensitivity, particularly in terms of impact and friction sensitivity, as well as thermal stability when compared to their counterparts that used inert polymeric binders. However, the challenge still remains: how to preserve this high-energy potential while further improving the safety and thermal stability of the system. As the field of energetic material moves toward a new generation of PBXs, there is a clear demand for materials that offer not only superior explosive performance, but also enhanced insensitivity characteristics. This study is driven by that very need to develop PBXs material that strike a better balance between energy output and sensitivity control. In this context, the use of GAP as an energetic binder that combined with low-sensitivity explosives such as NTO can present the ideal solution to candidate new materials able to use in insensitive ammunitions. This was detailed in the following sections.

2.4.4 High explosives as the main component of PBXs

The primary components of PBXs consist of highly energetic materials, involving both conventional and insensitive explosives. These high explosives typically exist in powdered form, serving as the primary source of energy for the system. They responsible for all the explosive characteristics including high detonation velocity, detonation pressure and temperature, brisance, and elevated heat of explosion [92]. When designing IM as discussed before, it is essential to consider three main components: the energetic material, the casing or architecture and the packaging [47]. The main response of different threats like bullet impact, rapid or slow heating, impact and friction stimuli primarily depends on the energetic material properties. In many cases, these materials are composed of different compounds rather than single substances. Therefore, the exploration of novel energetic compounds and mixtures serves as a driving force for many scientists and researchers. Here, we will discuss some of these energetic materials.

2.4.4.1 PBXs materials based on RDX

RDX (1,3,5-trinitro-1,3,5-triazinane) or hexogen, stands as the most crucial military high explosive in the world. RDX has both military and civil applications. It has important features including, high detonation velocity and temperature. Also, stable in storage. One of the most powerful and effective military high explosives is Semtex H, which consists of a mixture of RDX and PETN [93]. Several typical PBXs materials are detailed in Table 2-3.

Table 2-3 Typical PBXs materials based on RDX [79-81,93,94]

Name	Compositions	Velocity of detonation m/s	Application
C- 4	91% RDX / plasticizer/Binder /Mineral Oil	8100 / ρ = 1.65 g/cm^3	Demolition and old weapons
Semtex H	41.2% RDX / 40.9% PETN / plasticizer Antioxidant / Binder	7568 / ρ = 1.6 g/cm^3	Old weapons
Comp. A	91% RDX / wax	8470 /ρ = 1.61 g/cm^3	Main charges in land mines & rockets
Comp. C	RDX/polyisobutylene/ethylhexyl sebacate/ motor oil	-	Loading in shaped charges of warheads
HEXOWAX	RDX / Wax or Binder	8350 / ρ =1.71 g/cm^3	Pressed composition for main charges and
PBX 9007	RDX / Polystyrene / DOP	8009 / ρ = 1.66 g/cm^3	Weapons
PBX 9010	RDX, Kel-F 3700	8370 / ρ = 1.79	Nuclear weapons
PBXN-3	RDX / nylon	-	Missiles
PBXW-17	RDX / Polyacrylate	8100 / ρ =1. 66 g/cm^3	Pressed composition for shaped charges
PBX 9604	RDX / Kel-F 800	-	Not clear

2.4.4.2 PBXs materials based on HMX

HMX (1,3,5,7-tetranitro-1,3,5,7-tetrazocane) or octogen explosive consider also one of the significant secondary high explosives. Its detonation velocity is higher than RDX explosive compound that reached to 9100 m/s at density approximately 1.92 g/cm^3. The only two high explosives known to us that surpass the performance of HMX are CL-20 and octa-nitro-cubane (ONC). However, their synthesis is significantly more expensive. In particular, the production of CL-20 is much cost than that of HMX due to its multi-step synthesis process that requires the use of expensive catalysts [95]. Therefore, HMX stands out as a key energetic option capable of enhancing weapon performance. Table 2-4 illustrates several typical PBXs materials incorporating HMX.

Table 2-4 Typical PBXs materials based on HMX [80,95,96]

Name	Compositions	Velocity of detonation m/s	Application
EDC-29	95% HMX / 5% HTPB	-	UK composition
EDC-37	91% HMX / NC	-	-
LX-04-1	85% HMX / 15% Viton	8046 $\rho = 1.86$ g/cm^3	Nuclear weapon
LX-09-0	93% HMX / 4.6% BDNPA / 2.4% FEFO	-	Nuclear weapon
PBXN-5	95% HMX and 5% Viton	8800 $\rho = 1.86$ g/cm^3	Pressed composition for boosters
PBX 9011	90% HMX, 10% Estane	8500 $\rho = 1.77$ g/cm^3	Nuclear weapons
PBX9404	94% HMX / 3% NC / 3% CEF	8800 $\rho = 1.83$ g/cm^3	Naval shells
PBXN-3	HMX / Nylon	8370 $\rho = 1.73$ g/cm^3	High performance compositions for different
OCTOWAX	HMX / Wax or Viton	8850 $\rho = 1.78$ g/cm^3	Pressed composition for high performance warheads and
HMX/GAP	84%HMX /16%GAP	8384 $\rho = 1.64$ g/cm^3	High performance compositions

2.4.4.3 PBXs materials based on TATB

TATB (1,3,5-triamino-2,4,6-trinitrobenzene) is a high explosive known for its exceptional thermal and mechanical stability. TATB readily forms in many eutectic mixtures with other explosives materials including HMX, RDX, etc., TATB is widely regarded as one of the most thermally stable insensitive explosives available. Despite containing reactive amino groups, it exhibits far greater thermal and chemical stability compared to conventional nitroaromatic compounds. It is widely used in insensitive munitions due to its extremely low sensitivity to shock, friction, and heat [97]. Several PBXs materials based on TATB have been reported as main-charge explosive are summarized Table 2-5.

Table 2-5 Typical PBXs materials based on TATB [80,94,96,97]

Name	TATB	Other ingredients	Binder	Application
PBX-9502	95%	-	5% KelF 800	Main-charge explosive with very low explosiveness and shock sensitivity.
RX-26-AF	46.6%	49.3% HMX	4.1% Estane	Main charge explosive but increased shock sensitivity.
PBX-9503	80%,	15% HMX	5% Kel-F800	Booster.
PBXW-7	60%,	35% RDX	5% PTFE	Booster formulation with sufficient shock sensitivity.
BX3	60%	90% RDX / 10% HMX	5% Kel-F800	Booster formulation with cook-off resistant and sufficiently shock sensitive.

2.4.4.4 PBXs materials based on CL-20 (HNIW)

Hexanitrohexaazaisowurtzitane (CL-20) is a relatively advanced nitramine-based high explosive that offering approximately 20% greater energy output than HMX. CL-20 remains known for its high sensitivity as the reported impact sensitivity values ranging between 2.0 and 4.5 J. Then, many researchers classifying it as a high-performance explosive but sensitive explosive. CL-20 has potential applications across both military and civilian applications. The main drawback of its widespread use related to its cost, particularly its high production cost. To date, large-scale manufacturing remains a significant challenge, preventing CL-20 from replacing more cost-effective explosives like HMX or RDX in practical applications [98,99].

In recent decades, the use of traditional PBXs materials alone has proven insufficient in addressing significant challenges related to ammunition storage, transportation and handling where energetic materials are regularly subjected to extreme conditions. Moreover, ensuring protection against accidental initiation of the energetic materials such as immunity to fire and resistance to bullet impact has become a crucial priority. Hence, researches are focusing on explosives with high detonation characteristics and minimal sensitivity. Then, it is essential to use intrinsically low-sensitivity explosives in order to achieve the required level of safety.

2.5 3-Nitro-l,2,4-triazol-5-one (NTO)

NTO is one of the intrinsically low sensitive explosives used in PBX compositions. Its excellent resistance to friction and impact makes it highly suitable for IM and for use in propellant applications.

2.5.1 General properties of NTO

NTO is a heterocyclic compound having four nitrogen atoms. It has various nomenclature such as Oxynitrotriazole (ONTA) or 5-nitro-1,2,4-triazol-3-one, 3-nitro-1,2,4- triazol-5-one (NTO). It is a white crystalline solid that undergoes direct decomposition without melting. NTO explosive particles dissolved in water forming a yellow solution. It has acidic nature with a pK value of 3.67 [100]. Table 2-6 provides various properties of NTO.

Table 2-6 Properties of NTO explosive material [14,26,27,100-105]

N	Property	Information
1	Nomenclature	3-Nitro-1,2,4-triazole-5-one, 5-Nitro-1,2,4-triazole-3-one, 5-oxy-3-nitro-1,2,4-triazole (ONTA), Nitrotriazolone.
2	Empirical formula	$C_2H_2N_4O_3$
3	Molecular weight	130 g/mol
4	Crystal Density	1.93 (α-NTO), 1.87 (β -NTO) g/cm^3
5	Chemical structure	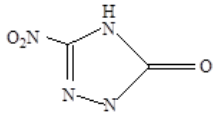
6	Decomposition temperature	253-279 °C (depending on purity and experimental conditions used)
7	Acidity	3.67 pKa
8	Crystal polymorphs	Two forms (α and β form)
9	Oxygen balance	-24.60 %
10	IR spectrum	NH: 3212, C=O: 1714, NO: 1547 cm^{-1}
11	Raman IR spectrum	1361 and 1329 cm^{-1}
12	Near IR spectrum	6250 and 4550 cm^{-1}
13	NMR Spectrum ppm	^{1}H :13.5 (H—N adjacent NO_2 and 12.8 (DMSO-d_6) ^{13}C: 154.4 (C—O and 148.0(C—NO_2) (DMSO-d_6) ^{14}N: -34.5.5 (H—N, -112.9 (N—H, -205.4, -207.4, -243.9)
14	Solubility	Soluble in: Water, Acetone, Acetonitrile, Dioxin, DMF and DMSO Restricted solubility: Toluene, Chloroform, Diethyl ether Insoluble: Dichloromethane
15	DTA exotherm	>236, 264 °C
16	Recrystallizes from	Water: large, Jagged, Rod-like crystals. Methanol and Ethanol: Spheroidal NTO
17	Toxicity	NTO and TO are non-toxic to mice, rats.
18	Vacuum stability is good	No detectable gas evolution at 120 C for 40 hours. Releasing 0.06 cm^3/g in 20 h at 110 °C. Releasing 1.45 cm^3/g in 193 h at 100 °C.
19	Impact sensitivity	Julius peter Apparatus CSI test 22 J, US sensitivity H50: 92 cm
20	Friction	353 N
21	Detonation velocity	8510 m/s (calculated) 7990 m/s at crystal density of 1.8 (g /cm^3).

NTO exists in two polymorphs, one of them is more stable and referred to as α-NTO, while the other is unstable and known as β-NTO which decomposes within a span of 6 months. The α-form materializes by gradually cooling a heated NTO solution in different solvents including water and subsequently refrigerating it. The resultant crystals take the shape of needles. On the other hand, β-NTO is produced via recrystallization from either methanol or ethanol solvents. Distinguishing between the α- and β-forms of NTO can be achieved using various techniques [101].

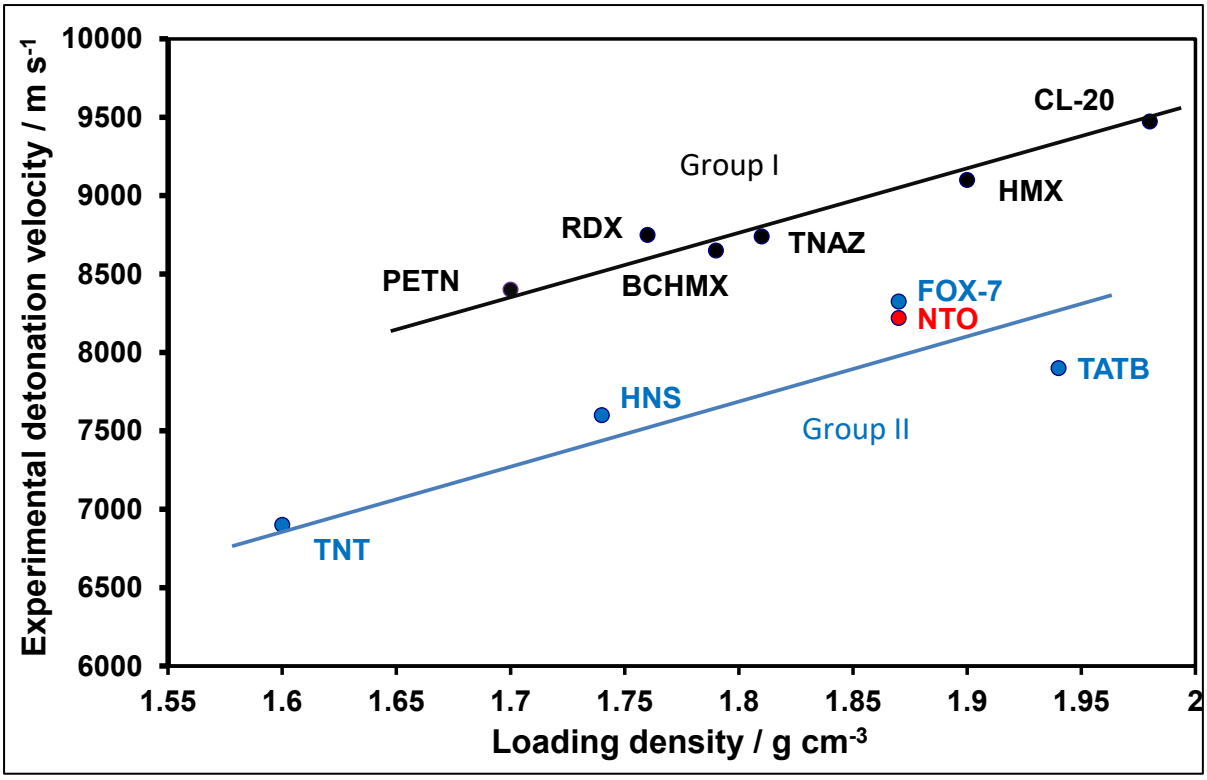

Figure 2-10 Dependence of detonation velocity on the density of explosives [106].

NTO exhibits lower sensitivity to friction and impact compared to RDX, HMX and PETN while its sensitivity is similar to TNT and TATB. However, it is slightly more sensitive to shock than TATB and less sensitive than PETN, RDX and HMX. As illustrated in Figure 2-10. Figure 2-11. illustrate the detonation velocities and sensitivity characteristics of NTO compared to other advanced and traditional explosives.

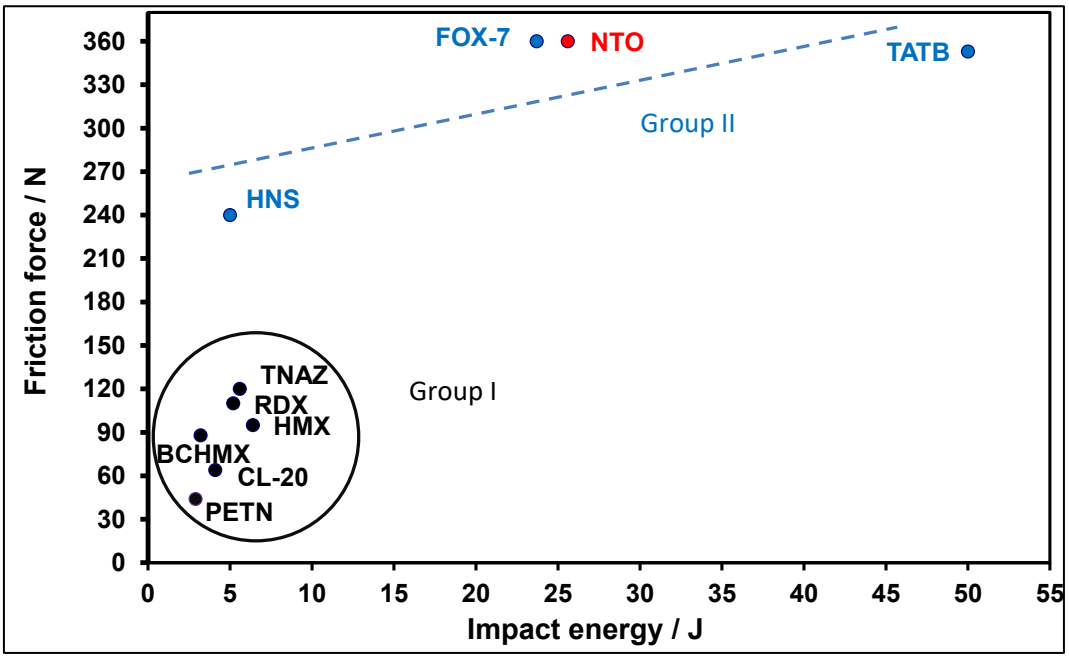

Figure 2-11 Impact energy of explosives compared with their friction force [106].

From Figure 2-10, two lines are present the detonation velocities of the explosives with respect to their densities. Group I is collecting the high-performance explosives based on their density; a linear relationship is observed; this group has explosives with high detonation velocities. Interestingly, group II is collecting explosives with high density while their detonation velocities are lower than group I. The reason of these differences might be understood using Figure 2-11. The high-performance explosives have high impact and friction sensitivities (see group I), while the explosives with lower detonation velocity appeared to be low sensitive (see group II). NTO and 1,1-diamino-2,2-dinitroethylene (FOX-7) have higher detonation velocity than both TATB and HNS. In addition, they have very low sensitivity (impact energy is higher than 20 J and friction sensitivity higher than 360 N). These figures confirm the importance of both NTO and FOX-7 as low sensitive explosives with detonation velocities slightly lower than the traditional explosives (RDX and PETN). Nevertheless, NTO also has some drawbacks; its acidic nature, negative enthalpy, high water solubility, large critical diameter for uniform detonation, poor adsorption affinity, and incomplete degradation in soils. These features have resulted in environmental concerns and potential toxic effects when exposed to high concentrations of NTO.

2.5.2 Synthesis of NTO

Several synthesis strategies have been adopted to improve the yield and the reaction process of NTO. It was found that the most common strategy to produce NTO depends on a two steps method. The first step is the formation of the intermediate 1,2,4-triazol-5-one (TO) and then the second step is the nitration using nitrating agent to obtain NTO explosive materials. The following sections compares the different strategies of synthesizing NTO explosive. Figure 2-12 clarifies the general methods used to prepare NTO.

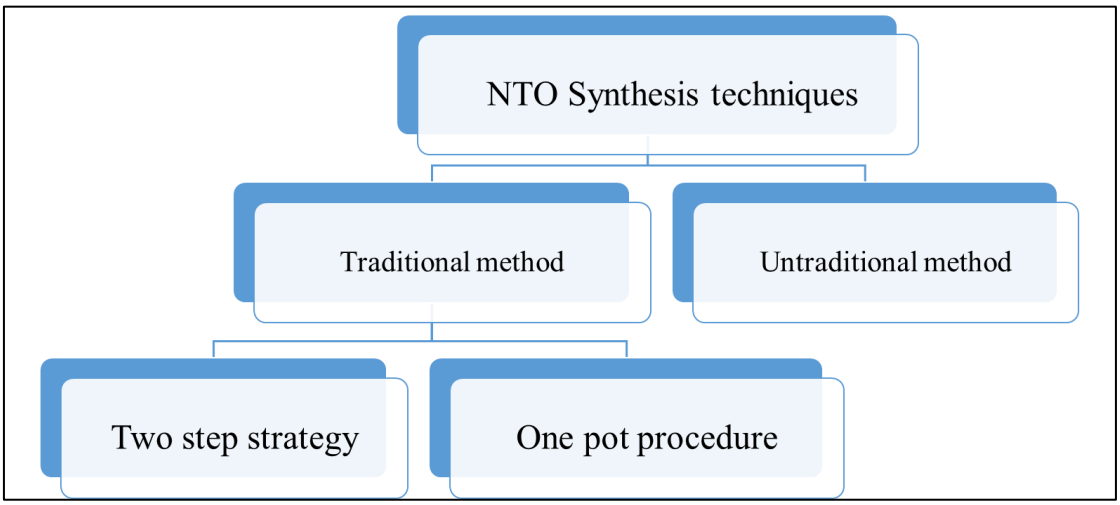

Figure 2-12 General methods used to prepare NTO.

A huge literature speak about the synthesis of NTO. The first attempt to synthesis NTO was published by Manchot and Noll in 1905 using two stages [25]. In 1966, Chipen et al. synthesized NTO and used different pathways to improve the yield (67.5%) and the purity of the NTO. They used different pathways to improve the yield and the purity of the NTO. Theses pathways include different nitrating agents and different routes to synthesis TO as illustrated in Figure 2-13 [27]. Lee and Cobura [26,107] succeeded in synthesis of NTO directly without separating the intermediate TO and they published the first report of NTO as an explosive material in 1985. Spears et al. [36] have tried to optimize several parameters which affect the yield and purity of NTO reporting a yield of NTO (77%). Becuwe and Delclos [108] improved the yielding of NTO up to 80%. While Smith and Cliff [14] synthesized NTO through a one-pot synthesis route reporting a yield of 77% for NTO. Saikia group [29] was the first group to use an unconventional heating source (microwaves) to produce NTO. This process significantly improved the nitration step and reducing

the time of nitration from 120 min. to just 10 min. Deshmukh and his group [109] explored an alternative nitrating mixture instead of nitric acid in 2014. The researchers utilized a nitrating system composed of cyclodextrin nitrate (CDN) and H_2SO_4 reporting a yield 88% of pure NTO. In 2014, Saikia explored a novel approach to synthesize NTO using metal nitrates instead of traditional nitric acid. This change was motivated by the negative environmental impact associated with nitric acid usage. The employed metal nitrates were sodium nitrate ($NaNO_3$), potassium nitrate (KNO_3) and silver nitrate ($AgNO_3$). The authors combined these materials with H_2SO_4 to form the nitrating mixture. The highest obtained yield of NTO was approximately 80% when they utilized $AgNO_3$ [28].

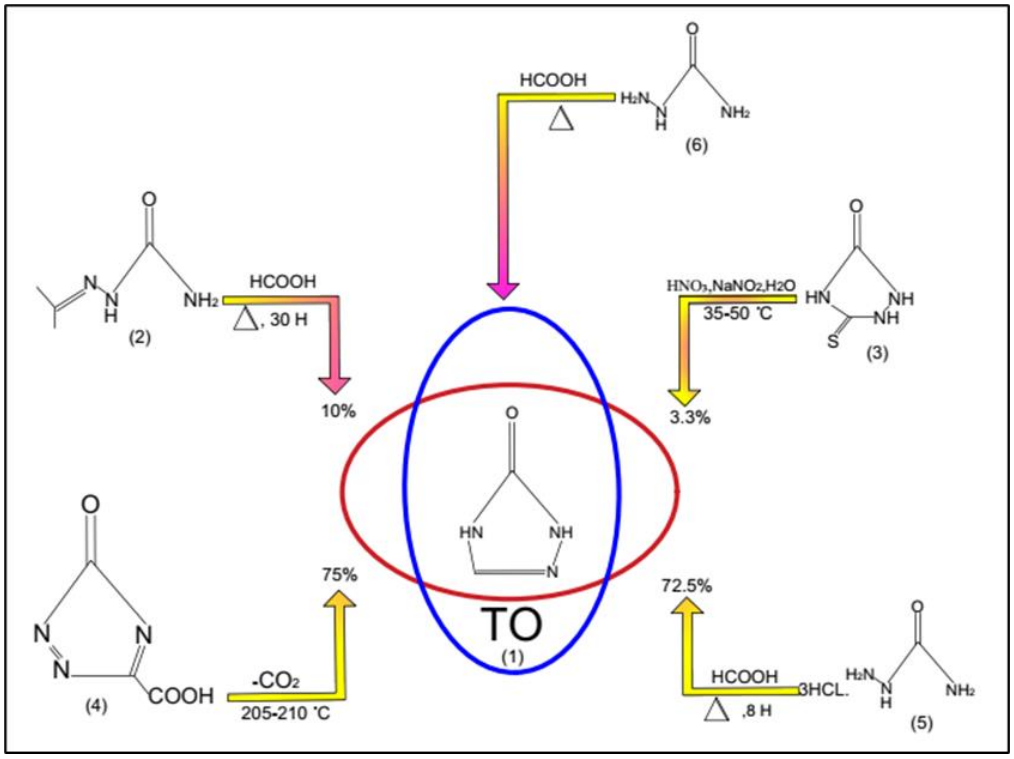

Figure 2-13 Synthesis paths of (1): 1,2,4-triazol-5-one (TO). (2) : acetone semi-carbazone, (3) Monothiourazole, (4): 3-oxo-3H-1,2,4 triazole-5-carboxylic acid, (5) : Semicarbazide hydrochloride, (6): Semicarbazide [27].

2.5.3 The optimum conditions for synthesis NTO

Based on the literature on NTO synthesis, researchers have found that the yield and purity of NTO are influenced by several factors such as reactants concentrations, reaction temperature, contact time of the reactants, the method of TO separation and nitrating agents as illustrated in Figure 2-14. These parameters can be optimized through the following sectors [26,27,36,108].

The Chipen group determined that the highest yield was achieved when reacting semi carbazide hydrochloride with an excess of 85% formic acid with a molar ratio of 1.0:2.5. And the most effective nitration agent was 75% nitric acid resulting in approximately 67.5% yield of NTO using the specific procedure outlined in their study [27]. The effective yield (70% TO) was achieved when using semicabazide hydrochloride in the reactions compared to only 35% yield when using semicabazide. Also, the presence of water did not impact the (TO) yield significantly, it helped to homogenize the mixture of semicabazide hydrochloride with formic acid. A nitration ratio of 5 moles of HNO_3 per mole of (TO) was preferred while starting the nitration process at a temperature close to 0 °C was recommended due to the highly exothermic nature of triazolone dissolution in nitric acid [26].

The optimal temperature for the nitration process was found to be 65 °C with a reaction time of 1.5 hours using a mixture of concentrated nitric acid and concentrated sulfuric acid resulted in a maximum yield of approximately 77%. The excessively high temperatures exceeding 100 °C during nitration led to poor NTO yield. Likewise, performing nitration at a lower temperature of 59 °C led to a decreased conversion of NTO [36].

The addition of a small amount of concentrated nitric acid approximately (0.05 mole per semicabazide hydrochloride) increased the TO yield by about 5%. Also, excess nitric acid (3 to 6 moles of HNO_3: 1 mole of TO) led to 82% yield of NTO when using a mixture of 60% nitric acid, 20% sulfuric acid and 20% water [110].

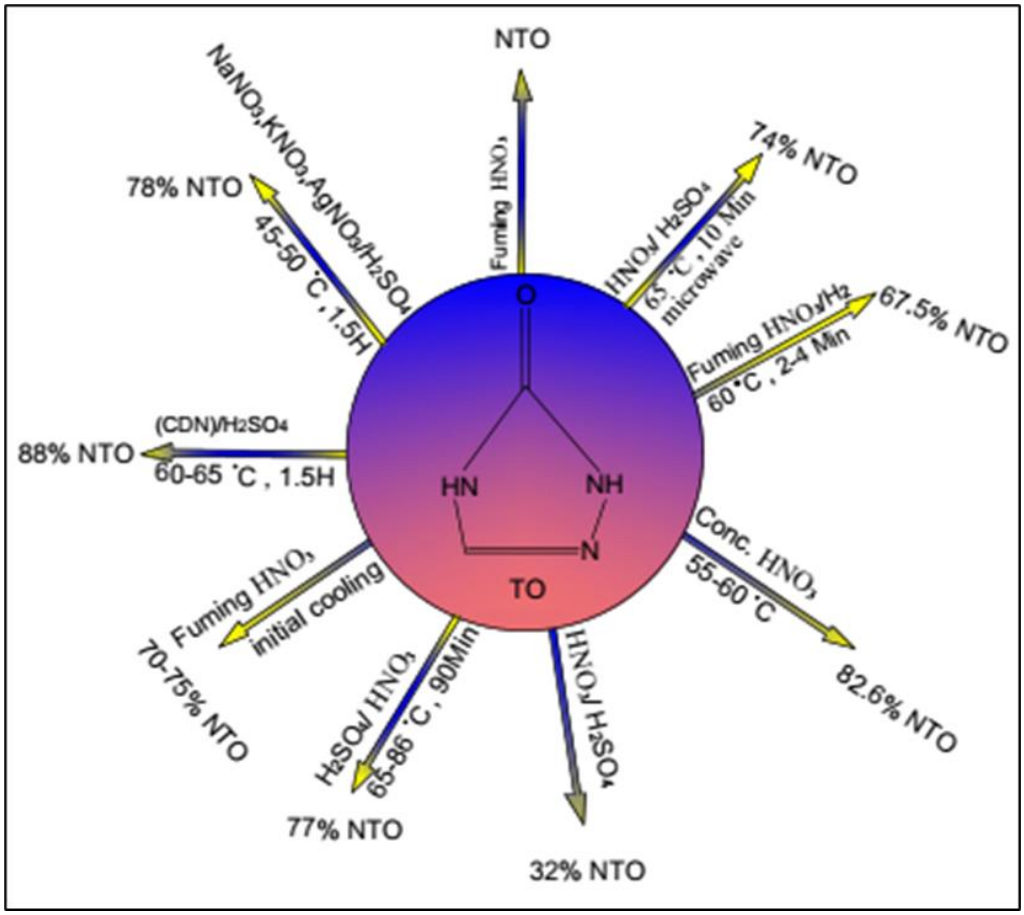

Figure 2-14 Synthesis of NTO from TO using different nitrating agent [26,27,36,107,108].

2.5.4 PBXs materials based on NTO

Various techniques are utilized to create compositions with NTO including melt casting [111], cast cured PBXs [112] and pressed PBXs [113]. Moreover, NTO and its derivatives find applications in gun propellants and rocket propellants [114-116].

2.5.4.1 Melt- cast explosives based on NTO

These compositions involve the addition of NTO particles to the explosive in a melt-phase material as TNT and DNAN. Smith and Cliff [14] have conducted a review of formulations containing TNT/NTO. Also, spyckerelle and colleagues [117] investigated formulations involving NTO/TNT/RDX/Al and the outcomes were evaluated through computational analysis utilizing CHEETAH version 2 that shown in Table 2-7.

Table 2-7 Explosives based on NTO/TNT and their properties utilizing CHEETAH [117].

Name	NTO	TNT	Additives	Binder	Density (g/cm^3)	Velocity of Detonation (m/s)
ONTALITE	50	50	-	-	1.7773	7630
ONTALITE	65	35	-	-	1.812	7885
ONTALITE	60	35	5 (RDX)	-	1.807	7908
ONTALITE	55	35	10 (RDX)	-	1.802	7930
ONTALITE	40	30	20 (AL)	10 (Wax)	1.744	6606
ONTALITE	34	30	20 (AL) + 6 (RDX)	10 (Wax)	1.738	6637
ONTALITE	28	30	20(AL) + 12 (RDX)	10 (Wax)	-	-

Nexter Munitions in France recently developed a melt-cast explosive named XF®13333 [118]. This explosive is based on NTO and comprises 31% TNT, 48% NTO,7.5% wax and 13.5% Al. It was specifically designed for the new 155 mm LU211 artillery shell and it successfully passed all the tests outlined in STANAG 4439 [3].

Trzcinski and his research group also [119] conducted a study on melt pour compositions consisting of 40% DNAN, 20% RDX and 40% NTO in melt casting. The impact sensitivity of the formulation was determined to be 25 J. The detonation velocity was measured to be around 7040 ± 50 m/s for a density of 1.64 g/cm^3 (in a copper tube with a 25 mm diameter) and approximately 7190 ± 200 m/s for an unconfined charge (with a 40 mm diameter). The detonation pressure recorded was 22.0 GPa, and the computed Gurney energy amounted to 2.85 MJ/kg.

A widely used insensitive formulation in the U.S. Army today is IMX-101 [4] developed by BAE Systems at the Holston Army Ammunition Plant (HSAAP). IMX-101 has been approved as a viable candidate to substitute TNT in filling 155 mm M795 and 105 mm M1 projectiles. It consists of 43.5% 2,4-dinitroanisole (DNAN), 19.7% NTO and 36.8% nitroguanidine. IMX-104 [4] has also been identified as a fitting substitute for comp B in U.S. munitions. Similar to IMX-101, it

was formulated by BAE Systems at HSAAP and is employed in 60, 81 and 120-mm mortar projectiles. It will serve as the primary explosive charge in the next-generation of 155 mm ammunition series. IMX-104 (formerly known as OSX-7) comprises 53% NTO, 31.7% DNAN and 15.3% RDX.

2.5.4.2 Cast cured PBXs based on NTO explosives

Cast-cured compositions are composed of castable polymers such as HTPB, polyacrylate or other suitable polymers. Zeman et al. [120] have developed a novel PBXs by combining two energetic materials BCHMX and NTO with a polydimethylsiloxane binder in a mass ratio of 44:44:12. The researchers found that this new formulation exhibited excellent thermal stability and favorable mechanical properties along with significant detonation characteristics.

Elbeih et al. [121] have developed PBX in the form of sheet explosives. They used 88 % NTO explosives with 9.14 % by weight HTPB binder and other ingredients on the preparation of the new sheet PBXs. NTO Sheet PBX has very low sensitivities (Impact sensitivity 34.2 J - Friction Sensitivity more than 360 N and its performance is high (The calculated detonation velocity was 7514 m/s at Density 1.59 g/cm3). Lan et el. [122] developed a low vulnerable PBX material based on NTO and CL-20 using the solution-water suspension method. They prepared several materials based on these two explosives. They concluded that the optimum formulation which passes the slow cook off test and released an acceptable energy should contain (CL-20, NTO, cellulose acetate butyrate (CAB), bis-dinitro propyl formal/acetal (BDNPF/A) and additional graphite) in a mass ratio (50%,44%,2.4%,3.6% and 0.5%) respectively. Recently, Huang et el. [123] studied the properties of PBXs based on NTO with fluoropolymer. Their results in terms of compatibility and sensitivity summarized as follows: NTO / PVDF > NTO / Viton A > NTO / F2611 > NTO / F2614 > NTO / PHFP. Tappan et el. [124] studied a new material based on two insensitive energetic materials NTO and 3,3′diamino-4,4′-azoxy furazan (DAAF) using cylinder expansion test. DAAF proves to be an ideal material to combine with NTO resulting in formulations that effectively balance high performance with enhanced sensitivity to external stimulus. Incorporating DAAF within the weight range of 20 -70% along with other ingredients such as NTO and Kel-F yields formulations that demonstrate reduced mechanical sensitivity to impact and friction.

2.5.4.3 Pressed PBXs based on NTO

Smith and Cliff [14] conducted an investigation on pressed formulations developed in collaboration between Switzerland and Norway as shown in Table 2-8. Li et al. [125] recently introduced a series of pressed PBXs utilizing NTO and HMX as illustrated in Table 2-9. They conducted a comprehensive study on the thermal characteristics of these compositions by employing an accelerating rate calorimeter (ARC), a modified cook-off experiment equipment and finite element numerical simulations. The researchers observed that as the content of NTO increased in the formulations the stability to mechanical stimuli (impact and friction) improve but the detonation characteristics decreased.

Table 2-8 Pressed PBXs based on NTO [14]

Name	NTO	HMX	BDNPA/F	Binder	Velocity of detonation (m/s)	BAM impact (J)	BAM friction (N)
GD-9	47.5	47.5	2.5	2.5 (Cari flex)	8360	4	192
GD-10	48.8	48.8	-	2.4 (Cari flex)	8430	3	192
GD-11	48	48	-	4 (Cari flex 1101)	-	-	-
GD-12	48	48	-	4 (Cari flex 1107)	7829	7.5	252
GD-13	48	48	-	2/2 HyTemp/DOA	8520	7.5	252
GD-14	48	48	-	4 (Estane)	8458	7.5	213
French 1	55.5	37	-	7/0.5(KelF /Graphite)	-	-	-

Table 2-9 NTO/ HMX Pressed explosives [125]

Designation	NTO	HMX	Binder	Wax	Density (g/cm^3)
NH-1	63.7	27.3	8	1	1.75
NH-2	45.5	45.5	8	1	1.781
NH-3	27.3	63.7	8	1	1.777

2.6 Overview of flow chemistry techniques

2.6.1 Flow chemistry

"Flow Chemistry" refers to the practice of conducting the chemical reactions in a continuous flow system rather than the traditional batch chemistry. This method uses channels or tubing to facilitate reactions in a continuous stream as opposed to using flasks within structured channels of miniaturized flow vessels known as microreactors. The benefits of continuous multistep synthesis have been proven in various fields, such as active pharmaceutical ingredients. Beyond pharmaceuticals, flow chemistry has extended its applications to specialty chemicals, polymers, and the synthesis of nanomaterials, including the production of metal and semiconductor nanoparticles. Furthermore, this approach has significantly reduced the time required for synthesizing peptides [126,127].

2.6.2 Micro reaction technology

Microreactors are small-scale devices that function as continuous mixers under pressure-driven flow. They consist of single or multiple parallel microchannels with specific dimensions. [128,129] These flow channels, often having diameters in the range of a few hundred microns, operate as continuous flow reactors. It can be defined as "*a casing for performing chemical reactions that is designed or selected to induce and exploit deliberately microflow phenomena".* [128]. Nowadays, laboratories in flow chemistry typically employ perfluoro alkoxy (PFA) or stainless-steel tubes

with simple T- and Y-mixers. Microstructured mixers are necessary for brief mixing durations. [130]. Typical microreactor systems as shown in Figure 2-15.

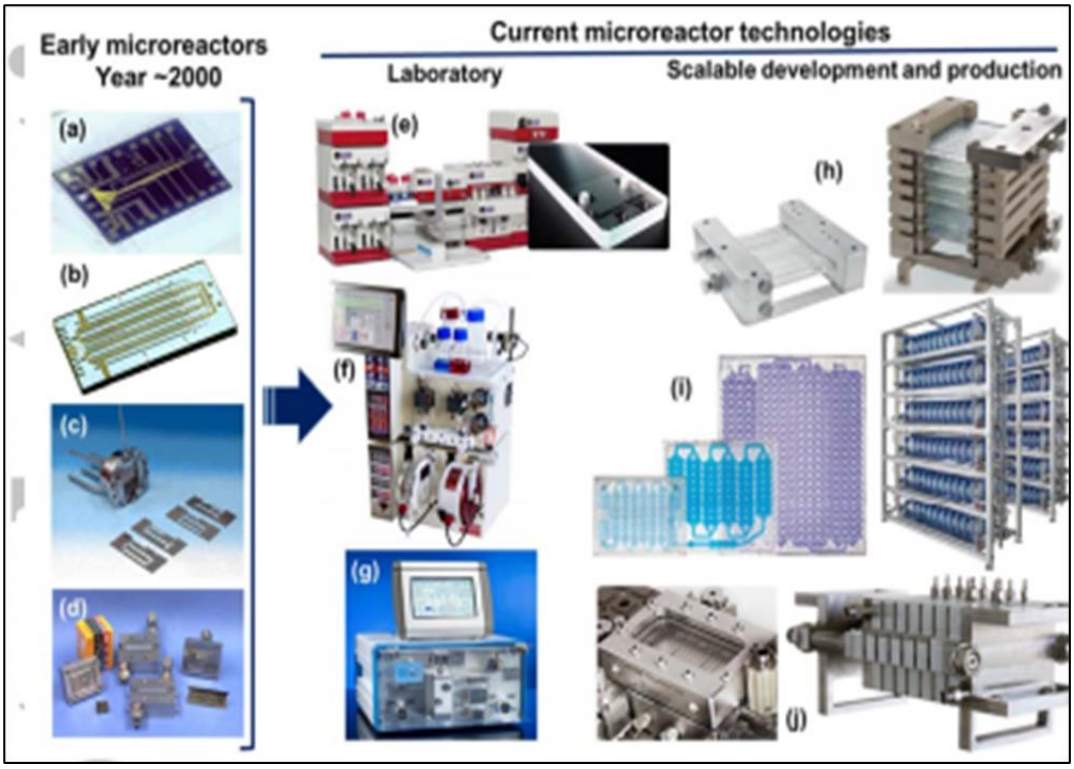

Figure 2-15 Typical microreactor systems [131]

2.6.3 Microreactor components

In continuous flow processes, microreactor systems are composed of various components including pumps, flow meters, reactors with controlled heating/cooling, separators, valves, and analysis tools. These components are organized into eight zones: fluid delivery, mixing, reactor, quenching, pressure regulation, collection, analysis, and purification as shown in Figure 2-16 [132]. The fundamental elements of the continuous flow setup can be summarized as follows:

- Fluid and Reagent Delivery

In a continuous flow process, precise fluid movement control is crucial, determining residence time and stoichiometry when multiple reagent streams merge. Various pumps are employed in continuous flow systems based on flow rates and pressure requirements as HPLC pumps, metering pumps and syringe pumps [133].

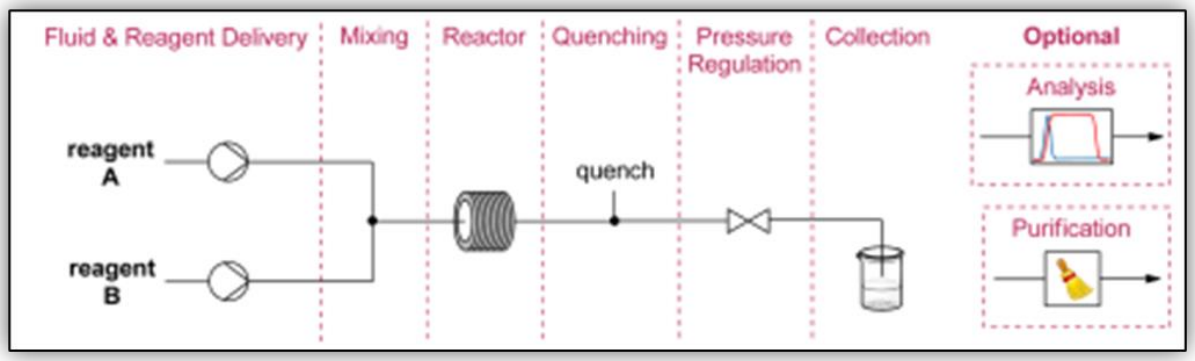

Figure 2-16 Zones of a standard two-feed continuous flow setup [132]

- Mixer

Mixing in continuous flow systems is very important operation that employs active and passive methods. Simple connections, like T or Y-shaped units, are used for slower reactions. Specialized micro-mixing units, such as T-mixers with small diameters or split and recombine techniques, reduce mixing time for fast reactions. An additional micro-mixing method entails dividing each stream into multiple segments as shown in Figure 2-17, followed by rotation and recombination (known as split and recombine, SAR). [132,134-136].

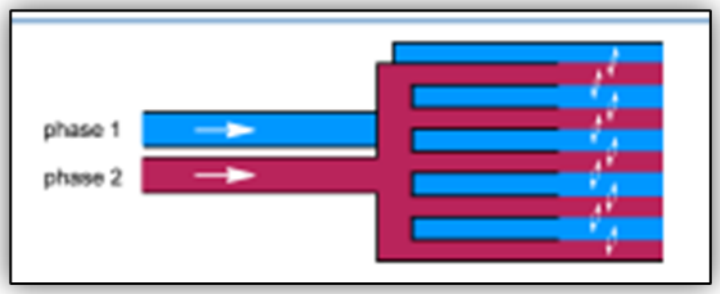

Figure 2-17 Mixers operate through the splitting of streams into a multitude of streams [132].

- Reactor Unit

The core unit of every flow system is where chemical reactions take place. Reactors can be chip, coil, or packed bed types as shown in Figure 2-18, chosen based on the specific transformation. Chip-based reactor units provide excellent heat transfer with high surface-to-volume ratios, allowing precise thermal control for accurate reactions. Coil-based reactor units are widely used in synthetic flow chemistry due to their cost-effectiveness and versatility, especially when compared

to chip-based reactors. These reactors are typically made from readily available tubing materials such as inert fluoropolymers or stainless steel (SST) with various diameters. Packed bed reactor units are employed when continuous chemical transformations require heterogeneous catalysts or reagents. [132,137-139].

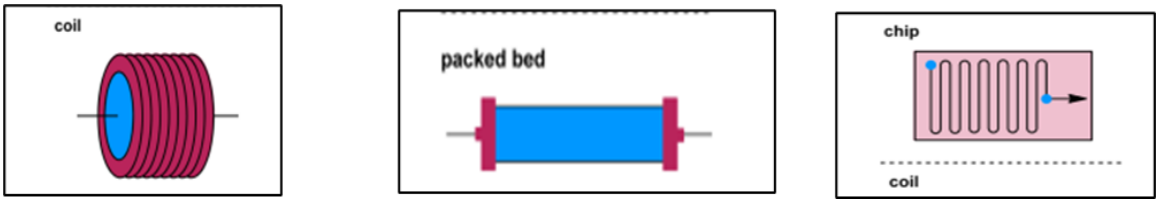

Figure 2-18 Typical types of microreactor [132]

- Quenching Unit, Pressure Regulating Unit, Collection Unit

Other key components of a continuous flow synthesis system including quenching unit that is essential for controlling reaction time, with methods such as thermal or chemical quenching depending on the specific reaction and flow process. The pressure regulating unit, employing back pressure regulators, maintains constant system pressure, crucial for operations involving volatile reagents. The collection unit, which follows depressurization, typically involves collecting the mixture in a flask, and for specific tasks, fraction collectors may be utilized. [132,140 -145]

2.6.4 Advantages of microreactors

Microreactors, characterized by their small size and intricate design, offer several advantages over traditional large-scale reactors. In summary, microreactors' unique features and advantages as follows [146-149]:

1- Advantages of Microreactors:

- High Surface-to-Volume Ratio: Microreactors are characterized by a significantly larger surface area relative to their small volume, which is especially advantageous for phase-boundary reactions.
- Efficient Mixing: Microreactors enable fast and efficient mixing due to their small dimensions, which allows for precise control of chemical reactions. Microreactors, due to

their small size, enable rapid mixing in less than a minute. Flow conditions in microreactors enhance mixing, allowing precise control of residence time and reducing side reactions.

- Temperature Control: These reactors facilitate rapid heating and cooling, leading to precise temperature control, making them suitable for various reactions.
- Residence Time Control: The residence time, or the time reactants spend in the reactor, can be precisely controlled by adjusting the length of microchannels. It can be varied by changing flow speed or the length/volume of the flow path.
- Safety and Selectivity: Microreactors enhance safety by minimizing material hold-up and allow for better control of product selectivity.
- Scale-Up Flexibility: By adding more microreactors, ensuring a flexible scale-up process by increasing dimensions and number of mixing units in such a way to keep the overall mass transfer characteristics the same.

2- Features of Microreactors:

- Mixing Mechanisms: Microreactors rely on diffusion and micro-mixing mechanisms for efficient mixing, which is particularly advantageous for fast reactions.
- Heat Transfer: Microreactors have a high heat transfer efficiency, allowing for rapid temperature changes and preventing hot spot formation.
- Mass Transfer: The high specific interfacial area in microreactors results in efficient mass transfer, especially in biphasic or multiphase reactions.

2.7 Carbon nanomaterials and energetic compositions

Several strategies have been employed to obtain new energetic materials that suitable for use in insensitive low vulnerable munitions. One of these strategies involves modifying the explosive materials through various approaches including coating them with polymers to produce PBXs where the explosive components are bound together by a polymeric binder forming a rubbery material which is less susceptible to shock and other stimuli as illustrated before [8] or coating them with different insensitive layers such as wax and carbon materials [150] or refining the explosive crystals through recrystallization techniques [9] or creating new insensitive explosive

materials such as TATB and NTO to replace some high vulnerable explosives by a certain amount of this insensitive explosive in the explosive compositions [10] or incorporating nano explosive materials into the explosive compositions [11] or co-crystallization techniques that have been explored leading to the formation of larger crystals with enhanced properties compared to the original individual explosives [12-151].

Carbon-based materials have shown great potential in improving safety while maintaining the performance of the explosive or having minimal impact on energetic properties [15,152]. Carbon nanomaterials are gaining a lot of interest because of their great properties like strength, electrical conductivity, radiation resistance, and large surface area. Also, they can be made in different shapes, sizes, and crystal forms [153]. Among them, graphene oxide (GO), reduced graphene oxide (RGO) and carbon nanotubes (CNTs) are seen as the most promising for use in energetic materials [154,155]. In this part of my study, I will give a quick overview of how CNMs, especially GO can affect the properties and behavior of energetic materials.

2.7.1 Preparation methods of GO

GO consider as important derivative of graphite due to the presence of oxygen containing functional groups on its basal planes and edges. It is synthesized through the chemical oxidation and exfoliation of graphite powders using strong oxidizing agents such as $KMnO_4$ in concentrated sulfuric acid. The following sections presents the different strategies of synthesizing GO:

- The first attempt to synthesis GO was published by Brodie in 1859 by using potassium chlorate ($KClO_3$) and strong oxidizing agents as fuming nitric acid producing a material that contains carbon, hydrogen and oxygen. This method is not preferred due to the long reaction time and liberation of toxic fumes during preparation [156].
- In 1898, Staudenmaier et al. also synthesized GO using the Brodie method, but introduced a modification by adding potassium chlorate in portions throughout the reaction, along with increasing the acidity of the medium through the addition of sulfuric acid [157].
- In 1958, Hummers and Offeman successfully introduced a new approach for preparing GO, in which sulfuric acid (H_2SO_4) and sodium nitrate ($NaNO_3$) were used to activate graphite,

while potassium permanganate ($KMnO_4$) was used as strong oxidizing agent. This method is widely used for the preparation of GO [158].

- Finally, James M. Tour et al. proposed an improved version of the Hummer method. In their modification, $NaNO_3$ was excluded and the amount of potassium permanganate was increased. The reaction was carried out in a mixture of two acids including sulfuric acid and phosphoric acid at a 9:1 ratio respectively. This method not only enhanced the oxidation efficiency of graphite but also produced a more hydrophilic and highly oxidized form of GO. Additionally, no toxic gases were generated during the synthesis process and allows better temperature control that making it more suitable for large-scale production [159].

2.7.2 Energetic materials based on GO

GO have several key characteristics that make it highly suitable for energetic materials applications. It has high theoretical specific surface area and abundant oxygen functional groups. GO offers also thermal reactivity, which is beneficial in energy releasing reactions. Additionally, it is more hydrophilic and dispersible compared to other carbon nanomaterials that reducing the agglomeration during coating processes and allowing for better encapsulation and desensitization of energetic materials [160,161]. For examples, Wang et al., successfully prepared and characterized the dihydroxylammonium-5,5′-bistetrazolyl-1,1′-diolate (TKX-50)/GO energetic material confirming that coating TKX-50 with GO led to a morphological transformation that led to altering its structure from tabular crystals to polyhedral shapes and the thermal stability of the TKX-50/GO remained largely unchanged while GO reduced both the impact and friction sensitivity of TKX-50 compared to its pure form [162]. Song et al., reported that GO can effectively encapsulate CL-20 and forming a stable energetic material. His results showed that the decomposition temperature of the CL-20/GO was 518.0 K, which remained nearly identical to that of raw CL-20 while the phase transition temperature increased slightly to 444.8 K indicating a minor stabilization effect of GO compared to pure CL-20 [163]. Li et al., reported that GO sheets exhibited a superior desensitizing effect compared to fullerene and carbon nanotubes. When 2.0 wt.% GO sheets were incorporated into raw HMX, the impact sensitivity dramatically decreased from 100% to 10%, while the friction sensitivity was reduced from 100% to 32%. Also, the activation energy of HMX increased by 23.5 kJ/mol upon the addition of 2.0 wt.% GO indicating

that GO enhances the thermal stability of HMX [164]. In another study Zeng et al., suggest the opposite results of the effect of GO on HMX confirming that the mean activation energy of pure HMX was 470 kJ/mol, whereas the activation energy of the GO/HMX decreased to 421 kJ/mol, indicating a reduction of approximately 50 kJ/mol [165]. This contradicts the previous study in terms of activation energy and thermal decomposition behavior. Chen et al. showed that the Graphene Oxide-Nickel effectively reduced the activation energy for Tri-aminoguanidine nitrate decomposition [166]. Hanafi et al. studied the effect of metal complexes of tri-aminoguanidine (T-Co, T-Zn) with and without GO on NTO thermal decomposition. These nano-catalysts altered the decomposition pathway and significantly reduced activation energy, with GO-T-Co-T achieving the lowest value (189 kJ/mol) [167]. Kumar et al. studied the catalytic effects of nanosized NiO and ZnO on the thermal decomposition of NTO finding that ZnO exhibited superior catalytic activity compared to NiO [168].

Based on the above literature, GO can either stabilize or catalyze the decomposition of NTO explosive materials and can increase or reduce the activation energy of NTO. Then, important part of our study investigates the effect of GO addition to NTO at varying concentrations (1%, 2%, 3%, 4% and 5%) to determine whether it increases or decreases activation energy or if it has no effect at all. Additionally, the impact of GO on the mechanical sensitivity of NTO will be evaluated. Furthermore, Metal Oxide Nanocrystals were found to catalyze the thermal decomposition of NTO [168]. Also, we explore the effect of incorporation different concentrations nano-scale copper oxide (CuO) in the coating layer GO with different proportions (5%, 15%, 25%, 35 & 45%) when applied to the coated NTO particles with GO to assess its influence on the thermal properties of NTO. The ultimate goal is to develop an optimized explosive composite with enhanced performance, improved mechanical sensitivity and controlled thermal stability and activation energy.

2.8 Characterization techniques

Characterization of NTO based explosives and their plastic bonded explosive materials must be carried to understander the relationship between material performance and its properties, leading to the development and optimization of materials. Starting from the morphological and structural characterization that focuses on identification, confirmation of the structure and surface properties that conducted using techniques such as fourier transform infrared spectroscopy (FTIR), nuclear magnetic resonance (NMR), scanning electron microscopy (SEM), energy-dispersive x-ray spectroscopy (EDX), transmission electron microscopy (TEM) and x-ray diffraction (XRD). These techniques provide insights into particle size, shape, coating uniformity and crystallographic structure. In addition, specific tests that determine the behavior of the material under thermal and mechanical stimuli, including impact and friction sensitivity [169], shock wave response, differential scanning calorimetry (DSC), thermogravimetric analysis (TGA), hot plate ignition temperature testing, vacuum thermal stability testing, electrostatic discharge sensitivity. One of the important tests is the performance assessment to the energetic materials including detonation velocity and detonation pressure measurements, brisance tests, bomb calorimetry for heat of combustion in accordance with ASTM D240 [170,171], as well as standard safety assessments such as fast and slow cook off test for IM. While not all these techniques were used in this thesis. Characterization was performed using instruments and facilities at Polytechnique Montréal and Defence Research and Development Canada (DRDC).

CHAPTER 3 OJECTIVES

3.1 Objective

The objective of this thesis is to design, synthesize, and characterize novel advanced plastic-bonded explosives (PBXs) with enhanced detonation performance, while maintaining mechanical sensitivity (impact and friction) within acceptable limits for use in insensitive munitions (IM). The study emphasizes the use of cast-cured compositions incorporating NTO as the primary intrinsically insensitive pure explosives and GAP as the energetic binder. In addition to the base explosive composition (NTO/GAP), modified PBXs materials incorporating NTO coated with GO and NTO coated with GO and nano-CuO were also prepared using the Thinky mixer. Additionally, this research introduces a novel microreactor-based synthesis method for NTO, designed to overcome the limitations associated with traditional batch processes. This novel approach seeks to improve the safety and thermal control of NTO synthesis. Ultimately, the research aims to produce novel PBX systems with superior performance and safety profiles compared to current IMX explosives and conventional PBXs materials. This chapter presents the specific objectives and research goals that guide the entire work, from the synthesis NTO explosive material via a novel microreactor based synthesis to the synthesis and characterization of advanced PBXs materials.

3.2 Specific objectives

In order to achieve the global objective, our research activities are divided into the specific objectives listed below:

1. Optimization of the conventional synthesis of NTO via batch and one-pot procedures: A study of key reaction parameters. This work aims to propose a safer and more efficient synthesis route that ensures a high yield of NTO while maintaining strict safety process. Reaction parameters, including the nitration temperature, the starting temperature for the nitration process, the use of different nitrating agents, and the optimal reaction time were systematically studied and optimized. The data obtained from this objective particularly the optimized nitration temperature is required for guiding the development of a new and safer method for NTO production inside the microreactor.

2. A novel microreactor approach for the safer and controlled synthesis of NTO explosive material. This work aims to develop a novel synthesis approach for NTO using a microreactor and flow chemistry, addressing the challenges and risks associated with conventional methods. One of the key advantages of this technology which has attracted significant interest in the field of explosive synthesis is its ability to ensure safety during chemical reactions, even at elevated temperatures and in the presence of hazardous reagents and products. These reactors facilitate rapid heating and cooling, leading to precise temperature control while minimizing the quantity of reagents mixed inside the system. Another advantage that makes microreactors a superior technology for synthesizing high explosives is their ability to mitigate hot spot formation during production. In this study, a systematic investigation of key synthesis parameters was conducted, including solvent selection for TO dissolution, solvent concentration, and reaction time. Each of these variables will be examined within the microreactor to identify the optimal conditions for maximizing NTO yield.
3. Development of novel NTO-based nanocomposites using graphene oxide and copper oxide coatings for enhanced thermal stability and reduced mechanical sensitivity. This work aims to the development of the explosive material itself based on NTO to exhibit enhanced energetic output, reduced mechanical sensitivity and controlled thermal stability. The objective is to achieve an optimal balance between energy and sensitivity by incorporating varying contents of graphene oxide (GO) and copper oxide (CuO) as nanoscale coatings on NTO particles. These coatings are intended to modify the thermal decomposition behavior and mechanical response of NTO, contributing to the development of a safer and more efficient energetic material suitable for use in advanced energetic compositions. In this objective, GO is synthesized using the improved Hummers method, and composite materials (GO/NTO and GO/CuO/NTO) are prepared via a solution-based ultrasonic dispersion technique. The effect of GO on the mechanical sensitivity and the thermal stability of NTO is evaluated, and different contents of nano-CuO are investigated to assess their influence on the thermal behavior of the coated NTO.
4. Creating an alternative technique instead of melt cast technique (IMX101-IMX104) for developing new PBXs materials based on NTO explosives and energetic binder GAP. This work aims to formulate new PBX materials based on NTO as the energetic component and GAP as the energetic binder, using the cast-cured technique. The objective of this study is to

systematically investigate the effects of increasing NTO content on the performance and sensitivity characteristics of GAP-based PBXs. Specifically, this work aims to determine the maximum NTO loading that can be homogeneously incorporated into the GAP binder while maintaining mixture stability. Additionally, the study seeks to evaluate the impact of coating NTO particles with GO and a combination of GO and nano-CuO on the thermal stability, mechanical sensitivity, and energetic performance of the resulting PBX compositions. The modified composites will be compared with the base NTO/GAP composition to assess their suitability for application in insensitive munitions.

5. The theoretical detonation parameters of the developed compositions of the PBXs are calculated using the EXPLO5 program. This work aims to calculate the theoretical detonation parameters of the prepared NTO-based PBX materials using the EXPLO5 program [172]. Key parameters including detonation velocity, explosion pressure, explosion temperature and heat of explosion are evaluated based on the measured density and chemical composition of each PBXs composition. In addition, a time-dependent simulation of the variable confinement cook-off test (VCCT) was carried out using COMSOL Multiphysics to assess the thermal behavior and safety of an NTO-GAP-based PBX under slow heating conditions. By coupling heat transfer with decomposition kinetics, the simulation provided critical insights into the composition's thermal stability and response. The ultimate goal is to select and propose an optimized explosive formulation suitable for use in insensitive munitions.

3.3 Coherence of the thesis

The following four chapters present the main research outcomes and represent the core of this thesis. Each chapter presents one of the specific research objectives, and collectively, they lead to the achievement of the general objective of this thesis.

Chapter 4 represents the first specific objectives "Optimization of the conventional synthesis of NTO via batch and one-pot procedures: A study of key reaction parameters". In this study, we replicated conventional procedures reported in the literature to synthesize 1,2,4-triazol-5-one (TO) from semicarbazide hydrochloride and formic acid. Subsequently, NTO was synthesized from TO using both the batch method and the one-pot nitration procedure. In the second phase, we conducted a series of experiments to address several significant safety challenges, particularly during the

nitration step especially when employing the one-pot method. This involved systematic modification of critical reaction parameters. Our focus was on optimizing key aspects of the NTO synthesis process, such as the nitration temperature (25, 40, 55, and 65 °C) and the overall reaction conditions to ensure a safer and more efficient synthesis. Additionally, we investigated the impact of the initial nitration temperature and the type of nitrating agents used, including 70% HNO_3, mixed acid (98% H_2SO_4 and 70% HNO_3) and even alternative nitrating salts like ammonium nitrate (NH_4NO_3), to maximize both the safety and the yield of the final NTO product. This chapter offer a preparation approach for NTO that ensures safety and high yield.

Chapter 5 Building on the challenges identified in the conventional synthesis of NTO discussed in the previous chapter, this chapter presents the results of the second specific objective "A novel microreactor approach for the safer and controlled synthesis of NTO explosive material". This work directly addresses the critical limitations of traditional approaches particularly the significant risks associated with the nitration step, which typically requires elevated temperatures (around 65 °C) sustained for 1.5 to 2 hours, leading to potential hazards. In this study, a novel approach was designed to synthesize NTO via in situ nitration of 1,2,4-triazol-5-one (TO) with nitric acid inside a microreactor. Unlike batch processes, the microreactor offers superior thermal control, reduced reaction volume, and increased safety, making it a promising alternative for handling sensitive energetic materials. To adapt this process for microreactor operation, the study was initiated by evaluating the solubility of TO in various solvents including dimethyl sulfoxide (DMSO), dimethyl formamide (DMF), acetonitrile, chloroform, ethyl acetate, dioxan to ensure compatibility with micro-scale flow systems. This step was critical to prevent clogging or blockage of the narrow reactor channels during NTO precipitation. Subsequently, a series of batch nitration experiments were performed by adding 70% nitric acid to different TO solutions to assess their reactivity and behavior under varying solvent conditions. Following this, a detailed parameter study was conducted within the microreactor. Key factors such as solvent selection, TO concentration starting with (0.2 ,0.4, 0.6,0.8,1) M and nitration time ranging from (0.5, 1.5, 2.5, 3.5, 5, 8) minutes were systematically varied to determine the optimal conditions that yield the highest NTO purity and efficiency. This microreactor-based synthesis not only enhances process safety but also represents a significant innovation in the field of energetic materials by introducing

a controlled, flow-based method for manufacturing a traditionally hazardous compound via the microreactor.

Chapter 6 presents the results of the third specific objective "Development of novel NTO-based nanocomposites using graphene oxide and copper oxide coatings for enhanced thermal stability and reduced mechanical sensitivity". In this study, a novel approach was introduced to enhance the energetic performance, reduce the mechanical sensitivity, and improve the thermal stability of NTO by applying nanoscale coatings of GO and CuO in varying proportions. The work is structured into several stages. First, graphene oxide (GO) is synthesized using a modified Hummers method. Then followed by the preparation of a novel GO/NTO nanocomposite using an ultrasonic dispersion technique. A systematic investigation is carried out by incorporating different weight fractions of GO (1%, 2%, 3%, 4%, and 5%) onto NTO particles to assess the effect of the GO coating on thermal properties and mechanical sensitivity. Subsequently, a second novel composite, GO/CuO/NTO was prepared using the same ultrasonic technique. In these compositions, the GO content was fixed at 3 wt.% relative to the NTO mass, while CuO nanoparticles were introduced into the GO matrix at varying weight ratios (5%, 15%, 25%, 35%, and 45%) relative to the GO content. As a result, the total CuO content in the final coating varied between less than and more than 1 wt.% of the overall composite, depending on the ratio used. This study introduces a novel strategy to simultaneously reduce the sensitivity and enhance the thermal stability of high-energy materials like NTO through nanostructured coatings. Most notably, it presents an innovative method for incorporating a metal oxide (CuO) into an energetic material without significantly compromising its thermal stability achieved by embedding CuO within a graphene oxide matrix as part of the coating layer. This novel composite design offers a promising balance between energy performance and safety in advanced explosive compositions.

Chapter 7 presents the results of the four specific objective "Creating an alternative technique instead of melt cast technique (IMX101-IMX104) for developing new PBXs materials based on NTO explosives and energetic binder GAP". In this chapter, we developed advanced explosive material using the cast-cured technique to formulate new PBXs designed for use in insensitive munitions (IM). The work presented in this chapter integrates and builds upon the findings of the previous objectives to deliver a comprehensive and practical formulation strategy. As a first step, recrystallization procedures are applied to NTO to improve particle morphology and increase the

packing density, thereby allowing for a higher explosive content within the PBX compositions. Subsequently, a series of PBX compositions were developed using thinky mixer (model ARV-310) to systematically investigate performance and sensitivity characteristics. The NTO content was gradually increased to determine the maximum loadable amount that could be homogeneously and stably incorporated into the GAP binder. A binder-to-curing agent ratio NCO/OH of 1.2 was selected based on visual and manual assessment of the cured PBX samples. At this ratio, the mixtures displayed good homogeneity and workability, and the cured binders were neither excessively hard nor brittle. In addition to the base formulation (NTO/GAP), novel modified PBX materials were prepared by incorporating NTO coated with graphene oxide (GO), and NTO coated with both GO and nano-CuO, using the same cast-cured method. These composites were evaluated against the base composition to assess their suitability for use in insensitive munitions. The morphological structure of the PBXs was examined using SEM spectroscopy, while their mechanical sensitivity (impact and friction) was compared with existing insensitive materials such as IMX-101 and IMX-104. Furthermore, the thermal stability and kinetic behavior of the PBX compositions were evaluated. The heat of combustion was measured experimentally using bomb calorimetry, and the detonation parameters were calculated using the EXPLO5 program.

Chapter 8 presents the numerical modeling results and analysis of the slow cook-off behavior of the developed NTO-based PBX composition. A time-dependent simulation of the variable confinement cook-off test (VCCT) was performed using COMSOL Multiphysics to assess the thermal response and decomposition behavior of the explosive under slow heating conditions. This chapter includes temperature distribution profiles, identification of critical regions, and evaluation of the risk of thermal runaway. The simulation results provide valuable insights into the thermal stability, ignition threshold, and compliance of the PBX materials with insensitive munitions requirements.

CHAPTER 4 OPTIMIZATION OF THE CONVENTIONAL SYNTHESIS OF NTO VIA BATCH AND ONE-POT PROCEDURES: A STUDY OF KEY REACTION PARAMETERS

4.1 General

This chapter introduces the outcomes of the first objective of this thesis, which focuses on the synthesis of NTO (3-nitro-1,2,4-triazol-5-one) using conventional methods, including both batch and one-pot techniques [14,26,27,36,108]. A series of experiments were conducted to address significant safety challenges, particularly during the nitration step which is especially critical in the one-pot synthesis method.

NTO is classified as an insensitive high explosive, offering a unique balance between low sensitivity to mechanical stimuli (impact and friction) and high thermal stability, while maintaining performance characteristics comparable to RDX. It demonstrates comparable detonation performance with lower sensitivity than RDX, HMX and PETN, and exhibits sensitivity levels closer to TNT and TATB [106]. NTO has already been incorporated into several advanced explosive compositions, such as XF®13333 [118], IMX-101 [4], IMX-104 [4], B2267A, B2268A [173] and pressed PBXs [14,113]. Since its discovery in 1905 [25], extensive research has been conducted on NTO synthesis mainly through two techniques: the two-step method and the one-pot procedure. The most common strategy involves a two-step process: first, the formation of the intermediate compound 1,2,4-triazol-5-one (TO), followed by its nitration using various nitrating agents to produce NTO.

Building on this background, our contribution focuses on enhancing both safety and yield in the conventional synthesis of NTO particularly within the one-pot method, where the high nitration temperature (typically 65 °C) and the strongly exothermic nature of the reaction led to operational hazards such as uncontrolled frothing and boiling. These challenges complicate temperature control and compromise process safety. The objective of this novel approach is to develop a safer and more efficient preparation method for NTO by systematically optimizing critical reaction parameters. This includes the nitration temperature (25, 40, 55, and 65 °C), the initial temperature of nitration (0 and 25 °C), and the selection of nitrating agents such as 70% HNO_3, mixed acid

(98% H_2SO_4 and 70% HNO_3), and alternative nitrating salts like ammonium nitrate (NH_4NO_3). The study presents synthetic approach to maximize both the safety and the yield/purity of NTO. Also evaluates each stage of the process, from the synthesis of the TO intermediate to the final nitration step ensuring control over exothermic reactions. To verify the success of the synthesized NTO, FTIR spectroscopy and DSC thermal analysis were employed.

4.2 Materials and methods

4.2.1 Chemicals and instruments

Semicarbazied hydrochloride ($N_3H_5CO.HCL$), Formic acid (CH_2O_2 88%) used in the preparation of TO was purchased from Sigma Aldrich. Nitric acid (HNO_3 70%), Concentric sulfuric acid (H_2SO_4 98%), Ammonium nitrate (NH_4NO_3) used as nitrating agents were also purchased from Sigma Aldrich. The starting material triazolone (TO) was prepared. Fourier transform-infrared (FTIR) techniques were recorded within the IR range of 400 - 4000 cm^{-1} using Perkin Elmer SP-65 FTIR spectrometer in an attenuated total reflectance (Miracle ATR) mode and thermal properties were evaluated through differential scanning calorimetry (SDT Q600 thermal analyzer (TA Instruments)).

4.2.2 Preparation of TO

TO was synthesized in a 500 mL three-necked flat-bottom flask equipped with a magnetic stirrer, thermometer and reflux system. TO was prepared by adding 59.68 mL of formic acid (88%) to 50 g of solid semicarbazide hydrochloride at ambient temperature [27,108]. The reaction scheme is presented in Figure 4-1. The mole ratio between the reactants was 1:2.5 (SC.HCl : formic acid), respectively. The resulting solution was then heated to 85-90 °C and stirred magnetically for 6-8 hours under reflux. After the reaction was completed, the excess formic acid was removed by evaporation until the triazolone precipitated. TO was washed with water and then evaporated again to ensure complete removal of formic acid. Subsequently, the dried product was dissolved in heated water and slowly cooled to induce precipitation of the TO product, followed by filtration and drying at 60 °C for 24 hours.

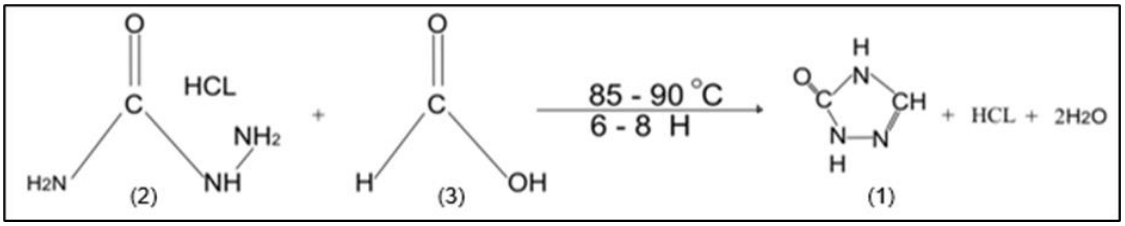

Figure 4-1 Batch synthesis of (1): 1,2,4 - triazole-5-one (TO). (2): Semicarbazide hydrochloride, (3): Formic acid.

4.2.3 Preparation of NTO

1- Batch technique

In the batch reactor, NTO was prepared by gradually adding nitric acid (HNO_3) drop by drop to solid triazolone (TO) until the entire amount of nitric acid was added. The mole ratio between TO and nitric acid was 1:5, as illustrated in Tables 4-1 and 4-2. The resulting mixture was stirred using a magnetic stirrer until the reaction was complete. The initial temperature for the nitration step (i.e., the addition of nitric acid to triazolone) was either 0 °C or 25 °C, as shown in Tables 4-1 and 4-2. Following the initial addition, the reaction temperature was gradually increased to the designated nitration temperature, which was maintained for a specified time until the formation of NTO was complete. To control the temperature during the nitration process, a 50:50 mixture of propylene glycol and water was used as a cooling medium. Upon completion of the reaction, the mixture was cooled to room temperature, followed by chilling in ice water. The resulting product was then filtered, washed with cold water and dried at 70 °C for 48 hours. Optimization of the reaction conditions focused on achieving not only high NTO yield but also a safe and controlled synthesis process, as presented in Tables 4-1 and 4-2. The corresponding reaction scheme is shown in Figure 4-2.

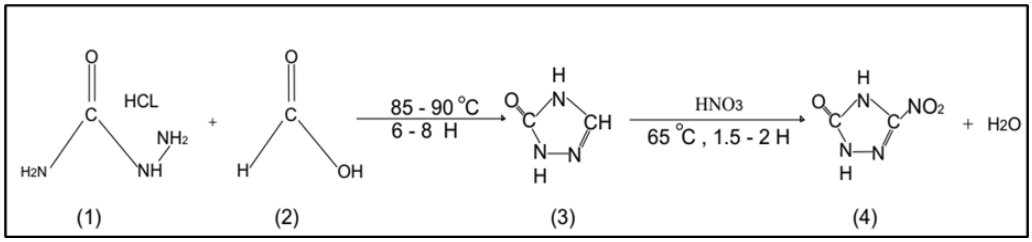

Figure 4-2 Synthesis of (4) NTO. (3): (TO), (1): Semicarbazide hydrochloride, (2): Formic acid.

Table 4-1 Results of TO nitration using 70 % HNO_3 by batch approach at 0 °C

Exp.	TO	70% HNO_3	Mole Ratio (TO: HNO_3)	Nitration temperature [° C]	Time [hour]	Obtained results (Yield) %
R1	10 g	38 ml	1:5	25	4-5	21.2
R2				40	3-4	39.6
R3				55	3-4	53.2
R4				65	2-3	66.71

Table 4-2 Results of TO nitration using 70 % HNO_3 by batch approach at 25 °C

Exp.	TO	70% HNO_3	Mole Ratio (TO: HNO_3)	Nitration temperature [° C]	Time [hour]	Obtained results (Yield) %
R5	10 g	38 ml	1:5	30	3- 4	25.7
R6				40	2-3	42.6
R7				55	2-3	56.2
R8				65	1.5 - 2	67.2

2- <u>One pot procedure</u>

NTO was also prepared using the same procedure described in the batch approach in section 1, as illustrated above, except that TO was not isolated as a separate intermediate product. Instead, the nitration was conducted directly in the same vessel used for TO synthesis. Optimization of the reaction conditions was performed similarly to the previous method, with a focus on achieving both a high yield of NTO and a safe synthesis route, as described in Tables 4-3 and 4-4. The subsequent processing steps, filtration, washing and recrystallization, were carried out in the same manner as in the previous approach.

Table 4-3 Results of TO nitration using 70 % HNO_3 by one-pot procedure at 0 °C

EXP.	TO	70% HNO_3	Mole Ratio (TO: HNO_3)	Nitration temperature [°C]	Time [hour]	Obtained results (Yield) %
R9	10 g	38 ml	1:5	25	3-4	35.2
R10				40	2.5-3	44.7
R11				55	2-2.5	56.9
R12				65	1.5 - 2	72.3

Table 4-4 Results of TO nitration using 70 % HNO_3 by one-pot procedure at 25 °C

EXP.	TO	70% HNO_3	Mole Ratio (TO: HNO_3)	Nitration temperature [°C]	Time [hour]	Obtained results (Yield)
R13	10 g	38 ml	1:5	30	1-1.5	41.9
R14				40	1-1.5	51.2
R15				55	-	-
R16				65	-	-

3- Preparation of NTO using different nitrating agents

The nitrating agents included concentrated nitric acid, mixed acid (HNO_3 and H_2SO_4) and ammonium nitrate. The objective is to compare the influence of these nitrating agents on NTO synthesis, and the experimental results are evaluated against data reported in the literature, as summarized in Table 4-5. Following the safe and controlled procedure described earlier for the batch technique, NTO was synthesized by gradually adding nitric acid or mixed acid drop by drop to solid triazolone (TO) until the entire volume of acid was added. The mixtures were then stirred magnetically until the reactions were complete. Subsequent steps, including cooling, filtration and product recovery, were carried out as detailed in section 4.2.3 (Batch technique) to obtain the final NTO product. In the case of using ammonium nitrate as the nitrating agent, the compound was added gradually to cooled sulfuric acid at 0 °C with continuous stirring

using a magnetic stirrer. Once the addition was complete, TO was introduced in small portions while maintaining the reaction temperature between 0-5 °C. The temperature was then allowed to rise to the nitration temperature (65 °C) and the reaction was continued for 2 hours. During this period, the color of the mixture gradually changed from white to yellow. The NTO product was subsequently recovered following the same procedure described earlier.

Table 4-5 Results of NTO synthesis using different nitrating agents

Research Group	Nitrating Agent	Nitration Temp. (°C)	Nitration time (min.)	Mole Ratio (TO: HNO_3)	Yield (%)
Chipen et al. [27]	Fuming Nitric Acid	60	(2-4)	-	67.5
Kröger et al. [174]	Fuming Nitric Acid	-	-	(3:2)	70
Lee et al. [26]	70% Nitric Acid	55 - 60	-	-	High
Spears et al. [36]	H_2SO_4/ HNO_3	65 - 86	90	-	77
Becawe et al. [108]	Fuming Nitric Acid	20 - 40	180	(5:1)	80
Smith et al. [14]	H_2SO_4/ HNO_3	65	90 -120	-	77
Cudziło et al. [110]	HNO_3/ H_2SO_4/ H_2O	65	120	-	65
Mukundan et al. [175]	Fuming Nitric Acid	60 -70	-	-	80
Our Group (Batch)	70% HNO_3	65	120-150	(5:1)	67.2
Our Group (One-pot)	70% HNO_3	65	90	(5:1)	72.3
Our Group (Batch)	70% HNO_3 / H_2SO_4	65	120	(5:1)	69.8
Our Group (Batch)	NH_4NO_3 / H_2SO_4	50-60	120	(2:1)	52.9

4.3 Results and discussion

4.3.1 Preparation of 1,2,4 triazole -5-one (TO)

Triazolone (TO) was prepared successfully by reacting solid semicarbazide hydrochloride with formic acid, as described in Section 4.2.2. The yield of the TO product was 71.45%. Based on the experimental results, the most effective approach for achieving a high yield of TO involves reacting semicarbazide hydrochloride with an excess of 88% formic acid for 8 hours at 65 °C, or for 6 hours at a temperature range of 85-90 °C. The yield of the TO product was found to be independent of the formic acid concentration, however, the presence of water in the reaction mixture was observed to influence the reaction rate. This finding aligns with previously published studies on the kinetics of triazolone formation [26].

4.3.2 Preparation of NTO

The results of NTO synthesis, presented in Table 4-1 and supported by experimental observations, indicate that when the entire amount of nitric acid was added to the intermediate TO at 0 °C, the nitration step proceeded safely. In this case, the reaction temperature was gradually increased from 0 °C to the target nitration temperatures of 25 °C, 40 °C and 55 °C. During the nitration period, the maximum recorded reaction temperature increased only slightly, reaching approximately 60-63 °C. However, under these conditions, the yields were relatively low 21.2%, 39.6% and 53.2% respectively.

In contrast, when the nitration temperature was set to 65 °C, the process remained safe, as the reaction temperature was again gradually increased from 0 °C to 55-60 °C. Following this, the exothermic nature of the reaction caused the temperature to increase to 85-90 °C. However, with active cooling and careful temperature regulation, the reaction mixture was brought back down and maintained at 65 °C throughout the remainder of the 2-hour nitration period. Under these optimized conditions, a significantly higher yield of 66.71% was achieved.

Additionally, notable visual changes in the reaction mixture were observed, indicating progression in the nitration process. The reaction changes color from a light-yellow solution to red during the nitration reactions as shown in Figure 4-3(a, b, c, d).

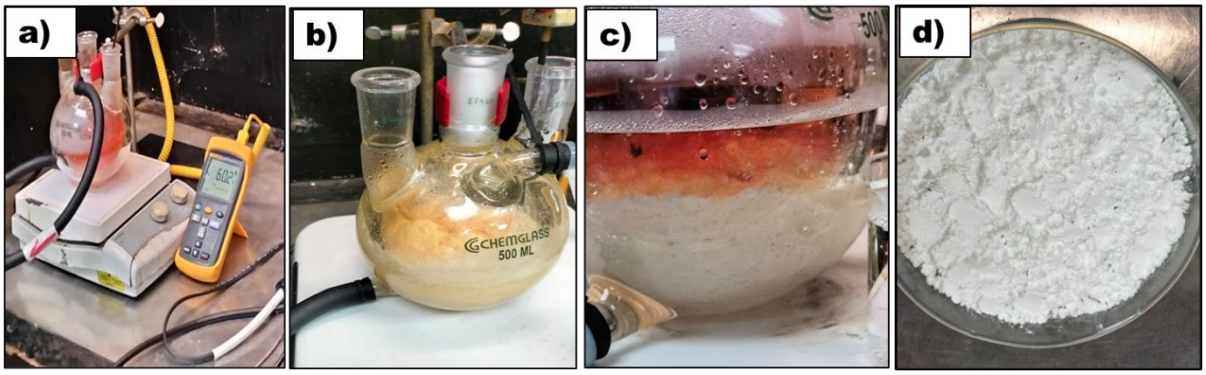

Figure 4-3 (a, b, c, d) visual changes images occurring during the NTO formation.

On the other hand, when the entire amount of nitric acid was added at 25° C to the TO as shown in Table 4-2, the nitration step was also safe because the temperature of the reaction was gradually increased to the nitration temperature. The same behaviour of the temperature increase was recorded and during the time of nitration, the maximum temperature of the reaction reached to (67-69) °C. It was increased to (90-92) °C, when the nitration temperature was 65°C but also, in a way that allow us to control the reaction and cooling it without any dangers. The yield was low 25.7%, 42.6%, 56.2% when the nitration reaction was 30 °C, 40 °C, 55 °C respectively and it reached 67.2% when the nitration temperature was 65 °C. These process takes less time to produce NTO, with an increase in yield compared to the previous experiment.

In the present work, the exothermic behavior during the nitration step was controlled by adding nitric acid to the intermediate TO gradually and at a controlled rate while closely monitoring the temperature. The slow addition of the acid, combined with the use of an external cooling bath around the reactor helped to prevent sudden increase in the temperature and ensured safe operation throughout the experiments. However, the setup used in this study was based on a magnetic stirrer, which provides limited mixing efficiency when gas evolution becomes significant. A mechanical overhead stirrer would offer improved mixing under these conditions and could therefore enhance heat dissipation and exotherm control. Also, employing a reactor equipped with special wider vent or outlet would facilitate the release of gases generated during nitration, preventing pressure build-

up that can otherwise intensify the exotherm. Temperature monitoring with a feedback-based control system could further stabilize the reaction and provide more precise thermal regulation.

In the one-pot synthesis approach, the gradual addition of nitric acid to the intermediate TO without separation as a separate product was carried out at 0 °C until the complete volume of acid had been added. During the nitration time, the temperature of the reaction was gradually increased to the nitration temperature 30 °C, 40 °C and 55 °C during the time of nitration, the temperature reaching a peak of 70-75 °C for a relatively short time. Under these conditions, the process was considered relatively less safe because the temperature was raised in short time compared to the previous method. However, the NTO yields obtained at these conditions were also relatively low 35.2%, 44.7% and 56.9% respectively as shown in Table 4-3. In contrast, when the nitration temperature was conducted at 65 °C, the behavior of the reaction was totally changed. Initially, the temperature was increased gradually from 0 °C to 35-40 °C, then it was raised rapidly to 65 °C and it jumped sharply to 95-100 °C in a very short time. This sudden rise in temperature decreases the safety of the process, requiring immediate cooling to bring the temperature back down to 65 °C. The temperature should to be carefully monitored and adjusted throughout the entire reaction time because this sudden increase in the temperature occurred more than one time during the nitration time. This process yielding NTO at 72.3% after approximately 1.5 hours. This high yield may be due to fewer material losses of TO or reduced chances for side reactions or decomposition. Keeping the whole process in a single continuous step may also maintain a more consistent acidic environment, which supports better conversion of TO to NTO. These explanations are only possible interpretations, as this work did not directly study the causes.

On the other hand, when the addition of nitric acid to the intermediate TO was carried out at 25 °C until the complete volume of acid had been added as presented in Table 4-4, the nitration step became significantly more hazardous. The reaction temperature was raised rapidly from 25 °C to 30 °C and then to 40 °C, eventually reaching to 55-60 °C within a very short period. This uncontrolled temperature increase resulted from the exothermic nature of the reaction outpacing the heat removal capacity of the reactor, making the process more difficult to control and also the process gave a relatively low yield 41.9% and 51.2% respectively. But, when the nitration process was conducted at even higher temperatures, such as 55 °C or 65 °C, the reaction became completely

unstable and the nitration step quickly escalated beyond control that leading to vigorous boiling and overflow of the reaction mixture from the reactor vessel.

As shown above from the experipments, several nitration temperatures were investigated (25 °C, 40 °C, 55 °C and 65 °C). These temperatures refer specifically to the target reaction temperature (bath temperature) of the reaction mixture, not the internal temperature of the mixture. However, in all experiments, the nitric acid was added to the TO starting at either 0 °C or 25 °C as the internal temperature of the mixture and the mixture was then allowed to reach and maintain that target temperature under controlled conditions. The external cooling bath was used only to regulate the reaction temperature and prevent uncontrolled exothermic rises.

To evaluate the effect of different nitrating agents on the yield and safety of NTO synthesis, we investigated the use of mixed acid (70% HNO_3 and H_2SO_4) and ammonium nitrate (NH_4NO_3) as shown in Table 4-5, the results indicate that there was no significant difference in yield between using 70% HNO_3 alone and its mixture with H_2SO_4 .In both cases, the yields were comparable and the processes remained safe when the nitration procedures outlined in section 4.3.2 were followed. However, when ammonium nitrate was used as nitrating agent, the yield dropped significantly to 52.9%. Despite the lower efficiency, this method was safer because the reaction temperature did not exceed on 65 °C. During the reaction, the color of the mixture changed from white to yellow and it was accompanied by the formation of bubbles and foam that needs effective agitation.

The compounds obtained from all experipments was submitted to FTIR analysis, DSC analysis and NMR analysis to confirm the structure of NTO explosive and its purity. Based on the FTIR spectra from Figure 4-4. The characteristically bonds of NTO compound were identified confirming the nitration reactions happen [14,103,107]. Also, the recorded ^1H NMR spectrum in DMSO-d6 displayed two prominent peaks: 13.5 ppm, corresponding to the H-N proton adjacent to the nitro group (-NO_2) and 12.8 ppm, attributed to the DMSO-d6 solvent as shown in Figure 4-5 that prove the purity of the prepared NTO explosive particles due to the absence of any unexpected peaks in the spectrum.

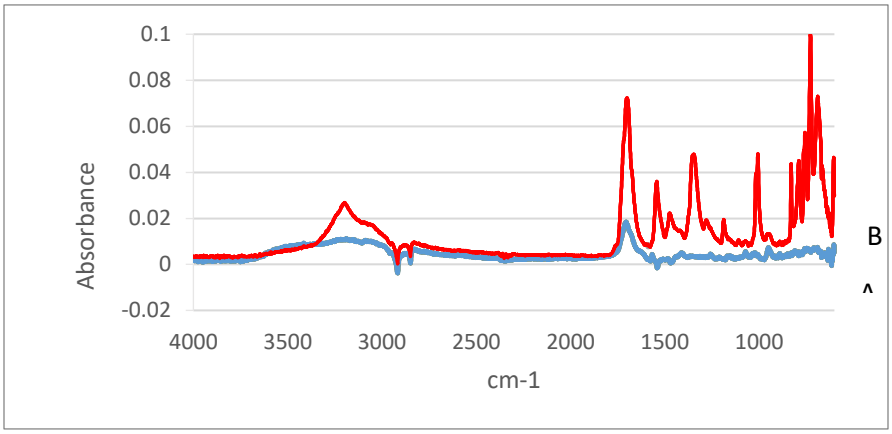

Figure 4-4 IR spectrum of TO (A) and NTO (B)

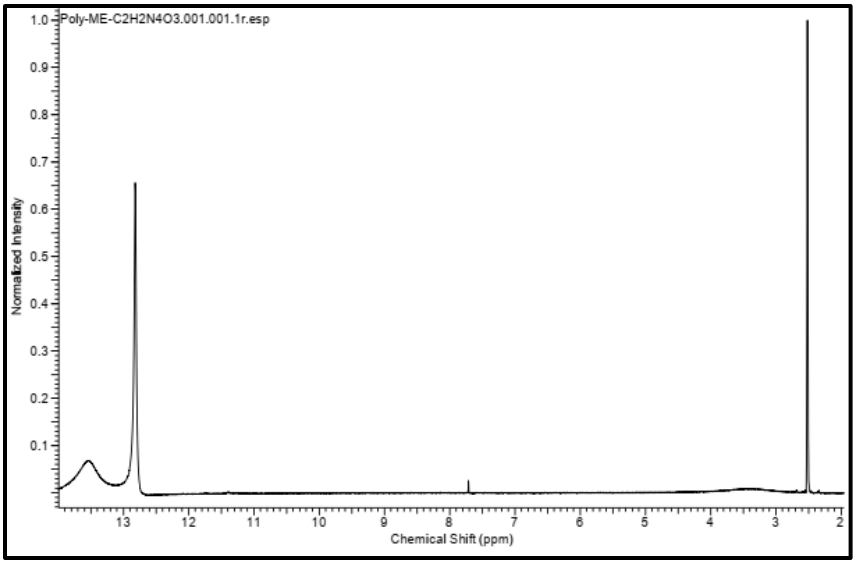

Figure 4-5 ^{1}H NMR spectrum of the NTO sample dissolved in d6-DMSO

The DSC curve of the prepared NTO exhibits a strong and sharp exothermic peak at approximately 265.3 °C, corresponding to the self-decomposition of NTO as shown in Figure 4-6. This result aligns well with values reported in the literature [14,103,107].

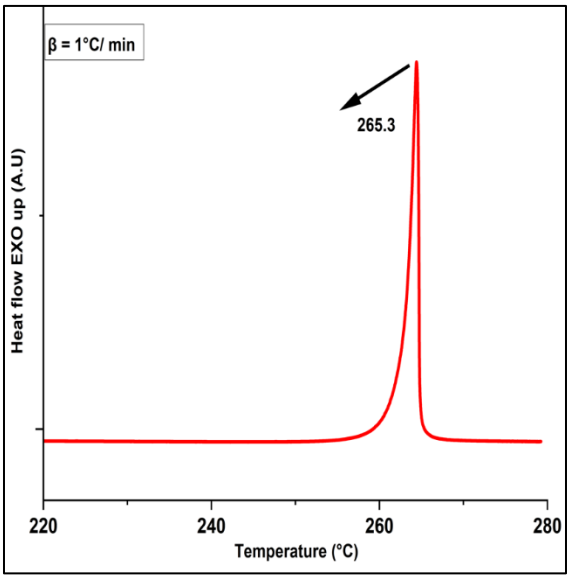

Figure 4-6 DSC curve heating rate 1 ° C/min for pure NTO

4.4 Conclusion

Triazolone was formed as a result of the condensation reaction of semicabazide hydrochloride with formic acid. The reaction proceeds more efficient with a slight molar excess of formic acid. NTO can be prepared safely at lower temperatures and with moderate yields using both the conventional two-step and one-pot approaches. Increasing the nitration temperature to 65 °C has been shown to significantly enhance the yield. NTO can be prepared more safely by starting the nitration at 25 °C, particularly using the batch technique, were increasing the nitration temperature to 65°C for approximately 2 hours significantly enhances the yield to 67.2% NTO. In contrast, the one-pot synthesis method demonstrated an additional safety requirement by gradually adding nitric acid at 0 °C under carefully controlled cooling conditions, the risk of frothing and thermal runaway was reduced with high yield approximately72.3%, indicating a promising route for scalable synthesis with some risks during the reaction. Additionally, using mixed acid produced yields similar to 70% HNO_3 alone. However, using ammonium nitrate with concentrated sulfuric acid resulted in a lower yield of 52.9%. This method also required careful control due to the formation of foam and bubbles which necessitate efficient agitation. These findings directly lead to the formulation of the second specific objective of this thesis, which is to explore and optimize the synthesis of NTO trough the microreactor.

CHAPTER 5 A NOVEL MICROREACTOR APPROACH FOR THE SAFER AND CONTROLLED SYNTHESIS OF NTO EXPLOSIVE MATERIAL

5.1 Introduction

The development of high explosive manufacturing has become a major focus for many scientists and researchers nowadays due to the serious problems and hazardous incidents associated with their production [23,24]. NTO is a heterocyclic compound having four nitrogen atoms [14,107,108]. Based on findings from the literature and the results of the first objective of this thesis, the conventional synthesis of NTO particularly using the one-pot method presents significant safety challenges and risks. Achieving high yields often requires conducting the nitration step at elevated temperatures, typically around 65 °C, for an extended duration of 1.5 to 2 hours. However, the strongly exothermic nature of the nitration reaction poses serious operational risks. During this period, the temperature can rise rapidly exceeding 100 °C within a few minutes [26,36,107]. To manage this, an intensive cooling system is required to reduce the temperature to a safer range of 55-65 °C. Maintaining this target temperature presents further challenges. Overcooling can cause the temperature to drop below 65 °C, necessitating reheating again to return the reaction to the optimal temperature range. This cycle of cooling and reheating may repeat multiple times during a single synthesis due to the long time of nitration, increasing the risk of thermal instability and complicating process control. These challenges highlight the urgent need for a novel, efficient, and inherently safer method for the synthesis of NTO explosive.

To address these issues, this chapter introduces a novel continuous flow microreactor-based process that transfers NTO synthesis from conventional batch methods to flow chemistry technology. This innovative approach refers to the practice of conducting the chemical reactions in a continuous flow system (microreactors) rather than the traditional batch chemistry. This technique uses channels or tubing to facilitate reactions in a continuous stream as opposed to using traditional flasks [128,129,146]. Microreactor systems are composed of various components including pumps, flow meters, reactors with controlled heating-cooling, separators, valves and analysis tools. Microsystems have a wide of applications including pharmaceuticals, polymers, nanomaterials, semiconductor and peptides [126,127]. One of the key advantages of this

technology which attracts many researchers in its use in explosives synthesis, is its ability to ensure safety during the chemical transformations even at elevated temperatures and in the presence of hazardous reagents and products. These reactors facilitate rapid heating and cooling leading to precise temperature control and by minimizing the amounts of reagents that mixed together inside the microreactor [147]. Another advantage that makes microreactors a superior technology for synthesizing high explosives is their ability to mitigate hot spot formation during the production. Microreactors enhancing the reaction efficiency and safety for these reasons [147,148].

(1) Enhanced Heat Transfer: The exceptionally high surface area to volume ratio of the microreactor allows rapid dissipation of heat from the reaction mixture to the reactor walls. The very small channel dimensions shorten the heat transfer distance, minimizing temperature gradients and preventing local hot spots in exothermic reactions. In addition, the reactor walls often made of materials with good thermal conductivity facilitate efficient heat exchange with external cooling or heating systems. Together, these features enable precise temperature control throughout the reaction.

(2) Efficient Mixing: Mixing is also significantly more efficient in microreactors because the narrow channels force fluids into close contact, increasing interfacial interaction between reactants. The reduced diffusion distance allows molecular diffusion to occur rapidly, even under laminar flow conditions typical of microreactors. The flow geometry creates strong velocity gradients that stretch and fold fluid layers, promoting uniform mixing without the need for turbulence. As a result, reactants are distributed quickly and uniformly, reducing residence time and limiting the formation of undesired by products.

(3) Increased Mass Transfer Rates: The microscale dimensions of microreactors facilitate efficient mass transfer of reactants and products. The increased mass and heat transfer rates contribute to higher reaction yields and selectivity.

Before implementing this technique, it was necessary to understand the microreactor design and operational principles to prevent any problems during synthesis especially when dealing with sensitive and hazardous materials. In microreactor systems, nitration reactions occur within narrow capillary tubes, so it was critical to ensure that these channels would not become blocked during NTO formation. This concern was informed by earlier observations during batch synthesis where

NTO particles began to precipitate before the reaction was complete indicating a risk of premature crystallization and clogging. To address this issue, a series of preliminary nitration experiments were conducted in batch reactors using different solvent systems. These tests aimed to identify the nature of the reaction during NTO synthesis and to evaluate the solubility of the precursor, TO under different media. The selected solvent system would also need to support continuous flow synthesis and efficient product collection. An effective strategy was developed for product recovery by cooling the collected reaction vials rather than relying on solvent evaporation, thereby avoiding the need to reinitiate the reaction or expose the system to additional thermal stress.

5.2 Materials and methods

5.2.1 Materials and instruments

All chemicals used in the synthesis of NTO within the microreactor were previously described in section 4.2.1. In addition, Dimethyl sulfoxide (DMSO), Dimethyl formamide (DMF), Acetonitrile, Chloroform, Ethyl acetate, Dioxan solvents were purchased from Sigma Aldrich. Acetone, isopropanol and sodium bicarbonate were purchased from commercial sources to clean the pumps of microreactor. Chemical analysis was employed using nuclear magnetic resonance (NMR) that used to confirm the structure of NTO explosive materials and measure the purity of the NTO explosives and FTIR techniques were recorded within the IR range of 400 - 4000 cm^{-1} using Perkin Elmer SP-65 FTIR spectrometer in an attenuated total reflectance (Miracle ATR) mode.

5.2.2 Preparation of TO

TO was synthesized by reacting formic acid (88%) with solid semicarbazide hydrochloride. The resulting compound, TO, was then used to produce the NTO explosive material inside the microreactor. The detailed preparation procedure for TO is described in section 4.3.1 [27,108].

5.2.3 Preparation of NTO

In order to begin the preparation of NTO explosive materials inside the microreactor, it was essential to ensure that the nitration process could be carried out without any operational issues. Since nitration in the microreactor takes place within narrow tubes, it was necessary to confirm that these channels would not become blocked during the formation of NTO. This precaution was

based on prior observations during batch synthesis, where NTO particles were found to form during the reaction, even before the process was fully completed.

Based on these observations, additional nitration experiments were conducted in batch reactors using various solvents. These experiments aimed to verify that NTO would precipitate prematurely during synthesis or not and to investigate the solubility of triazolone (TO) in different solvent systems. The goal was to identify a solvent environment suitable for use in the microreactor. The experimental procedures and findings are explained in the following sections.

5.2.3.1 Solubility of TO in different solvents

The solubility of TO in different organic solvents at atmospheric pressure (P = 0.1 MPa) and room temperature was investigated using the visual inspection technique by adding a known weight of TO on a known volume of the selected solvents, which included dimethyl sulfoxide (DMSO), dimethylformamide (DMF), acetonitrile, chloroform, ethyl acetate, and dioxane. The mixtures were then visually observed to determine whether TO completely dissolved, partially dissolved, or remained as a solid in the solvents.

5.2.3.2 Nitration of TO solutions with nitric acid

A series of nitration reactions of TO solutions using the solvents mentioned above were conducted. Approximately 5.5 g of TO and 100 mL of solvent were mixed at room temperature based on the solubility of TO in the respective solvents. Then, approximately 21 mL of 70% HNO_3 was gradually added drop by drop to the TO solution at room temperature with magnetic stirring until the entire amount of nitric acid was added. The nitration temperature was then gradually raised to 65 °C and the reaction was proceeded for 1-1.5 h. Once the reaction was completed, the mixture was cooled to room temperature, then further chilled in ice water, filtered and washed with cold water to yield NTO. Finally, the resulting NTO was dried at 70 °C for 48 hours as shown in Table 5-1. The use of DMF as a solvent for the nitration of TO with 70% nitric acid was carefully considered in light of the known hazards associated with DMF under nitrating conditions. All reactions were conducted with continuous monitoring of temperature to minimize the risk of uncontrolled side reactions or thermal runaway.

The choice of a microreactor system was motivated in part by its enhanced heat and mass transfer properties, which provide greater control and safety when handling potentially hazardous nitration reactions in the following section.

Table 5-1 Results of nitration of TO solutions using 70 % HNO_3 at 65 °C

Run	Solvent	Nitration temperature [°C]	Time [Min.]	Obtained results (Yield) %
R1	DMF	65	60-90	33.5
R2	DMF: H_2O (90:10)		60-90	30.6
R3	Acetonitrile: H_2O (60:40)		60-90	26.8
R4	DMSO: H_2O (90:10)		60-90	41.8
R5	DMSO: DMF (90:10)		60-90	43.7

5.2.3.3 Preparation of NTO utilizing the microreactor

Two Waters 515 HPLC pumps were utilized for the experiments after caliberated. The flow rate of the pumps was adjusted to achieve the required mole ratio between the reactants and the desired residence time in the reactor. Feed A and Feed B were combined and directed through the microreactor. The reaction scheme shown in Figure 5-1. The temperature of the nitrating reaction was approximately 65 °C using a Huber heater module. The flow rate was adjusted to maintain a fixed residence time of 5 minutes during the optimization of solvent and concentration. To ensure stable and uniform flow, the system was purged before initiating the reactions to eliminate any air bubbles. Throughout the experiment, strict safety precautions were implemented to minimize risks.

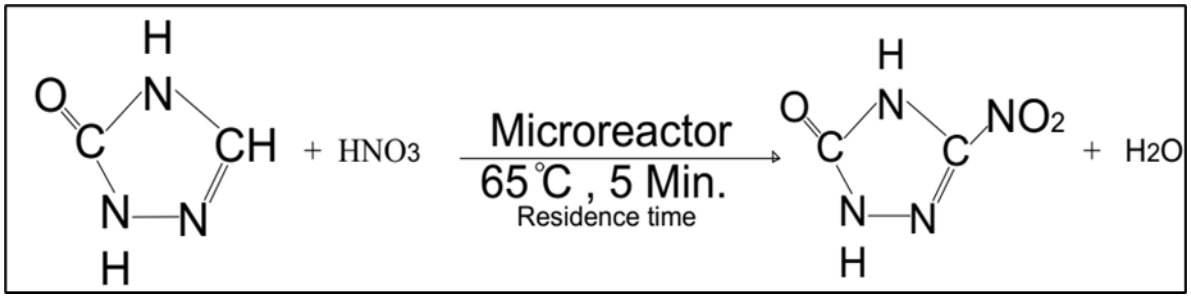

Figure 5-1 Synthesis of 5-niro-1,2,4 - triazole-5-one (NTO) in microreactor

Feed-A: Triazolone (TO) solutions of varying concentrations (0.2 M, 0.4 M, 0.6 M, 0.8 M and 1 M) were prepared in dimethylformamide (DMF) and other solvents, as shown in Table 5-2.

Feed-B: A 70% nitric acid (HNO_3) solution was used, following the optimized conditions in Table 5-2. All experiments were conducted using a molar ratio of TO:HNO_3 at 1:5 respectively. The flow rates of both the TO solutions and the stoichiometric excess of HNO_3 were maintained at constant values, along with the reaction temperature resulting in uniform residence times within the microreactor. The nitration reactions were performed in a stainless steel microreactor with an internal volume of 7 mL. The microreactor is equipped with two inlet ports for separate introduction of reactants and one outlet for product collection. Temperature was controlled using a heating jacket, and the reactor was fitted with a thermocouple for continuous temperature monitoring. Reagents were introduced using HPLC pumps, ensuring controlled flow rates and precise addition. At the microreactor outlet, the reaction mixture was directly collected in a product vial submerged in ice water for quenching. A 45 mL sample of the reaction mixture was collected

in each run for yield determination. The sample was then stored in a refrigerator for 24 hours to promote precipitation. The resulting NTO product was observed as a solid precipitate at the bottom of the vials. It was then filtered, washed with cold water and dried in an oven at 60 °C for 24 hours. The yield was calculated based on the amount of TO fed into the system and the volume of reaction mass collected. After drying and weighing, the NTO product was characterized using NMR and IR analysis.

To clean the pump used for acid delivery, multiple solvents and flushing cycles were employed. The cleaning process involved sequentially flushing the pump with water, followed by sodium bicarbonate solution, and then isopropanol. For the other pump, acetone and isopropanol were used for thorough cleaning. Schematic representation flow synthesis setup of NTO is presented in Figure 5-2. In order to optimize the synthesis of NTO explosive in the microreactor, solvents and concentrations that yielded the highest amount of NTO product were first evaluated, followed by residence time optimization as illustrated in Tables 5-2 and 5-3 respectively.

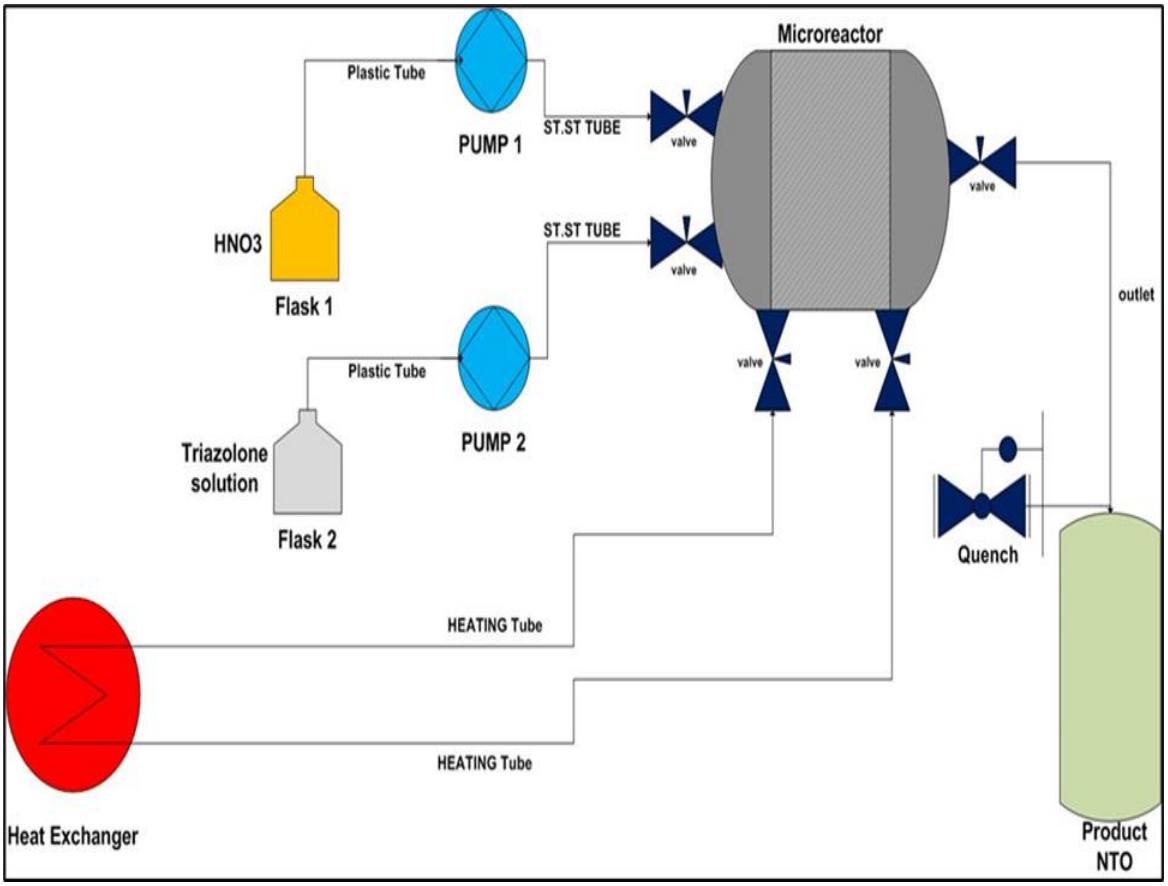

Figure 5-2 Schematic representation flow synthesis setup of NTO

5.3 Results and discussion

5.3.1 Solubility of TO in different solvents

In DMF and DMSO, the TO compound exhibited notable solubility allowing for the preparation of high-concentration solutions in these solvents. The maximum solubility of TO in DMF was found to be approximately 1 M, whereas in DMSO, it reached approximately 2.8 M under standard atmospheric pressure and room temperature. Conversely, the TO compound demonstrated limited solubility in acetonitrile and was insoluble in 1,4-dioxane, chloroform and ethyl acetate under standard atmospheric pressure and room temperature conditions.

5.3.2 Nitration of TO solutions with nitric acid

The nitration reaction of TO solutions with 70% nitric acid demonstrated a favorable safety profile, characterized by a gradual rather than sudden increase in temperature. The observed temperature rise typically remained within 3-5 °C above the target nitration temperature of 65 °C. Despite this controlled thermal behavior, the yield of NTO was relatively low as indicated in Table 5-1. Observations from the experiments revealed that the selected solvents did not cause any significant increase in temperature or foaming during the reaction. Furthermore, NTO did not precipitate during the reaction period, unlike what was observed in previous experiments. Instead, crystallization occurred only after the reaction mixture was allowed to cool to room temperature and then refrigerated for 24 hours. NTO crystals subsequently formed at the bottom of the reaction vessel. This outcome was particularly advantageous, as it enabled the reaction to be conducted within the microreactor without issues such as clogging or blockage.

5.3.3 Preparation of NTO utilizing the microreactor

NTO was successfully prepared in the microreactor by reacting triazolone (TO) solutions with 70% HNO_3 using a continuous flow chemistry approach. Various solvents and TO concentrations were evaluated to optimize the synthesis process. The results presented in Table 5-2 indicate that DMF, DMF: DMSO (80:20), and DMF: DMSO (70:30) mixtures were the most effective solvent systems among those tested, yielding NTO at approximately 57.41%, 59.39%, and 56.25% respectively.

These results may be explained by the presence of DMSO, which enhances the electrophilicity of nitronium ions (NO_2^+), thereby potentially increasing the nitration efficiency. In contrast, when TO was dissolved in aqueous or water-containing solutions, the yield of NTO was relatively lower, approximately 46.42%, compared to the aforementioned mixtures. This reduction could be attributed to the presence of water, which interferes with nitronium ion formation and thus reduces the overall efficiency of the nitration process. Additionally, at low TO concentrations, the yield of NTO was significantly reduced. This is likely due to that crystallization occurs when the reaction medium becomes supersaturated. At lower concentrations, the amount of NTO formed is insufficient to reach supersaturation, resulting in the product remaining dissolved in the reaction medium rather than precipitating out.

Table 5-2 Microreactor results for NTO preparation (optimization of solvent & concentration).

Run	Solvent	TO Concentration	HNO_3 [equiv]	Nitration temperature [°C]	Residence time [min.]	Yield %
R1	DMF	0.2 M	5	65	5	-
R2	DMF	0.4 M	5	65	5	-
R3	DMF	0.6 M	5	65	5	31.89
R4	DMF	0.8 M	5	65	5	51.06
R5	DMF	1 M	5	65	5	57.41
R6	Acetonitrile: H_2O (70:30)	0.56 M	5	65	5	29.90
R7	DMSO: H_2O (90:10)	0.8 M	5	65	5	43.12
R8	DMSO: H_2O (90:10)	1M	5	65	5	46.42
R9	DMSO: H_2O (80:20)	1M	5	65	5	41.82
R10	DMSO: DMF (80:20)	0.8 M	5	65	5	52.31
R11	DMSO: DMF (80:20)	1 M	5	65	5	59.39
R12	DMSO: DMF (70:30)	1 M	5	65	5	56.25
R13	DMSO: DMF (50:50)	1 M	5	65	5	50.36

The effect of different residence times on the yield of the NTO product was also evaluated. As shown in Table 5-3, these experiments were conducted using a solvent mixture of DMSO: DMF (80:20) at a concentration of 1 M. Various residence times were tested, ranging from 0.5 minutes to 8 minutes. According to the results and observations, at a short residence time of 0.5 minutes, no product was collected after cooling the reaction mixture for 24 hours, as no solid precipitate was formed. This suggests that the reaction between TO and nitric acid did not proceed significantly within this short time, resulting in incomplete conversion of TO into NTO. Additionally, even if a small amount of NTO was formed, it may have remained dissolved in the reaction mixture due to its low concentration, especially considering that the solvents used are capable of dissolving NTO effectively, thus preventing precipitation. As the residence time increased to 1.2, 2.5, and 3.5 minutes, the yield progressively increased to 23.2%, 31.8%, and 42.6%, respectively. This indicates that longer contact time between the reactants inside the microreactor enhances the conversion of TO into NTO. However, when the residence time was further increased to 8 minutes, some issues were encountered with irregular flow at the reactor outlet during product collection, and the experiment could not be completed. This irregularity in flow was believed to be due to partial blockage in the microreactor tubes. Two main reasons were considered for this blockage. First, when the residence time was set to 5 minutes, a yield of approximately 59.6% was obtained. Extending the residence time likely continued to increase the conversion rate, resulting in additional NTO formation. Although the solvent system (DMSO: DMF) can dissolve both TO and NTO, it may have reached saturation. Consequently, excess NTO could have started precipitating inside the tubes, disrupting the flow. The second possible explanation is based on our experiment observations. After stopping the reaction, the reactor was purged by operating both pumps at maximum flow rate using the appropriate cleaning solvents for each. Initially, the irregular flow at the reactor outlet persisted, but after several flushing cycles, the flow became smooth and consistent. This confirmed the presence of a partial blockage inside the microreactor, likely caused by precipitated NTO particles.

Table 5-3 Microreactor results for NTO preparation (optimization of residence time).

Run	Solvent	Concentration [M]	Temperature [°C]	Time [Min.]	Mole Ratio (TO: HNO_3)	Yield %
R1	DMSO: DMF (80:20)	1M	65	0.5	1:5	-
R2				1.5		23.2%,
R3				2.5		31.8%,
R4				3.5		42.6%
R5				8		-

5.3.4 Characterization of all prepared samples

All prepared samples (TO, NTO) were characterized to analyze and confirm their chemical composition, verify the structure of the NTO explosive material, and assess the purity of the explosives.

5.3.4.1 Nuclear magnetic resonance (NMR) analysis

NMR analysis was conducted on the NTO explosive to confirm its structural composition and purity. The recorded ^{1}H NMR spectrum in DMSO-d_6 displayed two prominent peaks: 13.5 ppm, corresponding to the H-N proton adjacent to the nitro group (-NO_2) and 12.8 ppm, attributed to the DMSO-d_6 solvent as shown in Figure 5-3. These results confirm the formation of the nitro-triazolone structure, as they align well with values reported in the literature for the ^{1}H NMR spectrum of NTO explosive [14,107]. Additionally, a minor peak at 7.7 ppm (0.4% of the 12.8 ppm peak) was observed, along with signals from water and residual DMSO. Based on the ^{1}H NMR spectra results, the purity of the prepared NTO explosive particles appears to be exceptionally high (>99%) due to the absence of any unexpected peaks, excluding water which could originate from the sample or solvent. Similarly, the ^{13}C NMR spectrum exhibited two distinct resonance peaks at 154.64 ppm, corresponding to the carbonyl group (C=O) and 136.5 ppm attributed to the carbon atom bonded to the nitro group (C-NO_2) as shown in Figure 5-4.

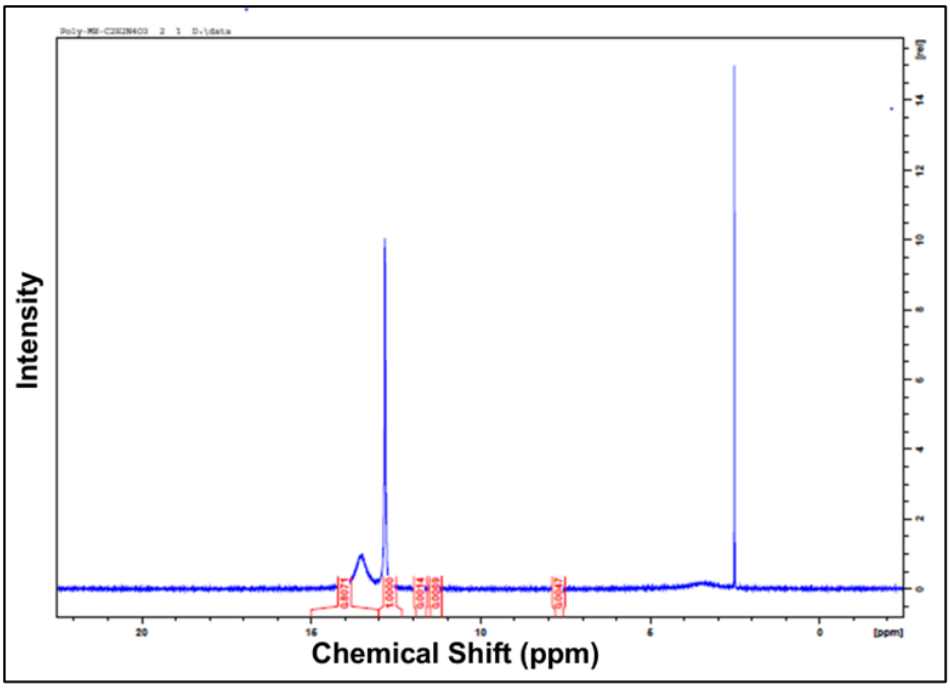

Figure 5-3 1H NMR spectrum of the NTO sample dissolved in d6-DMSO

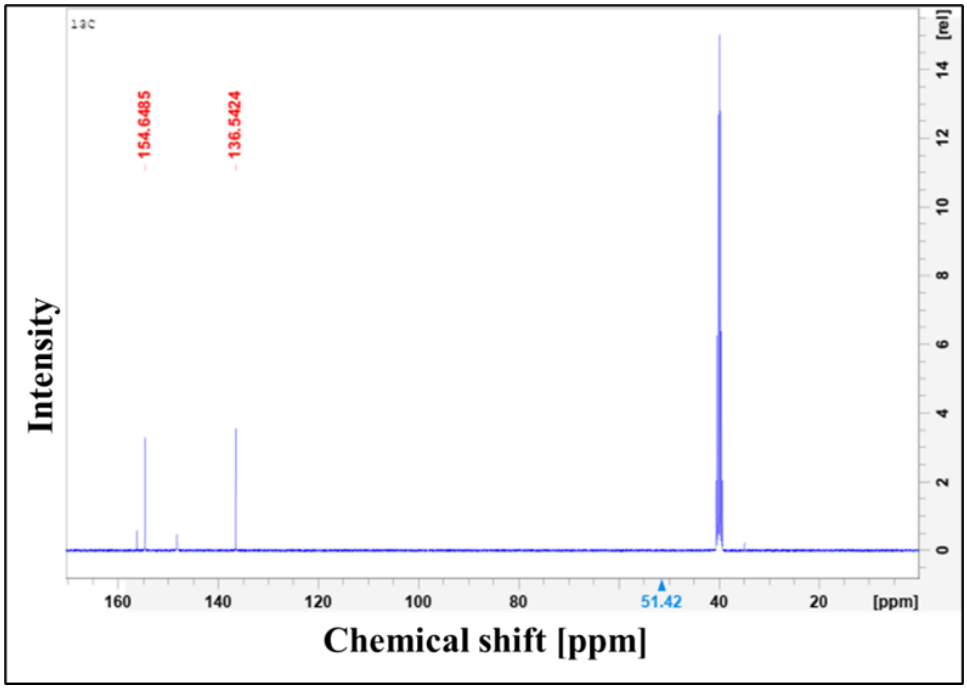

Figure 5-4 13C NMR spectrum of the NTO sample dissolved in d6-DMSO

5.3.4.2 Fourier transform infrared (FTIR) spectroscopy analysis

FTIR spectra of all prepared materials, including SC: HCl, TO, NTO were analyzed to confirm their structures. The FTIR spectrum shown in Figure 5-5 confirms the successful conversion of semicarbazide hydrochloride (SC: HCl) into TO, followed by its nitration to NTO. Several key characteristic absorption peaks were identified [14,103,107].

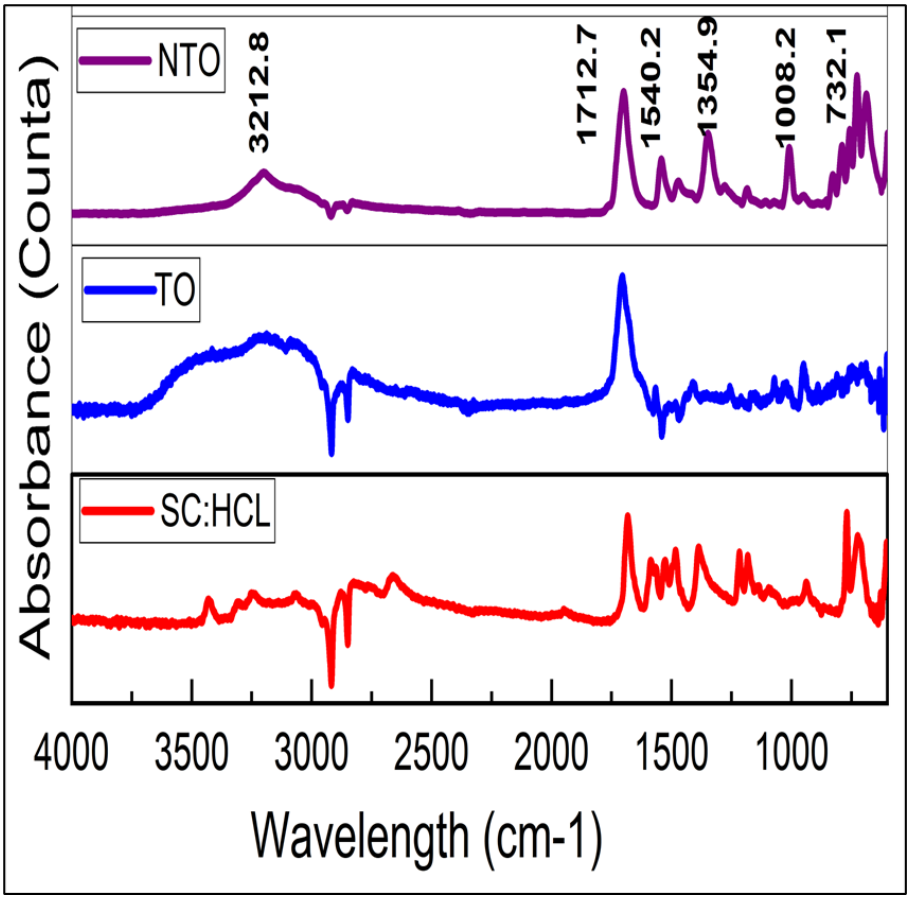

Figure 5-5 IR spectrum of the prepared samples (SC: HCL, TO, NTO).

5.4 Conclusion

The synthesis of energetic materials, particularly through hazardous processes such as nitration, inherently involves significant risks due to the release of large amounts of heat and the handling of highly sensitive compounds. Traditionally, NTO synthesis using batch processing requires approximately 3-4 hours to complete, with the nitration step alone typically lasting around 2 hours. This prolonged reaction time combined with inefficient heat dissipation and the evolution of substantial quantities of gas increases the likelihood of runaway reactions and makes the process less safe and more difficult to control. In contrast, this study introduces a novel approach to NTO synthesis based on continuous flow chemistry using a microreactor. This novel technique offers a safer, faster, and more controlled alternative to conventional batch processes. By nitrating triazolone solutions with 70% nitric acid in a flow microreactor, NTO was successfully synthesized with a yield of 59.6% using a DMF: DMSO solvent system (80:20) in just 5 minutes compared to 2 hours required in the batch method. The enhanced performance of this novel microreactor is primarily attributed to its microchannel architecture, which provides a high surface area to volume ratio. This structure significantly improves both mass and heat transfer allowing for superior temperature control and accelerated reaction kinetics. Moreover, unlike traditional batch reactors that are prone to heat accumulation and thermal instability, the microreactor design facilitates rapid heat dissipation, thereby minimizing safety hazards and improving process reliability.

CHAPTER 6 DEVELOPMENT OF NOVEL NTO-BASED NANOCOMPOSITES USING GRAPHENE OXIDE AND COPPER OXIDE COATINGS FOR ENHANCE THERMAL STABILITY AND REDUCED MECHANICAL SENSITIVITY

6.1 Introduction

Nowadays, there is rapid progress in the development of low-vulnerability munitions driven by significant advancements in the technological capabilities of modern military arms and defense systems. These types of munitions have attracted increasing interest among researchers because they are specifically designed to exhibit low sensitivity to unintended external stimuli such as shock, impact, weapon fragments, or heat [3]. One of the most critical properties of these munitions is their ability to resist detonation under severe unplanned conditions. Instead of detonating, they are designed to either ignite or deflagrate, thereby significantly reducing the risk of catastrophic failure and minimizing the loss of human lives and valuable assets. Additionally, these materials offer improved safety in terms of handling, storage and transportation [4].

NTO explosive material has emerged as a favorable candidate for use in LOVA applications due to its inherently low sensitivity to mechanical stimuli. It demonstrates much lower sensitivity to friction and impact compared to conventional high explosives such as RDX, HMX, and PETN [106]. However, despite its excellent insensitivity profile, there is still a need to further enhance the mechanical safety and thermal stability of NTO to meet the requirements of next-generation insensitive munitions. Several strategies have been used to develop low-vulnerability munitions [8-12]. One of these involves improving the explosive materials by applying coatings made of polymers or other substances. These coatings are engineered to tailor the sensitivity, stability, and energy release behavior of the base material.

Although NTO is already considered one of the best low-sensitivity explosives, the increasing demand for improved safety in defense applications necessitates the use of novel protective coatings that do not compromise performance. In this context, carbon-based nanomaterials particularly graphene oxide (GO) have shown great potential. GO possesses several unique features

that make it highly suitable for energetic material applications including a high theoretical surface area and an abundance of oxygen-containing functional groups that promote strong interactions with energetic compounds [160-161].

According to the literature, the incorporation of GO into explosive compositions has been reported to improve mechanical sensitivity (impact and friction) of these explosives. However, the influence of GO on thermal behavior varies significantly across studies. Some researchers have shown that GO enhances thermal stability by increasing activation energy, while others have reported the opposite effect, a reduction in activation energy. Some studies suggest that GO has no measurable effect on the thermal behavior of the energetic material [162,164,165]. These conflicting results highlight the need for investigation into the effects of GO on NTO.

In this chapter, GO is introduced as a novel additive with the objective of reducing the mechanical sensitivity of NTO-based explosives. A series of composite materials were prepared with varying GO contents (1%,2%, 3%, 4% and 5% by weight) to examine their influence on the thermal stability and sensitivity of NTO. The goal is to determine whether GO enhances or reduces the thermal stability or has no significant effect across different loading levels.

Furthermore, this study explores the novel incorporation of nano-scale copper oxide (CuO) into the GO coating layer aiming to assess its combined effect on the thermal behavior of NTO. CuO was introduced in varying proportions (5%, 15%, 25%, 35% and 45% relative to the GO content) to NTO particles previously coated with GO. This novel hybrid GO/CuO coating system is evaluated for its ability to regulate the thermal decomposition of NTO and improve the overall performance and safety profile of the composite.

The ultimate objective of this work is to develop an optimized and novel energetic composite that combines enhanced energetic performance, improved mechanical insensitivity and controlled thermal decomposition behavior and activation energy towards the way for safer and more effective applications in insensitive munitions.

6.2 Materials and methods

6.2.1 Materials and instruments

All the required chemicals for synthesis process that including semicarbazide hydrochloride ($N_3H_5CO.HCL$), formic acid (CH_2O_2 88%) and nitric acid (HNO_3 70%) used in the preparation of TO and NTO explosive were purchased from Sigma Aldrich. Sulfuric acid (H_2SO_4 98%), graphite powder, phosphoric acid (H_3PO_4), potassium permanganate ($KMnO_4$), hydrogen peroxide (H_2O_2), hydrochloric acid (HCL), Copper (II) Oxide (CuO), acetone and isopropanol used in the preparation of GO and coated explosives composition were purchased from Sigma-Aldrich. Chemical analysis was employed using FTIR techniques were recorded within the IR range of 400 - 4000 cm^{-1} using Perkin Elmer SP-65 FTIR spectrometer in an attenuated total reflectance (Miracle ATR) mode to confirm the structure of the prepared samples. Also, the composition of GO was checked by an CHNSO elemental analyzer flash smart. The morphology of pure NTO explosive and coated NTO with GO and GO/CuO was studied by a FEI Quanta FEG 450 SEM operated at 15 kV. XRD patterns were recorded on a Panalytical 3050/60 Xpert-PRO using CuKα radiation. Thermal stability properties were evaluated through differential scanning calorimetry (SDT Q600 thermal analyzer (TA Instruments)). Hermetically sealed aluminum pans were used in the DSC tests, and all measurements were conducted under a nitrogen flow. Only DSC data were analyzed because the focus of this study was on the thermal transition temperatures and heat-flow behavior, not on mass-loss information. While impact sensitivity and friction sensitivity were conduced in defence research and development Canada (DRDC) Valcartier. The heat of combustion was measured using a ParrTM 1341 Plain Jacket Calorimeter, a high-pressure bomb calorimeter in accordance with ASTM D240 [170,171]. The experiments were conducted three times for each sample and the average heat of combustion was calculated to ensure the accuracy and the results.

6.2.2 Preparation of TO and NTO

TO was prepared by reacting formic acid (88%) with solid semicarbazide hydrochloride. The resulting compound TO was then nitrated using 70% nitric acid (HNO_3) at 65 °C for 2 hours to produce NTO explosive material. Detailed preparation procedures for both TO and NTO are described in sections 4.3.1 and 4.3.2 [14,26,27,36,108].

6.2.3 Preparation of GO

Graphene oxide was prepared using a modified Hummer method. Graphite powder was treated with concentrated sulfuric acid and potassium permanganate ($KMnO_4$) as a strong oxidizing agent to achieve oxidation and exfoliation, as described in references [158-159]. Specifically, graphite powder (1 g) was used as the starting material and added to a 9:1 mixture of concentrated sulfuric acid (98%) and phosphoric acid (85%) (120 ml:13.3 ml) respectively, while stirring in an ice bath. Then, 6 g of potassium permanganate was gradually added slowly in portions while continuous stirring to maintain the temperature below 20 °C due to the slightly exothermic nature of the reaction. The mixture was stirred for 2-3 days at room temperature until it became a viscous brown product. This product was then slowly poured in portions into 1.5 L of distilled water while stirring vigorously at 350-400 rpm in an ice bath for approximately 1 hour. Afterward, hydrogen peroxide (10% H_2O_2) was carefully added to the mixture drop by drop through a titration funnel with continuous stirring until the color changed from dark brown to yellow- orange. The mixture was then stirred for an additional 20 minutes. GO particles were washed by decantation 2-3 times with 15% hydrochloric acid (HCl) to minimize the number of impurities. Finally, GO particles were collected by centrifugation (5000 rpm for 3 h) and washed with acetone. The schematic steps of synthesis are shown in Figure 6-1. Important visual changes observed during the progress of the reaction shown in Figure 6-2 (a, b, c).

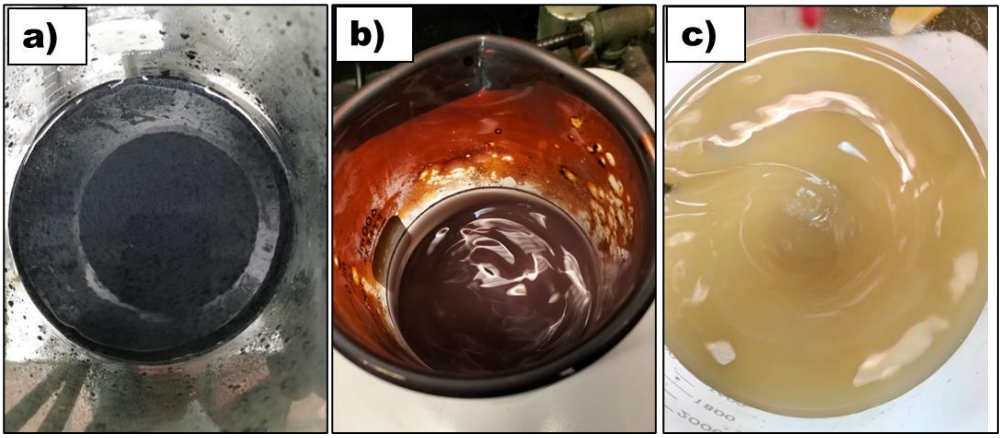

Figure 6-2 (a, b, c) visual changes images occurring during the GO formation.

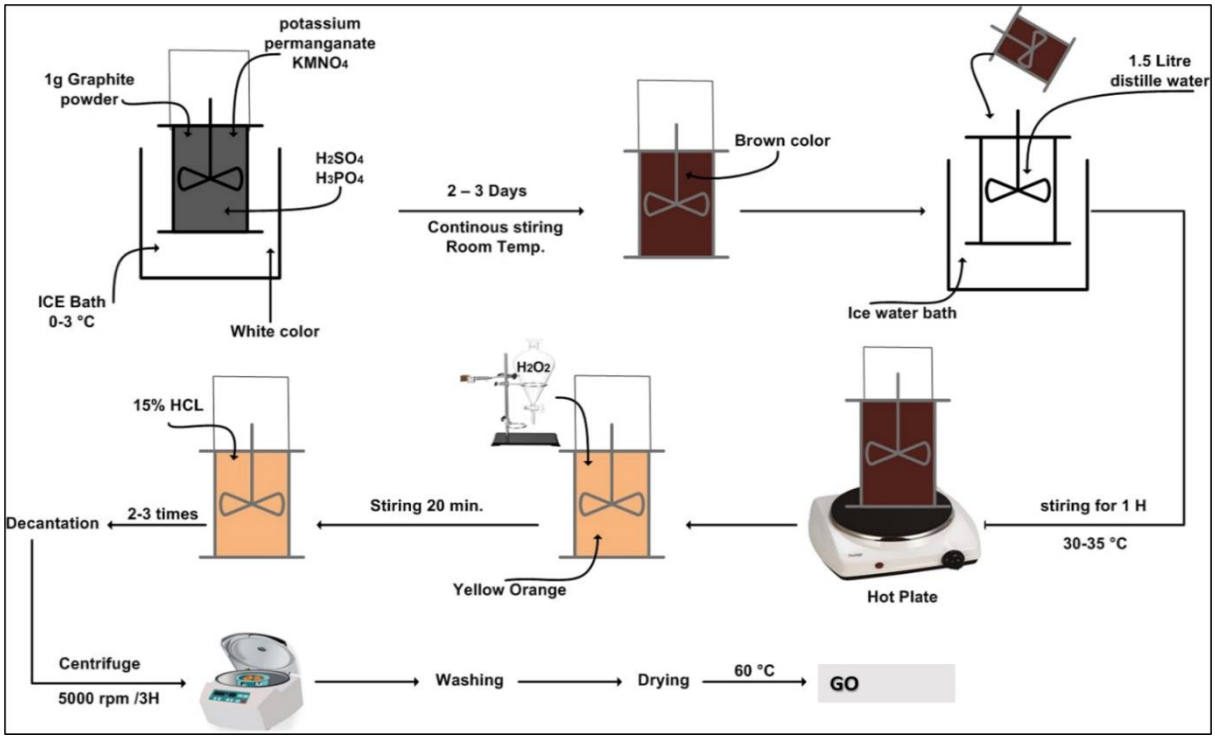

Figure 6-1 Schematic steps of synthesis of GO.

6.2.4 Preparation of NTO coated with GO layer

The GO/NTO explosive material composite was prepared using ultrasonication. First, GO powder was dispersed in a mixture of 30 mL of isopropanol and water (20:80 volume ratio) and sonicated for 30 minutes. NTO explosive was then carefully added to the mixture in portions with magnetic stirring for 1 hour in a water bath maintained at a temperature range of 5-10 °C. To ensure proper mixing, the samples were further processed in an ultrasonic bath (20 kHZ, 750 W, 120 V) for an additional 1 hour, with the water bath maintained at a temperature range of 3-5 °C. The ultrasonic bath was operated in a pulsed mode, with cycles 5 seconds on and 2 seconds off, the maximum temperature of the ultrasonic bath was 15 °C). GO was introduced to the NTO particles at different contents (1%,2%, 3%, 4% and 5% by weight) as shown in Table 6-1 (samples S1 to S5). The contents of the reaction flask were then filtered and washed several times with cold deionized water. Finally, the filtrate was dried in an oven at 60 °C for 12 hours under vacuum.

6.2.5 Preparation of NTO coated with GO/CuO composite layer

The GO/CuO/NTO explosive composite was prepared using the same technique by adding graphene oxide and copper oxide in varying proportions to the base material, NTO. First, GO powder was dispersed in 50 mL of acetone and sonicated for 30 minutes. Then, CuO nano powder was added to the dispersion followed by an additional 1 hour of sonication. NTO explosive was then carefully added to the mixture in portions with magnetic stirring for 1 hour. To ensure proper mixing, the samples were further processed in a sonic bath for 30 minutes in a water bath maintained at a temperature range of 5-10 °C. In these samples, the GO content was fixed at 3 wt.% relative to the NTO mass. CuO nanoparticles were incorporated into the GO matrix at different weight ratios (5%, 15%, 25%, 35% and 45%) relative to the total GO content. As a result, the CuO content in the final coating represented less than or more than 1 wt.% of the overall samples, depending on the specific ratio used in the experiments. A detailed summary of all prepared samples is provided in Table 6-1 (samples S6 to S10).

Table 6-1 Detailed summary of all prepared samples of GO/NTO and GO/CuO/NTO composite.

Sample ID	NTO %	GO %	CuO %
S0	100 %	0 %	0 %
S1	99%	1%	0 %
S2	98%	2%	0 %
S3	97%	3%	0 %
S4	96%	4%	0 %
S5	95%	5%	0 %
S6	97%	2.85%	0.15%
S7	97%	2.55%	0.45%
S8	97%	2.25%	0.75%
S9	97 %	1.95%	1.05%
S10	97 %	1.65%	1.35%

6.3 Results and discussions

6.3.1 Preparation of graphene oxide (GO)

GO was successfully prepared following the detailed steps outlined in section 6.2.3. The resulting material appeared in solution as a brownish-yellow aqueous dispersion after the oxidation and exfoliation steps. Visually, the product formed a stable suspension in water, indicating successful exfoliation of the graphite powder. The final yield of GO, calculated based on the initial mass of graphite and the mass after complete drying under vacuum at 60 °C for 24 hours was approximately 73.2%. The dried GO exhibited a brown color, as shown in Figure 6-3(d).

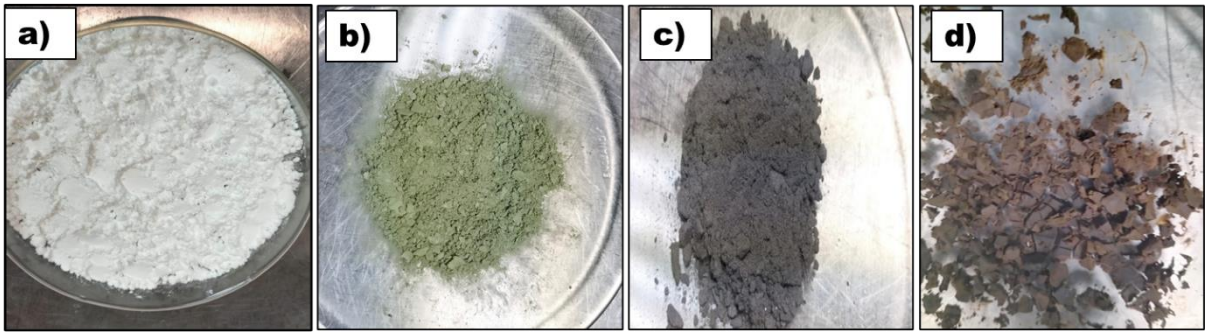

Figure 6-3 (a, b, c, d) Images of some prepared samples NTO, GO/NTO, GO/CuO/NTO and GO respectively.

To ensure the removal of all residual acids, the product was washed multiple times with acetone to eliminate any traces of sulfuric and phosphoric acid used during the synthesis process. Characterization by XRD and FTIR confirmed the successful preparation of GO in the following results. The elemental composition of the GO sample revealed a relatively high oxygen content by mass of w(O) = 0.6092±0.0201 and relatively low carbon w(C) = 0.3218±0.0179 indicating a highly oxidized structure prepared by the modified Hummers. Also, w(H) = 0.0282±0.0082, w(N) = 0.0017±0.0001 and w(S) = 0.0391±0.0006. From these results, the content of sulfur indicate that the sample needs further purification to reduce sulfur impurities. Also, the hydrogen and nitrogen contents fall within expected ranges.

6.3.2 Preparation of NTO coated with GO layer.

NTO explosive particles were successfully coated with GO. Visually, the color of the NTO particles changed to a dark green color, as shown in Figure 6-3(b). This may indicate the successful coating of NTO explosive powder with a uniform layer of GO, which was confirmed by the following results.

6.3.3 Preparation of NTO coated with GO/CuO composite layer

NTO explosive particles were also successfully coated with a hybrid GO/CuO composite. In these materials, the GO content was fixed at 3 wt.% relative to the NTO mass and CuO nanoparticles were incorporated into the GO matrix at different weight ratios (5%, 15%, 25%, 35% and 45%) relative to the total GO content. As a result, the CuO nanomaterial content in the final coating represented less than or more than 1 wt.% of the overall NTO material depending on the specific ratio used. Visually, the color of the NTO particles changed to a darker shade, as shown in Figure 6-3(c).

6.3.4 Characterization of all prepared samples

All prepared samples (TO, NTO, GO, NTO coated with GO and NTO coated with the GO/CuO composite material) were characterized to analyze and confirm their chemical composition, verify the structure of the NTO explosive material. The heat of combustion was also measured using a bomb calorimeter. In addition, the thermal decomposition kinetics of pure NTO, GO-coated NTO, and GO/CuO-coated NTO composites were evaluated using the Kissinger equation to assess the impact of the coating materials on the thermal behavior of pure NTO. This was done by conducting DSC experiments at different heating rates (0.5, 1, 2, 3 and 4 °C/min) for each sample. Moreover, mechanical sensitivity measurements were conducted at Defence Research and Development Canada (DRDC) Valcartier.

6.3.4.1 Fourier transform infrared (FTIR) spectroscopy analysis

FTIR spectra of all prepared materials, including SC: HCl, TO, NTO and graphite, were analyzed to confirm their structures and to serve as reference profiles for the coated explosives, GO/NTO and NTO/GO/CuO composites and GO material, to evaluate their structural modifications. The

FTIR spectrum shown in Figure 6-4 confirms the successful conversion of semicarbazide hydrochloride (SC: HCl) into TO, followed by its nitration to NTO. Several key characteristic absorption peaks were identified: a peak at 3212.8 cm^{-1} corresponding to the -HN-NH-alkyl fingerprint, which becomes more pronounced during the transformation from SC: HCl to NTO, and a peak at 1712.7 cm^{-1} assigned to the C=O functional bond, which was present in all three spectra (SC: HCl, TO and NTO). A peak at 1540.2 cm^{-1} in the fingerprint region was attributed to C=N stretching vibrations. This bond is absent in SC: HCl, appears in TO and becomes more intense in NTO. The nitro group appears at 1354.9 cm^{-1}, characteristic of the -C-NO_2 bond, which is not present in SC: HCl and TO but strongly appears in NTO, confirming the successful formation of the NTO explosive. These spectral changes validate the stepwise chemical conversion of SC: HCl into TO and its subsequent nitration to NTO. Additionally, the FTIR spectrum of GO was analyzed to identify functional group modifications compared to graphite powder. The results confirmed the presence of several characteristic functional groups, including a strong O-H stretching vibration at 3432.2 cm^{-1}, a carboxyl (C=O) stretching peak at 1718 cm^{-1} and a C=C stretching vibration at 1632 cm^{-1}. Peaks at 1118 cm^{-1} and 1232 c cm^{-1} were attributed to C-O stretching vibrations.

Furthermore, the FTIR spectra of NTO coated with GO and of NTO coated with a GO/CuO composite layer were analyzed to assess the impact of the coating materials on the structure of the NTO explosive. Comparison of the IR spectra of GO-coated NTO and GO/CuO-coated NTO with that of the reference NTO confirmed the presence of the same characteristic NTO peaks. This indicates that the coating process involved physical mixing without any chemical reactions. The FTIR spectra results for all samples align well with values reported in the literature for these materials [14,103,107,161,162,164].

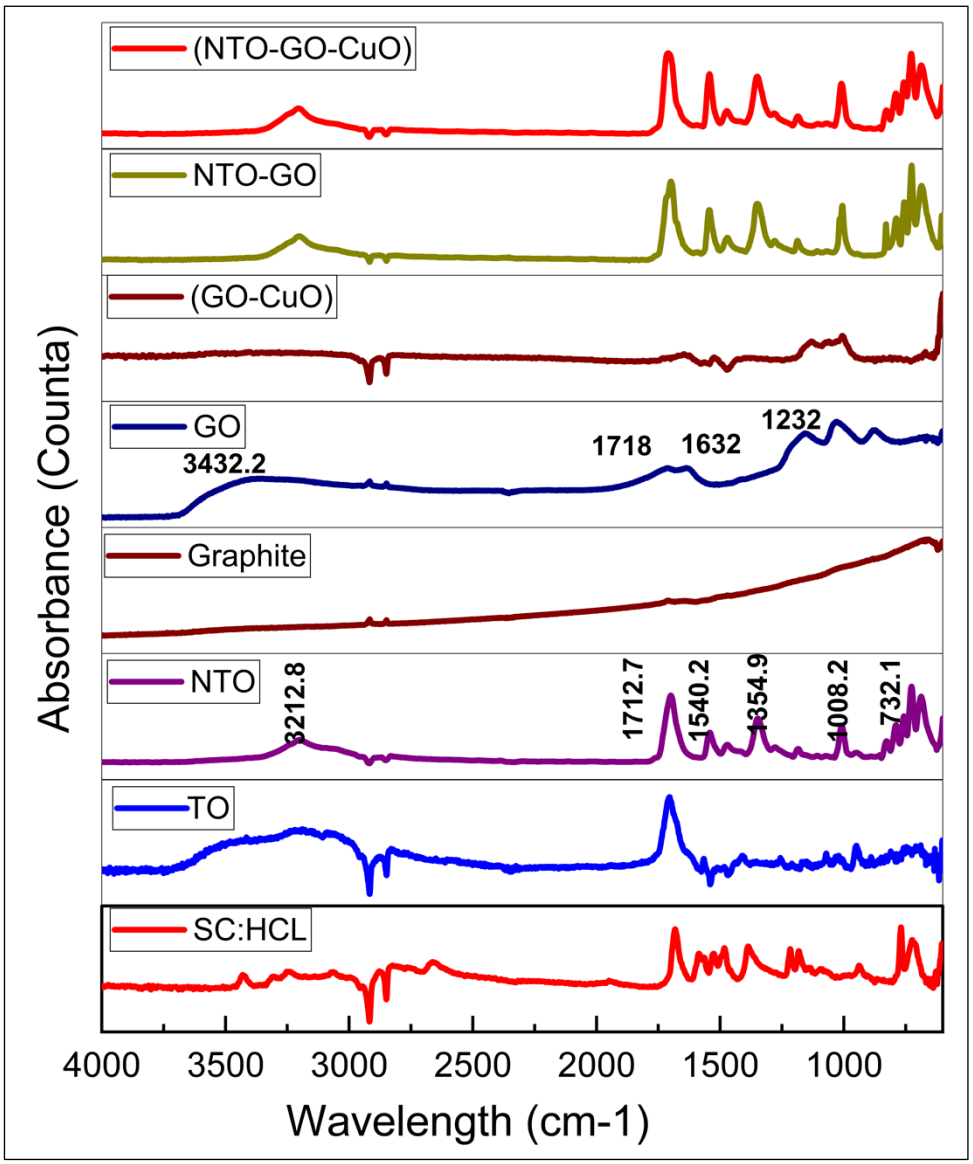

Figure 6-4 IR spectra of the prepared samples (SC: HCL, TO, NTO, Graphite, GO, GO-CuO, NTO-GO and NTO-GO-CuO).

6.3.4.2 X-ray diffraction analysis (XRD) results

X-ray diffraction (XRD) was also employed to analyze the structural properties of the prepared samples and to determine the interlayer spacing of GO. The XRD patterns of GO are presented in Figure 6-5. As shown, the pattern exhibits characteristic diffraction peaks at 2Θ = 12.8° and 26.1° corresponding to the (002) reflection of GO, with d-spacing values of 6.90 Å and 3.41 Å respectively. These values are significantly larger than that of natural graphite (3.34 Å), indicating

the successful introduction of oxygen-containing functional groups onto the GO. The XRD results align well with values reported in the literature [176]. Additionally, to investigate the impact of the coating process on the structure of NTO, XRD was conducted at the coated material because the goal was to evaluate whether coating NTO with GO or GO/CuO affected its crystalline structure. For NTO produced by conventional and flow methods, the product identity was already confirmed by NMR, FTIR, and DSC. The α-NTO phase was verified once using XRD and compared with literature data, and this pattern was used as the reference for coated NTO. This analysis was essential due to the polymorphic nature of NTO explosives. NTO exists in two polymorphic forms: α-NTO and β-NTO. Among these, α-NTO is more stable while β-NTO is unstable and decomposes within six months [101–103]. From the XRD patterns shown in Figure 6-5, the characteristic diffraction peaks of NTO are observed at 2Θ = 19.81°, 20.73°, 27.02° and 31.31° corresponding to the (111), (110), (025) and (006) crystal planes respectively. The alignment of these peaks with standard reference spectra confirm the presence of α-NTO.

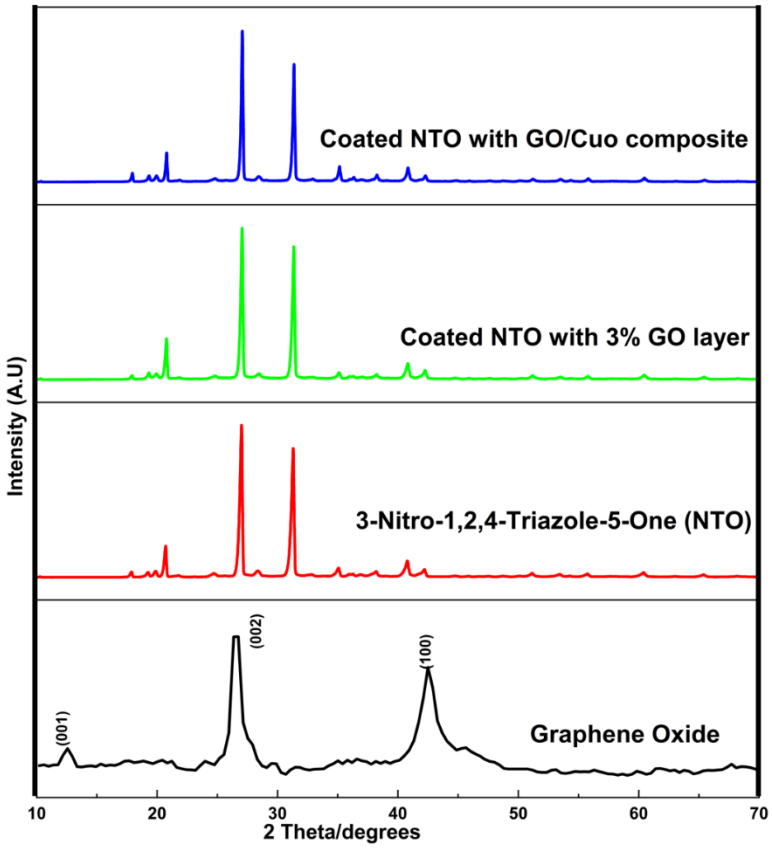

Figure 6-5 XRD patterns of prepared samples (GO, NTO, NTO/GO and NTO/GO/CuO).

For coated NTO, the diffraction pattern remains consistent with that of α-NTO indicating that the coating process does not induce a polymorphic transformation in NTO. Additionally, the characteristic peak of GO disappears in the diffraction pattern of the coated NTO-based material. This may be due to several factors reported in the literature. GO often loses its (001) diffraction peak when its layered structure becomes disordered due to exfoliation because strong interfacial interaction with the NTO particles led to interlayer spacing becomes non-uniform. Additionally, the relatively low GO content and the much stronger diffraction intensity of the highly crystalline NTO phase can overshadow the weak GO peak. These effects collectively lead to the absence of the GO signal in the coated NTO pattern.

6.3.4.3 Scanning electron microscopy (SEM) results

Scanning electron microscopy (SEM) was performed on the prepared samples using an FEI Quanta FEG 450 SEM, operated at 15 kV. SEM images were collected at different magnifications to illustrate the shape and distribution of the coated materials. As shown in Figure 6-6 (a, b, c) NTO particles exhibit a large, jagged cuboid shape with sharp, needle-like edges. Similarly, the NTO/GO crystals also display a large, jagged cuboid shape, indicating that the presence of a small amount of GO does not significantly alter the crystal morphology of NTO as shown in figure 6-7. However, a clear morphological difference is observed between pure NTO and GO-coated NTO. The surface of pure NTO appears smooth and clean (Figure 6-6) (b, c) while, after the addition of GO (1,3 wt.%), some wrinkles are visible on the crystal surface (Figure 6-7) (a, b, c, d, e, f), confirming that GO was successfully deposited on the surface of the NTO explosive particles.

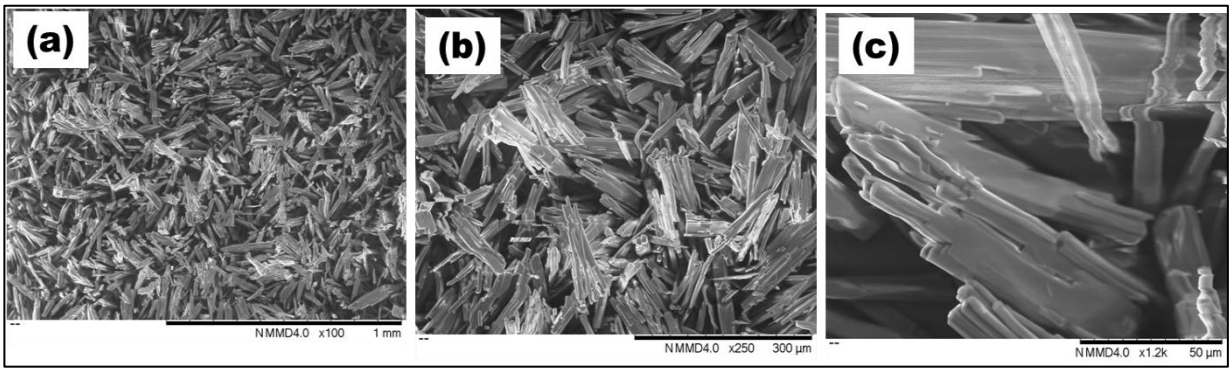

Figure 6-6 SEM of pure NTO at different magnification at (a, b, c).

On the other hand, when the GO content was increased to 4 wt.%, the nanomaterials appeared to be non-uniformly distributed across the surface of the NTO crystals, and agglomeration was observed, as shown in Figure 6-7 (h, j, k). This irregular distribution and agglomeration may potentially impact the thermal properties and overall stability of the coated samples, which will be discussed in detail in the following results.

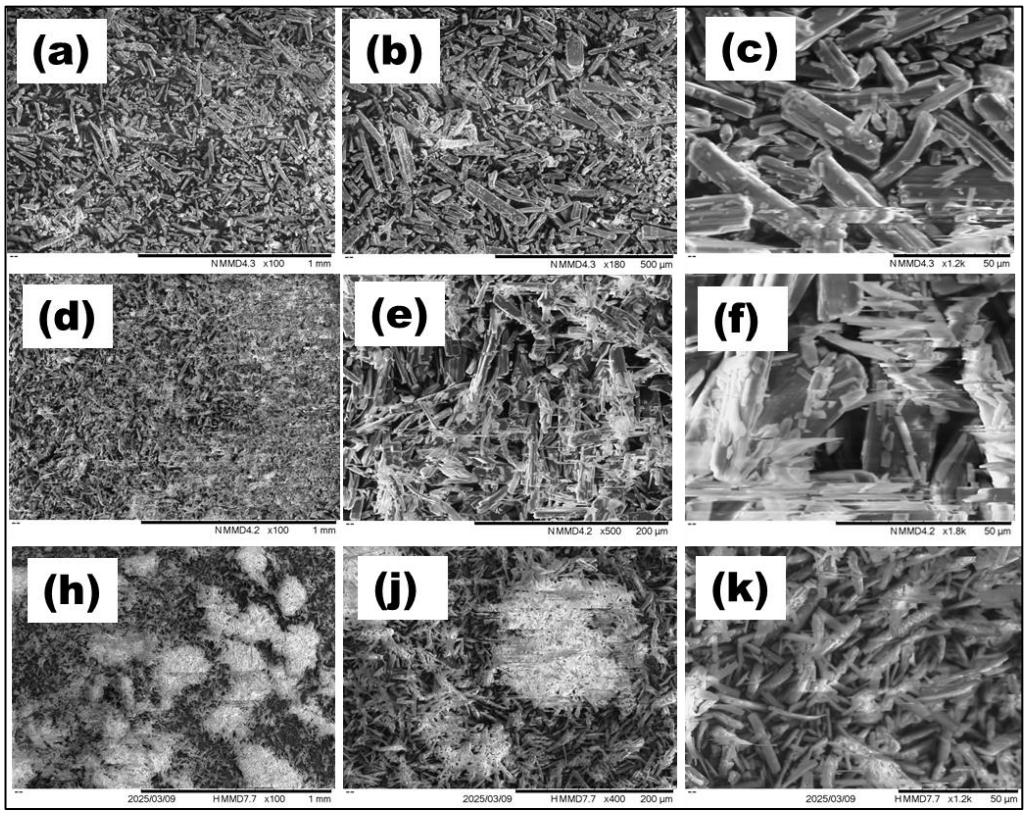

Figure 6-7 SEM of coated NTO with (1%,3%,4%) GO at different magnification at (a, b, c), (d, e, f), and (h, j, k) respectively.

Additionally, when nano CuO was incorporated into GO-coated NTO at different contents, distinct morphological differences were observed, as shown in Figure 6-8. At low CuO content, less than 1 wt.% relative to the overall NTO (corresponding to 5% CuO relative to the GO content), the nanomaterials were uniformly distributed across the entire surface of the NTO crystals without visible agglomeration, as shown in Figure 6-8 (a, b, c) respectively. A similar uniform coating effect was observed at 25% CuO, as shown in Figure 6-8 (d, e, f). However, at higher CuO contents, 45% (approximately more than 1 wt.% of the overall NTO), significant agglomeration of CuO

nanoparticles was observed, as shown in Figure 6-8 (g, h, j) respectively, leading to uneven surface distribution on the NTO crystals. This aggregation is expected to negatively impact both the mechanical sensitivity and thermal stability of the explosive material. This effect was further confirmed by thermal stability analysis and mechanical sensitivity as the following results, where samples with 35% and 45% CuO exhibited a significant decrease in decomposition temperature and activation energy, as detailed in the DSC results presented in the following results of this study.

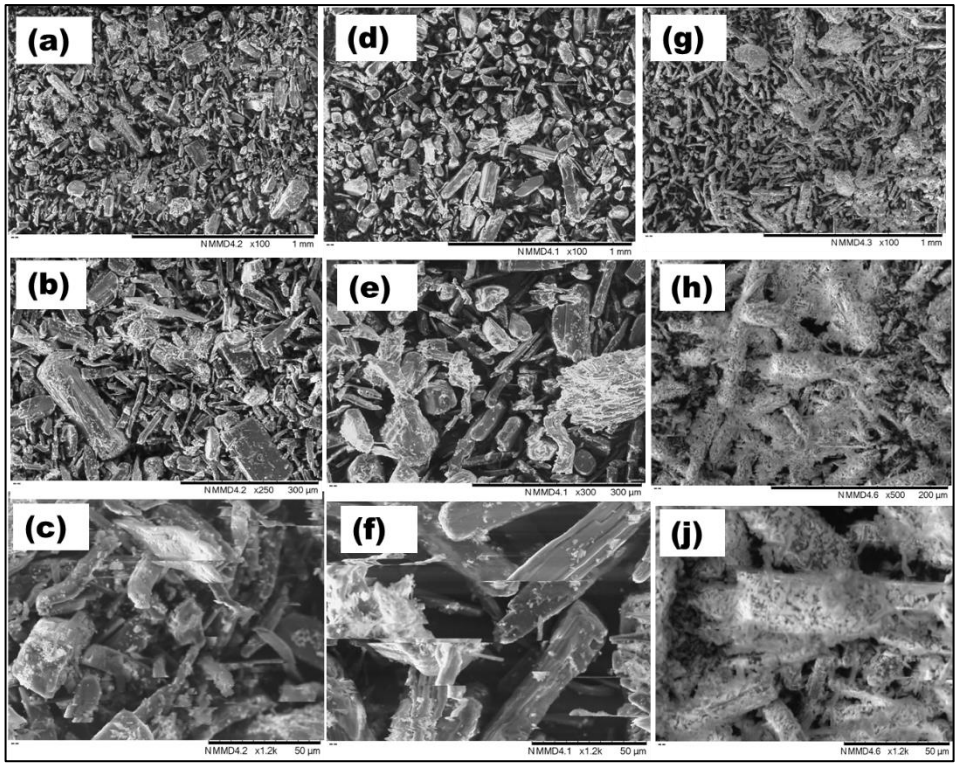

Figure 6-8 SEM images of (5%, 25%, 45%) CuO coating on NTO/GO explosive at different magnification at (a, b, c), (d, e, f), (g, h, j) respectively.

6.3.5 Thermal behavior results

Differential scanning calorimetry (DSC) was conducted to evaluate the thermal behavior of pure NTO explosive, as well as the coated materials, NTO/GO and NTO/GO/CuO composites, over a temperature range of 40 °C to 300 °C under a nitrogen (N_2) flow, with a heating rate of 1 °C /min. As shown in Figure 6-9 (a), the DSC curve of pure NTO exhibits a strong and sharp exothermic peak at approximately 264.4 °C, corresponding to the self-decomposition of NTO. This result is consistent with values reported in the literature [14,103,107]. The addition of GO or GO/CuO

composite as coating materials did not alter the nature of the exothermic peak of pure NTO, but these coatings significantly influenced both the onset and the maximum decomposition temperatures, as detailed in Table 6-2. The exothermic peak temperatures at a heating rate of 1 °C /min for NTO coated with varying GO content were recorded as 261.1 °C, 260.1 °C, 263.1 °C, 227.6 °C and 227.8 °C for 1%, 2%, 3%, 4% and 5% GO by weight respectively, as shown in Figure 6-9 (b, c) and Figure 6-10 (d, e, f). These results indicate that when the GO coating content is between 1 wt.% and 3 wt.%, the peak decomposition temperature remains relatively close to that of pure NTO.

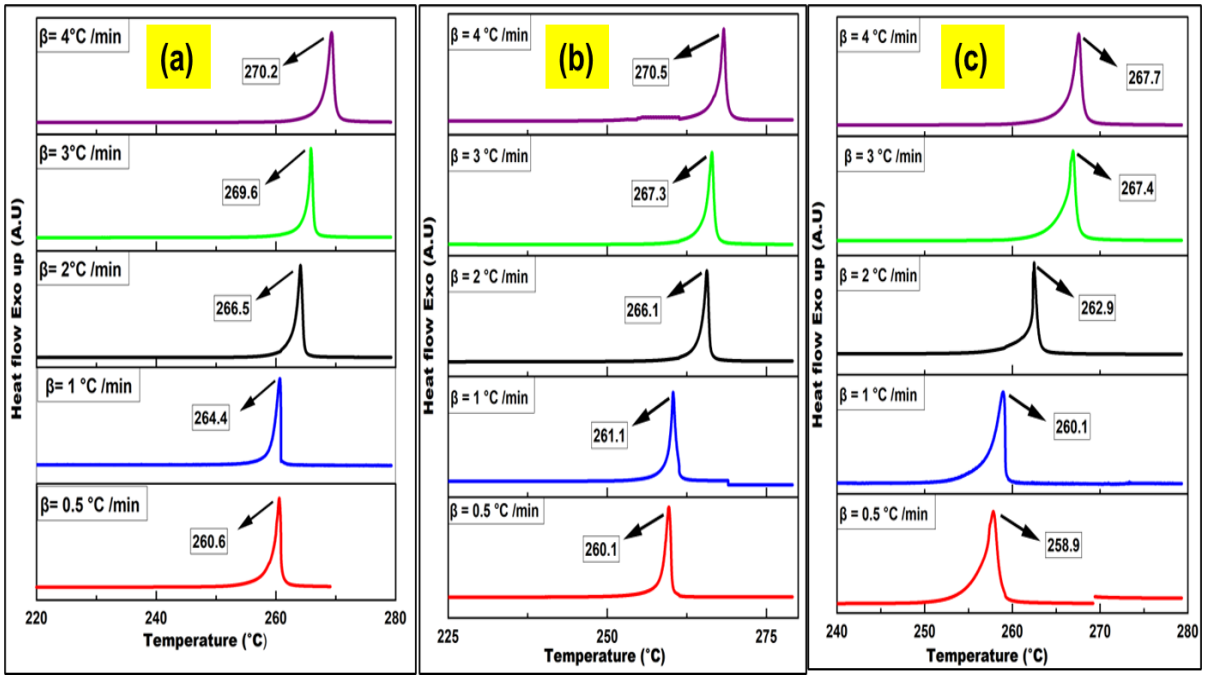

Figure 6-9 DSC curve at different heating rate (0.5, 1, 2, 3 and 4° C/min) for pure NTO and coated NTO/ GO materials with (1% and 2%) at (a, b, c) respectively.

However, when the GO coating increased to 4 wt.% and 5 wt.% there was a dramatic drop in the onset temperature from 260.3 °C in pure NTO to 221.8 °C and 221.4 °C for the 4 wt.% and 5 wt.% GO coated samples respectively. This onset temperature can be defined that the temperature at which the sample first shows a measurable deviation from the baseline due to the beginning of an exothermic event, it represents the start of the thermal decomposition before the reaction reaches its maximum rate. Similarly, the maximum decomposition temperature decreased from 264.4 °C in pure NTO to 227.6 °C and 227.8 °C respectively, suggesting a disruption in thermal stability. Furthermore, the difference in decomposition temperature between pure NTO and NTO coated

with 1-3 wt.% GO was less than 2 K, confirming that GO is thermally compatible with NTO at these concentrations. However, at higher GO contents (4 wt.% and 5 wt.%) this compatibility decreases likely due to the agglomeration of GO layers, which introduces defects in the thermal decomposition process and reduces stability.

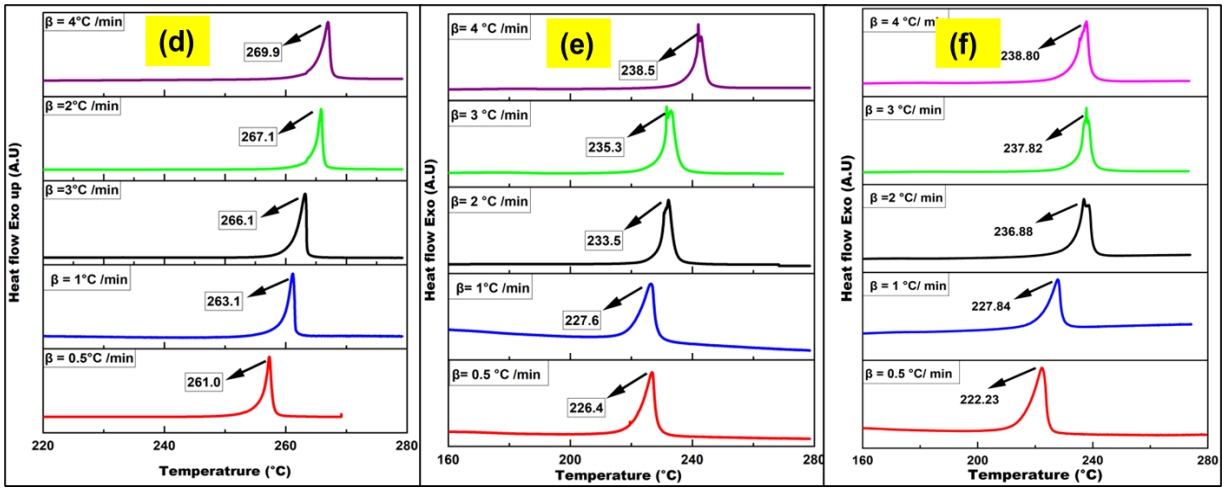

Figure 6-10 DSC curves at different heating rate (0.5, 1, 2, 3 and 4° C/min) for NTO/ GO materials with (3%,4%,5%) at (d, e, f) respectively.

Additionally, CuO nanoparticles were incorporated in different weight percentages into NTO coated with 3 wt.% GO while maintaining the total coating layer (GO/CuO) content at 3 wt.%. The decomposition peak temperatures corresponding to various CuO additions were recorded as 258.55 °C, 253.08 °C, 250.37 °C, 237.96 °C and 228.13 °C for 5%, 15%, 25%, 35% and 45% CuO by weight of the total coating layer, respectively, at a heating rate of 1 °C /min, as shown in Figure 6-11. These results indicate that when the CuO content is less than 25% of the 3 wt. % total coating layers (approximately equivalent to < 1 wt.% CuO on NTO) a moderate decrease in the peak decomposition temperature is observed from 264.4 °C in pure NTO to 258.55 °C, 253.08 °C and 250.37 °C for 5%, 15% and 25% CuO respectively. However, when the CuO content increases to 35% and 45% of the total coating layer (corresponding to more than 1 wt. % CuO on NTO) the decomposition temperatures drop sharply to 237.96 °C and 228.13 °C respectively. Also, Figure (6-11) (a, e) show slight distortions appeared in the shape of the exothermic peaks particularly at higher heating rates (3 °C/min.). These distortions do not reflect changes in the decomposition mechanism but are attributed to some limitations in the instrument's dynamic heat flow response.

The rapid and intense heat release from NTO based compositions can momentarily exceed the ability of calorimeter to compensate that leading to broadened or asymmetric peaks. Also, small variations in sample mass influence the rate of self heating and causing minor differences in the thermal feedback that affect the peak profile. In addition, the cooling and thermal equilibration capacity of the DSC instrument becomes more constrained at these conditions. Despite these effects, the onset and peak temperatures remained consistent across all heating rates.

These findings suggest that the catalytic effect of nano-metal oxides on NTO decomposition can be altered by the method of incorporation. It is well established that directly adding nano-metal oxides to NTO leads to a significant catalytic effect, lowering the decomposition temperature [168].

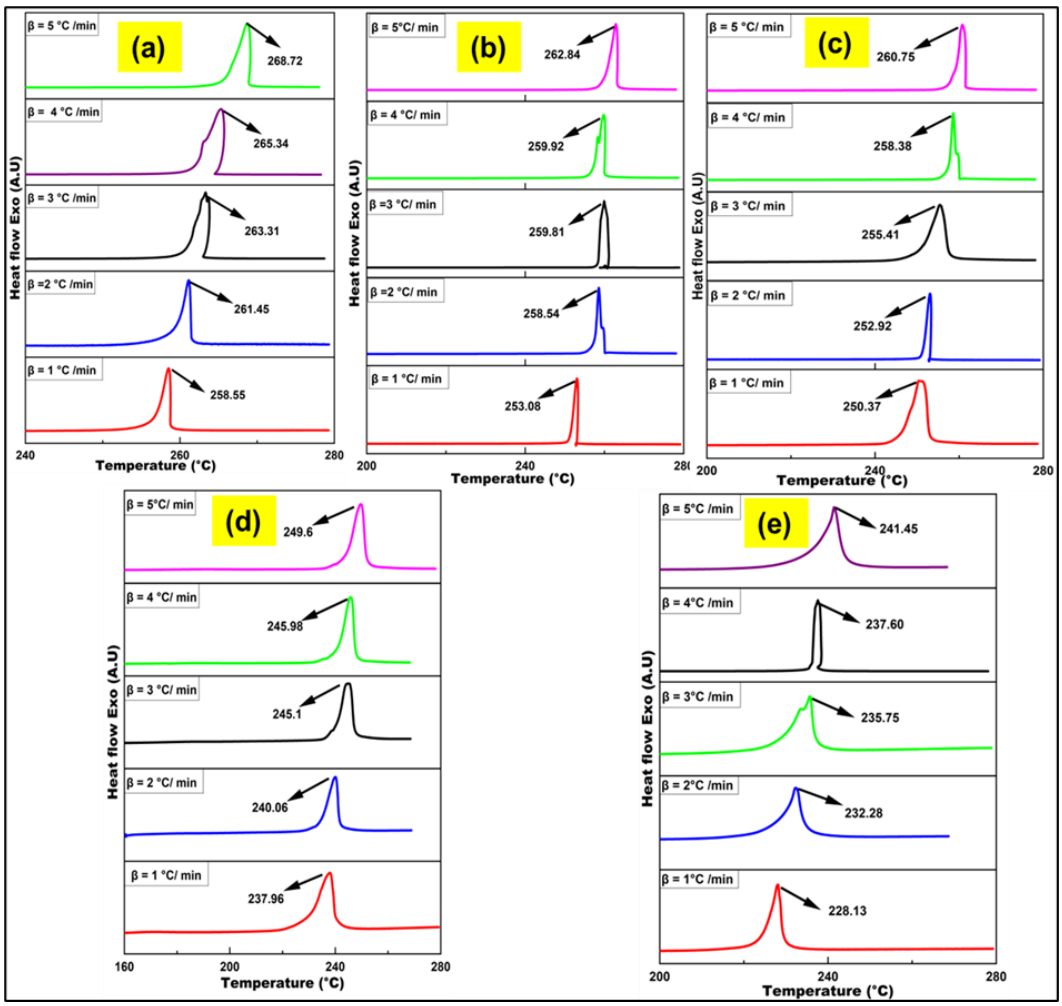

Figure 6-11 DSC curve at different heating rate (1, 2, 3, 4 and 5° C/min) NTO/CuO/ GO composite materials with (5% ,15%, 25%,35%,45%) at (a, b, c, d, e) respectively.

6.3.6 Kinetics and stability determination

To further evaluate the thermal decomposition kinetics of the coated materials NTO/GO and NTO/GO/CuO composites, kinetic parameters were calculated at different heating rates (0.5, 1, 2, 3 and 4 °C/min) using DSC measurements as shown in Figures 6-9, 6-10, and 6-11. The apparent activation energy (Ea) and the pre-exponential factor (A) were determined using the Kissinger equation, providing deeper insight into the role of GO and CuO on the thermal stability of NTO. The activation energy was calculated using Equation 6.1 [177].

$$\ln \frac{\beta}{T_p^2} = \ln \frac{A.R}{E} - \left(\frac{E}{R}\right) \frac{1}{T_p} \qquad \text{Equation (6.1)}$$

Where: (β represents the heating rate of the DSC experiment, Tp is the peak decomposition temperature at different heating rates, E is the activation energy (Ea), A is the pre-exponential factor and R is the universal gas constant).

For each heating rate, $\ln(\beta/T_p^2)$ was plotted against $1/T_p$, as shown in Figures 6-12 and 6-13. The resulting plots exhibit a linear relationship, indicating that the activation energy and pre-exponential factor can be determined from the slope and intercept of the corresponding regression lines. The calculated kinetic parameters for all prepared samples are summarized in Table 6-2. Additionally, as shown in Figures 6-9, 6-10 and 6-11, the decomposition peaks demonstrate that increasing the heating rate results in a shift toward higher peak temperatures in the exothermic decomposition curves are shown in Table 6-3. The calculated activation energy for pure NTO was approximately 505.03 kJ/mol, which aligns well with values reported in the literature [14,103,108].

The experimental results also revealed that when the GO content ranged between 1 wt.% and 3 wt.%, the activation energy remained relatively stable, thereby maintaining the thermal stability of NTO. The calculated activation energies were 443.3, 471.8 and 550.3 kJ/mol for 1%, 2% and 3% GO by weight respectively. However, at higher GO contents (≥4 wt.%) a significant reduction in activation energy was observed. Specifically, the calculated activation energies dropped to 331.2 kJ/mol and 230.2 kJ/mol for 4% and 5% GO respectively. This decline is likely attributed to the increased catalytic influence of the GO coating on the decomposition of NTO.

Based on these results, it can be concluded that when the GO content is precisely 3 wt.%, the activation energy increases by approximately 45 kJ/mol relative to pure NTO. This enhancement

is believed to result from the formation of a uniform, thin GO coating layer that effectively encapsulates the NTO particles. This interpretation is further supported by the SEM analysis, which showed no signs of particle agglomeration and confirmed the presence of a well-distributed coating. The observed improvement in activation energy at 3 wt.% GO may be attributed to several factors. Primarily, the GO layer acts as a thermal barrier that encapsulates the NTO particles. Its high thermal conductivity enables more uniform heat distribution, which prevents the formation of localized hotspots that could trigger premature decomposition. As a result, the decomposition of NTO shifts to a higher temperature, and the activation energy increases, indicating enhanced thermal stability. From the results, it was observed that at 3 wt.% GO, the coating does not introduce an excessive number of reactive functional groups on the NTO surface. This contributes to the stabilization of NTO without promoting its premature decomposition. In contrast, when the GO content was increased to 4 wt.% and 5 wt.% the decomposition process accelerated significantly. This was evidenced by the substantial drop in decomposition temperatures to 227.6 °C and 227.8 °C respectively, and the corresponding decrease in activation energy to 331.2 kJ/mol and 230.2 kJ/mol.

This marked reduction in activation energy at higher GO concentrations can be attributed to several factors. One primary reason is the increased presence of oxygen-containing functional groups (such as -OH, -COOH and C=O) at higher GO loadings. These groups enhance the chemical reactivity of the coating, particularly under elevated temperatures, thereby promoting earlier decomposition of the NTO and potentially catalyzing its breakdown. Furthermore, at high GO concentrations, the material appears to act more as a catalyst than as a stabilizer, thereby accelerating the thermal decomposition process. Another critical factor observed at these higher GO contents was the occurrence of particle agglomeration, as confirmed by SEM analysis.

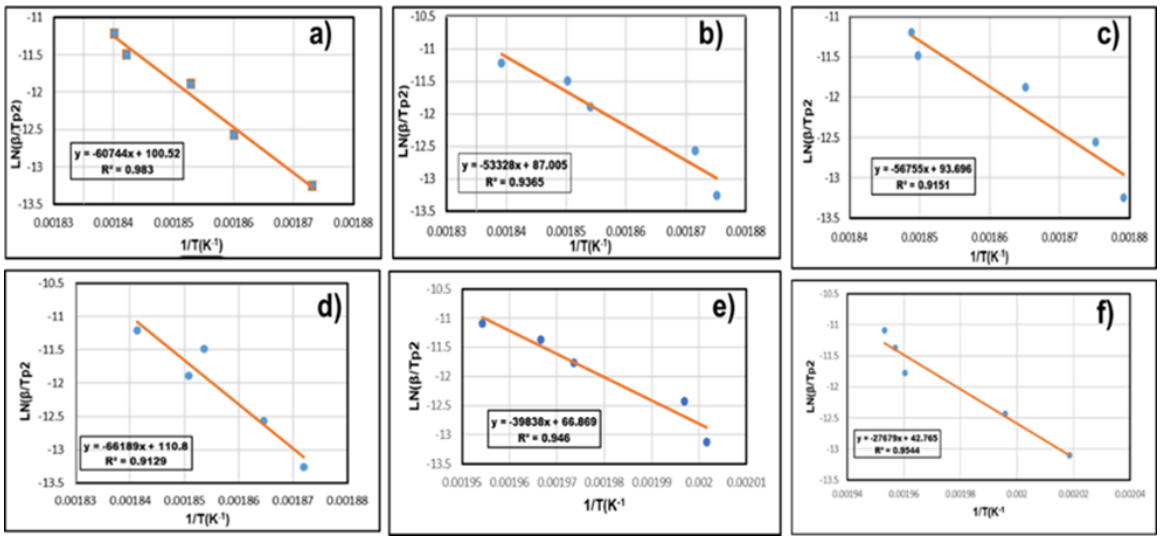

Figure 6-12 Fitted Kissinger activation energies results of NTO and NTO/ GO composite materials with (1% ,2%, 3%,4%,5%) at (a, b, c, d, e, f) respectively.

It was also found that at low CuO contents (5%-25% relative to the GO content, approximately equivalent to 1 wt.% CuO relative to NTO), the CuO/GO composite layer effectively maintained the thermal stability of NTO. This coating suppressed the typical catalytic effect of CuO nanoparticles, which are otherwise known to promote early decomposition of NTO. In this hybrid material, the presence of GO appeared to moderate the catalytic behavior of CuO. The observed peak decomposition temperatures, 258.55 °C, 253.08 °C and 250.37 °C, were very close to those of pure NTO and the 3 wt.% GO-coated NTO composite, confirming minimal thermal destabilization. This thermal behavior can be attributed to a synergistic interaction between GO and CuO. GO provides structural stability and high thermal conductivity, which helps disperse heat uniformly, while CuO acts as a controlled catalyst that enhances energy release without significantly reducing the decomposition temperature (by less than 10 °C). These findings suggest that the addition of CuO at low levels enhances the energy release rate of NTO without compromising thermal safety. This synergistic effect ensures a more regulated decomposition process and minimizes the risk of thermal runaway. Additionally, the high surface area of GO facilitates uniform dispersion and stabilization of CuO nanoparticles, improving their catalytic activity while maintaining thermal control. This controlled catalysis allows CuO to reduce the activation energy for decomposition in a manner that does not degrade the overall thermal performance of the NTO-based composite.

However, when the CuO content exceeded 25% of the coating layer, a significant reduction in both peak decomposition temperature and activation energy was observed. At 35% and 45% CuO, the decomposition temperatures dropped sharply to 237.96 °C and 228.13 °C, respectively. Correspondingly, the activation energies were drastically reduced to 291.85 kJ/mol and 255.51 kJ/mol. This decline in thermal stability is primarily attributed to the catalytic acceleration of the decomposition process. Given that CuO is both a strong oxidizer and an effective catalyst, its presence at high concentrations lowers the activation energy required for NTO decomposition, thereby promoting earlier and more rapid thermal breakdown.

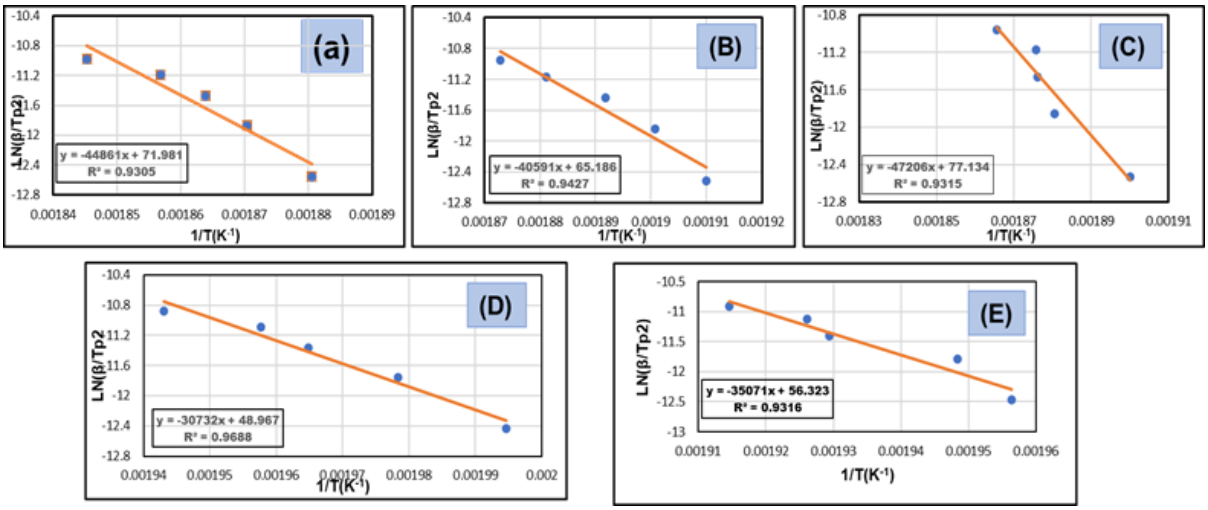

Figure 6-13 Fitted Kissinger activation energies results of NTO/CuO/ GO composite materials with (5% ,15%, 25%,35%,45%) at (a, B, C, D, E) respectively.

Table 6-2 Results of kinetic data for all studied samples.

Sample	T_o/°C					T_p/°C					T_e/°C				
	β /°C min $^{-1}$														
	0.5	**1**	**2**	**3**	**4**	**0.5**	**1**	**2**	**3**	**4**	**0.5**	**1**	**2**	**3**	**4**
NTO	259	260	264	266	266	260	264	266	269	270	262	265	269	271	274
S1	258	258	264	264	265	260	261	266	267	270	261	263	269	270	273
S2	257	257	258	258	259	258	260	262	267	267	260	263	265	269	270
S3	259	261	264	264	265	261	263	266	267	269	268	266	269	270	271
S4	220	221	227	227	231	226	227	233	235	238	230	234	239	243	245
S5	215	221	229	231	233	222	227	236	237	238	226	235	241	245	246
S6	256	256	260	259	266	258	261	263	265	268	264	265	267	268	277
S7	247	257	257	258	260	253	258	259	259	262	256	263	263	265	265
S8	247	249	251	256	259	250	252	255	258	260	261	263	265	267	267
S9	232	234	240	240	243	238	240	245	245	249	249	251	253	254	262
S10	213	216	216	227	220	228	232	235	237	241	240	243	246	242	252

Table 6-3 Results of DSC experipments at different heating rates for all studied samples.

Sample	Ea kJ / mol	R^2	Ln A/s^{-1}
NTO	505.03	0.98	107.4
S1	443.3	0.93	93.7
S2	471.8	0.91	100.5
S3	550.3	0.92	117.8
S4	331.2	0.95	73.3
S5	230.2	0.95	48.9
S6	372.9	0.94	78.6
S7	392.4	0.93	83.8
S8	337.4	0.94	71.7
S9	291.5	0.94	62.6
S10	255.5	0.97	55.2

6.3.7 Heat of combustion and sensitivity results

The average values of the heat of combustion for all prepared samples were measured experimentally using an oxygen bomb ParrTM 1341 Plain Jacket calorimeter and are summarized in Table 6-4. NTO has heat of combustion approximately 7292.3 J/g. This result for pure NTO showed strong agreement with literature values, which range from 7252 to 7654 J/g [14,103]. When NTO was coated with varying amounts of GO, a gradual decrease in the heat of combustion was observed. Specifically, the measured values were 7188.61, 6919.49, 6793.94, 6736.97 and 6682.24 J/g for GO loadings of 1%, 2%, 3%, 4% and 5% respectively. The decrease in heat of combustion is primarily due to the reduced fraction of NTO in the sample as GO is added. GO itself does not contribute to the combustion energy when compare with NTO, so the total energy per gram of sample decreases proportionally to the GO loading. However. the decrease in combustion heat was relatively minor and does not significantly impact the energetic performance of the material. On the other hand, incorporating CuO into the coating layer of GO/NTO particles resulted in a slightly higher heat of combustion compared to NTO coated only with GO. The

measured values were 6803.8, 6820.2, 6845.6, 6858.3, 6879.6 24 J/g for CuO loadings of 5%, 15%, 25%, 35% and 45% respectively. When NTO was coated with GO alone, the heat of combustion decreased because GO is non-energetic and reducing the fraction of NTO per gram of sample. Despite the oxygen-rich environment, which ensures sufficient oxidizer for complete combustion, the total energy per gram drops due to this dilution. In contrast, when NTO was coated with a GO/CuO composite, the heat of combustion increased compared to NTO/GO. Here, CuO acts as an energetic oxidizer and contributing additional chemical energy. The excess oxygen from the environment allows both NTO and CuO to fully react, so the net energy release is higher than in the NTO/GO sample, demonstrating that the difference in combustion enthalpy arises from the composition of the coating rather than oxygen availability. In contrast, the addition of GO improved the mechanical sensitivity of NTO by forming a uniform nanoscale coating that acts as both a thermal and physical barrier. Both friction and impact sensitivity was improved by increasing the content of GO. This layer reduces the likelihood of hot-spot formation under mechanical stress, thereby enhancing safety during handling and processing as shown in Table 6-4. The slight reduction in energy output was considered acceptable given the improvement in safety.

Table 6-4 Heat of combustion & (Impact - Friction) sensitivity results of the studied samples

Sample	Heat of combustion (J/g) (Exp.1)	Heat of combustion (J/g) (Exp.2)	Heat of combustion (J/g) (Exp.3)	Average Heat of combustion (J/g)	Impact sensitivity [J]	Friction sensitivity [N]
S0	7930.3	6722.9	7223.8	7292.3	7.5	220
S1	7169.0	7201.2	7195.6	7188.6	-	-
S2	6974.8	6959.6	6824.1	6919.5	-	-
S3	6844.2	6828.7	6708.9	6794.0	10	240
S4	6720.2	6780.5	6710.2	6736.9	-	-
S5	6702.1	6686.3	6658.3	6682.2	15	360
S6	6820.2	6790.3	6801.0	6803.8	-	-
S7	6730.2	6901.2	6829.2	6820.2	5	240
S8	6831.2	6842.4	6863.4	6845.6	-	-
S9	6827.3	6878.4	6869.2	6858.3	5	240
S10	6903.3	6872.4	6863.2	6879.6	-	-

6.4 Conclusion

NTO-based nanocomposites were developed by coating NTO particles with GO and CuO nanomaterials. GO was successfully synthesized using the modified Hummers method, and the nanocomposites (NTO/GO and NTO/GO/CuO) were prepared using an ultrasonic dispersion technique. The results demonstrated that the novel GO-coated NTO composites retained their original polymorphic crystal structure during the coating process, indicating structural stability. A significant observation was the impact of GO content on the thermal behavior of NTO. When the GO content exceeded 3 wt.%, the thermal stability began to deteriorate. At 4 wt.% GO, the activation energy dropped by approximately 174 kJ/mol and the initial decomposition temperature decreased by 34.3 °C compared to pure NTO. At 5 wt.% GO, the reductions became more pronounced, approximately 275 kJ/mol in activation energy and 38.4 °C in decomposition temperature. In contrast, the addition of 3 wt.% GO led to some enhancement, with the activation energy increasing by about 45 kJ/mol relative to pure NTO, indicating improved thermal stability at this particular concentration. A novel contribution of this work was the successful incorporation of CuO nanoparticles, approximately less than 1 wt.% relative to NTO into the GO coating layer, forming a hybrid NTO/GO/CuO nanocomposite. This was achieved without significantly accelerating the catalytic decomposition of NTO. At low CuO contents (5% to 25% relative to the GO coating) the GO/CuO hybrid coating effectively maintained the thermal stability of NTO. However, when CuO content exceeded 25% of the GO layer, a dramatic decrease in both peak decomposition temperature and activation energy was observed. At 35% and 45% CuO content, the decomposition temperatures dropped sharply to 238.0°C and 228.1 °C respectively, while the activation energy decreased to 291.9 kJ/mol and 255.5 kJ/mol. The heat of combustion measurements confirmed that GO coating on NTO slightly reduces energy output, while significantly enhancing safety by improving the mechanical sensitivity (impact and friction) of the NTO particles. These results clearly demonstrate the novel balance achieved in this study between enhancing energy release through CuO addition and preserving thermal stability through controlled composite design and improved the mechanical sensitivity of the composition.

CHAPTER 7 CREATING AN ALTERNATIVE TECHNIQUE INSTEAD OF MELT CAST TECHNIQUE (IMX101-IMX104) FOR DEVELOPING NEW PBXS MATERIALS BASED ON NTO EXPLOSIVES AND ENERGETIC BINDER GAP

7.1 Introduction

The main advancement in the field of energetic materials lies in the development of novel explosive compositions that combine high detonation performance, low mechanical sensitivity, and good thermal stability [178]. However, a well-known challenge in this area is the trade-off between performance and sensitivity because enhancing explosive power often leads to increased vulnerability to external stimuli [179-182]. The design of next-generation weapon systems demands energetic materials that strike a careful balance between powerful detonation characteristics and reduced risk during handling, storage, and transportation. To address this, researchers have formulated various energetic compositions aligned with the principles of insensitive munitions. These efforts have employed processing techniques such as melt casting and cast-cured methods to produce PBXs. PBXs are typically composed of crystalline explosive fillers embedded in a curable binder matrix. Traditionally, high-performance PBX materials have relied on nitramine explosives such as RDX, HMX and PETN combined with both inert and energetic binders. While these materials deliver excellent detonation properties, they are often associated with high sensitivity to impact and friction [69, 79,80-85, 95-100]. In response, melt-cast explosive compositions such as IMX-101 and IMX-104 were introduced to improve safety [4]. These compositions are based on low-sensitivity explosives like NTO and 2,4 Dinitroanisole (DNAN) effectively reducing impact and friction sensitivity. However, this improvement comes at the expense of detonation performance. The detonation velocities of IMX-101 and IMX-104 are 6885 m/s and 7420 m/s respectively, significantly lower than those of nitramine-based PBXs. Moreover, DNAN raises environmental concerns, further limiting its applicability [4, 105-108].

To overcome these limitations, it is essential to develop a novel class of energetic compositions that merges the high detonation performance of nitramine-based explosives with the low sensitivity profile of IMX materials. One promising route is the incorporation of 3-nitro-1,2,4-triazol-5-one

(NTO) into PBX matrices with energetic binder GAP. NTO offers a compelling combination of low sensitivity and reasonable performance making it a suitable candidate for next-generation IM compositions [14,103,106].

The work presented in this chapter integrates and builds upon the findings of the previous objectives to deliver a comprehensive and practical formulation strategy. As a first step, recrystallization procedures were applied to NTO to improve particle morphology and increase the packing density, thereby allowing for a higher explosive content within the PBX compositions. Subsequently, a series of novel PBX compositions were developed using a Thinky Mixer (model ARV-310) to systematically investigate performance and sensitivity characteristics. The NTO content was gradually increased to determine the maximum loadable amount that could be homogeneously and stably incorporated into the GAP binder. A binder-to-curative NCO/OH ratio of 1.2 was found to be optimal, providing improved elasticity and mechanical integrity across all compositions. In addition to the base composition (NTO/GAP), novel modified PBX materials were prepared by incorporating NTO coated with graphene oxide (GO), and NTO coated with both GO and nano-CuO, using the same cast-cured method. The morphological structure of the PBXs was examined using SEM spectroscopy, while their mechanical sensitivity (impact and friction) was compared with existing insensitive materials such as IMX-101 and IMX-104 and other nitramine-based PBXs materials. Furthermore, the thermal stability and kinetic behavior of the PBX compositions were evaluated using two methods. The heat of combustion was measured experimentally using bomb calorimetry, and the detonation parameters were calculated using the EXPLO5 program.

This chapter successfully fulfills the objective of formulating novel NTO-based PBXs incorporating GAP binder, offering enhanced detonation performance while improving or maintaining mechanical sensitivity (impact and friction) within acceptable limits for insensitive munitions applications.

7.2 Materials and methods

7.2.1 Materials and instruments

The required components for synthesis include NTO explosives that was prepared in the previous chapters, GAP 5527 prepolymer, GAP700 plasticizer, Dicyclohexylmethane 4, a-Diisocyanate (HMDI) $C_{12}H_{22}N_2O_2$, Desmodur N100 A (poly (hexamethylene diisocyanate) trimer (trifunctional ,3 NCO groups per molecule) (product no. 85806123), were obtained from defence research and development Canada. The analytical instruments and techniques used for characterization are as described in section 6.2. The density of PBX samples was determined using the Archimedes principle. Each sample was accurately weighed and then completely immersed in water. The volume of water displaced was measured and the density of the sample was calculated by dividing its mass by the displaced volume. The particle size of NTO was evaluated using scanning electron microscopy. For each SEM image, particles were measured and their individual lengths were recorded. The average particle size was calculated to determine the mean particle size of NTO before and after recrystallization. It should be noted that while this method provides an estimate of the average particle size, it does not provide a complete particle size distribution due to the limited number of particles analyzed.

7.2.2 Recrystallization of NTO explosive particles

To increase the explosive content in PBX compositions, the prepared NTO was recrystallized to adjust its particle size and morphology for improved packing density, this improved packing density allows for a higher solid loading of explosive in the PBX compositions, increasing the practical explosive content per unit volume. Recrystallization was performed using a stepwise cooling process. Specifically, crude NTO was dissolved in hot distilled water at approximately 95 °C in a 500 mL beaker equipped with an agitator and placed on a hot plate. After the NTO particles were completely dissolved, the saturated solution was gradually cooled to room temperature over a period of approximately 3 hours under ambient conditions. The solution was then transferred to a refrigerator maintained at 5-7 °C and held for 24 hours to complete the crystallization process. This sequential cooling approach promoted the growth of large NTO crystals.

7.2.3 Preparation of PBXs composite materials based on NTO and GAP binder

To optimize the processing conditions for the PBX materials, several compositions were prepared using a Planetary Centrifugal Vacuum Mixer (Thinky mixer) (model ARV-310) by adjusting the mixing time, mixing speed and vacuum level to achieve optimal homogeneity and blending quality. Different PBX compositions were also prepared to determine the ideal NCO/OH ratio, ranging from 0.9 to 1.5. Among these, a ratio of 1.2 was selected based on visual and manual assessment of the cured PBX samples. At this ratio, the paste displayed good homogeneity and workability, and the cured binders were neither excessively hard nor brittle. Consequently, all subsequent samples were prepared with an NCO/OH ratio of 1.2. Prior to use, NTO was dried at 60 °C for 24 hours and then weighed accurately. GAP-5527 polymer was blended with GAP-700 plasticizer and mixed at 40 °C for 30 minutes, followed by homogenization in the thinky mixer for 2 minutes. NTO was then gradually added into the binder system in 2-3 portions over a span of 30 minutes without vacuum to allow for controlled dispersion. Once all the NTO powder had been incorporated, the mixture was subjected to high-speed mixing at 2000 rpm under vacuum for 40 minutes to ensure complete coating and uniform distribution. Subsequently, the curing agents HMDI and N-100 were added, and the mixture was further mixed for an additional 30 minutes under the same vacuum and speed conditions. The final paste was cast into pre-prepared molds and cured under vacuum at 55-60 °C for 10-15 days. Similarly, PBX materials based on NTO coated with GO and those coated with GO/CuO were prepared following the same procedure. In all samples, a blend of course and fine NTO particles was employed to enhance packing density and reduce voids in the PBX matrix. This approach led to improved mechanical properties and enhanced detonation performance of the resulting PBX materials. A summary of all prepared samples is provided in Table 7-1.

Table 7-1 Summary of prepared PBXs samples

Sample ID	NTO (wt.)	NTO/GO	NTO/GO/CuO	GAP 5527 polymer	GAP 700 plasticizer	N-100	HMDI
F1	66 %	-	-	24%	5.3%	1%	3.5%
F 2	68 %	-	-	22.31%	5.3%	1%	3.28%
F 3	70 %	-	-	20.50 %	5.3 %	1%	3.05%
F 4	72 %	-	-	18.76%	5.3%	1%	2.83%
F 5	74 %	-	-	16.99%	5.3%	1%	2.60%
F 6	76.5 %	-	-	14.77%	5.3%	1%	2.32%
F 7	-	76.5 %	-	15.21%	5.3%	1%	2.38%
F 8	-	-	76.5 %	15.21%	5.3%	1%	2.38%

7.3 Results and discussion

7.3.1 Recrystallization of NTO explosive particles

The prepared NTO particles exhibited a jagged, rod-like morphology and appeared as a very fine white powder, as shown in Figure 7-1(a). This fine particle size led to agglomeration during mixing with the GAP binder and limited the achievable explosive loading in the PBX material. Based on our initial experiments, the maximum practical loading of NTO in the binder system was approximately 69 wt.%. Beyond this content, excessive agglomeration occurred on the binder surface, resulting in inhomogeneous mixtures. To increase the explosive content in PBX compositions, the prepared NTO was recrystallized to adjust its particle size and morphology for improved packing density, this improved packing density allows for a higher solid loading of explosive in the PBX compositions, increasing the practical explosive content per unit volume, as shown in Figure 7-1(b). SEM images of the recrystallized NTO are presented in Figure 7-2(a, b).

After recrystallization, the particle size of NTO ranged from 165 to 398 µm, with an average particle size of 311.2 µm. In comparison, the original synthesized NTO exhibited particle sizes ranging from 13.4 to 23.3 µm, with an average size of 19.1 µm, as shown in Figure 7-3(c, d).

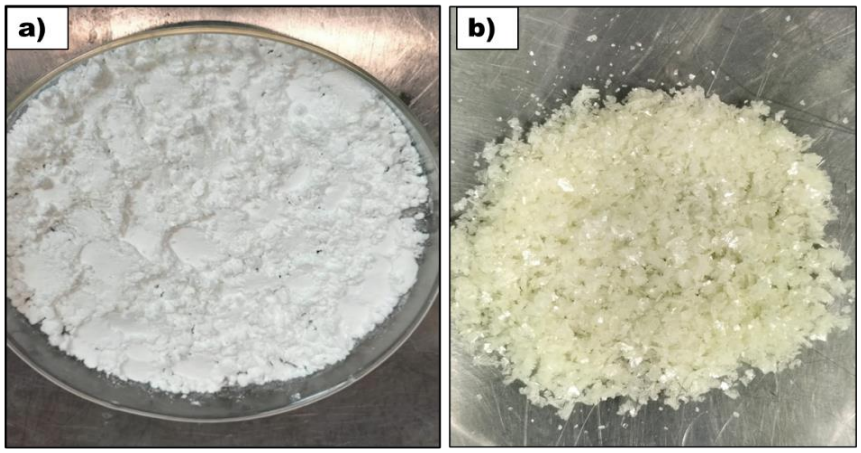

Figure 7-1 (a) NTO as very fine white powder before recrystallization, (b) NTO as coarse particles after recrystallization.

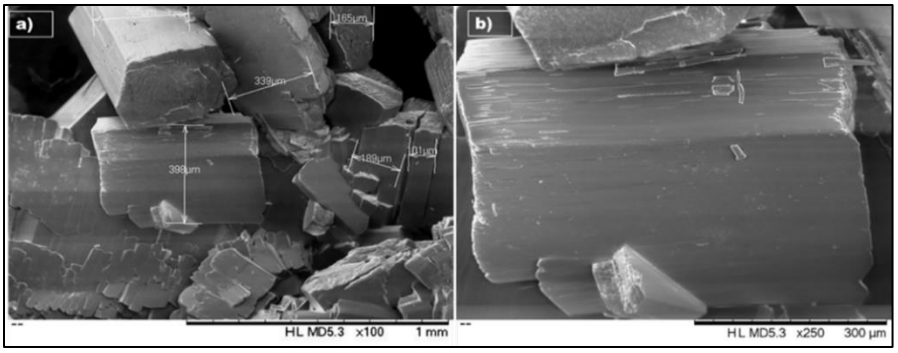

Figure 7-2 SEM images of recrystalized NTO at 1mm and 300 µm (a, b) respectively.

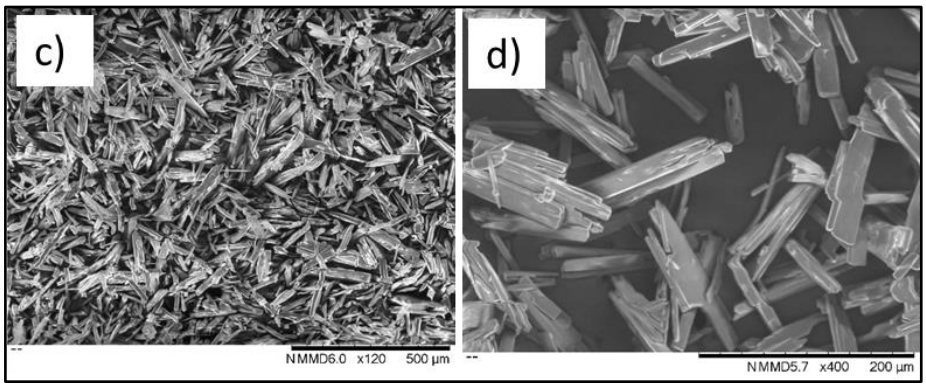

Figure 7-3 SEM images of NTO at 500 µm and 200 µm magnification (c, d) respectively

To confirm the crystal form of the recrystallized NTO samples, XRD analysis was performed, as shown in Figure 7-4, to investigate the impact of the recrystallization process on NTO particles. This analysis was crucial because the polymorphic nature of NTO significantly influences the performance of energetic materials, as previously discussed. NTO exists in two polymorphic forms: α-NTO and β-NTO. Based on the XRD patterns of both the original and recrystallized NTO particles, the diffraction pattern of the recrystallized NTO remained consistent with that of α-NTO. This indicates that the recrystallization process did not alter the polymorphic form of NTO.

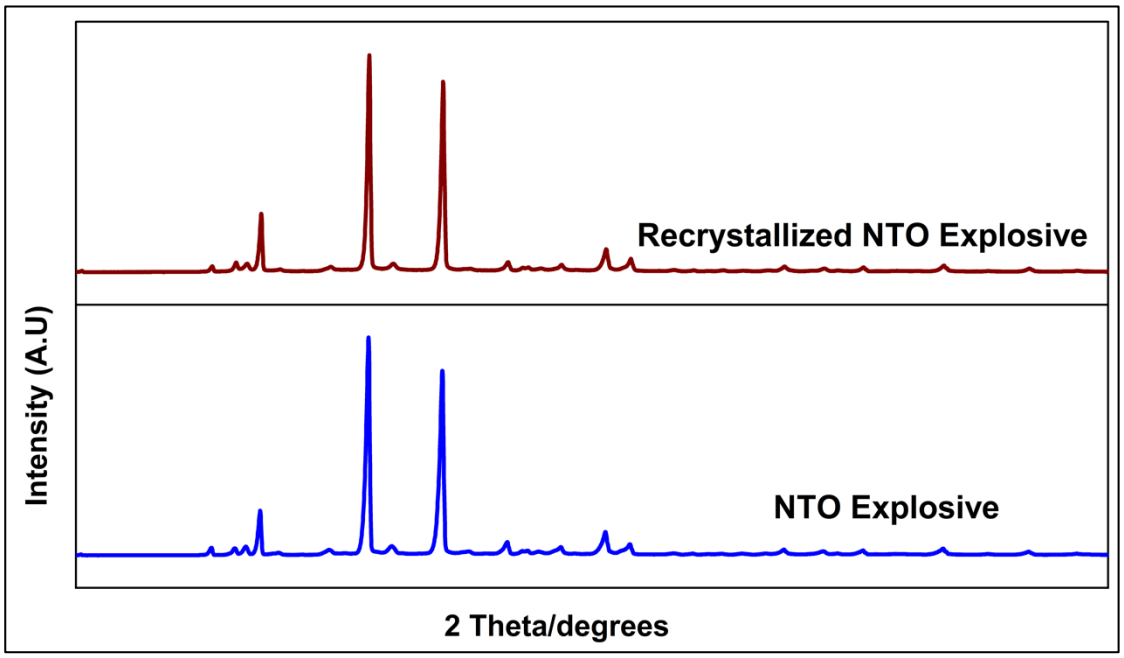

Figure 7-4 XRD patterns of NTO before and after recrystallization

7.3.2 Preparation of PBXs materials based on NTO and GAP binder

Several PBXs materials were prepared using a thinky mixer model ARV-310. A ratio of 1.2 for NCO/OH was selected for all PBXs materials prepared in this study. The high performance of an explosive is usually accompanied by an increase in explosive sensitivity. In our study, we aimed to develop PBXs materials that balance performance and sensitivity by using GAP polymer as an energetic binder to increase the overall performance of the prepared PBXs materials and at the same time reduce their mechanical sensitivity. synergistic balance of mechanical and energetic performance in PBX formulations. GAP-5527 contributes high energy due to its positive heat of

formation and offers structural cohesion, but its relatively rigid network can lead to some brittleness. Incorporating an energetic GAP plasticizer lowers the glass transition temperature, improves flexibility and processability and enhances compatibility within the polymer matrix. This compatibility is particularly important: if a different or non-matching plasticizer were used, phase separation, plasticizer migration or uneven mechanical properties could occur compromising long-term stability and safety. Because the GAP plasticizer is chemically compatible and also energetic, it preserves or even increases the overall energy output compared to inert alternatives. Combining both components allows fine-tuning of toughness, ductility, curing behavior and energy density achieving properties that neither GAP-5527 nor a GAP plasticizer alone could provide. To develop these PBXs materials, we used NTO as the core of the new PBXs composition. NTO coated with 3 wt.% GO was selected because this coated material (NTO/GO) at that GO content showed improved thermal stability based on our previous results. The coated NTO with 3 wt.% GO exhibited an activation energy approximately 45 kJ/mol higher than that of pure NTO. This modification was introduced to investigate whether incorporating GO-coated NTO into the PBXs material would enhance the thermal properties of the final formulation compared to the original PBXs composed only of NTO and GAP or whether it would result in a different thermal behavior. The results showed that the highest solid loading of NTO in the PBXs material was 76.5% by weight of the total PBXs composition. Beyond this percentage, the mixture became uneven, and NTO powder started collecting on the surface instead of blending properly into the paste. Also, the best combination of particle sizes was found to be 40% coarse NTO and 60% fine NTO by weight. This mix gave the highest packing density in the PBXs and allowed up to 76.5% NTO loading. It was observed from the experipments, using finer NTO content caused the particles to stick together (particle agglomeration) and made the mixture less uniform. On the other hand, using coarser NTO content made the large particles stand out and led to uneven distribution in the material.

7.4 Characterization of PBXs samples

7.4.1 Elemental analysis results

The carbon, hydrogen, and nitrogen contents of the prepared PBXs samples were measured using a flash smart CHNS-O elemental analyzer. Then, the measured nitrogen values were used to recalculate the exact chemical formulas of each PBXs material. The chemical formula for all

prepared PBXs material was shown in Table 7-2. These chemical formulas were later used as input data to calculate the detonation properties of the PBXs material using the EXPLO5 program.

7.4.2 Scanning electron microscopy (SEM) results

SEM was conducted on our PBXs materials, and their images are shown in Figure 7-5: (a, b) for the main composition PBXs material 76.5% NTO/GAP, (c, d) for 76.5% NTO/GO/GAP and (e, f) for NTO/GO/CuO/GAP. Based on the images below, the GAP binder appears to successfully encapsulate the NTO particles in all PBXs samples because no distinct needle-like NTO crystals were observed. This suggests that the binder effectively coats and surrounds the NTO particles. Also, among the images, the composite containing only NTO and GAP (a, b) exhibited the most uniform mixture, indicating excellent binder-explosive interfacial adhesion and homogeneous matrix distribution. In the second composition (c, d), the incorporation of GO at low content resulted in fairly well-dispersed nanoflakes throughout the binder matrix. This observation aligns with our previous results, which show that low GO loadings (≤3 wt.%) tend to promote uniform dispersion and no agglomeration. Slight variation was observed in the SEM images of the NTO/GO/CuO/GAP composite materials (e, f). This may be attributed to the interaction between GO and CuO particles, which can affect their distribution and compatibility with the polymer binder. Nevertheless, no major agglomeration or phase separation was detected, indicating an overall acceptable level of dispersion in the three PBXs materials.

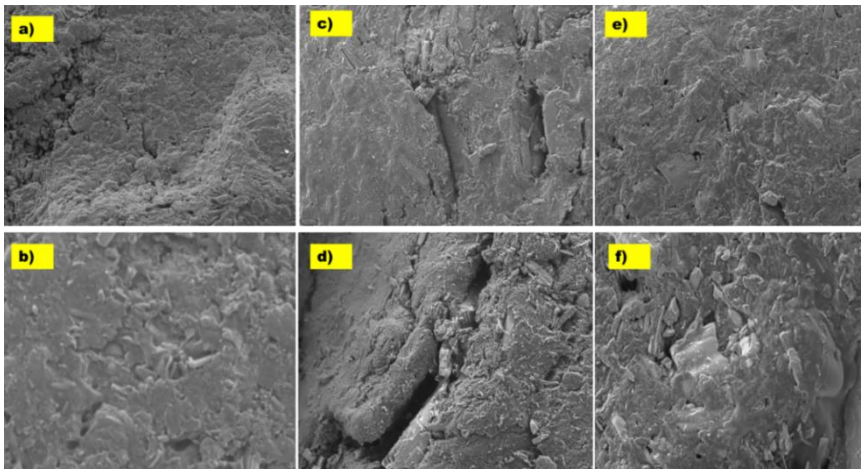

Figure 7-5 SEM images of (a, b) NTO / GAP, (c, d) NTO / GAP / GO, and (e, f) NTO / GAP/ GO / CuO composite materials respectively.

Table 7-2 Results of the experimental measurements of prepared PBXs.

No.	NTO content (wt.%)	Summary formula	Heat of combustion (J/g) (Exp.1)	Heat of combustion (J/g) (Exp.2)	Average combustion Heat (J/g)	Enthalpy of formation [kJ /mol]	Heat of explosion (kJ/kg)
F0	NTO	$C_2H_2O_3N_4$	6722.9	7223.8	6973.3	-129.4 [1]	4049.3
F1	66 NTO	$C_{3.01}H_{4.14}N_4O_{2.42}$	14826.0	14525.6	14675.8	206.2	4224.9
F2	68 NTO	$C_{2.81}H_{4.10}N_4O_{2.55}$	13617.9	14317.3	13967.6	190.0	4384.4
F3	70 NTO	$C_{2.75}H_{4.01}N_4O_{2.56}$	14087.1	13188.9	13638.1	173.2	4391.2
F4	72 NTO	$C_{2.73}H_{3.92}N_4O_{2.58}$	13064.6	13564.4	13314.5	141.5	4402.2
F5	74 NTO	$C_{2.58}H_{3.68}N_4O_{2.59}$	13173.1	12473.1	12823.1	153.7	4433.9
F6	76.5 NTO	$C_{2.45}H_{3.57}N_4O_{2.67}$	12153.0	12065.9	12109.9	120.3	4494.1
F7	76.5 NTO/ GO	$C_{2.89}H_{3.48}N_4O_{2.87}$	13121.9	12221.3	12671.6	141.6	4475.8
F8	76.5 NTO/GO/CuO	$C_{2.77}H_{3.77}N_4O_{2.97}$	13763.6	12263.2	13013.4	201.2	4727.0

7.4.3 Sensitivity and performance test results

The results of impact and friction sensitivity were shown in Table 7-3 of our PBXs martial and other explosive materials. The mechanical sensitivity significantly improved with respect to NTO explosives and other conventional and modern PBXs. The friction sensitivity results reveal that the PBX composition containing 76.5% NTO with GAP exhibits a significantly higher resistance to friction initiation (360 N) compared to insensitive explosives such as IMX-101 (240 N) and IMX-104 (160 N), representing improvements of 50% and 125% respectively. In comparison to other GAP-based PBXs, such as BCHMX/GAP (294 N) and CL-20/GAP (247 N), the NTO/GAP composition also shows enhanced friction insensitivity, with increases of 22% and 46% respectively. Moreover, the incorporation of GO further enhances the safety margin, as evidenced by a friction sensitivity exceeding 360 N for the 76.5% NTO/GO + GAP composition, and maintaining 360 N upon the addition of both GO and CuO (76.5% NTO/GO/CuO/GAP). These

results show that using the NTO/GAP system and adding nanomaterial additives materials like GO and CuO can markedly improving the friction sensitivity of PBX relative to traditional and modern insensitive munitions. The impact sensitivity results further demonstrate the advantages of our NTO/GAP-based PBX composition. Compared to insensitive explosives such as IMX-101 and IMX-104, as well as other GAP-based PBXs containing different energetic explosives, the NTO/GAP system exhibits reduced sensitivity to impact. Additionally, the incorporation of GO and copper oxide as additives provides an extra level of safety.

Table 7-3 Results of the experimental (Density- Impact- Friction) of the studied PBXs

Sample	Code designation	Experimental density (g/cm^3)	Impact Sensitivity [J]	Friction sensitivity [N]
F1	72 % NTO+ GAP	1.423	30	>360
F2	76.5 % NTO+ GAP	1.497	15	360
F3	76.5% NTO/GO + GAP	1.485	20	>360
F4	76.5% NTO/GO/CuO/GAP	1.520	20	360
F5	IMX-101 [4]	1.64	24.5	240
F6	IMX-104 [4]	1.778	28.5	160
F7	BCHMX / GAP [89]	1.62	7.7	294
F8	CL-20 /GAP [89]	1.73	8.4	247
F9	RDX/GAP [89]	1.59	11.5	360

Also, from Table 7-2, NTO has a relatively low heat of combustion and heat of explosion. This is mainly due to that it has low oxygen balance that limits the energy released during detonation. According to the results of the calculations using the EXPLO5 program that conducted in section 6.7, NTO has heat of explosion approximately 4049.3 kJ/kg. This value was clearly much lower than its heat of combustion that measured experimentally by bomb calorimetry which is 6973.3 kJ/kg. This difference is because the heat of combustion is measured in oxygen-rich conditions while the detonation assumes the explosive reacts without external oxygen. Compared

to other high-performance explosives from the literature, it was known that the NTO have moderate performance. For example. BCHMX has a heat of explosion of 6447 kJ/kg, β-HMX was 6075 kJ/kg, RDX was 6085 kJ/kg and ε-CL-20 reaches to 6455 kJ/kg [183]. These explosives not only release more energy but also tend to be more sensitive than NTO explosives. From the results in Table 7-2, it was clear that adding GAP binder to NTO-based PBXs material increased both the experimentally measured heat of combustion and the calculated heat of explosion. The highest values were observed when the PBXs material contained 66% NTO and 34% GAP that reaching to 14525.6 J/g for the heat of combustion and 4224.9 J/g for the heat of explosion higher than those of pure NTO. In the final PBXs material with 76.5% NTO, the values were 12109.9 J/g (combustion) and 4494.1 J/g (explosion). This increase in heat of combustion was mainly due to GAP being an energetic binder with azide groups that release extra energy especially in combustion process and also, help balance the oxygen deficiency in NTO during detonation. In the case of the PBX containing NTO/GAP/GO, the heat of combustion was increased to 12671.6 J/g and the heat of explosion to 4475.8 J/g. This indicates that GO slightly improves energy output due to its carbon content contributing as an additional fuel. Also, when CuO was added, the heat of combustion was increased further to 13013.4 J/g and the heat of explosion to 4727.0 J/g. This increase might be attributed to CuO acting as an oxidizer that is enhancing the exothermic reaction and improving the overall energy release.

7.4.4 Thermal analysis determination

DSC was conducted to evaluate the thermal behavior of pure explosive NTO and PBXs materials (76.5% NTO + GAP), (76.5% NTO/GO + GAP), (76.5% NTO/GO/CuO + GAP) composites over a temperature range of 40 °C to 300 °C under a nitrogen (N_2) flow with a heating rate of 2°C/min. As shown in Figure 7-6, the DSC curve of pure NTO exhibits a strong and sharp exothermic peak at approximately 266.5 °C, which corresponds to the self-decomposition of NTO and this result aligns well with values reported in the literature [14,103,107]. From the DSC curves, all the PBXs materials did not alter the nature of the exothermic peak, but it significantly affected both the onset and maximum temperature of decomposition as detailed in Table 7-4. The exothermic peak temperatures for PBXs materials (76.5% NTO + GAP), (76.5% NTO/GO + GAP), (76.5% NTO/GO/CuO + GAP) composites were recorded (228.8°C, 215.7°C, 222.9°C) respectively.

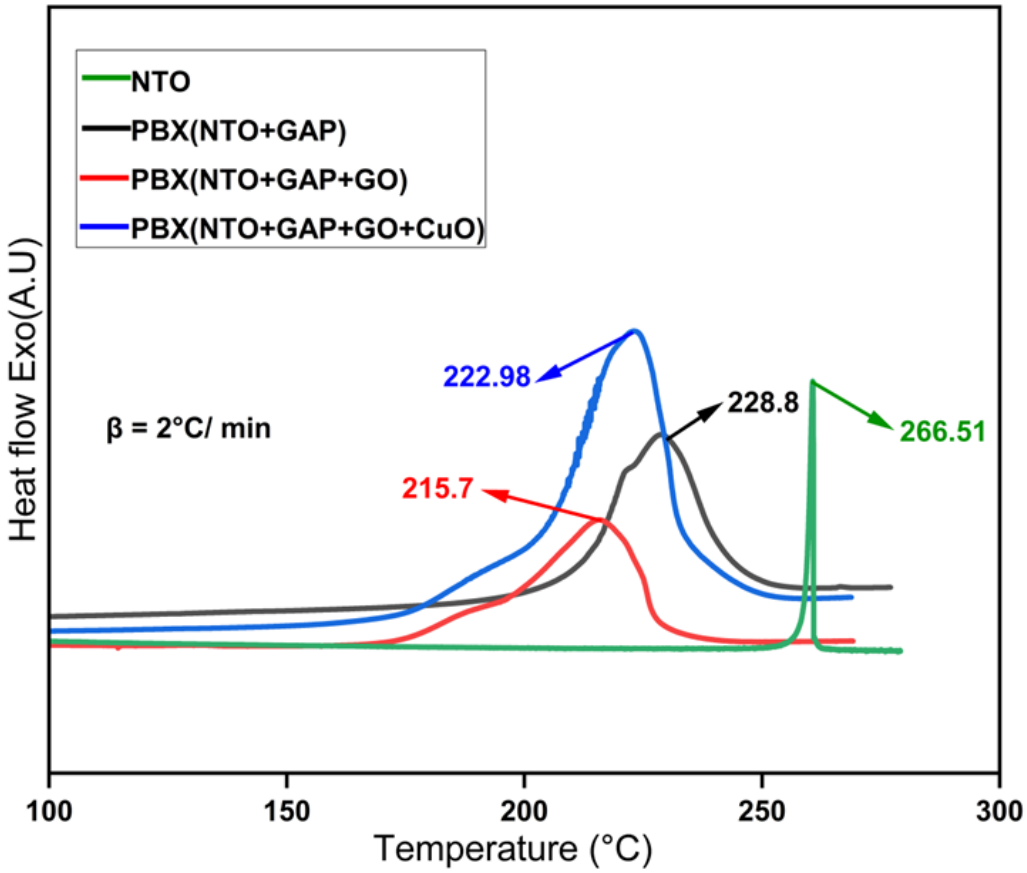

Figure 7-6 DSC curve at heating rate 2° C/min for NTO and PBXs materials (76.5% NTO + GAP), (76.5% NTO/GO + GAP), (76.5% NTO/GO/CuO + GAP) respectively.

From the results, there was a significant decrease in the onset and maximum decomposition temperatures of the PBXs materials compared to pure NTO explosives, as illustrated in Table 7-4. This notable drop may be attributed to the early decomposition behavior of NTO influenced by its interaction with the energetic polymer binder GAP. Since GAP begins to decompose at approximately 190 °C, it is believed that the heat released during its exothermic degradation promotes earlier decomposition of NTO. This suggests a thermal interaction between GAP and NTO within the mixture.

DSC analysis of all PBXs materials revealed that when one component undergoes exothermic decomposition, the overall exothermic peak of the mixture aligns with that of the component exhibiting the lower decomposition temperature. This indicates that GAP may act as a catalyst, accelerating the thermal decomposition of NTO, affecting both the onset and maximum decomposition temperatures.

Furthermore, analysis of the DSC peaks shown in Figure 7-6 indicates that the decomposition peaks of these mixtures are broader than those of pure NTO, indicating that the decomposition occurs over a wider temperature range. This implies a slower and more gradual reaction. Since the heat released during decomposition is related to the area under the DSC curve, the broader peaks suggest that more heat is released. This increased heat release, along with the shift in peak temperature, confirms that GAP likely accelerates the decomposition of NTO by acting as a catalyst and that the interaction between the components contributes to this enhanced heat release.

Table 7-4 Results of DSC at heating rate 2 °C min^{-1} for studied samples.

Sample	To/°C	Tp/°C	Te/°C	Ea kJ / mol
	β = 2 °C min −1			
NTO	264.9	266.5	269.9	505.03
F7: PBX (76.5 % NTO+GAP)	212.8	228.8	258.3	257.11
F8: PBX (76.5% NTO+GO+GAP)	189.1	215.7	253.2	147.24
F9: PBX (76.5% NTO+ GO+ CuO+ GAP)	205.7	222.9	254.8	118.29
Ea: Activation energy was calculated using the Kissinger equation				

7.4.5 Kinetics and stability determination of PBXs materials

The thermal decomposition kinetics of the PBXs materials and pure NTO were investigated over a range of temperatures using non-isothermal DSC measurements. This analysis aimed to ensure the safe processing, handling and storage of PBXs by understanding their thermal stability and decomposition behavior. The kinetic parameters, activation energy (Ea) and pre-exponential factor (A), for the decomposition reactions of pure NTO and the PBXs composites [(76.5% NTO + GAP), (76.5% NTO/GO + GAP) and (76.5% NTO/GO/CuO + GAP)] were determined using two methods. First, kissinger method was applied, as described by equation 7.1. DSC experiments were conducted at heating rates of 0.5, 1, 2, 3 and 4 °C/min as shown in Figures 7-7 through 7-10 for pure NTO and the PBXs composites [(76.5% NTO + GAP), (76.5% NTO/GO + GAP) and (76.5% NTO/GO/CuO + GAP)] respectively. The shift in peak decomposition temperatures with increasing heating rate was used to calculate the kinetic parameters. The results are summarized in Table 7-5.

$$\ln\frac{\beta}{T_p^2} = \ln\frac{A.R}{E} - \left(\frac{E}{R}\right)\frac{1}{T_p} \qquad \text{Equation (7.1)}$$

All terms of the equation were previously defined in section 6.1.6. Figure 7-11 shows a linear relationship between $\ln(\beta/T_p^2)$ and $(1/T_p)$ obtained by applying linear regression to the experimental data. These plots exhibit a linear relationship indicating that the activation energy and pre-exponential factor can be determined from the slope and intercept of the regression line.

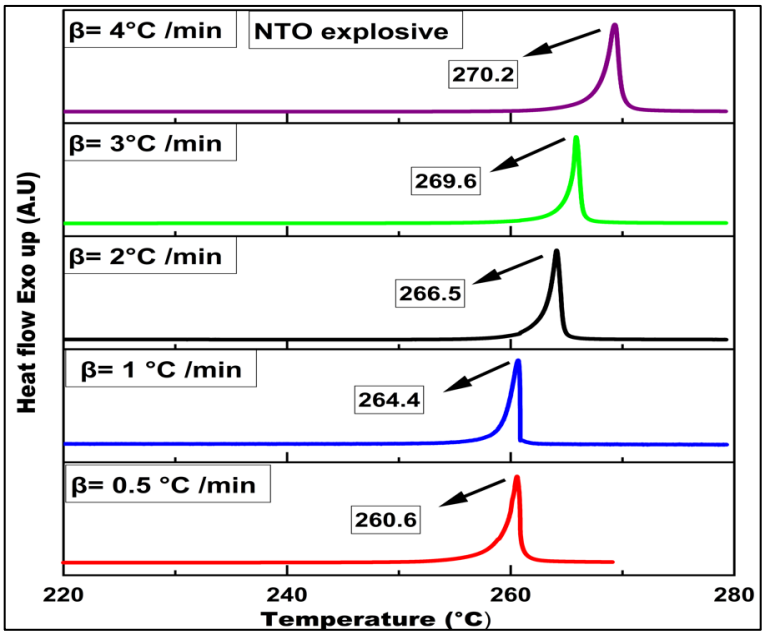

Figure 7-7 DSC curve at different heating rate (0.5, 1, 2, 3 and 4° C/min for NTO.

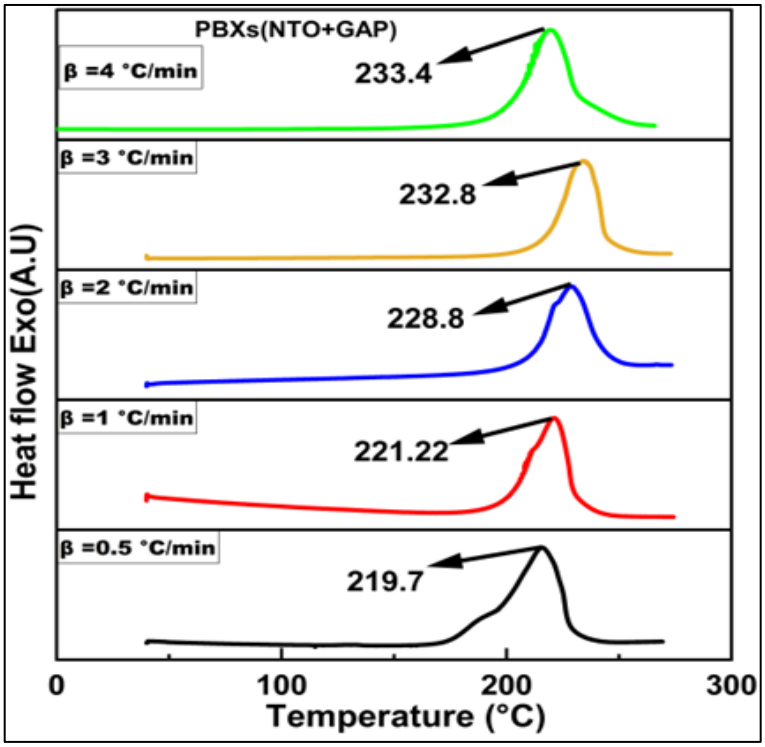

Figure 7-8 DSC curve at different heating rate (0.5, 1, 2, 3 and 4° C/min for PBXs material composed of (76.5% NTO + GAP)

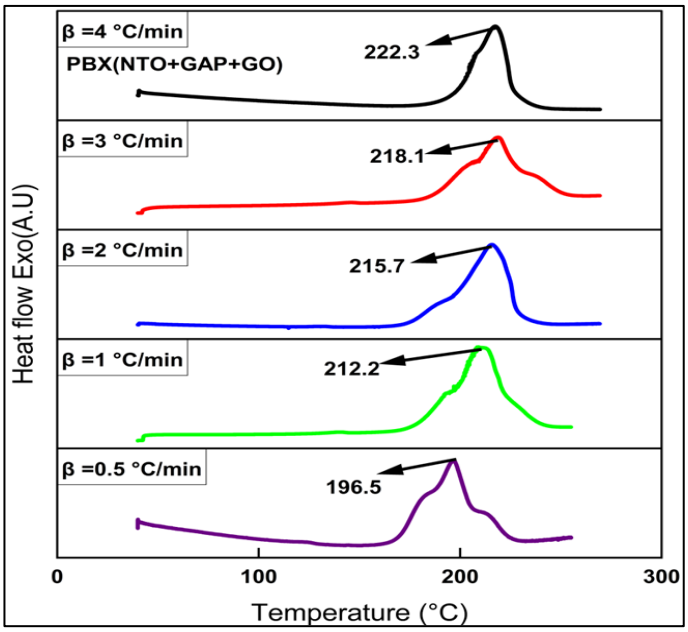

Figure 7-9 DSC curve at different heating rate (0.5, 1, 2, 3 and 4° C/min for PBXs material composed of (76.5% NTO +GO+ GAP).

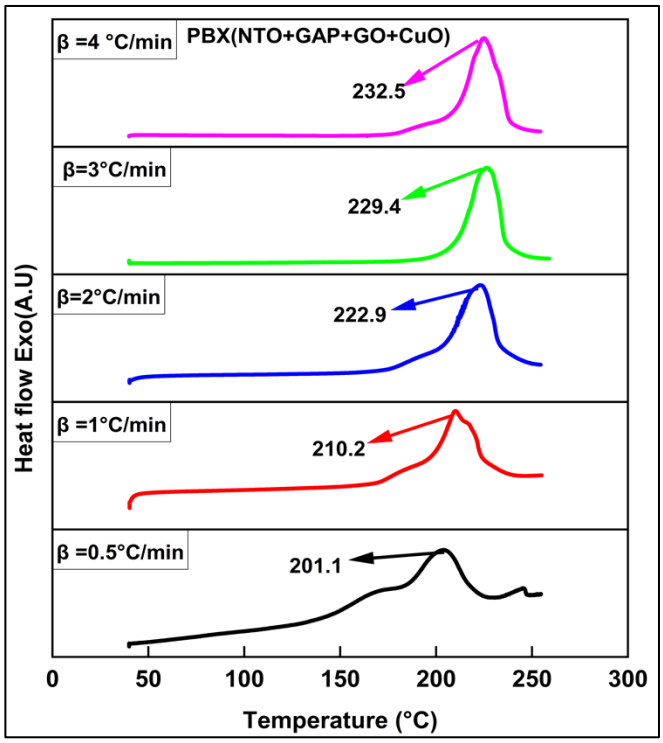

Figure 7-10 DSC curve at different heating rate (0.5, 1, 2, 3 and 4° C/min for PBXs material composed of (76.5% NTO +GO +CuO + GAP).

Table 7-5 Kinetic parameters of NTO and PBXs materials by Kissinger method.

Sample	B °C/ min	T_o °C	T_p °C	T_e °C	Ea kJ / mol	R^2	Ln A/s^{-1}
NTO	0.5	259.2	260.6	262.3	505.03	0.98	107.4
	1	260.3	264.4	265.9			
	2	264.9	266.5	269.9			
	3	266.1	269.6	271.3			
	4	266.9	270.2	274.8			
F7: PBX (76.5%NTO +GAP)	0.5	194.7	219.7	237.2	257.11	0.95	43.22
	1	202.0	221.2	250.9			
	2	212.8	228.8	258.3			
	3	222.7	232.8	267.2			
	4	219.2	233.9	260.0			
F8: PBX (NTO+GO+GAP)	0.5	176.3	196.7	232.5	147.24	0.90	30.25
	1	192.6	212.1	254.0			
	2	189.1	215.7	253.2			
	3	196.9	218.0	256.5			
	4	205.5	222.7	262.2			
F9: PBX (NTO+ GO+ CuO+ GAP)	0.5	179.0	201.1	233.8	118.29	0.99	22.48
	1	195.4	210.1	245.0			
	2	205.7	222.9	254.8			
	3	213.6	229.4	256.2			
	4	212.6	232.5	262.6			

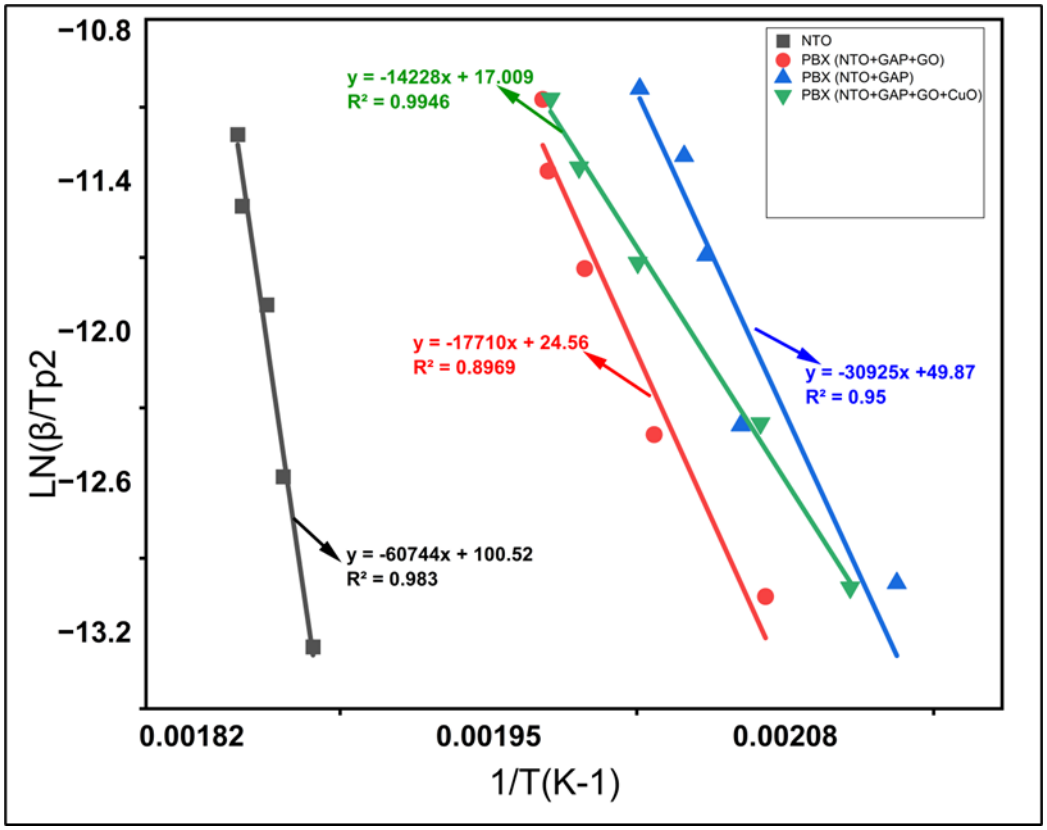

Figure 7-11 Fitted Kissinger activation energies results of NTO and PBXs materials.

On the other hand, the modified Kissinger-Akahira-Sunose (KAS) isoconversional method was used as a second approach to calculate the kinetic parameters of the prepared PBXs, as it is more accurate and provides a precise estimation of the kinetic parameters. This follows the recommendations of the international confederation of thermal analysis and calorimetry (ICTAC) [184]. The method allows for the determination of activation energy (Ea) over a wide range of conversion degrees (α), from 5% to 90% compared with the original Kissinger method, which determines the activation energy based on a constant degree of conversion during the reaction mechanism as shown in Figure 7-12 and Figure 7-13.

As shown in Table 7.6 and Table 7.7. The average activation energies for the PBXs materials [(76.5% NTO + GAP), (76.5% NTO/GO + GAP) and (76.5% NTO/GO/CuO + GAP)] were calculated to be 250.56 kJ/mol, 136.28 kJ/mol and 112.31 kJ/mol respectively, which are lower than that of pure NTO.

When comparing these results to those obtained using the original Kissinger method, it is evident that the activation energies from the original method are slightly higher, as it relies only on peak decomposition temperatures at each heating rate as presented in Table 7-5. The results obtained from both methods suggest that the activation energies of all PBXs materials are lower than that of pure NTO, as shown in Table 7-8. This reduction in activation energy may be due to the fact that NTO primarily decomposes through the cleavage of the C-NO_2 bond in the triazolone ring, typically beginning at 240 °C to 260 °C. In the presence of GAP binder, an energetic polymer containing azide groups, this behavior is changed and it is believed that upon GAP decomposition, reactive intermediates such as nitrenes are formed from azide group decomposition (-N_3 → -N:) especially at elevated temperatures.

The decomposition process of PBXs materials might therefore be attributed to two main factors: first, the exothermic decomposition of GAP, which generates localized heat and reactive species that initiate the breakdown of NTO and second, possible radical interactions that accelerate C-NO_2 bond cleavage or ring-opening reactions. These effects contribute to earlier onset decomposition and lower activation energy. The broader decomposition peaks observed in the DSC curves of PBXs (Figures 7-8, 7-9 and 7-10) compared to pure NTO (Figure 7-7) suggest that decomposition occurs over a wider temperature range, indicating a more gradual reaction. This can be attributed to the interaction between NTO and the GAP binder. Additionally, the logarithm value of the pre-exponential factor (A), which represents the frequency of effective collisions leading to reaction, was lower for the PBXs samples (18.17, 13.14 and 9.76 s^{-1}) than for pure NTO (46.6 s^{-1}) as shown in Table 7-5. Therefore, despite the reduced energy barrier, the lower frequency of effective molecular collisions implies that the PBXs do not decompose instantaneously. Instead, they break down gradually allowing time for heat dissipation and reducing the likelihood of hot spots or runaway reactions. This gradual decomposition is crucial for improving storage and handling safety. Additionally, due to the prolonged decomposition time, these PBXs may not detonate as violently as pure NTO making them more suitable for use in insensitive munitions.

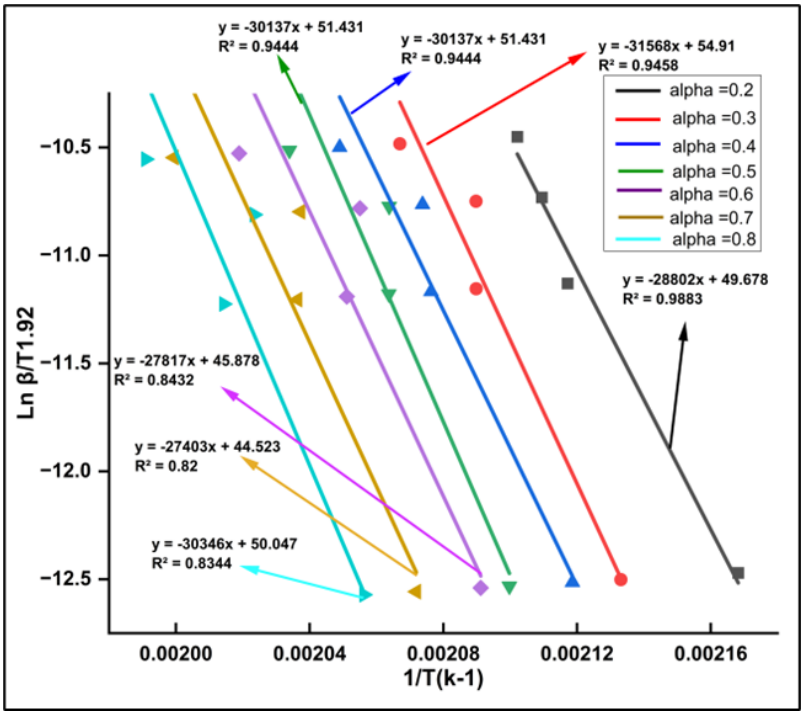

Figure 7-12 Fitted Kissinger-Akahira-Sunose (KAS) isoconversional method activation energies results of PBXs (76.5% NTO + GAP) materials.

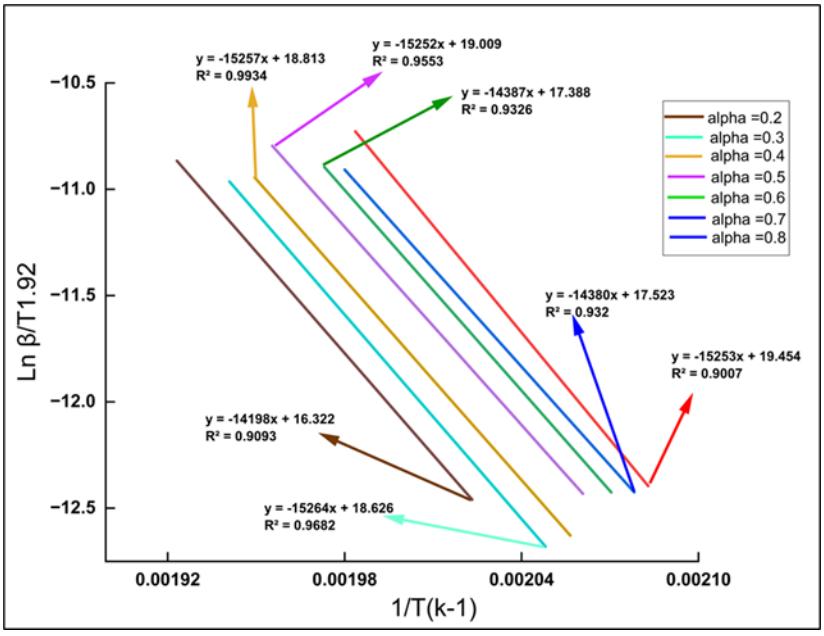

Figure 7-13 Fitted Kissinger-Akahira-Sunose (KAS) isoconversional method activation energies results of PBXs (76.5% NTO+GO +GAP) materials.

Table 7-6 Kinetic parameters of NTO-GAP by modified KAS method.

Conversion	Heating Rate β ° C/min						
α	0.5	2.0	3.0	4.0	E_a kJ/mol	Ln A s^{-1}	R^2
0.05	182.5	193.6	194.9	195.7	252.9	50.51	0.967
0.10	185.2	195.6	198.4	199.6	245.3	51.10	0.990
0.15	188.2	199.3	201.1	202.7	246.8	47.66	0.980
0.20	190.2	201.7	203.2	205.6	239.5	45.85	0.980
0.25	194.2	203.7	204.9	208.2	275.7	44.79	0.980
0.30	195.8	205.5	205.5	210.8	262.5	51.18	0.940
0.35	198.8	207.1	207.9	213.0	282.4	45.92	0.940
0.40	199.0	208.6	209.2	215.0	250.6	46.65	0.940
0.45	201.0	210.1	210.4	216.9	253.9	51.29	0.910
0.50	203.2	211.6	211.5	218.7	260.4	49.70	0.880
0.55	204.2	213.0	212.6	220.4	247.2	51.20	0.890
0.60	205.2	214.5	213.6	222.3	231.3	46.02	0.860
0.65	206.9	214.6	214.9	222.6	249.0	43.37	0.840
0.70	209.7	218.0	217.6	227.1	227.9	50.65	0.860
0.75	210.3	219.8	218.6	227.6	231.3	54.40	0.840
0.80	213.3	223.4	221.2	229.3	252.3	46.27	0.910
				Mean	250.56	46.66	0.919

In the second PBXs material, we used NTO particles coated with 3 wt.% GO. Based on our earlier results, GO improved the thermal stability of NTO as pure explosives by increasing its activation energy by approximately 45 kJ/mol compared to pure NTO as demonstrated in our previous study on the effect of GO on NTO explosive powder. Therefore, we initially expected that adding GO to the PBXs material would stabilize the entire composite. It was expected that GO would not only enhance the safety of the PBXs material but also improve its overall performance.

However, our experimental results revealed a completely opposite trend. When we performed DSC analysis and evaluated the thermal kinetics of the PBXs materials containing GO using two different methods, we observed that both the activation energy and the onset, maximum decomposition temperatures decreased. Specifically, the onset decomposition temperature dropped from 212.8 °C in the original PBXs (based on NTO + GAP) to 189.1 °C in the PBXs based on NTO/GO + GAP. Similarly, the maximum decomposition temperature decreased from 228.8 °C to 215.7 °C. In addition, the activation energy dropped from 257 kJ/mol in the original PBXs to 147 kJ/mol in the PBXs based on NTO/GO + GAP.

Table 7-7 Kinetic parameters of NTO/ GO-GAP by modified KAS method.

Conversion	Heating Rate β °C/min				E_a kJ/mol	Ln A s^{-1}	R^2
α	0.5	1.0	2.0	3.0			
0.05	204.9	208.5	212.0	220.2	215.4	48.02	0.943
0.10	205.5	208.6	212.6	223.2	178.5	38.54	0.916
0.15	206.6	209.0	213.5	225.2	163.4	34.59	0.900
0.20	207.0	211.0	223.2	231.1	131.8	26.26	0.974
0.25	207.1	210.0	227.2	232.2	114.9	21.95	0.959
0.30	208.19	211.95	230.1	233.7	112.3	21.15	0.964
0.35	209.2	212.6	231.2	233.8	114.2	21.61	0.953
0.40	209.9	213.6	231.2	233.8	119.8	22.97	0.959
0.45	211.2	216.2	230.2	235.6	129.7	24.84	0.979
0.50	211.2	216.2	230.2	235.6	123.2	23.66	0.974
0.55	212.8	217.2	232.2	239.2	120.2	22.98	0.969
0.60	213.2	225.2	235.2	239.9	129.5	25.01	0.995
0.65	214.3	228.3	236.3	240.2	132.7	25.71	0.979
0.70	211.0	213.3	221.9	236.5	130.0	24.93	0.984
0.75	211.8	213.3	222.4	236.5	125.6	23.74	0.995
0.80	212.0	212.0	223.2	230.5	124.4	23.41	0.974
0.85	212.0	213.3	224.2	237.9	131.6	25.08	0.969
0.90	214.0	214.0	225.3	238.95	155.3	30.47	0.995
				Mean	136.3	26.94	0.9661

To understand this unexpected behavior, we carefully examined the thermal decomposition profiles in more detail as shown in Figure 7-14. Unlike the original PBXs material composed of NTO and GAP, which displayed a typical single-step exothermic peak from onset to maximum decomposition temperature, the PBXs material containing GO exhibited a slightly more complex pattern. Although it still showed one broad exothermic peak, a noticeable irregularity appeared between the onset and the main decomposition peak, resembling a shoulder or very minor step along the slope of the curve. This suggested that an intermediate decomposition process was occurring prior to the main exothermic event possibly due to interactions between GO, NTO and the GAP matrix. These results indicate that, instead of enhancing thermal stability, the inclusion of GO in the PBXs material introduced a more complex which may have contributed to the earlier onset of decomposition and the reduction in activation energy.

This mechanism may be explained by the fact that GO undergoes a highly exothermic decomposition at relatively low temperatures, releasing significant heat during its decomposition process. This behavior was evident from the shoulder observed in the DSC curve, which appeared only in the PBXs materials containing GO, particularly at heating rates of 0.5 and 3 °C/min shown in blue and green spectra respectively in Figure 7-14. According to the literature, GO exhibits a substantial heat release of approximately 1032 J/g [154–162]. The rapid energy release during its decomposition can cause localized heating, which in turn may trigger the earlier decomposition of adjacent components such as GAP and NTO. As a result, although GO alone was previously shown to enhance the thermal stability of pure NTO by forming a stabilizing coating around the explosive particles, its combination with GAP in the PBXs material may lead to an overall reduction in thermal stability due to complex, synergistic decomposition behavior.

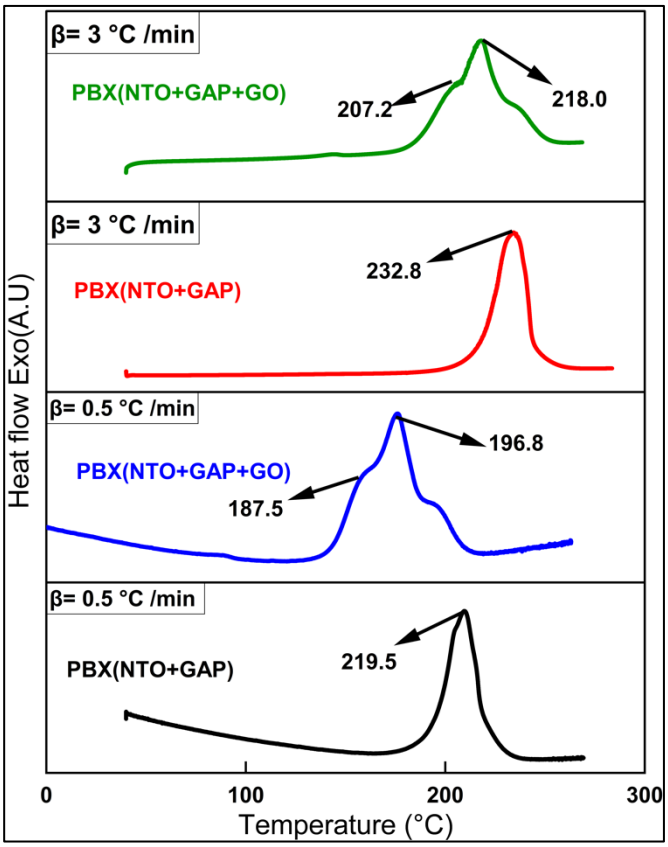

Figure 7-14 DSC curve at different heating rate (0.5 and 3° C/min for PBXs material composed of (76.5% NTO +GO+ GAP) and (76.5% NTO + GAP).

Table 7-8 Kinetic parameters of PBXs mixtures

Explosive material	E_a (Kissinger method) kJ/mol	E_a (KAS method) kJ/mol
NTO	505.03	-
PBXs (76.5% NTO + GAP)	257.11	250.56
PBXs (76.5% NTO/GO + GAP)	147.24	136.28
PBXs (76.5% NTO/GO/CuO + GAP)	118.29	112.31

The results of PBXs materials using NTO coated with GO and nano CuO, with GAP revealed that the onset decomposition temperature of the NTO/GO/CuO/GAP material around 205.5 °C was higher than that of the NTO/GO/GAP material, which was around 189.1 °C. However, despite this improvement in thermal onset, the activation energy of the NTO/GO/CuO/GAP composition was lower than that of both the NTO/GAP and NTO/GO/GAP materials. This behavior can be explained by the catalytic nature of nano CuO, which is known to promote the thermal decomposition of energetic materials by facilitating redox reactions and accelerating the breakdown of reactive groups such as nitro and azide groups. The observed increase in onset temperature compared to the NTO/GO/GAP material may be attributed to the stabilizing physical structure introduced by the GO/CuO hybrid coating. However, once the decomposition starts, the catalytic effect of CuO becomes dominant. Thus, the lower activation energy observed reflects the catalytic role of CuO during the main decomposition step, promoting faster reaction rates once thermal degradation begins.

7.5 Calculation of the detonation characteristics using EXPLO5 program

The theoretical detonation characteristics (detonation velocity, D, heat of detonation, Q, detonation pressure, P, number of moles of explosion products, n, specific volume, Vo, explosion temperature, T) of all the prepared PBXs material were calculated using EXPLO5 thermodynamic code. BKWN set of parameters for the BKW EOS was applied, these parameters are: $\alpha = 0.5$, $\beta = 0.298$, $\kappa = 14.71$, $\theta = 6620$ [185]. To evaluate the performance and calculate the detonation properties of the experimentally prepared PBXs martials, their densities were measured using Archimedes principle. Elemental composition analysis was conducted experimentally to determine the precise chemical formula of each PBXs. The heat of combustion was experimentally measured using a bomb calorimeter in order to calculate the actual heat of formation of the mixtures. Subsequently, the detonation velocities of the prepared PBXs were estimated using the Explo-5 program [185]. The obtained results are presented in Table 7-9.

Table 7-9 Explosive characteristics of PBXs that based on GAP binder using EXPLO5

No.	NTO content (wt.%)	Ob%	n (per mole of expel)	Qv (KJ/kg)	TC (K)	P (K bar)	D (m/s)	Vo (L/kg expel)
F0	NTO	-24.6	4.10	4049.2	3485.5	216.7	7439.4	706.8
F 1	66 NTO	-67.15	4.39	4224.9	3238.4	132.83	6304.9	727.4
F 2	68 NTO	-60.81	4.45	4384.4	3343.8	143.34	6486.9	740.0
F 3	70 NTO	-58.21	4.40	4391.2	3358.3	149.2	6586.3	739.2
F 4	72 NTO	-57.77	4.41	4402.2	3379.8	156.42	6705.6	737.8
F 5	74 NTO	-53.39	4.36	4433.9	3426.3	166.90	6847.7	738.7
F 6	76.5 NTO	-48.34	4.36	4494.1	3529.1	177.19	7030.7	741.9
F 7	76.5 NTO/ GO	-53.07	4.5	4475.8	3504.4	164.6	6793.0	719.2
F 8	76.5 NTO/GO/CuO	-50.69	4.61	4727.0	3621.8	184.41	7106.6	733.7

Tables 7-9 and Figure 7-15 show that the detonation velocity of the PBXs materials revealed a direct correlation between the high explosive content and the corresponding detonation velocity, with higher explosive loading leading to improved detonation performance as expected. Specifically, the detonation velocity reached 7030.7 m/s for the original PBXs material based on 76.5% NTO with a GAP binder. In contrast, the PBXs material incorporating GO exhibited a slightly lower velocity of 6793.0 m/s, likely due to the partial substitution of energetic material with GO which reduced the overall energy density. However, when both GO and CuO were included in the PBXs material, the detonation velocity increased to 7106.6 m/s. This improvement can be attributed to the increased density of this PBXs formulation, which exhibited the highest measured density of approximately 1.521 g/cm^3 as shown in Table 7-5.

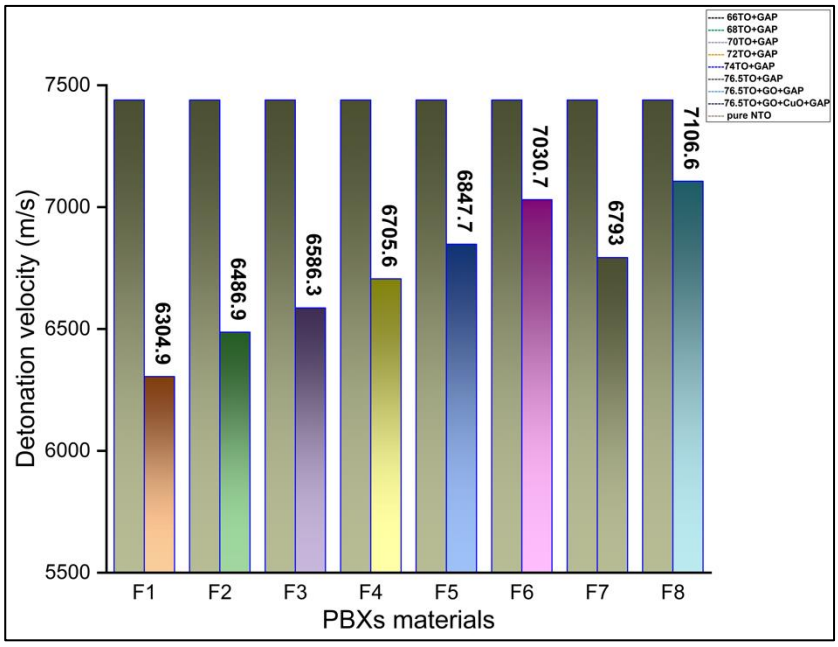

Figure 7-15 The detonation velocity of PBXs materials.

The explosion force (F) and brisance [186] were observed to increase with a higher proportion of explosive in the PBXs materials. This trend was clearly presented in Tables 7-10 and Figure 7-16.

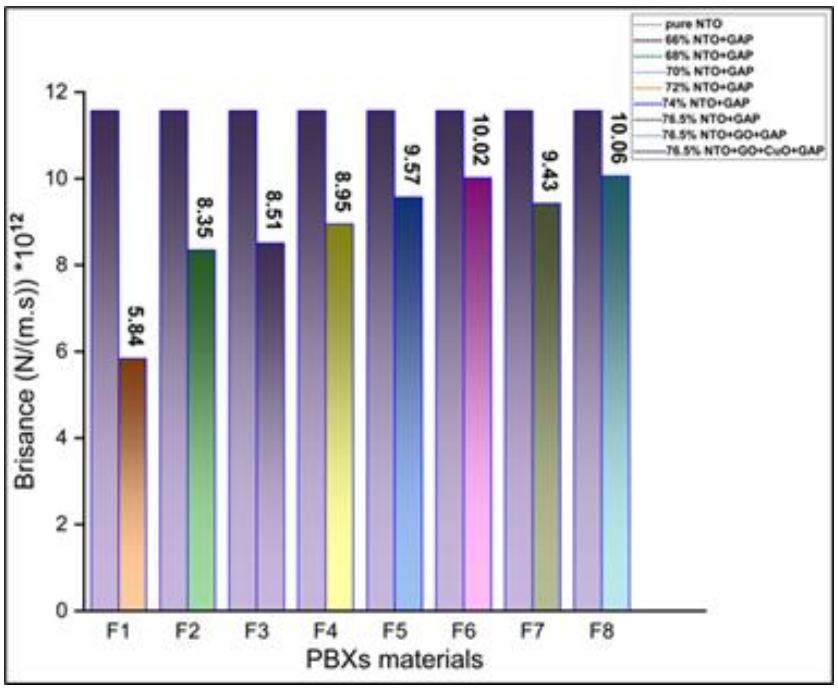

Figure 7-16 The brisance of PBXs materials

Table 7-10 Explosion force and brisance of the PBXs materials

Formulation	F 0	F 1	F 2	F 3	F 4	F 5	F 6	7	F 8
Explosion Force (kJ/kg)	914.9	675.5	918.2	916.1	924.19	939.47	970.59	935.25	987.05
Brisance (N/ (m.s) *10^{12}	11.5	5.8	8.3	8.5	8.95	9.57	10.02	9.43	10.06

As shown in Figure 7-17, a performance comparison was conducted between the PBXs materials developed in this study and the widely used insensitive munitions IMX-101 and IMX-104. The prepared PBX based on NTO explosive and GAP binder exhibited notable novelty in terms of safety, demonstrating lower mechanical sensitivity than conventional RDX and HMX based PBXs, while maintaining acceptable energetic performance. Moreover, compared to IMX systems, the developed PBX (F6) offered comparable safety with superior detonation performance exceeding the detonation velocity of IMX-101 by up to 145.7 m/s.

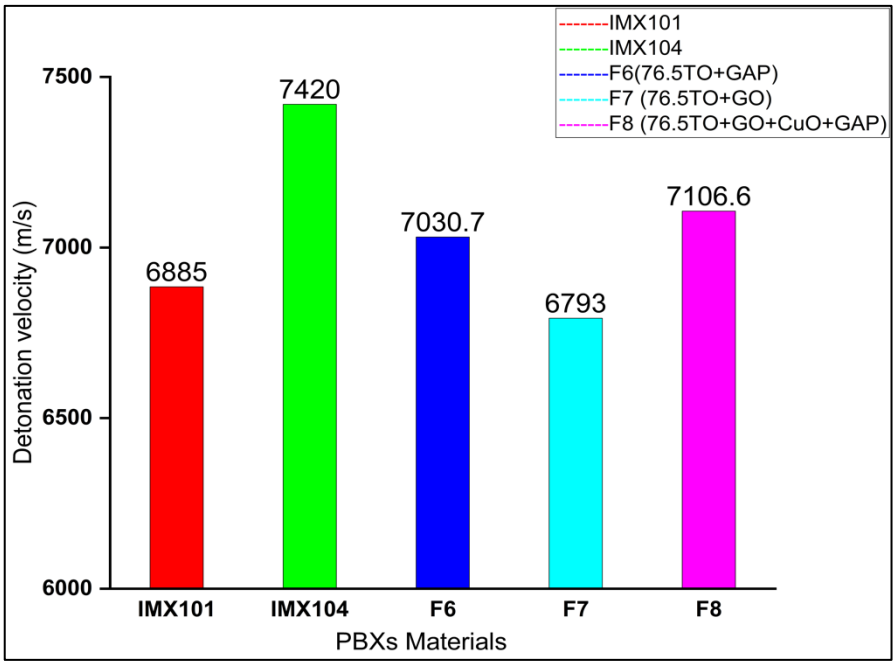

Figure 7-17 The detonation velocity of PBXs materials and IMX101 &IMX104

7.6 Conclusion

This study presents a novel contribution to the development of high-performance, low-sensitivity PBXs based on NTO and GAP using a cast-cured technique. A recrystallization process was successfully employed to modify the particle size of NTO, enabling a maximum solid loading of 76.5 wt.% through a bimodal distribution on PBXs materials. The prepared PBXs exhibited notable novelty in terms of safety, demonstrating lower mechanical sensitivity than conventional RDX and HMX based PBXs, while maintaining acceptable energetic performance. Moreover, compared to IMX systems, the developed PBXs offered comparable safety with superior detonation performance exceeding the detonation velocity of IMX-101 by up to 145.7 m/s. The inclusion of GAP binder not only enhanced the mechanical processability but also improved thermal behavior by increasing heat release, broadening the decomposition peaks compared with pure NTO. DSC analysis confirmed that decomposition in GAP-based PBXs occurs more gradually than in pure NTO suggesting improved thermal safety due to extended decomposition time, this behaviour allowing time for heat dissipation and reducing the likelihood of hot spots or runaway reactions. This gradual decomposition is crucial for improving storage and handling safety. Although GO alone improved the thermal stability of NTO, its incorporation with GAP in PBXs led to a synergistic effect reducing activation energy and decomposition temperature due to increased energy release. However, when CuO was introduced alongside GO, the formulation NTO/GO/CuO + GAP showed a higher onset decomposition temperature (205.5 °C) compared to NTO/GO + GAP (189.1°C) indicating improved initial thermal resistance. However, the reduced activation energy reflected CuO catalytic role in promoting rapid decomposition once initiated. The heat of combustion and explosion increased significantly with the addition of GAP, GO and CuO. These findings demonstrate that the developed novel NTO-based PBX compositions offer a balanced combination of enhanced performance, reduced sensitivity and improved thermal control.

CHAPTER 8 NUMERICAL SIMULATION

8.1 Introduction

Accidental initiation of ammunition can transition high explosives from a stable state into hazardous reactions such as burning, deflagration and potentially detonation. Minimizing the severity of this reaction often referred to as the “reaction level’’ is a key objective in many safety studies, especially those focused on unintentional exposure to heat during different stages of the ammunition lifecycle. IMs are engineered to withstand accidental stimuli such as bullet and fragment impacts, fast or slow heating and sympathetic detonation while still ensuring full operational performance upon reaching the target [187].

Among these threats, thermal hazards are of particular concern. When energetic materials are confined within sealed casings, as is common in missiles and artillery shells, they become highly susceptible to heat. If the rate of heat generation from slow thermal decomposition exceeds the system’s ability to dissipate it, a dangerous pressure buildup may occur, potentially resulting in deflagration or full-scale detonation. To address this, thermal risks are typically categorized into fast and slow heating scenarios. Fast heating simulates emergency fire events, such as those on ships or in storage areas. In contrast, slow heating is considered more insidious and dangerous, arising from gradual heat transfer during long-term storage [188-189].

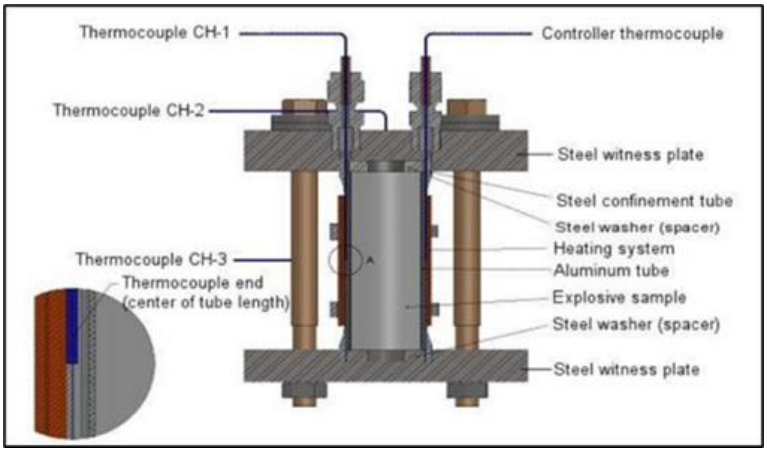

Figure 8-1 VCCT slow-heating test setup [190].

To evaluate these hazards, numerous experimental protocols have been established, particularly the slow cook-off test, which assesses how energetic materials respond to gradual heating under controlled conditions. These tests are designed to reduce the risks and costs associated with testing full-scale munitions. One widely recognized protocol is NATO's STANAG 4491, which outlines standardized procedures for evaluating thermal sensitivity and explosiveness [191]. Various test setups have been developed, such as the thermal explosion experiment (STEX), used for samples up to 750 g and relying on radiative heating, the sandia instrumented thermal ignition (SITI) test for smaller samples up to 6 g, and the variable confinement cook-off test (VCCT), which accommodates up to 50 g of explosive material with heating rates between 3.3 and 25 °C/h [192-194]. The VCCT and SITI use conduction heating and are shown in Figures 8-1 and 8-2 respectively.

Several factors, including chamber design, pre-conditioning duration and heating rate can significantly influence slow cook-off test outcomes. These experimental methods are critical for the early-stage screening and formulation of energetic materials before advancing to full-scale IM testing. Slow cook-off experiments with medium to low heating rates are time-consuming and costly, often requiring several hours to complete. To overcome these limitations, numerical simulation offers a promising solution. Simulating the cook-off behavior and estimating the time to thermal runaway can aid in experiment planning and provide preliminary data. The objective of this study is to investigate the slow cook-off behavior of our PBX composition by utilizing kinetic parameters obtained from modified Kissinger analysis and DSC experiments, and to analyze this behavior through simulation model established in previous research [190].

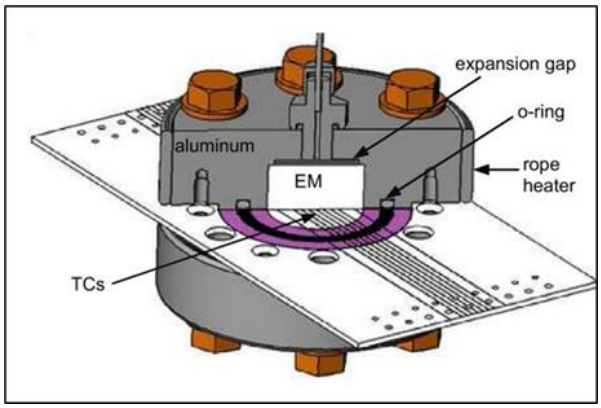

Figure 8-2 SITI slow-heating test setup [193].

8.2 Theoretical framework and simulation approach

The simulation model utilized in this work was originally developed by Professor Charles Dubois, as detailed in his study "Multiphysics Modelling of Variable Confinement Cookoff Test (VCCT)." For the purposes of this research, the model was adapted to our PBX composition to investigate the slow cook-off behavior to our materials [190].

Building upon this model, the following section provides a summary of the main steps and methodologies applied in this research.

In a standard variable confinement cook-off test (VCCT) setup, a cylindrical sample of energetic material enclosed within a confinement sleeve is subjected to controlled heating. During the test, all three fundamental modes of heat transfer are present: conduction, convection, and thermal radiation. All these models were shown in Figure 8-3.

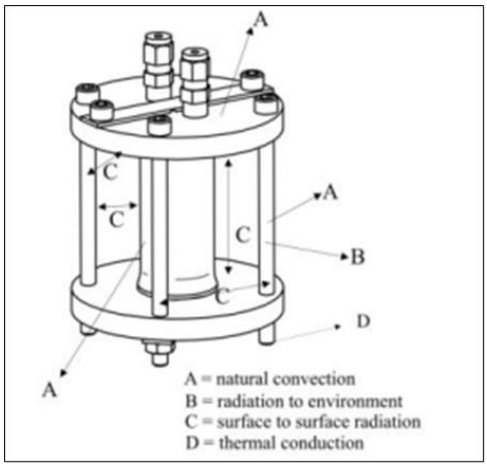

Figure 8-3 Schematic illustration of the standard VCCT setup with heat transfer modes [190].

Heat diffusion through solids is described by the transient three-dimensional form of Fourier's law as in equations 8.1 and 8.2 respectively [190]. To solve the heat conduction equation, appropriate boundary conditions were applied based on the nature of each interface within the system [190].

$$\rho\, Cp \frac{\partial T}{\partial t} = K\, \nabla^2\, T + S(T) \qquad \text{Equation (8.1)}$$

$$S(T) = \rho\, Q\, A\, e^{\frac{-Ea}{R\,T}} \qquad \text{Equation (8.2)}$$

where, k is the thermal conductivity (W/m. K), T is the temperature (K), ρ is the density (kg/m^3), C_p is the heat capacity (J/kg. K), t is the time (s), ∇ represents the Laplacian operator, Ea is activation energy, was obtained using the Kissinger-Akahira-Sunose (KAS) method, A is the pre-exponential factor and Q is the measured decomposition enthalpy from DSC.

Three types of solid-solid were identified in the VCCT configuration that shown in Figure 8-3. The first scenario assumes perfect thermal contact, where no thermal resistance exists at the interface. In this case, both the temperature and heat flux remain continuous across the boundary between two solids as in equations 8.3 and 8.4 respectively [190].

$$T_A = T_B \qquad \text{Equation (8.3)}$$

$$q_A = q_B \qquad \text{Equation (8.4)}$$

The second senarion, in practical applications, micro-gaps often lead to imperfect thermal contact. This results in a temperature discontinuity or thermal jump, at the interface due to finite thermal contact resistance as described by equations 8.5 and 8.6 respectively as shown in Table 8 -1. [190].

$$q = \frac{(T1-T3)}{\frac{\Delta XA}{KA*A}+\frac{1}{hc*A}+\frac{\Delta xB}{kB*A}} \qquad \text{Equation (8.5)}$$

$$hc = \frac{1}{Lg}\left(\frac{Ac}{A} * \frac{2\,kA\,KB}{KA+KA} + \frac{AV}{A}\,Kf\right) \qquad \text{Equation (8.6)}$$

Table 8-1 Symbols, Descriptions and Units for equations (8.5) and (8.6).

Parameter	Defintion	Units
T_1, T_3	Temperatures at the outer surfaces of solid A and solid B.	°C, K
ΔX_A, ΔX_B	Thickness of solids A and B.	m
K_A,K_B	Thermal conductivities of solids A and B.	(W/m.K)
A	Contact area.	m^2
h_c	Thermal contact conductance between the two surfaces.	(W/m².K)
Q	Heat flux through the whole layered structure.	W/m²
L_g	Gap thickness between two parts.	M
A_C	Contact area (metal-metal) between solids A and B.	m^2
A_V	Void area (air-filled gaps, non-contacting regions).	m^2
A	Total interface area = A_C+ A_V	m^2
k_f	Thermal conductivity of filler or air in the voids	W/m.K

The third type of interface occurs between solid surfaces, such as the outer metal walls of the VCCT assembly and the surrounding air. Heat transfer takes place via both convection and thermal radiation as equation 8.7 [190].

$$-kA\left.\frac{dT}{dx}\right| = q = hA\,(Tw - T\infty) + F\varepsilon\, Fg\, \sigma A\,(\mathrm{T^4\,W - T^4S}) \qquad \text{Equation (8.7)}$$

An essential component of this model is the heat transfer coefficient (h). This coefficient is not constant, it varies depending on the flow regime (natural or forced convection), surface geometry and temperature differences. To estimate it accurately, empirical correlations based on the Nusselt number were used as equation 8.8 as shown in Table 8-2. [190].

$$\mathrm{Nu} = \frac{h\,D}{K} = \mathrm{f\,(Re, Pr)} = \mathrm{M\,Re^a\,Pr^b} \qquad \text{Equation (8.8)}$$

Table 8-2 Symbols, Descriptions and Units for equations (8.7) and (8.8).

Parameter	Defintion	Units
T_w	Wall temperaturethe.	°C, K
T_∞	Ambient air temperature.	°C, K
H	Convective heat transfer coefficient..	$W/m^2.K$
F_ε	Surface emissivity.	-
F_g	Geometrical view factor from the wall to the surroundings.	-
Σ	Tefan-Boltzmann constant 5.67×10^{-8}	$W/m^2.\,K^4$
A	Exposed surface area.	m^2
T_S	Temperature of the surrounding surfaces for radiation balance.	°C, K
k_f	Thermal conductivity of filler or air in the voids	W/m.K
Nu	Nusselt number. dimensionless heat transfer ratio.	-
D	Characteristic length.	M
Re	Reynolds number.	-
Pr	Prandtl number.	-
M, a, b	Empirical constants.	-

8.3 Modeling of slow heating cook off test

In this work, the necessary convective heat transfer coefficients were taken from the built-in coefficient's library available in COMSOL Multiphysics. These correlations are calculated automatically when the "convective cooling" boundary condition is applied.

In our current study, the explosive composition under investigation, based on NTO and GAP was found experimentally to follow a single-step decomposition mechanism. This conclusion was supported by differential scanning calorimetry (DSC), which revealed a single exothermic peak in the thermal decomposition profile. The presence of only one peak suggests that all major components decompose in a closely overlapping temperature range, making a single global reaction model a reasonable assumption for thermal modeling. This behavior is consistent with published literature. Studies on GAP-based PBXs containing other nitramines such as RDX or HMX also showed that GAP can shift decomposition temperatures and cause overlapping thermal events, resulting in a single broad peak in DSC measurements. Then, this single peak indicates that a simplified one-step global kinetic model in thermal simulations. In this case, the heat released during decomposition contributes to further heating of the material, which in turn accelerates the reaction, a self-reinforcing feedback loop known as thermal runaway. If not dissipated properly, this process can lead to a violent event such as deflagration or detonation. Therefore, to account for this phenomenon, an internal heat source term is introduced in the heat transport equation to represent the energy released by the chemical reaction as descripted in equations 8.1 and 8.2 respectively. To build our model, thermal and kinetic parameters were obtained through DSC experiments and analyzed using standard methods based on the modified Kissinger Akahira-Sunose (KAS) method to extract kinetic parameters from the non-isothermal DSC data.

The model was built in 3D, the geometry of the VCCT model was first created in COMSOL Multiphysics [195]. Material properties such as thermal conductivity, specific heat, and density were assigned to each part. The geometry was then meshed and then, solver settings were configured for a transient (time-dependent) study, and the simulation was run with time stepping until the final simulation time was reached and convergence was achieved.

8.3.1 Small-scale slow heating modeling simulations

Slow cook-off behavior of PBXs material was simulated using COMSOL Multiphysics to evaluate the thermal response of the PBXs material and the decomposition characteristics of it under gradual heating condition. The model included temperature-dependent material properties (thermal conductivity and specific heat) for the PBXs domain, while the density of the explosive was assumed to remain constant during heating, as supported by literature showing minimal change (less than 3%) in HMX density between 300-500 K [196]. At the end of the simulation, we can determine the temperature distribution in the explosive charge. Also, the simulation calculated the maximum temperature during the heating.

8.3.2 The geometry

A detailed three-dimensional geometry of the variable confinement cook-off test (VCCT) was constructed using COMSOL Multiphysics. The model replicates the experimental setup, including all major components such as the confinement sleeve, energetic sample, top and bottom plates, heater block, and supporting rods. The final geometry allows for accurate representation of thermal conduction, convection and radiation within the VCCT assembly during the cook-off simulation. Figure 8-4 shows the 3D geometry of the VCCT model constructed in COMSOL program.

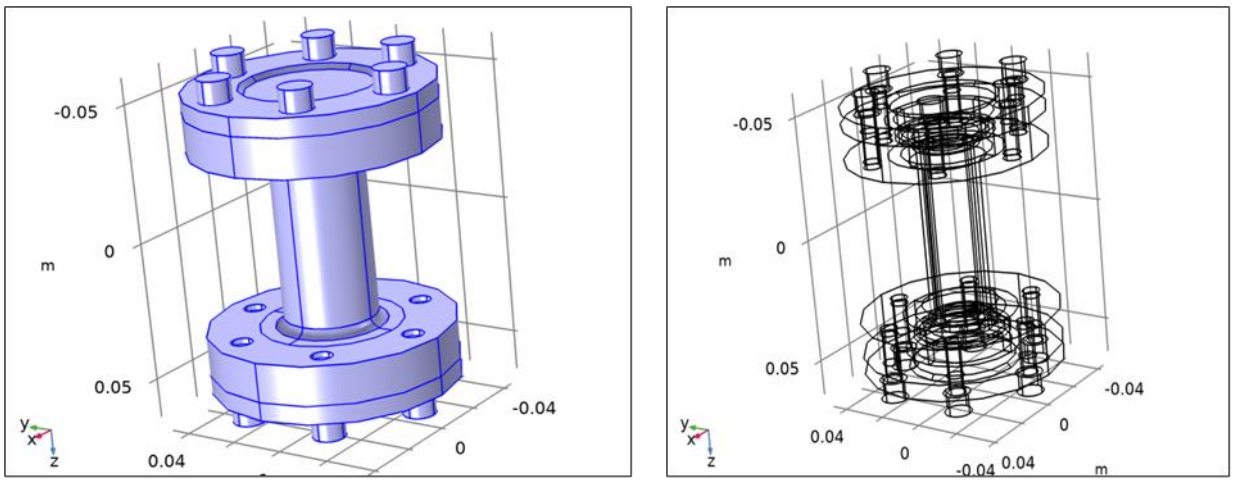

Figure 8-4 3D geometry of the VCCT model constructed in COMSOL program.

8.3.3 Materials

The model consists of different material regions (Explosive Core and the casing).

- Explosive Core (PBX Material):

The central component of the modeled geometry consisted of a plastic-bonded explosive (PBX) formulation containing 76.5 wt.% NTO as the primary energetic ingredient, combined with a GAP-based energetic binder, as illustrated in Figure 8-5. Due to the temperature-dependent self-decomposition behavior of the explosive material, an internal heat generation term, $S(T)$ was incorporated into the model to represent the exothermic nature of the decomposition process as temperature increases. The slow cook-off scenario was simulated by applying a gradual heating rate of 3.3 °C per hour, which mirrors the conditions used in experimental slow cook-off tests conducted in thermally controlled chambers. The temperature-dependent reaction rate was defined using kinetic parameters (pre-exponential factor A and activation energy Ea) are shown in Table 8-3.

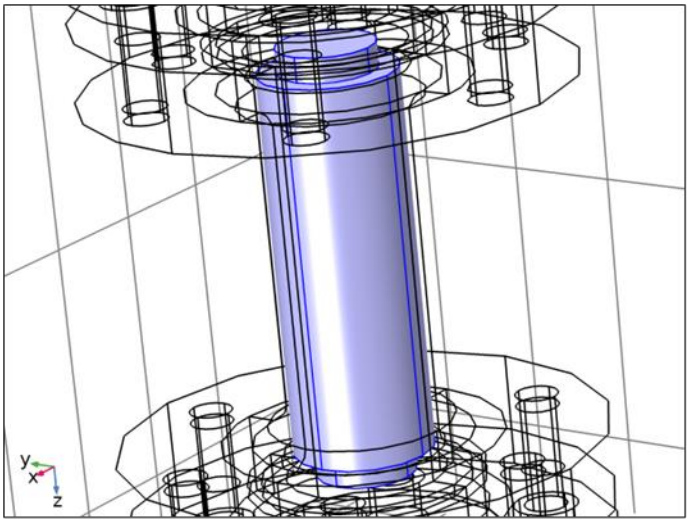

Figure 8-5 PBX component location on the VCCT model constructed in COMSOL program.

In addition to the PBX sample, the remaining components of the VCCT assembly were modeled using appropriate engineering materials to accurately reflect the physical structure and thermal behavior of the system. These components include structural and support parts made of AISI 4340 steel, AISI 1020 steel, AISI 1045 steel, aluminum and copper, each selected based on their real usage in the experimental setup.

8.3.4 Mesh and solver configuration

A refined mesh was applied near boundaries and within regions expected to exhibit steep temperature gradients to enhance solution accuracy as presented in Figure 8-9.

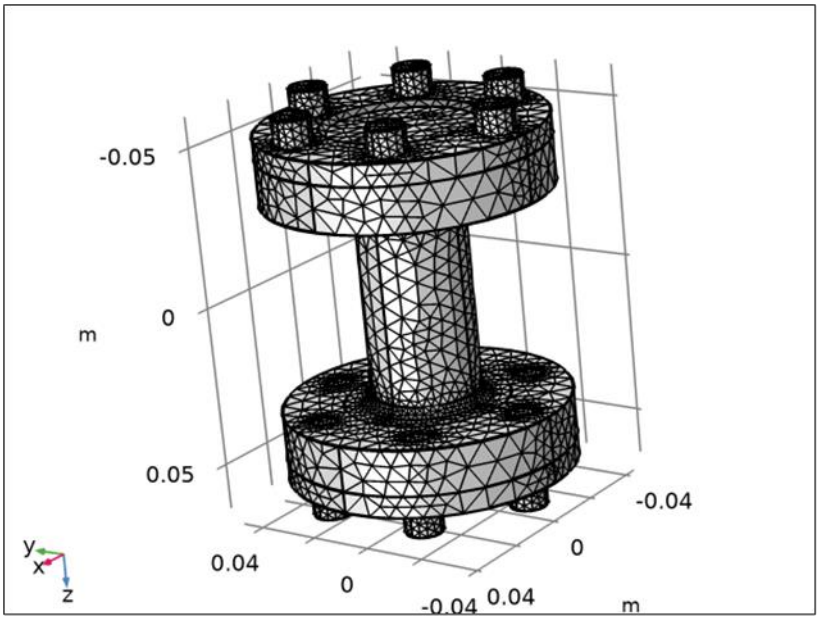

Figure 8-6 Meshed 3D Model of VCCT model constructed in COMSOL program.

Table 8-3 Kinetics parameter for 76.5wt.%NTO + GAP explosive material

Parameters	**76.5wt.%NTO + GAP**
Density, ρ (g/cm^3)	1.497
Activation energy, Ea (kJ/mol)	250.56
Heat of reaction, Q (J/g)	2792
Specific heat capacity, cp (kJ/kg ·K)	Cp = 0.25297+0.01181T
Thermal conductivity, k (W/m. °C)	0.64
Pre-exponential factor, A (1/s)	1.064* 10^{20}

8.3.5 Thermal distribution results

A time-dependent study was conducted over a simulation interval of 0 to 24500 seconds (approximately 6 hours) and two physics interfaces were used, heat Transfer in solids for modeling transient conductive heat transfer within the solid domains and transport of diluted species to account for temperature-driven species transport associated with material decomposition. Figure 8-10 shows the temperature distribution in the energetic charge at the final simulation time (24500 s) under a slow cook-off heating profile in a VCCT configuration. The PBX cylinder reaches a maximum temperature of 213°C (486 K) at its center.

This simulated peak temperature closely matches the decomposition onset temperatures determined experimentally by DSC, which ranged from 194.7°C (at 0.5°C/min) up to 222.7°C (at 4 °C/min), with intermediate values of 202.0°C, 212.8°C and 219.2°C corresponding to different heating rates of 1, 2 and 3°C/min respectively. Then, the simulated temperature falls between the DSC onset values observed at 0.5,1 and 2 °C/min, indicating that under these modeled conditions the PBX composition may reach or slightly surpass the threshold for thermal decomposition. This close match shows that there is a real and important risk of decomposition during slow heating.

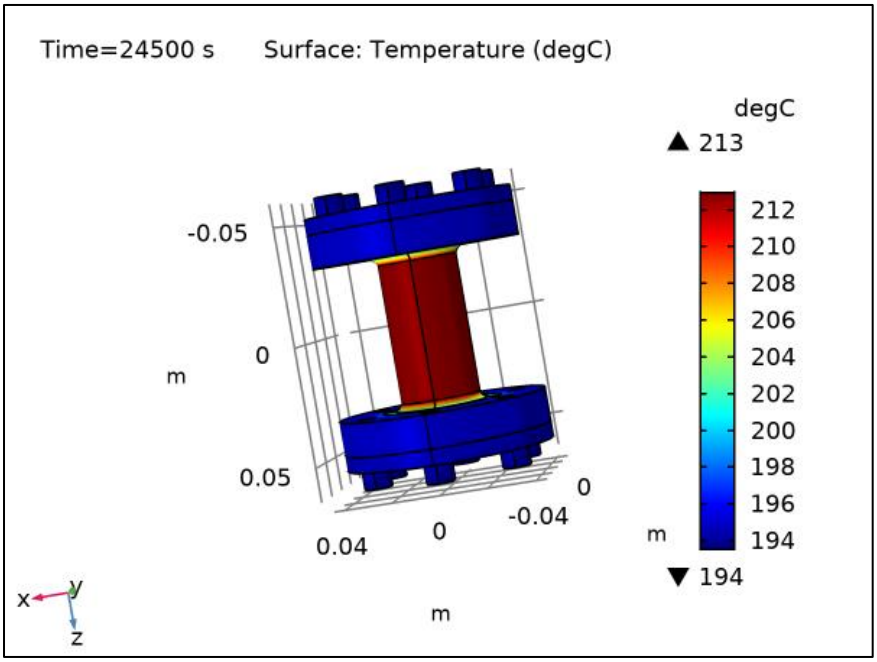

Figure 8-7 Temperature distribution in the energetic charge at the final simulation time.

The heating profile that presented in Figure 8-11 was modeled based on a controlled temperature ramp extracted from a CVVT, as shown the initial steep increase in temperature corresponds to surface and near-surface nodes reacting quickly to the external heating where the temperature spread between the colored curves in the figure indicates the temperature gradient within the PBX due to conduction limits, this shows the thermal lag between different points inside the PBX, especially between outer layers and core regions. The second slope change around 10000 s to 20000 s suggests the start of exothermic decomposition of the PBX material. This aligns with a thermal runaway behavior where the decomposition reaction releases heat, accelerating the temperature rise in some regions with temperatures increasing linearly up to a final steady state between 480 K and 500 K after approximately 22,000 s. The final temperatures exceed the experimentally observed onset for decomposition as the PBX cylinder reaches a maximum temperature of 213°C (486 K) at its center, this indicates that our PBX material may not passes the slow cook-off test under this condition.

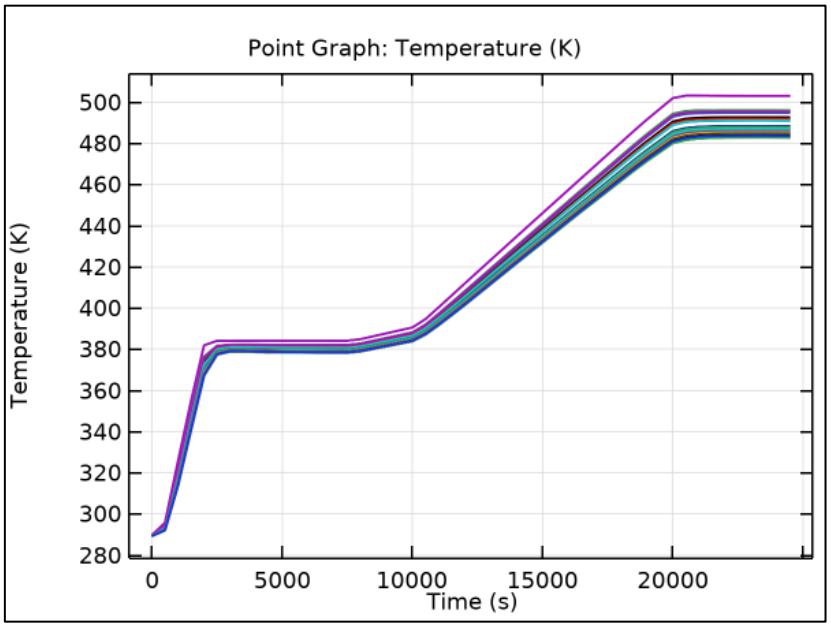

Figure 8-8 Temperature Profiles for PBX.

CHAPTE 9 GENERAL DISCUSSION

This research aims to advance the design of modern explosive materials by addressing the critical trade-off between performance and sensitivity. Specifically, it focuses on the composition of next-generation PBXs using 3-nitro-1,2,4-triazol-5-one (NTO), a high-energy and relatively insensitive explosive as the energetic component. As we mentioned earlier, two classes of traditional systems, nitramine-based PBXs and melt-cast IMX-type explosives, each present key limitation. While nitramine-based PBXs (RDX, HMX, PETN-based) offer high detonation performance, they suffer from high mechanical sensitivity. Conversely, melt-cast IMX systems achieve excellent insensitivity using ingredients like DNAN but at the cost of reduced energetic output. The novelty of this work lies in the development of cast-curable PBXs that integrate NTO with glycidyl azide polymer (GAP), an energetic binder. GAP contributes positively to the total energy content of the PBX due to its azide functionalities, while also improving mechanical properties. However, GAP has impact sensitivity approximately (8 J) raises some concerns, as it could increase the sensitivity of the explosive mixture when used at high contents. In the same time, despite NTO has inherently favorable insensitivity, its mechanical sensitivity and thermal stability still require improvement to fully meet the demands of next-generation insensitive munitions. To address all of this, a novel coating strategy was employed using carbon nanomaterials (CNMs), particularly graphene oxide (GO) to coat NTO crystals. GO is used to suppress the mechanical sensitivity of the NTO crystals and by extension that of the overall PBX composition. Its high surface area and functional oxygen groups facilitate strong interactions with energetic materials, acting as a buffer layer that mitigates impact and friction sensitivity. Additionally, CuO nanoparticles were embedded within the GO coating to enhance thermal decomposition behavior and overall energetic performance. While CuO has catalytic effect is well known, this research highlights a key distinction, when CuO is introduced as part of a GO-CuO composite coating, its catalytic influence is better controlled, maintaining a balance between improved energy release and safety. Another innovation in this study is the synthesis of NTO using a continuous flow microreactor, offering precise reaction control and enhanced safety compared to conventional batch synthesis. This technique directly addresses the critical limitations of traditional approaches particularly the significant risks associated with the nitration step, which typically requires elevated temperatures (around 65 °C) sustained for 1.5 to 2 hours, leading to potential hazards. The combination of these elements, GAP

as an energetic binder, GO as a sensitivity-reducing nanomaterial, CuO for catalytic enhancement, and microreactor-synthesized NTO, results in a new class of PBXs that demonstrate improved safety and performance.

Conventional synthesis techniques for NTO were first applied in this study to investigate the fundamental reaction mechanisms and to identify key parameters influencing the nitration step. The main objective was to optimize these parameters in order to achieve high product yield while maintaining a safe and efficient synthesis pathway. A significant challenge encountered during this stage was controlling the reaction temperature during nitration. Due to the highly exothermic nature of the reaction, the temperature of the reaction often exceeds above 95-100 °C causing the mixture to boil and releasing a substantial volume of gases which posed serious safety risks especially by one pot synthesis method. Through systematic variation of the initial reaction temperature, a notable improvement was achieved. Specifically, initiating the nitration reaction at 25 °C rather than 0 °C, resulted in a considerably higher NTO yield of 67.2% at a reaction temperature of 65 °C. This approach also reduced the reaction time and allowed for better temperature control enhancing both efficiency and safety in the batch process. In contrast, the one-pot synthesis method demonstrated an additional safety requirement by gradually adding nitric acid at 0 °C under carefully controlled cooling conditions, the risk of frothing and thermal runaway was significantly reduced. This modification led to an even higher yield of 72.3%, indicating a promising route for scalable synthesis with some risks during the reaction.

A novel approach for synthesizing NTO using a microreactor was developed in the second part of this study. Unlike conventional batch processes, the microreactor provides superior thermal control, reduced reaction volume and significantly improved safety, making it an attractive alternative for handling sensitive energetic materials. This method directly addresses the major challenges associated with conventional NTO synthesis, particularly the requirement for a sustained high nitration temperature (65 °C) over an extended period (1.5-2 hours) and the highly exothermic nature of the reaction, both of which pose serious safety concerns. Before implementing this technique, it was necessary to understand the microreactor design and operational principles to prevent any problems during synthesis especially when dealing with sensitive and hazardous materials. In microreactor systems, nitration reactions occur within narrow capillary tubes, so it was critical to ensure that these channels would not become blocked during NTO formation. This

concern was informed by earlier observations during batch synthesis where NTO particles began to precipitate before the reaction was complete indicating a risk of premature crystallization and clogging. To address this issue, a series of preliminary nitration experiments were conducted in batch reactors using different solvent systems. These tests aimed to identify solvent conditions that prevent early precipitation of NTO during synthesis and to evaluate the solubility of the precursor, TO under different solvents. The selected solvent system would also need to support continuous flow synthesis and efficient product collection. An effective strategy was developed for product recovery by cooling the collected reaction vials rather than relying on solvent evaporation, thereby avoiding the need to reinitiate the reaction or expose the system to additional thermal stress. As a result, a novel microreactor-based synthesis method was successfully established. It reduced the nitration time dramatically from 2 hours in the batch process to just 5 minutes, while achieving a comparable yield of 59.6% using a DMF: DMSO (80:20) solvent system. This demonstrates not only enhanced efficiency but also improved process safety. Compared to traditional batch synthesis, the microreactor system offers several advantages: it prevents heat accumulation, enables precise temperature control and allows for rapid heat and mass transfer due to its high surface-area-to-volume ratio. These features collectively reduce the risk of runaway reactions and establish a scalable and safer platform for synthesizing sensitive energetic materials like NTO.

The third part of this study focused on developing an optimized and novel energetic composite based on NTO, aimed at enhancing energetic performance, improving mechanical sensitivity and controlling thermal decomposition behavior. This was achieved by applying nanoscale coatings of graphene oxide (GO) and copper oxide (CuO) in varying proportions onto NTO particles. The preparation of the GO/NTO nanocomposites was successfully conducted using an ultrasonic dispersion technique, although several experimental challenges were encountered and addressed. One major issue was the selection of a suitable solvent system: NTO is soluble in water, which is also an effective medium for dispersing GO. To overcome this, a mixture of water and isopropanol was used. This combination enabled efficient dispersion of GO while preventing the dissolution of NTO. Additionally, due to the heat generated during ultrasonic treatment which can exceed 50 °C, experiments were conducted in an ice bath to maintain safe operating conditions especially in the existence of NTO explosive materials and extend the sonication time allowing sufficient coating without compromising safety.

A significant challenge in this phase of the research was the conflicting findings in the literature regarding the thermal effects of GO on energetic materials. While GO has been consistently reported to reduce the mechanical sensitivity (impact and friction) of explosives, its influence on thermal behavior remains controversial. Some studies have shown that GO improves thermal stability by increasing the activation energy, whereas others report the opposite (a reduction in thermal stability) or either no effect in thermal stability even within the same energetic material. To systematically investigate this, GO was incorporated at different contents by weight relative to NTO to examine its effect on both thermal stability and sensitivity. The results revealed a critical threshold: when the GO content exceeded 3 wt.%, thermal stability dramatically decreased. At 4 wt.% GO, the activation energy dropped by approximately 174 kJ/mol and the initial decomposition temperature decreased by 34.27 °C compared to pure NTO. Conversely, the incorporation of 3 wt.% GO yielded a novel improvement. The activation energy increased by approximately 45 kJ/mol over that of pure NTO and the decomposition temperature remained relatively stable. This enhancement is likely due to the encapsulating effect of the GO layer around NTO particles. GO may act as a thermal barrier: its high thermal conductivity allows heat to dissipate more evenly reducing localized hotspots that could initiate premature decomposition. Moreover, at this optimal content (3 wt.% GO), GO does not introduce an excess of reactive functional groups that could destabilize the explosive. In contrast, higher GO contents (<3 wt.% GO) likely introduce an overabundance of oxygen-containing groups (-OH, -COOH, C=O) which increase reactivity particularly under elevated temperatures leading to catalytic decomposition behavior rather than stabilization.

Building on these results, a hybrid composite of GO/CuO/NTO was also developed using the same ultrasonic dispersion technique. In this composition, the GO content was fixed at 3 wt.% based on its demonstrated optimal performance (thermal stability and mechanical sensitivity), while CuO nanoparticles were introduced in varying amounts relative to the GO content. The decomposition peak temperatures of these hybrid materials remained close to that of both pure NTO and the 3 wt.% GO-coated NTO indicating that the GO layer effectively moderated the catalytic influence of CuO when approximately less than 1 wt.% relative to NTO into the GO coating layer.

One of the new innovations was the successful incorporation of approximately less than 1wt.% CuO as a nano-metal oxide in the NTO without significantly accelerate the catalytic decomposition of NTO and in the same time increase the energy release of NTO by combination the coating layer with GO. This composite design provides a new and innovative strategy for tuning the performance and safety of NTO-based energetic materials through nanoscale surface coating.

The fourth part of this study builds upon previous findings to develop high-performance, low-sensitivity PBXs based on NTO and GAP using a cast-cured technique. A series of PBX materials were successfully prepared, targeting improvements in both detonation performance and mechanical safety. In addition to the base NTO/GAP composition, modified PBXs incorporating NTO coated with GO and NTO coated with a GO/nano-CuO composite were also fabricated using a thinky mixer to ensure uniform dispersion

One major challenge encountered was increasing the explosive content within the PBX matrix. It was observed that using a single particle size of NTO did not allow for optimal packing density. To address this, a recrystallization process was applied to produce NTO with a bimodal particle size distribution. This approach significantly improved the particle morphology and enabled higher solid loading within the explosive material ultimately achieving a composition with 76.5 wt.% explosive content. To further optimize the processing conditions, several compositions were mixed using a thinky ARV-310 mixer, which is specifically designed for highly viscous materials and offers better consistency compared to manual or traditional mechanical mixing. Parameters such as mixing time, speed and vacuum level were systematically varied to achieve optimal homogeneity and high-quality blending. Another key optimization parameter was the isocyanate to hydroxyl (NCO/OH) ratio in the curing system. Multiple PBX materials were prepared with NCO/OH ratios ranging from 0.9 to 1.5. Among these, a ratio of 1.2 was found to be optimal providing enhanced elasticity and favorable mechanical properties. The outcome was the development of a novel PBX material using NTO and GAP via the cast-cured method that exhibited significantly reduced mechanical sensitivity compared to conventional RDX and HMX based PBXs and also IM explosive systems. The friction sensitivity results reveal that the PBX composition containing 76.5% NTO with GAP exhibits a significantly higher resistance to friction initiation (360 N) compared to insensitive munitions such as IMX-101 (240 N) and IMX-104 (160 N), representing improvements of 50% and 125% respectively. The impact sensitivity results

further demonstrate the advantages of our NTO/GAP-based PBX composition. Compared to insensitive munitions such as IMX-101 and IMX-104. At the same time, it demonstrated superior detonation performance outperforming IMX-101 by up to 145.7 m/s. This represents a unique balance between sensitivity and detonation performance.

Moreover, the use of GAP as an energetic binder introduced several advantages. It improved the processability of the PBX and increased the overall heat release. Although GO alone improved the thermal stability of NTO, its incorporation with GAP in PBXs led to a synergistic effect reducing activation energy and decomposition temperature due to increased energy release. However, when CuO was introduced alongside GO, the formulation NTO/GO/CuO + GAP showed a higher onset decomposition temperature (205.5 °C) compared to NTO/GO + GAP (189.1°C) indicating improved initial thermal resistance. However, it's activation energy was reduced reflected CuO catalytic role in promoting rapid decomposition once initiated.

Finally, I conducted a time-dependent simulation of the variable confinement cook-off test (VCCT) using COMSOL Multiphysics based on previous developed model as described before to evaluate the thermal response and decomposition behavior of a PBX composition based on NTO and GAP. The simulation was performed over a 6-hour period under a controlled heating rate of 3.3 °C/h, in accordance with standard slow cook-off protocols. The heater temperature was defined through an interpolation profile, reaching a maximum of 230 °C, which exceeds the experimentally determined onset decomposition temperature of the material which ranged from 194.7°C (at 0.5°C/min) up to 222.7°C (at 4 °C/min), with intermediate values of 202.0°C, 212.8°C and 219.2°C corresponding to different heating rates of 1, 2 and 3°C/min respectively. This setup was intentionally chosen to evaluate the PBX response under worst-case thermal conditions and to identify the onset of thermal instability. The results clearly showed that the maximum temperature within the PBX core reached approximately 213 °C, Then, the simulated temperature falls between the DSC onset values observed at 0.5,1and 2 °C/min, indicating that under these modeled conditions the PBX composition may reach or slightly surpass the threshold for thermal decomposition. Overall, this modeling approach enabled a predictive assessment of the PBXs safety behavior.

CHAPTE 10 CONCLUSIONS AND RECOMMENDATIONS

This chapter presents a summary of the conclusions drawn from the objectives discussed in the previous chapters, followed by recommendations addressing the identified limitations and potential directions for future research.

10.1 Conclusions

This dissertation focuses on the design, synthesis, and characterization of novel advanced plastic-bonded explosives (PBXs) with enhanced detonation performance, while maintaining mechanical sensitivity (impact and friction) within acceptable limits for insensitive munitions (IM) applications. The study emphasizes the use of cast-cured PBXs incorporating NTO as the primary intrinsically insensitive high explosive and GAP as the energetic binder. In addition, this work introduces a novel microreactor-based synthesis method for NTO, developed to address the limitations of conventional batch processes. This innovative approach enhances both the safety and thermal control of NTO production.

The first part of this study explores the preparation of NTO explosives using conventional methods. Unlike prior studies, this work addresses critical gaps in the literature by combining high-yield strategies with enhanced process safety, particularly in batch and one-pot synthesis approaches. The key conclusions drawn from this part of the work are summarized as follows:

1- A novel enhancement in batch synthesis was achieved by initiating the nitration reaction at 25 °C instead of 0 °C, resulting in a significantly higher NTO yield (67.2) at 65 °C and reduced reaction time, while maintaining safe operational conditions.

2- The modified one-pot synthesis, involving gradual nitric acid addition at 0 °C, reduced frothing and thermal runaway risks and achieved a high yield of 72.3% that offering a scalable route with some reaction hazards.

3- Alternative nitrating agents such as mixed acids offered similar yields to nitric acid alone. Also, the use of ammonium nitrate improved thermal control and safety despite yielding only 52.9%.

The second part of this study presents a novel approach for synthesizing NTO via in situ nitration of 1,2,4-triazol-5-one (TO) with nitric acid inside a microreactor. Unlike conventional batch

techniques, the microreactor offers enhanced thermal control and improved safety, making it a promising alternative for handling sensitive energetic materials. This novel technique directly addresses the challenges associated with traditional NTO synthesis methods, particularly the risks posed by the high nitration temperature (65 °C) that sustained for 1.5-2 hours. The key conclusions drawn from this part of the work are summarized as follows:

1- A novel microreactor-based synthesis method was developed as a safer and more efficient alternative to the conventional batch process. It significantly reduced the nitration time from 2 hours to just 5 minutes while achieving a comparable yield (59.6%) using a DMF: DMSO solvent system demonstrating superior reaction efficiency.

2- Compared to the traditional batch method, the novel microreactor system offers superior safety and process reliability by eliminating heat accumulation and improving thermal control. Its high surface-area-to-volume ratio enables enhanced heat and mass transfer resulting in reducing the nitration time from 2 hours to just 5 minutes.

The third part of this study presents the development of NTO-based nanocomposites using graphene oxide (GO) and copper oxide (CuO) coatings aimed at enhancing thermal stability and reducing mechanical sensitivity by coating its particles with nanoscale layers of GO and CuO in varying proportions. The key conclusions drawn from this part of the work are summarized as follows:

1- GO-coated NTO nanocomposites was successfully developed, preserving the original polymorphic crystal structure of NTO during the coating process. A significant finding was that 3 wt.% GO provided a good enhancement in thermal stability, increasing the activation energy by 45 kJ/mol compared to pure NTO, whereas higher GO contents ≥ 4 led to a reduction in thermal stability.

2- A novel hybrid nanocomposite of NTO/GO/CuO was achieved by incorporating CuO into the GO coating. At low CuO contents (5-25% of the GO layer), the composite maintained thermal stability comparable to pure NTO, illustrating a novel balance between catalytic activity and thermal control enabled by GO of CuO effects. However, at higher CuO concentrations (35-45% of the GO layer), thermal stability was decreased, highlighting the critical role of composite design in tailoring the decomposition behavior of NTO-based explosives

3- The heat of combustion measurements confirmed that GO coating on NTO slightly reduces energy output due to the non-energetic nature of GO compared with NTO, while significantly enhancing safety by improving the mechanical sensitivity (impact and friction) of the NTO particles.

The fourth part of this study presents a novel contribution to the development of high-performance, low-sensitivity PBXs based on NTO and GAP using a cast-cured technique. A series of PBXs materials were successfully developed to enhance both performance parameters and sensitivity characteristics. In addition to the base material (NTO/GAP), modified PBXs materials incorporating NTO coated with GO and NTO coated with GO and nano-CuO were also successfully prepared using the thinky mixer. The key conclusions drawn from this part of the work are summarized as follows:

1- PBX material was developed using NTO and GAP via a cast-cured technique, where a successful recrystallization process enabled a high solid loading of 76.5 wt.% through a bimodal particle size distribution. This composition exhibited significantly lower mechanical sensitivity (impact and friction) than conventional RDX and HMX based PBXs and compared to insensitive explosives such as IMX-101 and IMX-104, while achieving superior detonation performance surpassing IMX-101 by up to 145.7 m/s, demonstrating a unique balance between sensitivity and high energy output.

2- The incorporation of GAP binder introduced multiple advantages, including enhanced processability, increased heat release and broadened decomposition behavior allowing gradual decomposition that is crucial for improving storage and handling safety.

3- Synergistic effect was observed when GO and CuO were integrated into the NTO-GAP matrix, although GO alone improved the thermal stability of NTO, its incorporation with GAP in PBXs led to reducing the activation energy and decomposition temperature due to increased energy release. Also, inclusion of CuO in the PBXs matrix decreases the activation energy and reduced the thermal stability of the PBXs compared with the original PBXs that composed from NTO and GAP only.

4- A COMSOL-based simulation of the VCCT was used to assess the thermal behavior of an NTO-GAP PBX under slow heating conditions. With a heating rate of 3.3 °C/h and a heater

temperature reaching 230 °C, the maximum temperature within the PBX core reached approximately 213 °C that falls between the DSC onset values, indicating that under these modeled conditions the PBX composition may reach or slightly surpass the threshold for thermal decomposition.

10.2 Recommendations

This research provided valuable insights into the development of PBX materials that balance performance and sensitivity characteristics. It also introduced a novel step toward synthesizing the explosive material NTO using a microreactor via a continuous flow chemistry approach. However, several aspects remain unexplored and are recommended for future investigation:

1. In the second part of this research, the solvent system (the type and the concentration of the solvent) was optimized for NTO synthesis in the microreactor, and residence time was partially explored. Future studies should focus on other parameters such as reaction temperature, reagent molar ratios to improve yield and safety.
2. In the PBX section, the results showed that GO catalyzed the thermal decomposition of the PBX material. Therefore, future studies should investigate other nanomaterials, such as reduced graphene oxide (RGO), to evaluate their effects on the behavior and stability of PBX formulations.
3. It is recommended to experimentally evaluate the full performance of the developed PBX compositions by measuring key parameters such as detonation velocity and brisance.
4. In this study, GAP was used as the energetic binder. However, future research should explore other binder systems such as PolyNIMMO, nitrated HTPB to evaluate their impact on the performance and sensitivity of PBX materials.
5. Investigate the compatibility of NTO with other advanced high-energy explosives such as BCHMX and CL-20 within PBX systems using GAP binder. This will help assess the combined effects on energetic output and mechanical sensitivity.

REFERENCES

[1] Baker, W. E., Cox, P. A., Kulesz, J. J., Strehlow, R. A., & Westine, P. S. (2012). Explosion hazards and evaluation. Elsevier.

[2] Agrawal, J. P. (2005). Some new high energy materials and their formulations for specialized applications. Propellants, Explosives, Pyrotechnics: An International Journal Dealing with Scientific and Technological Aspects of Energetic Materials, 30(5), 316-328.

[3] NATO STANAG 4439. (2010).Policy for Introduction and Assessment of Insensitive Munitions, Edition 3.

[4] Frem, D. (2023). A Review on IMX-101 and IMX-104 Melt-Cast Explosives: Insensitive Formulations for the Next-Generation Munition Systems. Propellants, Explosives, Pyrotechnics, 48(1), e202100312.

[5] Agrawal, J. P. (2010). High energy materials: propellants, explosives and pyrotechnics. John Wiley & Sons.

[6] May, C. M., & Tarver, C. M. (2014, May). Short pulse duration shock initiation experiments plus ignition and growth modeling on Composition B. In Journal of Physics: Conference Series (Vol. 500, No. 5, p. 052045). IOP Publishing.

[7] Kim, H. S., & Park, B. S. (1999). Characteristics of the Insensitive Pressed Plastic Bonded Explosive, DXD-59. Propellants, Explosives, Pyrotechnics, 24(4), 217-220.

[8] van der Steen, A., & Verbeek, R. (1990). Initiation and detonation of RDX and HMX HTPB-Based Plastic-Bonded Explosives. Propellants, explosives, pyrotechnics, 15(1), 19-21.

[9] Kim, Y. H., Lee, K., Koo, K. K., Shul, Y. G., & Haam, S. (2002). Comparison study of mixing effect on batch cooling crystallization of 3-Nitro-1, 2, 4-triazol-5-one (NTO) using mechanical stirrer and ultrasound irradiation. Crystal Research and Technology: Journal of Experimental and Industrial Crystallography, 37(9), 928-944.

[10] Bellamy, A. J., Ward, S. J., & Golding, P. (2002). A New Synthetic Route to 1, 3, 5-Triamino-2, 4, 6-Trinitrobenzene (TATB). Propellants, Explosives, Pyrotechnics: An

International Journal Dealing with Scientific and Technological Aspects of Energetic Materials, 27(2), 49-58.

[11] Jena, S., & Gupta, A. (2018). Nano-energetic materials for defense application. In Nano-energetic materials (pp. 81-108). Singapore: Springer Singapore.

[12] Aakeröy, C. B., & Sinha, A. S. (Eds.). (2018). Co-crystals: preparation, characterization and applications (Vol. 24). Royal Society of Chemistry.

[13] Ampleman, G. (2010). Development of a new generation of insensitive explosives and gun propellants. International Journal of Energetic Materials and Chemical Propulsion, 9(2).

[14] Smith, M. W., & Cliff, M. D. (1999). NTO-based explosive formulations: a technology review.

[15] Chi, Y., Huang, H., & Li, J. (2005, October). Influences of CNTs on Thermal decomposition and mechanical sensitivity of HMX. In International Autumn Seminar on Propellants. Explosives and Pyrotechnics (2005IASPEP). Beijing, China (pp. 319-321).

[16] Li, H., Ren, H., Jiao, Q., Du, S., & Yu, L. (2016). Fabrication and properties of insensitive CNT/HMX energetic nanocomposites as ignition ingredients. Propellants, Explosives, Pyrotechnics, 41(1), 126-135.

[17] Alam, S. N., Sharma, N., & Kumar, L. (2017). Synthesis of graphene oxide (GO) by modified hummers method and its thermal reduction to obtain reduced graphene oxide (RGO). Graphene, 6(01), 1.

[18] Shen, J., Liu, Z., Xu, B., Chen, F., Zhu, Y., Fu, Y., & Wang, Z. (2020). Tuning the thermal, mechanical, and combustion properties of NC-TEGDN-RDX propellants via incorporation of graphene nanoplates. Journal of energetic materials, 38(3), 326-335.

[19] Wu, S.X., Zhou, C.Y., Hu, Q.W., Chen, L., & Zhang, T. (2019). Study on combustion characteristics of graphene-coated al particles in HTPB propellant. In Proceedings of the International Annual Conference of the Fraunhofer ICT, Karlsruhe, Germany, pp. 1–5.

[20] Anoop Anand, K., & Rani, J. (2006). Polymer Nanocomposites: Crystallization, Reinforcement and Conductivity through SWNTs (Doctoral dissertation, Cochin University of Science & Technology).

[21] Gayathri, S., & Reshmi, S. (2017). Nitrato functionalized polymers for high energy propellants and explosives: recent advances. Polymers for Advanced Technologies, 28(12), 1539-1550.

[22] Tang, C. J., Lee, Y., & Litzinger, T. A. (1999). Simultaneous temperature and species measurements of the glycidyl azide polymer (GAP) propellant during laser-induced decomposition. Combustion and flame, 117(1-2), 244-256.

[23] Weifei, Y., Zhiyong, W., Ruijuan, X., Mei, F., Sen, L., & Guangcheng, Y. (2020, March). Explosive synthesis: novel intrinsically safe method and application with micro-channel reactor. In Journal of Physics: Conference Series (Vol. 1507, No. 2, p. 022030). IOP Publishing.

[24] Ménard, A. D., & Trant, J. F. (2020). A review and critique of academic lab safety research. Nature chemistry, 12(1), 17-25.

[25] Manchot, W., & Noll, R. (1905). Ueber derivate des Triazols. Justus liebigs annalen der chemie, 343(1), 1-27.

[26] Lee, K. Y., Chapman, L. B., & Cobura, M. D. (1987). 3-Nitro-1, 2, 4-triazol-5-one, a less sensitive explosive. Journal of Energetic Materials, 5(1), 27-33.

[27] Chipen, G. I., Bokalder, R. P., & Grinshtein, V. Y. (1966). 1, 2, 4-Triazol-3-one and its nitro and amino derivatives. Chemistry of heterocyclic compounds, 2(1), 79-83.

[28] Saikia, A., Sivabalan, R., Gore, G. M., & Sikder, A. K. (2014). Synthesis of some potential high energy materials using metal nitrates; an approach towards environmental benign process.

[29] Saikia, A., Sivabalan, R., Gore, G. M., & Sikder, A. K. (2012). Microwave-assisted quick synthesis of some potential high explosives. Propellants, Explosives, Pyrotechnics, 37(5), 540-543.

[30] da Costa Mattos, E., Moreira, E. D., Diniz, M. F., Dutra, R. C., da Silva, G., Iha, K., & Teipel, U. (2008). Characterization of polymer-coated RDX and HMX particles. Propellants, Explosives, Pyrotechnics: An International Journal Dealing with Scientific and Technological Aspects of Energetic Materials, 33(1), 44-50.

[31] Liang, Y., Zhang, J., & Jiang, X. (2008). HMX content in PBX booster measured by visible spectro-photometric method. Chin. J. Energ. Mater, 16, 531-534.

[32] Schmid, H. (1986). Coating of explosives. Journal of hazardous materials, 13(1), 89-101.

[33] Nie, P., Jin, S., Kou, X., Du, L., Li, L., Chen, K., & Wang, J. (2022). Study on the Effect of NTO on the Performance of HMX-Based Aluminized Cast-PBX. Materials, 15(14), 4808.

[34] Pelletier, P., Lavigne, D., Laroche, I., Cantin, F., Phillips, L., & Fung, V. (2010, October). Additional properties studies of DNAN based melt-pour explosive formulations. In 2010 Insensitive Munitions and Energetic Materials Technology Symposium, 11–14 October, Munich, Germany.

[35] Singh, S., Jelinek, L., Samuels, P., Di Stasio, A., & Zunino, L. (2010, October). IMX-104 characterization for DoD Qualification. In 2010 Insensitive Munitions & Energetic Materials Technology Symposium, Munich (pp. 11-14).

[36] Spear, R., Louey, C., & Wolfson, M. (1989). A preliminary assessment of 3-Nitro-1, 2, 4-Triazol-5-One(NTO) as an insensitive high explosive.

[37] Field, J. E. (1992). Hot spot ignition mechanisms for explosives. Accounts of chemical Research, 25(11), 489-496.

[38] Kim, E. S., Lee, H. S., Mallery, C. F., & Thynell, S. T. (1997). Thermal decomposition studies of energetic materials using confined rapid thermolysis/FTIR spectroscopy. Combustion and Flame, 110(1-2), 239-255.

[39] Witte, L. C., & Cox, J. E. (1973). Thermal explosion hazards. In Advances in Nuclear Science and Technology (pp. 329-364). Academic Press.

[40] Asay, B. W. (2010). Cookoff. In Shock Wave Science and Technology Reference Library, Vol. 5: Non-Shock Initiation of Explosives (pp. 403-482). Berlin, Heidelberg: Springer Berlin Heidelberg.

[41] Krawietz, T. R., McKenney Jr, R. L., & Ortiz, R. J. (2002). Characterization of the unconfined slow cook-off response of nitramines and nitraminecomposites with TNT. In 12 th International Detonation Symposium. San Diego (pp. 79-86).

[42] Yang, J., Li, H. B., Jin, P. G., Gao, Z., Ren, S. T., Jiang, X. B., & Zhang, W. J. (2024). Study on bullet impact performance of the HATO-based explosives. Vibroengineering Procedia, 54, 180-185.

[43] Chen, L., Wang, C., Feng, C. G., Lu, F., Lu, J. Y., Wang, X. F., & Guo, X. (2013). Study on random initiation phenomenon for sympathetic detonation of explosive. Defence technology, 9(4), 224-228.

[44] Dickson, P. (2019). The Response of Explosives to Accidental Stimuli (No. LA-UR-19-21843). Los Alamos National Laboratory (LANL), Los Alamos, NM (United States).

[45] Sivaraman, S., & Varadharajan, S. (2021). Investigative consequence analysis: a case study research of Beirut explosion accident. Journal of Loss prevention in the Process industries, 69, 104387.

[46] Accident Photographs from Beirut explosion. (2020). Available : https://en.wikipedia.org/wiki/2020_Beirut_explosion.

[47] Powell, I. J. (2016). Insensitive munitions–design principles and technology developments. Propellants, Explosives, Pyrotechnics, 41(3), 409-413.

[48] Moulard, H., Kury, J. W., & Delclos, A. (1985, July). The effect of RDX particle size on the shock sensitivity of cast PBX formulations. In Proc. 8th Symp.(Int.) on Detonation (ed. JM Short) (pp. 902-913).

[49] Köhler, J., Meyer, R., & Homburg, A. (2012). Explosivstoffe. John Wiley & Sons.

[50] Lee, K. E., Balas-Hummers, W. A., Di Stasio, A. R., Patel, C. H., Samuels, J., Roos, B. D., & Fung, V. (2010, October). Qualification testing of the insensitive TNT replacement explosive IMX-101. In Insensitive Munitions and Energetic Materials Technology Symposium (pp. 1-13).

[51] Kaneshige, M. J., Renlund, A. M., Schmitt, R. G., & Erikson, W. W. (2004). Development of scalable cook-off models using real-time in situ measurements. In AIP Conference Proceedings. American Institute of Physics. (Vol. 706, No. 1, pp. 351-354) .

[52] NATO Standardization Office, “AOP 4240. (2018). Fast Heating Munition Test Procedures”.

[53] NATO Standardization Office, “AOP 4382. (2020). Slow Heating Test Procedures For Munitions”.

[54] Provatas, A. (2000). Energetic polymers and plasticisers for explosive formulations: a review of recent advances (pp. 26-27). Melbourne: DSTO Aeronautical and Maritime Research Laboratory.

[55] Hopler, R. B. (1998). The history, development, and characteristics of explosives and propellants. Forensic Investigation of Explosives.

[56] Primasheet flexible sheet explosive. http://www.eba-d.com/products/primasheet-flexible-sheet-explosive.

[57] Li, Y., Wu, P., Hua, C., Wang, J., Huang, B., Chen, J., & Yang, G. (2019). Determination of the mechanical and thermal properties, and Impact sensitivity of pressed hmx-based PBX. Central European Journal of Energetic Materials, 16(2), 295-315.

[58] Nouguez, B., Mahe, B., & Vignaud, P. O. (2009). Cast PBX related technologies for IM shells and warheads. Sci. Technol. Energ. Mater, 70(5-6), 135-139.

[59] Strohecker, D. E., Carlson, R. J., Porembka, S. W., & Boulger, F. W. (1964). Explosive forming of metals (Vol. 203). Defense Metals Information Center, Battelle Memorial Institute.

[60] Akhavan, J. (2022). The chemistry of explosives 4E. Royal Society of Chemistry.

[61] Samudre, S. S., Nair, U. R., Gore, G. M., Kumar Sinha, R., Kanti Sikder, A., & Nandan Asthana, S. (2009). Studies on an improved plastic bonded explosive (PBX) for shaped charges. Propellants, Explosives, Pyrotechnics: An International Journal Dealing with Scientific and Technological Aspects of Energetic Materials, 34(2), 145-150.

[62] Nouguez, B., & Eck, G. (2016). From synthesis to formulation and final application. Propellants, Explosives, Pyrotechnics, 41(3), 548-554.

[63] Hamad, M. H., Mostafa, H. E., & Seleet, M. M. (2014, May). Study of Advanced Plastic Bonded Explosives. In The International Conference on Chemical and Environmental Engineering (Vol. 7, No. 7th International Conference on Chemical & Environmental Engineering, pp. 1-10). Military Technical College.

[64] Flower, P., & Marshall, E. (1993). Comparison of the production of PBXs by reaction injection moulding (RIM) and conventional techniques. 24th International Annual Conference of ICT. Karlsruhe, Germany.

[65] Kasprzyk, D. J., Bell, D. A., Flesner, R. L., & Larson, S. A. (1999). Characterization of a Slurry Process Used to Make a Plastic-Bonded Explosive. Propellants, Explosives, Pyrotechnics, 24(6), 333-338.

[66] Hofmann, H., & Rudolf, K. (2005). U.S. Patent No. 6,884,307. Washington, DC: U.S. Patent and Trademark Office.

[67] Elsharkawy, K. K. (2012). Advanced PBX Formulations used with Fragmentation Warhead. (M.Sc. thesis, MTC, Cairo).

[68] Leach, C., Flower, P., Hollands, R., Flynn, S., Marshall, E., & Kendrick, J. (1998). Plasticisers in energetic materials formulations- A UK overview. Energetic materials-Production, processing and characterization, 2-1.

[69] Teipel, U. (Ed.). (2006). Energetic materials: particle processing and characterization. John Wiley & Sons.

[70] Zalewski, K., Chyłek, Z., & Trzciński, W. A. (2022). Rheokinetic studies on the curing process of energetic systems containing RDX, HTPB with high content of 1, 2-vinyl groups and hydantoin-based bonding agent. Polymer Testing, 111, 107611.

[71] Cheng, T. (2019). Review of novel energetic polymers and binders–high energy propellant ingredients for the new space race. Designed Monomers and Polymers, 22(1), 54-65.

[72] Parker, G. R., Holmes, M. D., Heatwole, E. M., Broilo, R. M., Pederson, M. N., & Dickson, P. M. (2020). Direct observation of frictional ignition in dropped HMX-based polymer-bonded explosives. Combustion and flame, 221, 180-193.

[73] Anniyappan, M., Talawar, M. B., Sinha, R. K., & Murthy, K. P. (2020). Review on advanced energetic materials for insensitive munition formulations. Combustion, Explosion, and Shock Waves, 56, 495-519.

[74] Yu, L., Jiang, X., Guo, X., Ren, H., & Jiao, Q. (2013). Effects of binders and graphite on the sensitivity of ε-HNIW. Journal of thermal analysis and calorimetry, 112, 1343-1349.

[75] Liao, S. R., Luo, Y. J., Sun, J., & Tan, H. M. (2012). Preparation of WPU-g-SAN and its coating on HNIW. Hanneng Cailiao/Chinese Journal of Energetic Materials, 20(2), 155-160.

[76] Yu, L., Ren, H., Guo, X. Y., Jiang, X. B., & Jiao, Q. J. (2014). A novel ε-HNIW-based insensitive high explosive incorporated with reduced graphene oxide. Journal of Thermal Analysis and Calorimetry, 117, 1187-1199.

[77] Gao, J., Jin, S., Wang, N., Wu, N., Zhang, R., Li, L., & Chen, K. (2025). Study on the Properties of CL-20/NTO Based Pressed Mixed Explosive Under Typical Binder System. ChemistrySelect, 10(1), e202404766.

[78] Singh, H. (2005). Current trend of R&D in the field of high energy materials (HEMs): an overview. Explosion, 15(3), 120-133.

[79] Urtiew, P. A., Vandersall, K. S., Tarver, C. M., Garcia, F., & Forbes, J. W. (2008). Shock initiation of composition B and C-4 explosives: Experiments and modeling. Russian Journal of Physical Chemistry B, 2, 162-171.

[80] Meyer, R., Köhler, J., & Homburg, A. (2016). Explosives. John Wiley & Sons.

[81] Liang, Y., Zhang, J., & Jiang, X. (2008). HMX content in PBX booster measured by visible spectro-photometric method. Chin. J. Energ. Mater, 16, 531-534.

[82] Chen, L. Y. (2002). New explosive charge of warhead. Chinese Journal of Explosives and Propellants, 25(3), 26-27.

[83] Pisharath, S., & Ang, H. G. (2007). Synthesis and thermal decomposition of GAP–Poly (BAMO) copolymer. Polymer Degradation and Stability, 92(7), 1365-1377.

[84] Kubota, N., & Sonobe, T. (1988). Combustion mechanism of azide polymer. Propellants, Explosives, Pyrotechnics, 13(6), 172-177.

[85] Hartdegen, V. (2016). Energetic polymers and plasticizers based on organic azides, nitro groups and tetrazoles (Doctoral dissertation, lmu).

[86] Kubota, N., Sonobe, T., Yamamoto, A., & Shimizu, H. (1990). Burning rate characteristics of GAP propellants. Journal of Propulsion and Power, 6(6), 686-689.

[87] Nazare, A. N., Asthana, S. N., & Singh, H. (1992). Glycidyl azide polymer (GAP)-an energetic component of advanced solid rocket propellants-a review. Journal of Energetic Materials, 10(1), 43-63.

[88] Reed Jr, R., & Chan, M. L. (1983). U.S. Patent No. 4,379,903. Washington, DC: U.S. Patent and Trademark Office.

[89] Hussein, A. K., Elbeih, A., & Zeman, S. (2018). The effect of glycidyl azide polymer on the stability and explosive properties of different interesting nitramines. RSC advances, 8(31), 17272-17278.

[90] Yanju, W., Jingyu, W., Chongwei, A., Hequn, L., Xiaomu, W., & Binshuo, Y. (2017). GAP/CL-20-based compound explosive: a new booster formulation used in a small-sized initiation network. Journal of Energetic Materials, 35(1), 53-62.

[91] Zeng, C., Yang, Z., Wen, Y., He, W., Zhang, J., Wang, J., & Gong, F. (2021). Performance optimization of core-shell HMX@(Al@ GAP) aluminized explosives. Chemical Engineering Journal, 407, 126360.

[92] Politzer, P., & Murray, J. S. (2017). High performance, low sensitivity: the impossible (or possible) dream?. In Energetic Materials: From Cradle to Grave (pp. 1-22). Cham: Springer International Publishing.

[93] Hobbs, J. R. (1993, February). Analysis of semtex explosives. In Advances in Analysis and Detection of Explosives: Proceedings of the 4th International Symposium on Analysis and Detection of Explosives, September 7–10, 1992, Jerusalem, Israel (pp. 409-427). Dordrecht: Springer Netherlands.

[94] Badgujar, D. M., Talawar, M. B., & Mahulikar, P. P. (2017). Review of promising insensitive energetic materials. Central European Journal of Energetic Materials, 14(4).

[95] Badgujar, D. M., Talawar, M. B., Asthana, S. N., & Mahulikar, P. P. (2008). Advances in science and technology of modern energetic materials: an overview. Journal of hazardous materials, 151(2-3), 289-305.

[96] Yan, Q. L., Zeman, S., & Elbeih, A. (2012). Recent advances in thermal analysis and stability evaluation of insensitive plastic bonded explosives (PBXs). Thermochimica acta, 537, 1-12.

[97] Sabatini, J. J., & Oyler, K. D. (2015). Recent advances in the synthesis of high explosive materials. Crystals, 6(1), 5.

[98] Simpson, R. L., Urtiew, P. A., Ornellas, D. L., Moody, G. L., Scribner, K. J., & Hoffman, D. M. (1997). CL-20 performance exceeds that of HMX and its sensitivity is moderate. Propellants, Explosives, Pyrotechnics, 22(5), 249-255.

[99] Zou, H. M., Chen, S. S., Li, X., Jin, S. H., Niu, H., Wang, F., & Shu, Q. H. (2017). Preparation, thermal investigation and detonation properties of ε-CL-20-based polymer-bonded explosives with high energy and reduced sensitivity. Materials Express, 7(3), 199-208.

[100] Xue, H., Gao, H., Twamley, B., & Shreeve, J. N. M. (2007). Energetic salts of 3-nitro-1, 2, 4-triazole-5-one, 5-nitroaminotetrazole, and other nitro-substituted azoles. Chemistry of Materials, 19(7), 1731-1739.

[101] Bolotina, N. B., Zhurova, E., & Pinkerton, A. A. (2003). Energetic materials: variable-temperature crystal structure of β-NTO. Applied Crystallography, 36(2), 280-285.

[102] Toghiani, R. K., Toghiani, H., Maloney, S. W., & Boddu, V. M. (2008). Prediction of physicochemical properties of energetic materials. Fluid Phase Equilibria, 264(1-2), 86-92.

[103] Viswanath, D. S., Ghosh, T. K., Boddu, V. M., Viswanath, D. S., Ghosh, T. K., & Boddu, V. M. (2018). 5-Nitro-2, 4-Dihydro-3H-1, 2, 4-Triazole-3-One (NTO). Emerging Energetic Materials: Synthesis, Physicochemical, and Detonation Properties, 163-211.

[104] Sikder, A. K., & Sikder, N. (2004). A review of advanced high performance, insensitive and thermally stable energetic materials emerging for military and space applications. Journal of hazardous materials, 112(1-2), 1-15.

[105] Singh, G. (2015). Recent advances on energetic materials. Recent Adv Energy Mater, 1-411.

[106] Gibbs, T. R., & Popolato, A. (Eds.). (2023). LASL explosive property data (Vol. 4). Univ of California Press.

[107] Lee, K. Y., & Coburn, M. D. (1988). U.S. Patent No. 4,733,610. Washington, DC: U.S. Patent and Trademark Office.

[108] Becuwe, A., & Delclos, A. (1993). Low-sensitivity explosive compounds for low vulnerability warheads. Propellants, Explosives, Pyrotechnics, 18(1), 1-10.

[109] Deshmukh, M. B., Wagh, N. D., Sikder, A. K., Borse, A. U., & Dalal, D. S. (2014). Cyclodextrin nitrate Ester/H2SO4 as a novel nitrating system for efficient synthesis of insensitive high explosive 3-nitro-1, 2, 4-triazol-5-one. Industrial & Engineering Chemistry Research, 53(50), 19375-19379.

[110] Szala, M., Cudziło, S., & Lewczuk, R. (2011). Process optimization for synthesis of 3-nitro-1,2,4-triazol-5-one (NTO). Bul. Watts.

[111] Vadhe, P. P., Pawar, R. B., Sinha, R. K., Asthana, S. N., & Subhananda Rao, A. (2008). Cast aluminized explosives. Combustion, explosion, and Shock waves, 44, 461-477.

[112] Mukundan, T., Nair, J. K., Purandare, G. N., Talawar, M. B., Nath, T., & Asthana, S. N. (2006). Low vulnerable sheet explosive based on 3-nitro-1, 2, 4-triazol-5-one. Journal of propulsion and power, 22(6), 1348-1352.

[113] Yu, R., Chen, S., Lan, G., Li, J., Wei, C., & Jin, S. (2019). Thermal hazards evaluation of insensitive JEOL-1 polymer bonded explosive. Materials Express, 9(6), 596-603.

[114] Trache, D., Klapötke, T. M., Maiz, L., Abd-Elghany, M., & DeLuca, L. T. (2017). Recent advances in new oxidizers for solid rocket propulsion. Green Chemistry, 19(20), 4711-4736.

[115] Szala, M., & Trzciński, W. A. (2017). Synthesis and energetic properties of imidazolium and 2-methylimidazolium salts of 3-nitro-1, 2, 4-triazol-5-one. Propellants, Explosives, Pyrotechnics, 42(9), 1027-1031.

[116] Lee, K. Y., & Stinecipher, M. M. (1989). Synthesis and initial characterization of amine salts of 3-nitro-1, 2, 4-triazol-5-one. Propellants, explosives, pyrotechnics, 14(6), 241-244.

[117] Spyckerelle, C., Songy, C., Eck, G., & France, I. M. (2010, October). IM melt cast compositions based on NTO. In 2010 Insensitive Munitions & Energetic Materials Technology Symposium, Munich, Germany.

[118] Weckerle, A., & Coulouarn, C. (2010, October). A step further for the XF® explosive family dedicated to insensitive munitions (IM). In 2010 Insensitive Munitions & Energetic Materials Technology Symposium, Munich, Germany.

[119] Trzciński, W., Cudziło, S., Dyjak, S., & Nita, M. (2014). A comparison of the sensitivity and performance characteristics of melt-pour explosives with TNT and DNAN binder. Central European Journal of Energetic Materials, 11(3), 443-455.

[120] Hussein, A. K., Elbeih, A., & Zeman, S. (2017). Thermal decomposition kinetics and explosive properties of a mixture based on cis-1, 3, 4, 6-tetranitrooctahydroimidazo-[4, 5-d] imidazole and 3-nitro-1, 2, 4-triazol-5-one (BCHMX/NTO). Thermochimica Acta, 655, 292-301.

[121] Elbeih, A., Elnogomy, M., Elshenawy, T., Saleh, A., Azazy, A., Zaky, M. G., & Ahmed, H. S. (2022, August). High Performance Sheet of PBX based on NTO. In Journal of Physics: Conference Series (Vol. 2305, No. 1, p. 012019). IOP Publishing.

[122] Lan, G., Jin, S., Chen, M., Li, J., Lu, Z., Wang, N., & Li, L. (2020). Preparation and performances characterization of HNIW/NTO-based high-energetic low vulnerable polymer-bonded explosive. Journal of Thermal Analysis and Calorimetry, 139, 3589-3602.

[123] Huang, Y., Guo, Q., Gou, R., Zhu, S., Zhang, S., Yuan, X., & Chen, Y. (2022). Theoretical investigation on interface interaction and properties of 3-nitro-1, 2, 4-triazol-5-one (NTO)/fluoropolymer polymer-bonded explosives (PBXs). Theoretical Chemistry Accounts, 141(11), 74.

[124] Tappan, B. C., Bowden, P. R., Lichthardt, J. P., Schmitt, M. M., & Hill, L. G. (2018). Evaluation of the Detonation Performance of Insensitive Explosive Formulations based on 3, 3 Diamino-4, 4-azoxyfurazan (DAAF) and 3-Nitro-1, 2, 4-triazol-5-one (NTO). Journal of energetic materials, 36(2), 169-178.

[125] Li, J. C., Jiao, Q. J., Gong, Y. G., Wang, Y. Y., Liang, T., & Sun, J. (2018). Explosive performance of HMX/NTO co-crystal. In IOP Conference Series: Materials Science and Engineering (Vol. 292, No. 1, p. 012032). IOP Publishing.

[126] Elvira, K. S., i Solvas, X. C., Wootton, R. C., & Demello, A. J. (2013). The past, present and potential for microfluidic reactor technology in chemical synthesis. Nature chemistry, 5(11), 905-915.

[127] Sebastián, V., & Jensen, K. F. (2016). Nanoengineering a library of metallic nanostructures using a single microfluidic reactor. Nanoscale, 8(33), 15288-15295.

[128] Ehrfeld, W., Hessel, V., & Lower, H. (2000). New technology for modern chemistry. Microreactors: New Technology for Modern Chemistry.

[129] Hessel, V., Renken, A., Schouten, J. C., & Yoshida, J. I. (Eds.). (2009). Micro process engineering, 3 volume set: a comprehensive handbook (Vol. 1). John Wiley & Sons.

[130] Hartman, R. L., McMullen, J. P., & Jensen, K. F. (2011). Deciding whether to go with the flow: evaluating the merits of flow reactors for synthesis. Angewandte Chemie International Edition, 50(33), 7502-7519.

[131] Schwolow, S., Hollmann, J., Schenkel, B., & Röder, T. (2012). Application-oriented analysis of mixing performance in microreactors. Organic Process Research & Development, 16(9), 1513-1522.

[132] Plutschack, M. B., Pieber, B., Gilmore, K., & Seeberger, P. H. (2017). The hitchhiker's guide to flow chemistry‖. Chemical reviews, 117(18), 11796-11893.

[133] Guetzoyan, L., Nikbin, N., Baxendale, I. R., & Ley, S. V. (2013). Flow chemistry synthesis of zolpidem, alpidem and other GABA A agonists and their biological evaluation through the use of in-line frontal affinity chromatography. Chemical science, 4(2), 764-769.

[134] Soleymani, A., Yousefi, H., & Turunen, I. (2008). Dimensionless number for identification of flow patterns inside a T-micromixer. Chemical Engineering Science, 63(21), 5291-5297.

[135] Nagaki, A., Togai, M., Suga, S., Aoki, N., Mae, K., & Yoshida, J. I. (2005). Control of extremely fast competitive consecutive reactions using micromixing. Selective Friedel− Crafts aminoalkylation. Journal of the American Chemical Society, 127(33), 11666-11675.

[136] Ghanem, A., Lemenand, T., Della Valle, D., & Peerhossaini, H. (2014). Static mixers: Mechanisms, applications, and characterization methods–A review. Chemical engineering research and design, 92(2), 205-228.

[137] Jensen, K. F., Reizman, B. J., & Newman, S. G. (2014). Tools for chemical synthesis in microsystems. Lab on a Chip, 14(17), 3206-3212.

[138] Munirathinam, R., Huskens, J., & Verboom, W. (2015). Supported catalysis in continuous-flow microreactors. Advanced synthesis & catalysis, 357(6), 1093-1123.

[139] Hook, B. D., Dohle, W., Hirst, P. R., Pickworth, M., Berry, M. B., & Booker-Milburn, K. I. (2005). A practical flow reactor for continuous organic photochemistry. The Journal of organic chemistry, 70(19), 7558-7564.

[140] Yoshida, J. I., Takahashi, Y., & Nagaki, A. (2013). Flash chemistry: flow chemistry that cannot be done in batch. Chemical communications, 49(85), 9896-9904.

[141] Bedore, M. W., Zaborenko, N., Jensen, K. F., & Jamison, T. F. (2010). Aminolysis of epoxides in a microreactor system: a continuous flow approach to β-amino alcohols. Organic Process Research & Development, 14(2), 432-440.

[142] Reizman, B. J., & Jensen, K. F. (2016). Feedback in flow for accelerated reaction development. Accounts of chemical research, 49(9), 1786-1796.

[143] Vladisavljević, G. T., Kobayashi, I., & Nakajima, M. (2012). Production of uniform droplets using membrane, microchannel and microfluidic emulsification devices. Microfluidics and nanofluidics, 13, 151-178.

[144] Hessel, V., Löwe, H., & Schönfeld, F. (2005). Micromixers—a review on passive and active mixing principles. Chemical engineering science, 60(8-9), 2479-2501.

[145] Yoshida, J. I., Kim, H., & Nagaki, A. (2011). Green and sustainable chemical synthesis using flow microreactors. ChemSusChem, 4(3), 331-340.

[146] Méndez Portillo, L. S. (2011). Free-Radical Polymerization of Polystyrene Using Microreaction Technology (Doctoral dissertation, École Polytechnique de Montréal).

[147] Yao, C., Bai, W., Geng, L., He, Y., Wang, F., & Lin, Y. (2019). Experimental study on microreactor-based CNTs catalysts: Preparation and application. Colloids and Surfaces A: Physicochemical and Engineering Aspects, 583, 124001.

[148] Jähnisch, K., Hessel, V., Löwe, H., & Baerns, M. (2004). Chemistry in microstructured reactors. Angewandte Chemie International Edition, 43(4), 406-446.

[149] Sen, N., Singh, K. K., Mukhopadhyay, S., & Shenoy, K. T. (2020). Continuous synthesis of tributyl phosphate in microreactor. Progress in Nuclear Energy, 126, 103402.

[150] Cowey, K., Day, S., & Fryer, R. (1985). Examination of Wax-Coated RDX by scanning electron microscopy and X-ray photoelectron spectroscopy. Propellants, explosives, pyrotechnics, 10(3), 61-64.

[151] Wu, J. T., Zhang, J. G., Li, T., Li, Z. M., & Zhang, T. L. (2015). A novel cocrystal explosive NTO/TZTN with good comprehensive properties. Rsc Advances, 5(36), 28354-28359.

[152] Benhammada, A., Trache, D., Kesraoui, M., & Chelouche, S. (2020). Hydrothermal synthesis of hematite nanoparticles decorated on carbon mesospheres and their synergetic action on the thermal decomposition of nitrocellulose. Nanomaterials, 10(5), 968.

[153] Lin, C., Liu, J., Gong, F., Zeng, G., Huang, Z., Pan, L., .& Liu, S. (2015). High-temperature creep properties of TATB-based polymer bonded explosives filled with multi-walled carbon nanotubes. RSC Advances, 5(27), 21376-21383.

[154] Yan, Q. L., Gozin, M., Zhao, F. Q., Cohen, A., & Pang, S. P. (2016). Highly energetic compositions based on functionalized carbon nanomaterials. Nanoscale, 8(9), 4799-4851.

[155] Wang, L., Wu, J., Yi, C., Zou, H., Gan, H., & Li, S. (2012). Assemblies of energetic 3, 3′-diamino-4, 4′-azofurazan on single-walled carbon nanotubes. Computational and Theoretical Chemistry, 982, 66-73.

[156] Brodie, B. C. (1859). XIII. On the atomic weight of graphite. Philosophical transactions of the Royal Society of London, (149), 249-259.

[157] Dimiev, A. M., & Eigler, S. (Eds.). (2016). Graphene oxide: fundamentals and applications. John Wiley & Sons.

[158] Hummers Jr, W. S., & Offeman, R. E. (1958). Preparation of graphitic oxide. Journal of the american chemical society, 80(6), 1339-1339.

[159] Marcano, D. C., Kosynkin, D. V., Berlin, J. M., Sinitskii, A., Sun, Z., Slesarev, A., & Tour, J. M. (2010). Improved synthesis of graphene oxide. ACS nano, 4(8), 4806-4814.

[160] Wu, J., Lin, H., Moss, D. J., Loh, K. P., & Jia, B. (2023). Graphene oxide for photonics, electronics and optoelectronics. Nature Reviews Chemistry, 7(3), 162-183.

[161] Ojha, K., Anjaneyulu, O., & Ganguli, A. K. (2014). Graphene-based hybrid materials: synthetic approaches and properties. Current Science, 397-418.

[162] Wang, J., Chen, S., Yao, Q., Jin, S., Zhao, S., Yu, Z.,. & Shu, Q. (2017). Preparation, characterization, thermal evaluation and sensitivities of TKX-50/GO composite. Propellants, Explosives, Pyrotechnics, 42(9), 1104-1110.-10.

[163] Song, X., Huang, Q., Jin, B., & Peng, R. (2021). Fabrication and characterization of CL-20/PEI/GO composites with enhanced thermal stability and desensitization via electrostatic self-assembly. Applied Surface Science, 558, 149933.

[164] Li, R., Wang, J., Shen, J. P., & Yang, G. C. (2013). Preparation and characterization of insensitive HMX/graphene oxide composites. Propellants, Explosives, Pyrotechnics, 38(6), 798-804.

[165] Zeng, G. Y., Zhou, J. H., & Lin, C. M. (2015). The thermal decomposition behavior of graphene oxide/HMX composites. Key Engineering Materials, 645, 110-114.

[166] Chen, S., He, W., Luo, C. J., An, T., Chen, J., Yang, Y., ... & Yan, Q. L. (2019). Thermal behavior of graphene oxide and its stabilization effects on transition metal complexes of triaminoguanidine. Journal of Hazardous Materials, 368, 404-411.

[167] Hanafi, S., Trache, D., He, W., Xie, W. X., Mezroua, A., & Yan, Q. L. (2020). Catalytic effect of 2D-layered energetic hybrid crystals on the thermal decomposition of 3-nitro-2, 4-dihydro-3H-1, 2, 4-triazol-5-one (NTO). Thermochimica Acta, 692, 178747.

[168] Kumar, D., Kapoor, I. P., Singh, G., Siril, P. F., & Tripathi, A. M. (2011). Preparation, characterization, and catalytic activity of nanosized NiO and ZnO: part 74. Propellants, Explosives, Pyrotechnics, 36(3), 268-272.

[169] Ikhlas, A. (2003). Study of Initiation and Detonation of Low Sensitive Explosives by Jet Attack and Bullet Impact (M.Sc. thesis, MTC, Cairo).

[170] Standard, A. S. T. M. (2007). D240-02. Standard test method for heat of combustion of liquid hydrocarbon fuels by bomb calorimeter. Annual Book of ASTM Standards; American Society for Testing of Materials: West Conshohocken, PA, USA.

[171] Al-Ghouti, M., Al-Degs, Y., & Mustafa, F. (2010). Determination of hydrogen content, gross heat of combustion, and net heat of combustion of diesel fuel using FTIR spectroscopy and multivariate calibration. Fuel, 89(1), 193-201.

[172] Sucéska, M. (2004). EXPLO5. 4 program, Zagreb, Croatia, 2010 Search PubMed;(b) M. Sucéska. In Mater. Sci. Forum (pp. 465-466).

[173] Helen, S., Geneviève, E., Philippe, C., Songy, C., Nouguez, B., & AB, E. B. Recent developments in the formulation of high explosives. Strain, 7(6.0), 8-6.

[174] Kröger, C. F., Miethchen, R., Frank, H., Siemerl, M., & Pilz, S. (1969). Über 1.2. 4-Triazole, XVII. Die Nitrierung und Bromierung von 1.2. 4-Triazolonen. Chemische Berichte, 102(3), 755-766.

[175] Mukundan, T., Purandare, G. N., Nair, J. K., Pansare, S. M., Sinha, R. K., & Singh, H. (2002). Explosive nitrotriazolone formulates. Defence Science Journal, 52(2), 127.

[176] Pendashteh, A., Mousavi, M. F., & Rahmanifar, M. S. (2013). Fabrication of anchored copper oxide nanoparticles on graphene oxide nanosheets via an electrostatic coprecipitation and its application as supercapacitor. Electrochimica Acta, 88, 347-357.

[177] Kissinger, H. E. (1957). Reaction kinetics in differential thermal analysis. Analytical chemistry, 29(11), 1702-1706.

[178] Elbeih, A., Zeman, S., Jungova, M., & Akstein, Z. (2012). Effect of different polymeric matrices on the sensitivity and performance of interesting cyclic nitramines. Central European Journal of Energetic Materials, 9(2), 131-138.

[179] Licht, H. H. (2000). Performance and sensitivity of explosives. Propellants, Explosives, Pyrotechnics, 25(3), 126-132.

[180] Myint, P. C., & Nichols III, A. L. (2017). Thermodynamics of HMX polymorphs and HMX/RDX mixtures. Industrial & Engineering Chemistry Research, 56(1), 387-403.

[181] Zeman, S., & Jungová, M. (2016). Sensitivity and performance of energetic materials. Propellants, Explosives, Pyrotechnics, 41(3), 426-451.

[182] Klapötke, T. M. (2022). Chemistry of high-energy materials. Walter de Gruyter GmbH & Co KG.

[183] Zeman, S., Elbeih, A., & Akštein, Z. (2011). Preliminary study on several plastic bonded explosives based on cyclic nitramines. Energetic Materials, 19(1), 8-12.

[184] Vyazovkin, S., Burnham, A. K., Favergeon, L., Koga, N., Moukhina, E., Pérez-Maqueda, L. A., & Sbirrazzuoli, N. (2020). ICTAC Kinetics Committee recommendations for analysis of multi-step kinetics. Thermochimica acta, 689, 178597.

[185] Sućeska, M. (2004). Calculation of detonation parameters by EXPLO5 computer program. In Materials Science Forum (Vol. 465, pp. 325-330). Trans Tech Publications Ltd.

[186] Dolezal, V., & Janda, V. (1974). Theory of explosives. Czech Republic.

[187] Hazard Classification of United States Military Explosives and Munitions. (2012). U. S. Army Defense Ammunition Center, LogisticsReview and Technical Assistance Office, McAlester, OK, Revision 15

[188] Asay, B. W. (2010). Cookoff. In Shock Wave Science and Technology Reference Library, Vol. 5: Non-Shock Initiation of Explosives (pp. 403-482). Berlin, Heidelberg: Springer Berlin Heidelberg.

[189] Krawietz, T. R., McKenney Jr, R. L., & Ortiz, R. J. (2002). Characterization of the unconfined slow cook-off response of nitramines and nitraminecomposites with TNT. In 12 th International Detonation Symposium. San Diego (pp. 79-86).

[190] Pelletier, M., & Dubois, C. (2013). Multiphysics Modelling of Variable Confinement Cookoff Test (VCCT). In Proceedings of the Insensitive Munitions & Energetic Materials Technology Symposium, San Diego, CA.

[191] NATO STANAG 4491. (2002). Thermal sensitiveness and Explosiveness tests.

[192] Wardell, J. F., Maienschein, J. L., Yoh, J. J., Nichols, A. L., & McClelland, M. A. (2003). Towards An Ideal Slow Cookoff Model For PBXN-109 (No. UCRL-CONF-201173). Lawrence Livermore National Lab.(LLNL), Livermore, CA (United States).

[193] Kaneshige, M. J., Renlund, A. M., Schmitt, R. G., & Erikson, W. W. (2002). Cook-off experiments for model validation at Sandia National Laboratories. Albuquerque, NM, 87185, 10.

[194] Alexander, K., Gibson, K., & Baudler, B. (1996). Development of the Variable Confinement Cookoff Test. Discover the World's Research, 9(4).

[195] COMSOL - Heat transfer module User Guide.

[196] Myint, P. C., & Nichols III, A. L. (2017). Thermodynamics of HMX polymorphs and HMX/RDX mixtures. Industrial & Engineering Chemistry Research, 56(1), 387-403.